Robust LPV multivariable Automotive Global Chassis Control

Charles Poussot-Vassal

Grenoble Institut Polytechnique

No. attribué par la bibliothèque

THESE

pour obtenir le grade de

DOCTEUR de Grenoble INP

Spécialité: **AUTOMATIQUE-PRODUCTIQUE**

préparée au Département Automatique du GIPSA-lab

dans le cadre de l'Ecole Doctorale:
Electronique, Electrotechnique, Automatique, Traitement du Signal

présentée et soutenue publiquement

par

Charles POUSSOT-VASSAL

le 26/09/2008

Titre:

Commande Robuste LPV Multivariable de Châssis Automobile

Co-Directeurs de thèse:

Luc Dugard	Directeur de Recherche, CNRS
Olivier Sename	Professeur, Grenoble INP

Jury:

Président:	Michel Basset	Professeur, Université de Haute Alsace
Rapporteurs:	Brigitte d'Andréa-Novel	Professeur, Ecole des Mines de Paris
	Sergio M. Savaresi	Professeur, Politecnico di Milano (Italie)
Examinateur:	Peter Gáspár	Directeur de Recherche, Académie des Sciences (Hongrie)
Co-directeurs:	Luc Dugard	Directeur de Recherche, CNRS
	Olivier Sename	Professeur, Grenoble INP

Remerciements

Je tiens tout d'abord à remercier l'ensemble du personnel du département Automatique du GIPSA-lab, qui m'a permis de passer ces trois années dans un climat convivial et stimulant.

En particulier, ma gratitude va à Olivier Sename et à Luc Dugard, qui m'ont accueilli dans leur équipe et qui m'ont pris sous leur responsabilité pendant ces trois ans de thèse. Ils ont toujours été présent pour répondre à mes questions et à me transmettre leur connaissances scientifiques, et ce, dans la bonne humeur (voir même dans la dérision...). Ils ont été à la fois pointilleux sur nombre de détails, et m'ont toujours encouragé et soutenu dans mes démarches et idées (quelques fois pas très malignes). Je les remercie également pour leurs qualités humaines, car c'est probablement ces qualités qui ont fait que ces trois ans ont été un réel plaisir. Leur attitude a été et sera pour moi un moteur dans les années à venir.

Je remercie également Brigitte d'Andréa-Novel et Sergio M. Savaresi, les rapporteurs de ce mémoire de thèse qui ont accepté de me consacrer une partie de leur temps précieux (notamment pendant leurs vacances) pour me faire part de leurs remarques et questions. Je remercie également Michel Basset et Peter Gáspár, les examinateurs de mon jury de thèse, pour avoir participé à ce jury et pour l'intérêt qu'ils ont porté à mon travail tout au long de ces trois ans. Je les remercie tous d'avoir participé à la soutenance et d'avoir contribué à faire de ce jour un grand moment pour moi.

Je remercie toute l'équipe administrative, en particulier Virginie, Marielle, Marie-Rose, Marie-Thérèse, Patricia et Ophélie qui m'ont bien aidé à affronter les lourdeurs administratives, à préparer les missions, toujours dans la bonne humeur. Je remercie également l'équipe technique, notamment Daniel, Pascal (merci encore pour SLRacer!), Olivier, Jonathan, Thierry, Denis et le frère caché de Corentin qui m'ont aidé à passer trois années assez sereines.

Je remercie également Jozsef Bokor, Peter Gáspár et Zoltan Szabó, qui se sont occupés de moi lors de mes multiples séjours à Budapest, et qui ont contribué à ce que ces déplacements me soient extrêmement bénéfiques (Köszönöm !), j'espère avoir d'autres occasions de travaillez avec vous.

Je remercie Ricardo Ramirez et Aline Drivet, pour leurs contributions dans la collaboration Mexicaine et pour m'avoir accueilli dans le magnifique campus du Tec (avec ces paons...).

Ma gratitude va également à mes enseignants de l'ESISAR, qui ont su me donner envie de persévérer dans la technique et plus particulièrement dans l'automatique (trop succombent aux charmes du management...). En particulier, je remercie Eduardo Mendès pour sa pédagogie, pour ses conseils toujours pertinents et pour m'avoir supervisé à plusieurs occasions (projet industriel, stage); je remercie Damien Koenig (et ses observateurs de systèmes singuliers non linéaires, commutés, tolérants aux fautes, à retards variant dans un anneau, et qui font le café!) pour sa bonne humeur et son soutien constant.

Je remercie ma famille et mes proches: mes parents, sans qui je n'aurai rien fait et qui continuent à me supporter dans mes décisions, à Camille qui a la charge de me supporter au quotidien. Je remercie aussi mon grand frère Guilhem, Myriam, Gaël et ... qui ont toujours été là pour me soutenir et qui ont fait le déplacement. Bien évidement, je remercie ma petite soeur Claire (auteur de l'illustration de la première page), mon petit frère Robin et Joffrey, avec qui on a passé de bonnes soirées, de super journées de ski et des vacances énormes, etc; je souhaite que ça ne s'arrête pas!

Je remercie aussi les tontons Danielle, Etienne, Alain, Véronique (toujours présente), Eric et Maggy. Sans oublier les cousins de France: Thomas, Jérémy, Clara et Elena et d'outre Atlantique: Hélène (qui m'a hébergé à San Francisco pendant deux semaines), Cécile et Pierre.

Je remercie également Marc, Isabelle, Raymond et Irène, Sandra et Cyrille d'avoir fait le déplacement le jour de la soutenance et pour leur soutient tout au long de ces années.

Je remercie également mes collègues de "galère" doctorale, avec qui j'ai pu discuter plus ou moins sérieusement de modèles, de commande robuste, de convexité et autres sujets forts passionnants (et oui y'en a que ça intéresse...), mais pas que de ça non plus. En désordre structuré: merci à Corentin, Sébastien, Antoine et Sylvain, mes acolytes de bureau (avec qui ont aura résolu un paquet de problèmes scientifiques fondamentaux pendant ces trois ans, mais pas que...). Merci au toulousains Yassine, Wilfried et sa turbine de poche, ont ce sera bien gavé à Eindhoven (on a quand même rencontré dieu!) et à Reims (qui l'eu cru). A Gaëtan et Christophe, avec qui j'ai passé de bons moments que ce soit en Californie ou à Mulhouse... Merci à Luc, Fanny, Carolina, Lara, Sylvain et Alexandre (désolé t'es dans la case des thésards...) pour les repas, les pauses café, les soirées et ces moments sympas passés ensemble.

Un grand merci aux thésards et post-docs qui sont passés par le GIPSA-lab: Christophe, David, Hala, Hanane, Chady, Antoine, Maher, Marouane, Do Hieu, etc. Et bonne chance à ceux qui commencent.

Je remercie également les permanents avec qui j'ai passé de très bon moments (que ce soit au bureau, en bureau d'étude ou aux conférences) et avec qui j'ai pu discuter de tout. Merci à l'équipe SLR bien sûr! et particulièrement à John et Emmanuel, bonne chance pour la suite. Je remercie également Carlos, Nicolas, Mazen et Hayate.

Je me souviendrai longtemps de Séoul... Alors rien que pour ça, merci à Ko, Denis, Alexandre,

Carlos et Nicolas (vive les boui-bouis coréens). J'espère bien qu'il y en aura d'autre des congrès comme celui-là!

Durant cette thèse, j'ai eu la chance de co-encadrer quelques stagiaires. J'espère qu'ils ont appréciés autant que moi les moments passés ensemble. Merci donc à Joris, Elena, Sebastien, Christian et Stan.

Je garde également de très bon souvenirs avec les étudiants de l'IEG, d'HMG et de Polytech' Grenoble qui ont été assez indulgents avec moi. J'espère ne pas en avoir trop dégouté de l'automatique, et surtout qu'ils ont passé de relativement bons moments pendant les BE, TD et TP. En tout cas moi, je ne me suis pas ennuyé.

Je remercie également la team de l'UPMF 9 et manière plus générale, les "droiteux" de Grenoble. Quelle équipe, quelles victoires & défaites (principalement), mais surtout quelles soirées pré et post match. Merci à Lolo, Bastien (gasquette broquette), Jezzon, Pat (bogosse), mon très vieux pote Matthias, Jérémie (Gothiax), Bibi, Vince (la berlande), La bellevallée, Nadia, Jibé (ρta-β!), mon unique soutien), Jean-Loup, Chloé, La charpente, Margot, Vio et Tom, Sofiane, Maël, etc. Sans oublier, notre gardien de choc... Lucky Luke.

Comment ne pas remercier aussi les champions qui m'ont accompagné précédemment et que j'espère revoir encore; à savoir, mon binôme, le PI02 et le d2p crew. Plus particulièrement, René (BGB touch'), Eric, Tib (PI02 for ever, PI02 for fever), Vince, Kylie, Britney, Alyssa (on y croit ouai...). Vive les soirées chez les autruches, au Divan, et dans le salon de Chauve jusqu'à épuisement... de Red Bull. Je remercie aussi Sandie, Mib', Gladen, Hervé, Virginie, Tony, Alice, Manu, Fufu, Choupin[1] et la Verrue[2], Arnaud, Matthieu Jean Jacques. Merci à la famille ESISAR: La sermette, Ian et Ben.

Je remercie mes potes d'enfance (Jean-Jaurès, Stendhal crew & co)! Merci à mon grand pote Baptiste, à Gilou, Cyril, François, Amandine, Rémi, Magalie, Jane, Florence, Perrine, Emmanuel, Maud et Marlène. Merci à Audrey, Mathilde, Chacha. J'espère qu'on se reverra rapidement pour des soirées revival d'anthologie.

Je remercie tous ceux que j'ai oublié...

Je dédie ce manuscrit à Bernard, Simone et Charly...

[1] ©"c'est un bon Choupin!"
[2] ©"c'est ça ouai!"

Notations

$\mathbb{R}$	Real values set
$\mathbb{C}$	Complex values set
M^*	Conjugate of $M \in \mathbb{C}$
M^T	Transpose of $M \in \mathbb{R}$
$(*)^T$	Defines the conjugate (or transpose) element of a matrix $\in \mathbb{C}$ ($\in \mathbb{R}$)
σ	Singular value ($\sigma(T)$ defines the eigenvalues of the operator T s.t. $(T^*T)^{1/2}$)
j	Complex value
$Re(.)$	Real part of a complex number
$Im(.)$	Imaginary part of a complex number (j is the imaginary unit)
$M \prec (\preceq) 0$	Matrix M is symmetric and negative (semi)definite
$M \succ (\succeq) 0$	Matrix M is symmetric and positive (semi)definite
$\mathbf{Tr}(M)$	Trace of M matrix (sum of the diagonal elements)
$\mathbf{Co}(X)$	Convex hull of set X
$A = A^T$	Matrix A is real symmetric
$A = A^*$	Matrix A is hermitian
$AA^* = A^*A = I$	Matrix A is unitary
s	Laplace variable $s = j\omega$, where ω is the pulsation

GCC	Global Chassis Control
ABS	Anti-locking Braking System
ESC(P)	Electronic Stability Control (Program)
ABC	Active Body Control
LTI	Linear Time Invariant
LPV	Linear Parameter Varying
LMI	Linear Matrix Inequality
BMI	Bilinear Matrix Inequality
SDP	Semi-Definite Programming
EMB	Electro-Mechanical Braking
MRD	Magneto-Rheological Damper
DOF	degree of freedom
COG	center of gravity
iff.	if and only if
w.r.t.	with respect to
s.t.	such that / so that
resp.	respectively

Summary

This thesis is concerned with the modeling, analysis and control synthesis of dynamical ground vehicles through the use of advanced gain-scheduled robust control techniques. More specifically, the general aim is to improve vehicle comfort and safety through the control of the following actuators:

- The suspension system (either active or semi-active).
- The braking system.
- The steering system.

The main objectives underlying the thesis, is to propose new control synthesis methodologies in order to:

- Provide a new synthesis framework and solutions for semi-active controlled suspension (ensuring the dissipative constraint).
- Provide an efficient control methodology in order to synthesize Global Chassis Controllers in order to improve safety and comfort according to the driving situation, through the use of the suspension, braking and steering systems.

For that purpose, the thesis is subdivided in six Chapters, that can be gathered in three parts.

- The first part, composed by Chapters 2 and 3, is devoted to first recall some historical facts in control theory developments that led the (robust) control community to the use of the Linear Matrix Inequalities (LMIs). Then, Linear Parameter Varying (LPV) modeling and control tools and the recent developments in vehicle control (with an emphasis on suspension and global chassis control) are described. Secondly, the introduction and formal definitions of the theoretical basis of the robust control formalism and the LMI control design approach for LTI and LPV systems are described.
- The second part, composed by Chapters 4 and 5, first describes and gives analysis of the main elements that constitute a vehicle (namely tires, wheels and suspensions). Then it provides different vehicle models (widely used in the automotive community) that will be involved for control, and analysis purpose.
- The third part, composed by Chapters 6 and 7, describes the control strategies developed in the thesis and provides the main contributions of this thesis concerning suspension and global chassis control. The contributions on suspension control, either active or semi-active, using different robust approaches, are given in Chapter 6. Then, Chapter 7, describes the Global Chassis Control approaches that involve suspensions, braking and/or steering actuators.

Introduction and structure of the thesis

Thesis framework

This thesis is the result of a three years work (from October 2005 to October 2008), performed in the SLR[3] team from the Control Systems department of the GIPSA-lab[4] (former LAG[5]), on the **Robust Multivariable Linear Parameter Varying Control of Automotive Chassis**, under the supervision of **Olivier Sename** (Professor, Grenoble INP[6]) and **Luc Dugard** (Research Director, CNRS[7]). The general framework of this thesis is concerned with two main topics:

- The automotive field (more specifically, suspension and global chassis modeling and control).
- The robust Linear Parameter Varying control design, involving LMIs.

This thesis can be inserted in the continuity of previous works undertaken in the same research team, by:

- **Ricardo Ramirez-Mendoza** (see Ramirez-Mendoza, 1997), "Sur la modélisation et la commande de véhicules automobiles", which was the first study in the automotive field yield in the research team, where focus was done on the description and modeling of vehicles with first attempts on control methodologies, mainly for active cruise control.
- **Damien Sammier** (see Sammier, 2001), "Sur la modélisation et la commande de suspension de véhicules automobiles", where the focus was put on modeling and control design of a single active suspension (especially using the LTI/$\mathcal{H}_\infty$ control approach). A first attempt on semi-active suspension modeling and control was made on semi-active damper characteristics provided by PSA Peugeot-Citroën (containing multiple damping rules).
- **Alessandro Zin** (see Zin, 2005), "Sur la commande robuste de suspensions automobiles en vue du contrôle global de châssis", which extends the previous works with a strong attention on LPV/$\mathcal{H}_\infty$ control of a single active suspension in order to improve robustness properties. A sketch of global chassis control through the use of the four suspensions was also derived using an anti-roll distribution.

Moreover, throughout these three years, I had the chance to collaborate with some experts in LPV robust control theory, suspension and automotive modeling and control (both from industrial and academic horizons). Then I have participated in formal collaborations with the:

[3] System Linéaire et Robustesse (Linear Systems and Robustness)
[4] Grenoble Image Parole Signal Automatique (Grenoble Image Speech Signal Control Systems)
[5] Laboratoire d'Automatique de Grenoble (Grenoble Control Systems Laboratory)
[6] Grenoble INstitut Polytechnique (Grenoble Institute of Technology)
[7] Centre National de la Recherche Scientifique (National Scientific Research Center)

- **MTA-STZAKI** Computer and Automation Research Institute from the Hungarian Academy of Sciences (Budapest, Hungary)
  with **Jozsef Bokor** (Control Department Head Director), **Peter Gáspár** (Senior Research Fellow) and **Zoltan Szabó** (Senior Research Fellow).
  Thanks to the PAI[8] Balaton Project (2006-2007), we worked especially on LPV control design for automotive global chassis involving suspension and braking systems (multiple kind of actuators).

- **Tecnologico de Monterrey** (Monterrey, Mexico)
  with **Ricardo Ramirez-Mendoza** (Mechatronics Department Head Director) and **Aline Drivet** (PhD. student).
  Thanks to the LAFMAA[9] Project (2005-2008), we worked on semi-active suspension modeling and control, and on multi-body vehicle modeling in order to validate the proposed control approaches.

Collaborations have also been initiated with:

- **SOBEN**, a young high technology damper builder (Alès, France).
  with **Benjamin Talon** (Company CEO) and **Sébastien Aubouet** (PhD. student).
  Collaboration has been initiated in order to model, analyze and control a new kind of semi-active damper for automotive applications.

- **MIPS-MIAM** laboratory (Mulhouse, France)
  with **Michel Basset** (Professor, UHA).
  Collaboration has been initiated in order to work on the validation of control algorithms with model uncertainties, identified on real vehicles, observation and fault detection.

General introduction and motivations

Main problematic & starting point. Automotive vehicles are very complex systems composed by a multitude of subsystems that aim at improving comfort and safety through either passive (e.g. vehicle structure, seats belt, etc.) or active (e.g. ESC, ABS, etc.) solutions which are related to many different engineering areas like control, mechanics, electronics, sensors, actuators, structure, networks, etc. Then, the global dynamical behavior of automotive vehicles results to be very complex to design, model, analyze and control. In this thesis, the work is concerned with active systems i.e. systems that are (or at least, can be) controlled.

Due to the growing demand for vehicles with ever better driving characteristics in which efficiency, safety, reliability and performances are ensured (such as passenger comfort, road-holding, rollover stability, yaw stability, energy consumption, etc.), the number of controlled subsystems in commercial cars is drastically increasing. Additionally, the need for performance and robustness, in presence of actuator limitations or failure, leads control engineers to more and more work load and validation procedures in order to make the actuators collaborate each others in a good (and if possible, optimal) way.

Nowadays, most vehicle control solutions, like suspensions, braking and steering control systems, are synthesized separately and their limitations are not always handled in good way. Therefore, implementation parameters and collaboration between actuators are tuned using empirical rules, derived

[8] Projet d'Action Intégrée
[9] Laboratoire Franco-Mexicain d'Automatique Appliquée

thanks to the global knowledge of automotive engineers, or by the addition of other modules that solve a specific situation. It results in a very complex control structure which may lead to conflicting control performances, suboptimal control choices and unsolved problems. Consequently, it also contributes to a rising price in term of energy consumption, data flow, etc.

More generally, the electrical architecture, communication protocols and process reliability became more and more complex. Indeed, no global vehicle dynamical strategy (or Global Chassis Control) is involved in commercial cars to solve all the critical driving situations, using all the available actuators (see Figure 1).

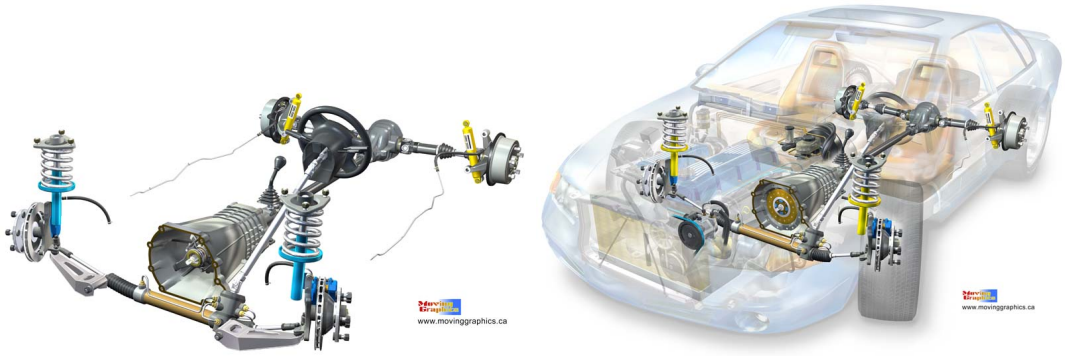

Figure 1: Vehicle chassis architecture with suspensions, braking and steering systems (from Moving Graphics web site).

Problem illustrations. As an illustration of the vehicle architecture complexity, suspensions are usually designed to improve either comfort, thanks to soft suspensions or Active Body Control (ABC) solution, or road-holding, through stiff suspensions) according to the considered vehicle. Then, comfortable cars will not be well adapted in critical driving situations because of the uneven load transfer that will introduce undesirable dynamical performances and bad handling performances. On the other hand, road-holding suspension tuning will provide a non comfortable vehicle, undesirable for usual customer. Without lost of generality and abuse of language, one denotes as a "road-holding" vehicle, a vehicle with hard (or stiff) suspensions that focusses on road adhesion, and a "comfort" vehicle, having soft suspensions and focussing on passenger comfort more than road contact.

Another illustration concerns the braking system, that usually acts in emergency situations to avoid slipping (ABS, Anti-locking Braking System, locally set for each wheel). Thus it is coupled to the ESC/ESP (Electronic Stability Control / Program) to prevent for important yaw rate, when the driver might loose control of the vehicle due to uneven road conditions. Then CBC, Cornering Braking Control system, is a module that may be added to these functions to adjust the braking force during cornering, or EBD, Electronic Brake force Distribution, to adjust braking according to the load transfer. But as far as the author knows, no collaboration with the suspension system is done in the ESP actual strategies. Nevertheless, as we will see in Chapter 5, suspensions play an important role in the load transfer control (pitch and roll), hence in the braking efficiency.

Toward Global Chassis Control (GCC). Even if these solutions, individually set, provide good results in specified situations (e.g. ABS for braking purpose, ESC for trajectory tracking and ABC

for comfort improvement), they are somehow contradictory and cannot solve all together vehicle dynamical problems like uneven road conditions, actuator failure, wind disturbances, obstacle avoidance situations, understeering etc. As far as the author knows, ESC is able to control vehicle trajectory by only acting on braking forces, and no suspension strategy is set to act in the same sense for such a situation (indeed, new ESP strategies now involve active steering). Moreover, solutions finally implemented on the vehicle might turn to be sub-optimal in the sense that all the actuator control strategies are not built in the same objective and do not collaborate each other, but actually, solve local problems only. Then, there is no GCC strategy where the control design is synthesized in global vehicle dynamical framework. Then general control and monitoring structures result to be very complex.

Indeed, as the controlled system (vehicle) is in this case a multi-input multi-output system, actuators should cooperate together in all situations towards a unified global chassis control objective. Today, the new trend in vehicle control design, is the collaboration of all the devices in contact with the ground and linked to the chassis, such as brakes, suspensions, steering wheels, etc. Hence, the aim is now at controlling the global behavior of the vehicle (Chou and d'Andréa Novel, 2005) and to propose innovative integrated control structures.

This motivates an intensive industrial and academic research in the GCC field, that aims at improving both comfort and safety on commercial cars through the development of integrated control methods that could handle different driving situations, using many different actuators, in a common objective (Shibahata, 2005).

Which control solution, and tools? According to these remarks, it is clear that, from the control point of view, GCC for ground vehicles leads to various control engineering problems which are related to very important practical vehicle properties and problematic, but also to academic and theoretical challenges such as:

- Multiple-Input Multiple-Output (MIMO) controller synthesis (vehicles are composed of many different actuators and sensors; and variables to be controlled is large).
- Robustness and performance analysis (as vehicle parameters and available measurements are not always well known and accurate).
- Performance variations (the vehicle performance objectives should vary according to the driving situation e.g. normal/dangerous/critical).
- Performance specifications (energy, comfort, road-holding) should be formalized and introduced using formal metrics.
- Actuators structural limitations requirements (like semi-active and saturations limits)
- Fault detection, monitoring and control reconfiguration (vehicle driving situation and actuators fault detection) should be handled by the control structure.

In this framework, the robust control approach, initially set for Linear Time Invariant (LTI) systems, provides interesting tools to control MIMO systems, such as vehicles. Through the use of frequency based performance specifications (like e.g. $\mathcal{H}_\infty$, $\mathcal{H}_2$, multi-objective performance criteria), it is possible to design global chassis controllers that supervise the whole vehicle dynamics and monitor the different actuators. Moreover, thanks to recent advances in Semi-Definite Positive (SDP) programming, Linear Matrix Inequalities (LMI) became a central tool in control theory and allows to

treat a large variety of problems. The extension of the robust analysis and design to Linear Parameter Varying (LPV) systems may be applied to global chassis control to handle these problems. This framework allows then to design gain-scheduled controllers that can tackle system non linearities, improving robustness of the closed loop system, and reaching adaptive performances.

Structure of the thesis & Road map

According to the previous general introduction, the thesis is structured as follows:

The first two chapters are intended to the introduction of the the main problematic faced in this thesis and provide mathematical (control) tools to understand the approaches involved in this thesis.

- **Chapter 2** gives some historical facts in order to understand the growing importance and the place of LMIs in control. The robust control and its perspectives trough the LPV theory are introduced at a fairly high level. The state of the art on recent advances in automotive control is presented with some fairly new interesting results, together with the new challenges in automotive control (focussing on suspension and global chassis control). Note that in this chapters some notions are used but not clearly defined. Thus it is more adapted to experimented reader who already have some background on control and vehicle notions).

- **Chapter 3** is devoted to the introduction of the key notions in robust control (system definitions, spaces, signals, system norms) and in LMI based controller synthesis procedure for LTI and LPV systems. This Chapter introduces the tools used in the thesis and provides an approach on the robust control for both LTI and LPV systems. Mathematical equations and formal definitions are given in order to give to the reader all the required tools to understand the main contributions of the thesis.

Chapter 4 introduces the technology and the physical phenomena related to suspension, tire, braking and steering systems. Then, in Chapter 5, the vehicle models involved in this thesis and in the literature are introduced and studied in order to illustrate the limitations and challenging points. Evaluation criteria that will be used for control performance efficiency measurement are introduced.

- **Chapter 4** is concerned by the physical description of the main vehicles subsystems and phenomena that will be used for modeling and control purpose. Attention is more paid at suspension (passive, active and semi-active), braking (both actuator and tire/road contact) and steering systems. In this chapter, two industrial suspension are analyzed to illustrate the semi-active principles.

- **Chapter 5** first introduces the different nonlinear, LTI and LPV vehicle models involved in the thesis. Then, thanks to a given performance criteria, frequency and time domain evaluations are performed. This chapter aims at providing a global understanding of the inner performances of the systems and on the expected improvements thanks to the control apport.

The two last chapters contain the thesis contributions. The first (Chapter 6) is concerned with the design of active and semi-active suspension controllers. The second one (Chapter 7) is concerned with the design of global chassis controllers.

- **Chapter 6** focusses on suspension control. Firstly both LTI and LPV designs of active suspension systems are derived and validated (using a multi-objectives control approaches). Then, a

novel approach to semi-active suspension control of a single suspension, based on LPV/$\mathcal{H}_\infty$ control methods, that ensures dissipative constraints and actuator limitations, is proposed and compared to other existing approaches.

- **Chapter 7** introduces robust control methods extended to full vehicle involving different kinds of actuators. The global chassis control is studied through various control architectures. Firstly, a four suspension based control design is introduced, in order to extend the single quarter car model control with an additional control law that represents an anti-roll repartition (based on results proposed in perspectives of Zin (2005)). Secondly, gain-scheduled suspension and braking strategies are introduced to solve comfort/road-holding balance and yaw stability critical situation. Finally a gain-scheduled braking and steering control design, involving a local braking strategy, is introduced in order to show the global chassis dimension of the proposed design.

Contributions

Main contributions. This thesis aims at providing tools and control design methodologies in order to improve comfort and safety in automotive vehicles, through the robust control tools. The main contributions are concerned with the:

- **Suspension control**, especially the new LPV based semi-active methodology developed where a novel approach to ensure the dissipative constraint of controlled dampers in introduced through a dynamical output feedback control (see Chapter 6). The main advantages of this approach rely on the frequency based degree of freedom and its "simple" structure (which should be appropriate for implementation purpose).
- **Global Chassis Control**, involving different kinds of actuators, playing the role of vehicle supervisor or monitor that controls the different actuators in order to reach a general vehicle dynamical objective (see Chapter 7). The interest of such a structure is to provide a methodology to construct controllers that monitor the vehicle actuators in order to reach a given general dynamical and attitude objective. Such an approach represents a new framework and provides new perspectives in vehicle active safety improvement: the GCC is a "super controller" that supervises the local controllers in order to make them work together in a unified objective.

Software development. A toolbox, working together with MATLAB/Simulink software, has been developed during the thesis. Additionally, together with Pascal Bellemain[10], user friendly 3D visualization software is now proposed to visualize the vehicle dynamics. The toolbox presents the following main features:

- Provides embedded MATLAB and Simulink functions and blocks, ready for simulation and control synthesis of the quarter, bicycle, half, full, etc. vehicle models (either LTI, LPV and nonlinear).
- Provides embedded MATLAB functions to synthesize LTI and LPV LMI based controller guaranteeing $\mathcal{H}_\infty$, $\mathcal{H}_2$, multiobjective performance criterion, using YALMIP interface (Lofberg, 2004).
- Provides a simulation interface, with user friendly environment, working together with MATLAB/Simulink, allowing 3D visualization of the vehicle (built with Pascal Bellemain).

[10] Engineer from the technical team of the GIPSA-lab.

Publication list

International journal papers

J1 *Discussion paper on: "Combining Slip and Deceleration Control for Brake-by-Wire Control Systems: a Sliding-Mode Approach"* (C. Poussot-Vassal),
In **European Journal of Control**, Vol. 13(6), December, 2007.

J2 *Attitude and Handling Improvements based on Optimal Skyhook and Feedforward Strategy with Semi-active Suspensions* (C. Poussot-Vassal, O. Sename and L. Dugard),
In **International Journal of Vehicle Autonomous Systems**, Special Issue on: Modeling and Simulation of Complex Mechatronics Systems (Accepted, In press, in December 2007).

J3 *A New Semi-active Suspension Control Strategy Through LPV Technique* (C. Poussot-Vassal, O. Sename, L. Dugard, P. Gáspár, Z. Szabó and J. Bokor),
In **Control Engineering Practice**, Vol. 16(12), pp 1519-1534, December, 2008.

International conference papers with proceedings

C1 *Optimal Skyhook control for semi-active suspensions* (C. Poussot-Vassal, O. Sename, L. Dugard, R. Ramirez-Mendoza and L. Flores),
In Proceedings of the 4^{th} **IFAC Symposium on Mechatronics Systems** (Mechatronics), Heidelberg, Germany, September, 2006.

C2 *Multi-objective qLPV $\mathcal{H}_\infty$/$\mathcal{H}_2$ control of a half vehicle* (C. Poussot-Vassal, O. Sename, L. Dugard, P. Gáspár, Z. Szabó and J. Bokor),
In Proceedings of the 10^{th} **Vehicle System Dynamics, Identification and Anomalies** (VSDIA), Budapest, Hungary, November, 2006.

C3 *Toward global chassis control by integrating the brake and suspension systems* (P. Gáspár, Z. Szabó, J. Bokor, C. Poussot-Vassal, O. Sename and L. Dugard),
In Proceedings of the 5^{th} **IFAC Symposium on Advances in Automotive Control** (AAC), Aptos, California, August, 2007.

C4 *A LPV based semi-active suspension control strategy* (C. Poussot-Vassal, O. Sename, L. Dugard, P. Gáspár, Z. Szabó and J. Bokor),
In Proceedings of the 3^{rd} **IFAC Symposium on System Structure and Control** (SSC), Iguaçu, Brazil, October, 2007.

C5 *Performance analysis and simulation of a new industrial semi-active damper* (S. Aubouet, O. Sename, B. Talon, C. Poussot-Vassal and L. Dugard),
In Proceedings of the 17^{th} **IFAC World Congress** (WC), Seoul, Korea, July, 2008.

C6 *A self tuning suspension controller for a multi-body quarter vehicle model* (C. Poussot-Vassal, A. Drivet, O. Sename, L. Dugard and R. Ramirez-Mendoza),
In Proceedings of the 17^{th} **IFAC World Congress** (WC), Seoul, Korea, July, 2008.

C7 *Attitude and Handling Improvements Through Gain-scheduled Suspensions and Brakes Control* (C. Poussot-Vassal, O. Sename, L. Dugard, P. Gáspár, Z. Szabó and J. Bokor),
In Proceedings of the 17^{th} **IFAC World Congress** (WC), Seoul, Korea, July, 2008

C8 *Commande Robuste LPV Tolérante aux Défauts pour l'Amélioration de la Sécurité des Véhicules* (C. Poussot-Vassal, O. Sename and L. Dugard),
In Proceedings of the 5^{th} **Conference Internationale Francophone d'Automatique** (CIFA), Bucharest, Roumania, September, 2008.

C9 *A Global Chassis Controller for Handling Improvements Involving Braking and Steering Systems* (C. Poussot-Vassal, O. Sename and L. Dugard),
In Proceedings of the 47^{th} **IEEE Conference on Decision and Control** (CDC), Cancun, Mexico, December, 2008

National conference papers with proceedings

N1 *Contrôle robuste LPV: Application aux véhicules automobiles* (C. Poussot-Vassal, O. Sename and L. Dugard),
In Proceedings of the 2^{nd} **Journée Doctorales/Journées Nationales MACS** (JD/JN MACS), Reims, France, July, 2007.

N2 *Commande Robuste LPV Tolérante aux Défauts pour l'Amélioration de la Sécurité des Véhicules* (C. Poussot-Vassal, O. Sename and L. Dugard),
In Proceedings of the Conférence Internationale Francophone d'Automatique (CIFA), Bucarest, Romania, September, 2008.

International conference papers without proceedings

S1 *A self tuning LPV/$\mathcal{H}_\infty$ suspension controller for a multi-body quarter vehicle model* (C. Poussot-Vassal, A. Drivet, O. Sename, L. Dugard and R. Ramirez-Mendoza),
At the 20^{th} **Symposium of the International Association for Vehicle System Dynamics** (IAVSD), Berkeley, California, August, 2007.

S2 *Global chassis control using braking and suspension systems* (P. Gaspar, Z. Szabo, J. Bokor, C. Poussot-Vassal, O. Sename and L. Dugard),
At the 20^{th} **Symposium of the International Association for Vehicle System Dynamics** (IAVSD), Berkeley, California, August, 2007.

Submitted journal and conference papers

J4 *Integrated Global Chassis Control Through Gain-scheduled Suspensions and Brakes Control* (C. Poussot-Vassal, O. Sename, L. Dugard, P. Gáspár, Z. Szabó and J. Bokor),
Submitted to **IEEE Transaction on Control System Technology** (under review).

J5 *Attitude and Handling Improvements Through Gain-Scheduled Suspensions and Brakes Control* (C. Poussot-Vassal, O. Sename, L. Dugard, P. Gáspár, Z. Szabó and J. Bokor),
Submitted to Control Engineering Practice: Special Issue of the 17^{th} IFAC World Congress.

C10 *Robust Vehicle Dynamic Stability Controller Involving Steering and Braking Systems* (C. Poussot-Vassal, O. Sename and L. Dugard),
Submitted to the 9^{th} European Control Conference (ECC), Budapest, Hungary, August, 2009.

C11 *Semi-active $\mathcal{H}_\infty$/LPV control for an industrial hydraulic damper* (S. Aubouet, O. Sename, L. Dugard, C. Poussot-Vassal and B. Talon),
Submitted to the 9^{th} European Control Conference (ECC), Budapest, Hungary, August, 2009.

Contents

List of Figures

List of Tables

Chapter 1

Introduction et résumé détaillé

1.1 Introduction

Cette thèse est le résultat de trois années de travail (Octobre 2005 - Septembre 2008) effectué au sein de l'équipe Systèmes Linéaires et Robustesse (SLR) du département Automatique du GIPSA-lab (ancien LAG) sur la **Commande Robuste Multivariable LPV de Châssis Automobile**, sous la direction de Olivier Sename (Professeur, Grenoble INP) et de Luc Dugard (Directeur de Recherche, CNRS). Les principaux thèmes développés concernent:

- La modélisation, l'analyse et le contrôle de la dynamique des véhicules automobiles.
- Le contrôle robuste de systèmes Linéaires à Paramètres Variants (LPV), utilisant les outils des Inégalités Linéaires Matricielles (LMIs).

Cette thèse s'insère dans la continuité d'autres travaux précédemment développés dans l'équipe, notamment ceux de:

- **Ricardo Ramirez-Mendoza** (voir Ramirez-Mendoza, 1997), "Sur la modélisation et la commande de véhicules automobiles", qui fût la première étude dans le domaine des véhicules automobile réalisée dans l'équipe SLR, où l'accent était mis sur la description et la modélisation des véhicules automobiles. Des premiers résultats concernant la commande de suspension et le contrôle longitudinal furent développés.
- **Damien Sammier** (voir Sammier, 2001), "Sur la modélisation et la commande de suspension de véhicules automobiles", où l'accent a été mis sur la modélisation et la commande de suspension active (utilisant l'approche LTI/$\mathcal{H}_\infty$). Des premiers résultats utilisant des suspensions semi-actives sont présentés, utilisant des données fournies par PSA Peugeot-Citroën.
- **Alessandro Zin** (voir Zin, 2005), "Sur la commande robuste de suspensions automobiles en vue du contrôle global de châssis", qui étend les résultats précédents en utilisant les méthodes LPV pour le contrôle de suspensions actives, garantissant de meilleures performances de robustesse. Un schéma de contrôle impliquant les quatre suspensions est également présenté utilisant les notions de répartition anti-roulis.

Au long des ces trois ans, j'ai eu l'opportunité de travailler avec des experts en LPV, théorie de la commande robuste, modélisation et commande de suspensions et de véhicules (à la fois du coté industriel et académique). Ainsi, j'ai travaillé de manière formelle avec le:

- **MTA-STZAKI** Computer and Automation Research Institute de l'Académie des Sciences Hongroise (Budapest, Hongrie)
  avec **Jozsef Bokor** (Directeur du département de théorie de la commande), **Peter Gáspár** (Senior researcher) et **Zoltan Szabó** (Senior researcher).
  Grâce au projet Balaton PAI[1] (2006-2007), nous avons pu travailler sur la commande LPV appliquée au contrôle du châssis, utilisant les actionneurs de suspensions et freinage.

- **Tecnologico de Monterrey** (Monterrey, Mexique)
  avec **Ricardo Ramirez-Mendoza** (Directeur du département mécatronique) et **Aline Drivet** (étudiante en Thèse de doctorat).
  Grâce au projet LAFMAA[2] (2005-2008), nous avons travaillé sur la modélisation et le contrôle de suspensions semi-actives, et sur la modélisation multi-corps de véhicules pour valider des algorithmes de commande complexes.

D'autres collaborations ont été initiées avec:

- **SOBEN**, une jeune entreprise fabriquant des amortisseurs pilotés pour véhicules (Alès, France).
  avec **Benjamin Talon** (Fondateur) et **Sébastien Aubouet** (étudiant en Thèse de doctorat).
  La collaboration à pour but de modéliser, d'analyser et de contrôler un nouveau type d'amortisseur piloté.

- Le laboratoire **MIPS-MIAM** (Mulhouse, France)
  avec **Michel Basset** (Professeur).
  La collaboration a pour but de valider les méthodes de commande robuste sur des modèles de véhicule avec des paramètres incertains, identifiés sur des véhicules réels. De plus nous souhaitons réaliser plus d'études sur l'observation et la détection de fautes afin de les intégrer à des méthodes de commande reconfigurables.

1.2 Introduction générale et motivations

1.2.1 Problématique principale & Point de départ

Les véhicules sont des systèmes extrêmement complexes, composés d'une multitude de sous-systèmes qui ont pour objectif d'améliorer le confort et la sécurité au travers de solutions passives (telles la structure du véhicule, les ceintures de sécurité, etc.) ou actives (tel l'ESC, l'ABS, les suspensions pilotées etc.). Ces solutions impliquent différents domaines de compétences dans l'ingénierie, comme le contrôle commande, l'analyse de structure, la mécanique, l'électronique, les capteurs et actionneurs, les réseaux, etc. Ainsi, la dynamique globale du véhicule est extrêmement complexe à analyser, modéliser et contrôler. Dans cette thèse, nous nous intéressons à ce que l'on appelle la sécurité active, i.e. les systèmes qui peuvent être pilotés en temps réel pour améliorer les performances du véhicule (e.g. la sécurité et le confort).

Dû au besoin croissant de performances et de sécurité, les défis dans le secteur automobile, spécialement en ce qui concerne le contrôle/commande, n'ont cessé de croître (confort passager, tenue de route, stabilité du véhicule, consommation d'énergie, etc.). De plus, le besoin récurrent de robustesse vis-à-vis de perturbations externes, de disfonctionnements d'actionneurs ou d'incertitudes de modélisation fait que le travail de l'ingénieur se complexifie grandement et l'amène à une charge de travail

[1] Projet d'Action Intégrée
[2] Laboratoire Franco-Mexicain d'Automatique Appliquée

grandissante ainsi qu'à une multiplication de tests pour valider les méthodes de contrôle et faire en sorte que les actionneurs collaborent entre eux (et si possible d'une manière optimale).

Dans les véhicules actuels, la plupart des solutions de contrôle/commande sont synthétisées de manière séparée et les limitations et couplage ne sont pas toujours pris en compte de manière explicite; c'est le cas des suspensions, du système de freinage, de la direction. Ainsi, la collaboration entre les différents actionneurs est faite a posteriori à partir des connaissances des ingénieurs véhicule, sur la base de "l'essai et erreur" ou en ajoutant des blocs pour traiter des situations spécifiques de conduite. Il en résulte une architecture de plus en plus compliquée qui peut difficilement être optimale et qui résulte en un prix, une consommation d'énergie et un flux de données toujours croissant et difficile à gérer.

D'une manière plus générale, l'architecture électrique, les protocoles de communication et la sureté de fonctionnement deviennent des points de plus en plus complexes. De fait, à ce jour, aucune solution de Contrôle Global de Châssis (CGC) permettant de piloter de manière unie et synchronisée tous les actionneurs disponibles, n'existe encore sur les véhicules commercialisés (voir Figure 1.1).

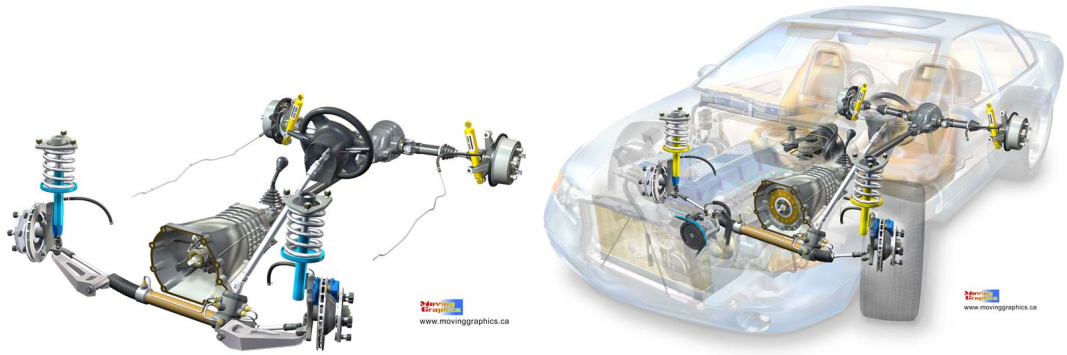

Figure 1.1: Châssis d'un véhicule: architecture avec systèmes de suspensions, freinage et direction (image de Moving Graphics).

1.2.2 Illustration de quelques problèmes

En guise d'illustration de ce qui peut se faire actuellement dans le secteur automobile, illustrant la complexité de l'architecture de contrôle de la dynamique véhicule, on constate que les suspensions sont souvent utilisées (pilotées si tel est le cas) dans le but d'améliorer le confort perçu par les passagers (ABC, Active Body Control) ou la tenue de route (en rigidifiant les supensions), en fonction du type de véhicule. Il en résulte un compromis classique entre confort de conduite et sécurité, qui peut s'avérer dangereux dans des situations de conduite où le report de charge devient important, ou mener à un mauvais ressenti du véhicule (ce qui n'est bien sûr pas du goût des constructeurs automobile).

Une autre illustration des problèmes liés à la dynamique et au contrôle global concerne le système de freinage, réalisé de manière locale sur chaque roue pour limiter, voire empêcher les phénomènes de glissements (ABS, Anti-locking Braking System). Ce genre de système est souvent couplé avec un ESC/ESP (Electronic Stability Control / Program) qui permet de garder le contrôle du véhicule (d'un point de vue conducteur et automaticien) en cas de faible adhérence de la route. De plus, on ajoute souvent un module type CBC (Cornering Braking Control) pour prendre en considération le freinage en courbe, puis un module EBD (Electronic Brake force Distribution) pour ajuster le freinage en cas de fort report de charges, etc. Mais, très peut de collaborations avec le système de suspension existent

dans les ESP actuels, alors que celles-ci jouent un rôle non négligeable dans la dynamique latérale, longitudinale et de lacet des véhicules (voir Chapitre 5).

1.2.3 Vers une commande globale de châssis (CGC)

Même si ces solutions, réalisées de manière individuelle et dissociée permettent d'obtenir de bons résultats dans des situations spécifiques (e.g. ABS pour le pilotage du système de freinage, l'ESC pour la poursuite de trajectoire utilisant freinage et volant, l'ABC pour l'amélioration du confort au travers des suspensions), ces performances sont d'une certaine manière contradictoires et ne peuvent résoudre ensemble un problème global de dynamique véhicule comme par exemple des situations d'adhérence non uniforme (droite/gauche), l'évitement d'obstacle à vitesse rapide, le sur/sous virage, la reconfiguration en cas de disfonctionnement d'un actionneur, etc. Ainsi, les solutions mises en oeuvre sur les véhicules actuels n'utilisent pour la plupart qu'un seul type actionneur à la fois; de fait, les performances obtenues sont sous-optimales et sous évaluées par rapport à ce que l'on pourrait obtenir en faisant collaborer tous les actionneurs en même temps afin de résoudre un problème de dynamique globale au lieu de se cantonner à des résultats locaux. Actuellement, la collaboration entre actionneurs dans les véhicules est faite via des essais, c'est à dire que les situations sont traitées au cas par cas et les sous systèmes re-réglés pour résoudre chaque problématiques; il en résulte une architecture extrêmement complexe qui laisse place à de nombreux tests de validations (expliquant des phases de développement longues et coûteuses).

Comme le système à piloter (le véhicule) est un systèmes multi-entrées/multi-sorties, les actionneurs doivent coopérer dans toutes les situations dans un but unifié de contrôle de la dynamique globale. C'est pourquoi, aujourd'hui, la nouvelle tendance en contrôle de dynamique véhicule est de faire collaborer les actionneurs de suspension, freinage, direction etc. afin d'atteindre un objectif commun. Ainsi, l'objectif est de contrôler la dynamique globale du véhicule et de proposer des solutions de commande intégrées innovantes (Chou and d'Andréa Novel, 2005).

Cet objectif mène à de plus en plus de recherche (qu'elle soit privée ou publique) dans le domaine de la CGC, avec pour objectif d'améliorer à la fois le confort et la sécurité des véhicules au travers de développements de contrôleur globaux efficaces dans différentes situations de conduite, utilisant tous les actionneurs disponibles (si besoin est), et ce, dans un objectif commun (Shibahata, 2005).

1.2.4 Quelle solution et quels outils?

Ces constats font paraître clairement que, du point de vue de l'automaticien, la CGC des véhicules routiers mène à de nombreux problèmes pratiques, qui sont également liés à des problématiques du monde académique comme:

- La synthèse de contrôleurs MIMO (les véhicules étant composés d'une multitude d'actionneurs et de capteurs, très différents structurellement, et de nombreuses variables de décisions).
- L'analyse et la garantie de performance et de robustesse en présence d'incertitudes (dans un véhicule, tout n'est pas forcement mesuré et connu).
- L'évaluation et même la définition des objectifs de performances (en effet dans une voiture, ceux-ci sont amenés à changer en fonction de la situation de conduite, e.g. normale / dangereuse / critique et de l'environnement).
- La définition des objectifs de performance (confort, tenue de route, pertes énergétiques, etc.) doit être formalisée au travers de métriques.

- La prise en compte des limitations des actionneurs (e.g. actionneurs dissipatifs, saturations, etc.).

- La propriété de fournir des algorithmes de commande tolérants aux fautes, et capables de se reconfigurer et d'assurer un certain niveau de performance en présence de défaillances.

Dans ce cadre, le formalisme de la commande dite robuste, initialement développée pour les système Linéaires à Temps Invariant (LTI), fournit des outils de développement intéressants pour le contrôle des sytèmes MIMO, comme les véhicules automobiles. Grâce à des approches permettant de définir des propriétés fréquentielles (comme les critères de performance $\mathcal{H}_\infty$, $\mathcal{H}_2$, multi-objectifs, etc.), il est alors possible de synthétiser des contrôleurs pilotant tout les actionneurs disponibles et supervisant la dynamique globale du véhicule tout en garantissant certaines propriétés de robustesse en présence d'incertitudes et de limites sur les actionneurs. De plus, grâce aux récents développements dans le domaine de la Programmation Semi-Definie (SDP), les Inégalités Linéaires Matricielles (LMIs) sont devenues un outils central dans la théorie de la commande des sytèmes dynamiques, permettant de traiter et de résoudre une large variété de problèmes. Parmi ces problèmes, l'extension de la commande robuste aux systèmes dits Linéaires à Paramètres Variants (LPV), permettant notamment de prendre en compte des incertitudes et d'étendre le domaine de validité des modèles linéaires, nous permet de synthétiser des contrôleurs à gains séquencés prenant en compte les non linéarités du modèle et de faire varier les performances du système bouclé en fonction de l'état du véhicule, permettant ainsi d'atteindre des performances adaptatives.

1.3 Principales contributions

1.3.1 Contributions scientifiques

Mon travail de thèse a concerné la synthèse de contrôleurs robustes à gain séquencés (aussi appelés LPV), dans le but de commander la dynamique globale du véhicule en utilisant les actionneurs de suspension, de freinage et de direction. Cette problématique nous confronte à des systèmes non linéaires, à dynamiques variées et complexes (tout particulièrement dans les situations critiques de conduite où le pilotage des sous-systèmes est crucial).

Au delà de l'analyse et de la simulation numérique de la dynamique du véhicule, cela m'a conduit à porter plus particulièrement mes recherches et mon attention sur les derniers développements en matière de commande robuste, d'optimisation convexe (au travers des LMIs) et de système LPV (modélisation et contrôle). Dans ce contexte, je me suis impliqué dans les récentes avancées liées aux méthodes basées sur la résolution de LMIs appliquées aux systèmes LPV, ainsi qu'aux problématiques et challenges industriels liés aux véhicules. Mes principales contributions concernent la mise en oeuvre de méthodes innovantes, utilisant des outils de l'automatique moderne, pour piloter les sous-systèmes et la dynamique globale du véhicule automobile. Ainsi, durant la thèse, les thèmes suivants ont été successivement développés (classés par thématique):

1. **La commande de suspensions**: Dans la mesure où mes travaux s'insèrent dans une continuité au sein de l'équipe SLR du GIPSA-lab, mes premiers résultats concernent la commande des suspensions actives et semi-actives.

   (a) **Commandes actives**:

   - Dans [C1], nous présentons une méthode basée sur un critère de performance fréquentiel pour ajuster les paramètres de la commande Skyhook (commande de suspension

bien connue dans la littérature). Cette commande, bien qu'elle soit appliquée sur un système semi-actif, est structurellement active.

- Dans [J1], les résultats de [C1] sont étendus et appliqués à chaque suspension du modèle complet du véhicule. En plus de ces commandes locales, une loi d'anticipation permettant de faire une répartition anti-roulis de manière à influencer le comportement sur/sous vireur de la voiture est étudiée. Ce travail illustre le fait que les suspensions peuvent également influencer le comportement latéral du véhicule, justifiant l'intérêt d'investigations sur le contrôle global.
- Dans [C2], nous présentons une commande LPV $\mathcal{H}_\infty/\mathcal{H}_2$ qui prend en compte les non linéarités des raideurs des suspensions de façon à rendre la boucle fermée plus robuste. De plus nous étudions le compromis inhérent à la synthèse de contrôleurs mixtes (via une analyse de courbe de Pareto). Cette analyse montre également que la synthèse mixte peut s'avérer très utile pour des systèmes physiques, notamment pour la minimisation énergétique.
- Dans [C4] et [C9], un contrôleur à gains séquencés en fonction de l'état de la suspension est synthétisé. Le contrôleur obtenu est validé en co-simulation avec un logiciel de simulation multi-corps (ADAMS), permettant de modéliser plus finement le quart de véhicule (avec prise en compte des inerties des masses, de la géométrie, etc.).

Il est à noter que l'étude de suspensions actives a une vocation plus théorique puisque les challenges dans ce domaine, tant industriels qu'académiques, concernent plus la mise oeuvre de commandes de suspensions semi-actives (c'est à dire d'amortisseurs pilotés).

(b) **Commandes semi actives**:

- Dans [C3], [C7] et [J3], une nouvelle méthode de commande de suspensions semi-active est présentée. Son originalité consiste à assurer des performances en boucle fermée (de type $\mathcal{H}_\infty$), tout en garantissant une commande dissipative. En effet, les suspensions semi-actives (amortisseur contrôlable) sont des actionneurs qui peuvent dissiper de l'énergie à différentes vitesses, mais pas fournir de l'énergie au système. Ainsi, cet actionneur peut être vu comme une saturation variable (dépendante de l'état du système). Dans la littérature, ce type de système est souvent piloté par des approches prédictives et/ou non linéaires (commutées ou port Hamiltonien). L'approche choisie est basée sur la méthodologie LPV, permettant d'obtenir un contrôleur simple à implémenter. Cette approche permet également de garantir la dissipativité de l'actionneur tout en proposant à l'ingénieur automaticien une large palette de degrés de liberté pour ajuster les performances du système en boucle fermée. Ainsi, la solution proposée permet notamment d'atteindre des performances de tenue de route (alors que dans la littérature, les performances atteintes concernent plus le confort). Une étude comparant les performances obtenues par la solution proposée avec des solutions connues dans la littérature est faite dans cette thèse.
- Dans [C8] une étude des performances atteignables par une suspension semi-active industrielle (développée par la société SOBEN) est faite en utilisant les critères développés dans [C1]. Un premier schéma de commande de ce type de système est proposé.
- Dans [C12] (soumis), la stratégie de commande développée dans [J3] est appliquée à la suspension industrielle de la société SOBEN (avec laquelle une collaboration a été initiée). Les premiers résultats (de simulation) fournissent des résultats encourageant quant à la possibilité de mise en oeuvre.

2. **La Commande Globale de Châssis (CGC)**: L'extension naturelle des travaux autour des suspensions, qui mène au deuxième volet de mes recherches concerne la Commande Globale de Châssis (CGC), utilisant différents types d'actionneurs (suspensions, freins et direction). Les domaines suivants ont été étidiés:

   (a) **Contrôle du Freinage**:
   - Dans [J1], une discussion d'une nouvelle stratégie d'ABS est faite. Cette analyse fait ressortir l'importance d'une commande conjointe de freinage et de suspension pour diminuer la distance de freinage et garantir la stabilité du glissement longitudinal (notion très complexe en véhicule). Cet article propose (simulation à l'appui) des extensions au papier initialement soumis pour améliorer les performances de freinage, via une commande conjointe (frein & suspension).

   (b) **Commande de Suspensions et Freinage**:
   - Dans [C5], [C6] et [C10], les méthodes de commande robuste LPV sont appliquées au véhicule complet pour piloter de manière unifiée les systèmes de suspension et de freinage afin de garantir le confort et la sécurité en fonction de la situation de conduite. Une des originalités de [C10] réside dans le fait que la stabilité du système de freinage (habituellement garantie par l'ABS) est préservée grâce à un séquencement de gains du contrôleur. Une version améliorée de ce papier a été soumise [J5].
   - Dans [J4] (soumis), nous proposons une stratégie d'ABS innovante, s'intégrant dans un CGC, utilisant le système de freinage et de suspension.

   Dans ces résultats, les contrôleurs synthétisés pilotent directement tous les actionneurs, à partir d'un modèle global.

   (c) **Commande de Freinage et Direction**: Dans les approches développées ici, l'objectif est de synthétiser un CGC afin de superviser tous les actionneurs et sous-systèmes et non de réaliser un contrôleur pilotant directement chaque sous-système. Ainsi, le but est de superviser la dynamique du véhicule.
   - Dans [C11], nous développons un CGC pour améliorer la sécurité des véhicules, en utilisant les actionneurs de freinage et de direction. Ce résultat propose une structure de CGC hiérarchisée, supervisant les sous systèmes de contrôle. Dans cet article, le CGC fournit des références aux systèmes de freinage et de direction. L'algorithme d'ABS discuté dans [J1] est réutilisé ici pour garantir la stabilité locale des roues et éviter le glissement. Cette approche permet notamment de hiérarchiser la commande tout en proposant une loi qui supervise les sous-systèmes et garantit des performances globales. De plus cette structure se montre très flexible quant aux possibilités de mise en oeuvre.
   - Dans [C13] (soumis), les résultats de [C11] sont étendus. La contribution consiste à utiliser une structure de contrôleur particulière pour éviter les phénomènes de saturation inhérents à la synthèse de contrôleurs via des approches linéaires et à fournir des paramètres de haut niveau pour définir les filtres de performances (utilisés dans la commande robuste) de manière simple et efficace.

1.3.2 Développements méthodologiques (outil)

Durant ma thèse de doctorat, j'ai également développé une Toolbox (boîte à outil) Matlab/Simulink pour la simulation et l'analyse de la dynamique de véhicule et la synthèse de contrôleurs LTI & LPV

par approche polytopique, utilisant YALMIP et SeDuMi. Cet outil est librement téléchargeable sur la page web de l'équipe.

L'intérêt de ce développement (coûteux en temps) est de fournir aux différents partenaires de nos collaborations (Mexique, Hongrie, Mulhouse...), les outils que nous utilisons pour la synthèse et la validation, de manière à pouvoir échanger et comparer rapidement les résultats. Il est à noter que cette Toolbox n'en est qu'à un stade préliminaire, mais sous condition de quelques efforts de structuration, celle-ci pourrait très bien être utilisée et agrémentée par la communauté pour la recherche (voire utilisée à des fin éducative). Les principales fonctionnalités (non exhaustives) sont listées ci-après.

1.3.2.1 Modélisation et simulation du véhicule

Toolbox Matlab/Simulink pour simulation et commande de la dynamique globale de châssis.

1. Ensemble de blocs Simulink paramétrisables, permettant de gérer et de simuler les suspensions, les freins, la direction, le châssis...
2. Fonctions modèle de véhicule $1/4$, $1/2$, Bicyclette, Complet (Linéaire & Non linéaire)
3. Modèles d'actionneurs de suspensions et de pneumatiques
4. Ensemble de données véhicule identifiées sur véhicule réel (avec le MIPS de Mulhouse)
5. Fonctions graphiques orientées véhicule (pour affichage des résultats)

1.3.2.2 Synthèse de contrôleurs robustes LTI & LPV

Toolbox Matlab/Simulink pour la synthèse de contrôleurs et l'analyse de systèmes.

1. Fonctions de synthèse de contrôleurs LTI et LPV avec performances $\mathcal{H}_\infty$, $\mathcal{H}_2$, Mixte... utilisant l'approche LMI et les outils de prototypage rapide YALMIP
2. Fonctions d'évaluation de performances des systèmes non linéaires (fonctions réalisant des pseudo-Bode, la mesure de densité spectrale de puissance...)

Cette Toolbox, libre d'accès (également sur le site de l'équipe SLR du GIPSA-lab) n'est pas encore complètement finalisée, mais pourrait être un outil intéressant à l'avenir. Elle a déjà été utilisée par des stagiaires et d'autre doctorants (au sein du GIPSA-lab, mais également dans d'autres laboratoires).

1.3.3 Impact du travail de thèse (rayonnement)

Comme les travaux de cette thèse se sont inscrits dans plusieurs projets de collaborations (voir ci-dessus), ils ont (et auront) un impact au sein de ces projets et les équipes/laboratoires associés. Ainsi, cette thèse a permis, entre autres:

1. De tisser des relations avec la jeune entreprise SOBEN, en matière de modélisation et commande de suspension semi-active. Actuellement, Sébastien Aubouet, un étudiant que j'ai co-encadré en Master, réalise une thèse CIFRE avec cette entreprise.

2. La collaboration, prenant initialement la forme d'un PAI Balaton, avec l'Académie des Sciences de Hongrie (Senior researchers Jozsef Bokor, Peter Gáspár et Zoltan Szabó) devrait se poursuivre dans les années qui suivent sous la forme d'un PICS[3] CNRS.

3. La mise en place d'une collaboration avec le Politecnico di Milano, Italie (Professeur Sergio M. Savaresi) où je vais réaliser un séjour post-doctoral dès début 2009 avec de nombreuses extensions de mes travaux de recherche.

4. De lancer un projet d'ANR[4] (en cours de rédaction) avec notamment l'école des Mines de Paris (Professeur Brigitte d'Andréa-Novel) et l'Université de Haute Alsace (Professeur Michel Basset) sur les problématiques de détection de fautes, de reconfiguration de contrôleurs et de développement de logiciel orienté dynamique véhicule.

5. De mettre en place une plateforme de simulateur de véhicule (encore en phase expérimentale, mais librement disponible sur le site de l'équipe[5]).

6. Le commencement d'une nouvelle thèse dans le domaine du contrôle global de châssis en 2008 (Anh Lam Do).

Cet ensemble de partenariats initiés de manière dissociée, autour de la commande robuste et des problématiques véhicules (au sens large), me semble être une opportunité intéressante de monter dans les années à venir une collaboration à dimension européenne.

1.4 Contrôle de suspensions semi-actives

Dans cette section, après avoir présenté les suspensions semi-actives, les technologies et commandes associées, nous présentons une des contributions de ce travail de thèse: une nouvelle méthodologie de contrôle de suspension semi-active.

1.4.1 Problématiques

Les suspensions semi-actives, dans le domaine automobile (mais aussi civil), sont de plus en plus utilisées et étudiées. Elles présentent le principal intérêt:

- par rapport à des suspensions passives, de pouvoir être contrôlées, et ainsi, dissiper l'énergie du système à des vitesses variées (gain en performances)

- par rapport à des suspensions actives, d'être bien plus légères, moins chères et plus rapides (gain économique)

Une manière très largement utilisée pour caractériser le type de suspension (passive, semi-active ou active) est illustrée sur la Figure 1.2

[3] Projet International de Coopération Scientifique
[4] Agence Nationale de la Recherche
[5] http://www.gipsa-lab.inpg.fr/index.php?id=663

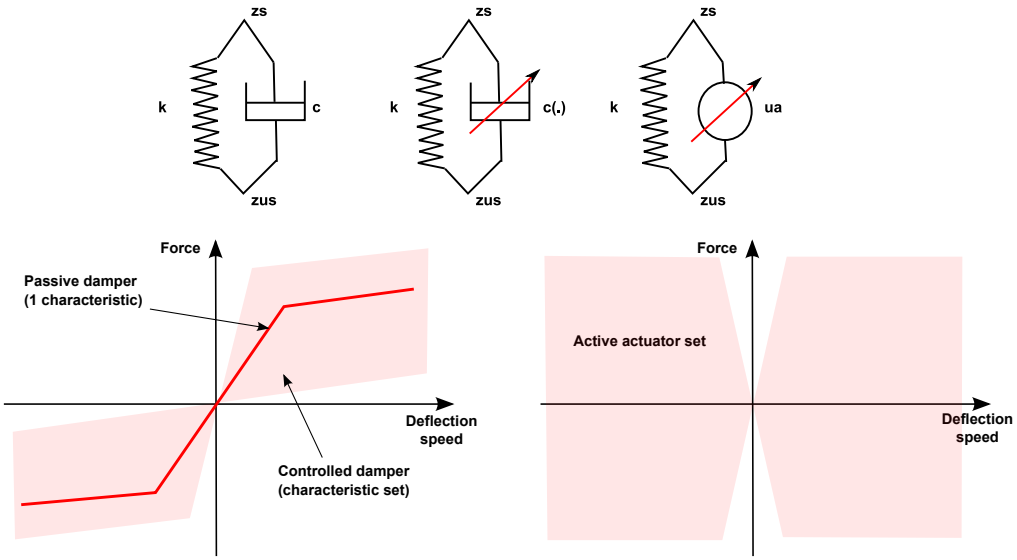

Figure 1.2: En haut: les différents types de suspensions (de gauche à droite): passive, semi-active et active. En bas: le représentation Force / Vitesse de débattement caractérisant le type de suspensions.

Le principal problème lié aux actionneurs semi-actifs est qu'ils sont limités à ne pouvoir que dissiper de l'énergie (voir en bas à gauche de la Figure 1.2). Cette limitation rend difficile leur pilotage en utilisant les outils usuels de la commande linéaire.

Comme précédemment indiqué, les suspensions semi-actives (ou contrôlées) sont de plus en plus étudiées, que ce soit dans le milieu industriel ou académique. Ainsi, différentes technologies et méthodes sont apparues ces dernières années, afin de piloter le comportement vertical du véhicule. Ci-après, nous dressons un rapide panorama des technologies et méthodes de commande développées.

1.4.1.1 Technologies: Amortisseurs pilotés

Différentes technologies de suspensions semi-actives ont été développées ces dernières années. Parmis ces technologies, nous pouvons souligner les suivantes (voir Figure 1.3 et Spelta (2008)):

- **Amortisseurs Magnéto-Rhéologiques** (MR damper), qui sont actuellement les plus étudiés car ils présentent d'intéressantes propriétés dynamiques et sont peu onéreux. Récemment, ce type d'amortisseur a équipé les nouvelles Audi TT. Le principe de fonctionnement consiste à modifier, à l'aide d'un flux magnétique, la visquosité du fluide à l'intérieur du cylindre (i.e. son amortissement). De plus en plus de fournisseurs automobiles proposent aujourd'hui ce type de système (voir e.g. Sachs, 2008; Delphi, 2008; Lord, 2008). Des études de modélisation sont également menées (voir e.g. Ahmadian and Song, 1999; Koo *et al.*, 2004; Savaresi *et al.*, 2005*b*).

- **Amortisseurs Electro-Hydrauliques** (ER damper), qui sont également très largement utilisés pour les applications auto et moto. L'intérêt principal est qu'ils présentent un fonctionnement linéaire, ce qui est très appréciable pour le contrôle. Certaines voitures Volvo et motos BMW utilisent aujourd'hui ce type de système piloté. Les amortisseurs électro-hydrauliques utilisent différentes propriétés mécaniques: le flux peut par exemple être modifié de manière continue en changeant les sections de passage.

- **Systèmes d'amortisseurs à air**, qui est une technologie récente, consistant à modifier la raideur de l'amortisseur en utilisant une pompe à pression. L'amortissement est réglé en modifiant la résistance du gaz. Bien qu'intéressante, cette technologie est difficile à modéliser et a contrôler précisément.
- **Amortisseur Electro-Mécanique** (brevet SOBEN), où le coefficient d'amortissement est modifié au travers de vis, modifiant les sections de passage du fluide présent dans l'amortisseur. Un des aspects intéressants de cette solution technologique est que la compression et la détente du système peuvent être réglées de manière indépendante (voir Aubouet *et al.*, 2008).

Figure 1.3: De gauche à droite: MR damper, ER damper et Air damper.

1.4.1.2 Méthodes de commande

Parallèlement aux développements technologiques, de nombreuses approches pour le contrôle de suspensions semi-actives ont été développées. Ces approches sont détaillées dans le Chapitre 2. On peut toutefois retenir les suivantes:

- LQ, Skyhook, $\mathcal{H}_\infty$, etc. **clipped** (voir Falcone *et al.*, 2007*a*; Sammier *et al.*, 2003): qui consistent à réaliser une commande active avec une méthodologie issue des méthodes linéaires ou non linéaires (sans tenir compte de la contrainte de dissipativité) puis de la rendre semi-active en saturant le signal de commande. Le principal défaut de cette approche est que les performances et la stabilité ne sont vérifiées qu'a posteriori.
- Les approches **Model Predictive** (voir Canale *et al.*, 2006; Giorgetti *et al.*, 2006; Giua *et al.*, 2004) qui fournissent un cadre de travail simple à utiliser mais qui ont pour principal inconvénient d'introduire une optimisation en ligne (coûteuse en temps de calcul et en mémoire), de nécessiter la mesure de l'état entier du système et de ne fournir aucune garantie de robustesse.
- Les méthodes **ADD** (Acceleration Driven Damper) ou **Mixed SH-ADD** (Skyhook-ADD mixte) (voir Savaresi *et al.*, 2005*a*; Savaresi and Spelta, 2007) qui ont la particularité d'être structurellement simple. Ces stratégies sont orientées confort, au détriment des performances de tenue de route.

1.4.2 Principe de la solution

D'une manière générale, toutes les méthodes proposées ci-dessus tendent vers une amélioration du confort et utilisent des méthodes de contrôle de type non linéaire. La solution proposée ci-après

est basée sur l'approche robuste des systèmes Linéaires à Paramètres Variants (LPV). Pour réaliser une commande garantissant la contrainte dissipative de l'actionneur (amortisseur piloté), un modèle statique des limitations de l'actionneur est utilisé (voir Figure 1.4).

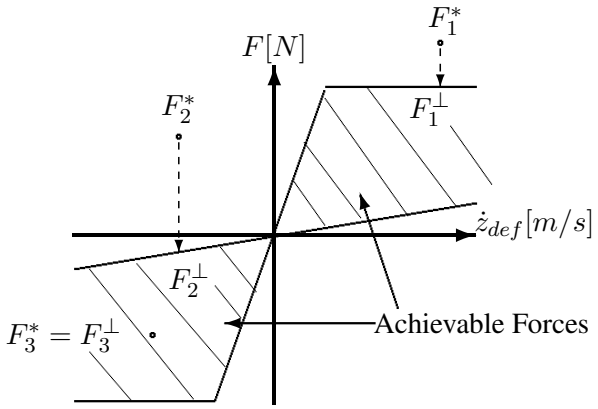

Figure 1.4: Modèle statique de l'amortisseur piloté: domaine atteignable $D(\dot{z}_{def})$.

Ensuite, l'idée est de synthétiser un contrôleur LPV, séquencé par un paramètre ρ représentant l'appartenance ou non de la commande fournie (u) au domaine de force acceptable par l'actionneur considéré (voir la zone hachurée de la Figure 1.4).

Le schéma de contrôle généralisé est donné en Figure 1.5. L'idée consiste à définir des fonctions de pondération pour spécifier les performances désirées (W_{z_s} et $W_{z_{def}}$) et une fonction de pondération $W_u(\rho)$ sur le signal de commande, linéairement dépendante du paramètre ρ.

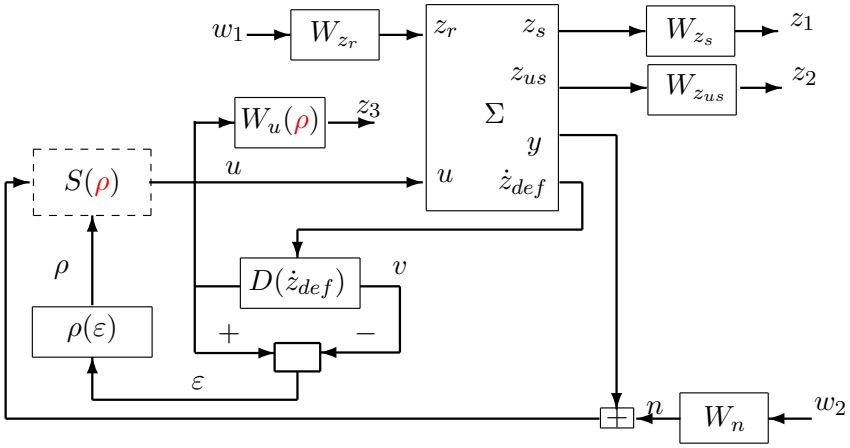

Figure 1.5: Système généralisé & Loi de séquencement.

Ce type de système généralisé est alors défini comme suit:

$$\begin{bmatrix} \dot{x} \\ z_\infty \\ y \end{bmatrix} = \begin{bmatrix} A(\rho) & B_\infty(\rho) & B \\ C_\infty(\rho) & D_{\infty w}(\rho) & D_{\infty u} \\ C & 0 & 0 \end{bmatrix} \begin{bmatrix} x \\ w_\infty \\ u \end{bmatrix} \tag{1.1}$$

avec,

$$\left\{\begin{array}{rcl} x & = & \left[\begin{array}{cc} x_s & x_w \end{array}\right]^T \\ z_\infty & = & \left[\begin{array}{ccc} W_{z_s} z_s, & W_{z_{us}} z_{us}, & W_u(\rho) u \end{array}\right]^T \\ w_\infty & = & \left[\begin{array}{cc} W_{z_r}^{-1} z_r, & W_n^{-1} n \end{array}\right]^T \\ y & = & z_{def} \\ \rho & \in & \left[\begin{array}{cc} \underline{\rho} & \overline{\rho} \end{array}\right] \end{array}\right. \tag{1.2}$$

où z_∞ et w_∞ sont respectivement les sorties à contrôler et entrées exogènes du système. La sortie de mesure est définie par y. Les fonctions de pondération sont définies comme suit,

$$\left\{\begin{array}{rcl} W_{z_s} & = & \frac{\frac{s}{\omega_{11}}+1}{\frac{s}{\omega_{12}}+1} \\ W_{z_{def}} & = & \frac{1}{\frac{s}{\omega_{21}}+1} \\ W_{z_r} & = & 7.10^{-2} \\ W_n & = & 10^{-4} \\ W_u(\rho) & = & \rho \frac{1}{\frac{s}{1000}+1} \\ \rho & \in & \left[\begin{array}{cc} 0.01 & 10 \end{array}\right] \end{array}\right. \tag{1.3}$$

avec x_s et x_w les états du système et des filtres de pondération. Ensuite, les performances sont données par $\omega_{11} = 1rd/s$, $\omega_{12} = \sqrt{\frac{k_t}{m_{us}}} rd/s$ et $\omega_{21} = \sqrt{\frac{k_t}{m_s+m_{us}}} rd/s$. Sur la Figure (1.6), les pondérations de $1/W_{z_s}$, $1/W_{z_{def}}$ et $1/W_u(\rho)$ sont illustrées.

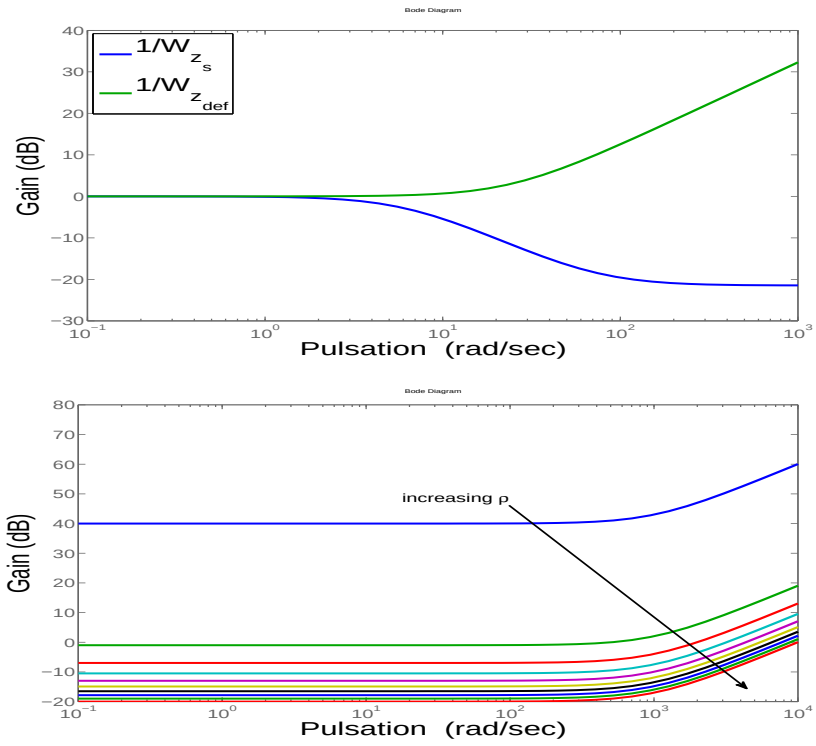

Figure 1.6: Fonctions de pondération pour la synthèse LPV $\mathcal{H}_\infty$.

Ainsi, lorsque ρ est faible, la pondération sur la commande $W_u(\rho)$ est faible, laissant agir la commande. De manière équivalente, lorsque ρ est grand, le signal de commande est attenué de manière très forte, et n'agit presque plus.

La synthèse du contrôleur LPV par approche polytopique permet d'obtenir les contrôleurs dynamiques $S(\underline{\rho})$ et $S(\overline{\rho})$ garantissant la stabilité et des performances au sens $\mathcal{H}_\infty$ pour l'ensemble des variations du paramètre ρ. Les informations sur la résolution ce problème avec l'approche polytopique sont données au Chapitre 3. La loi de commande ainsi obtenue s'écrit de la façon suivante (1.4):

$$\begin{aligned} u &= c_0.\dot{z}_{def} + u^{\mathcal{H}_\infty} \\ u^{\mathcal{H}_\infty} &= \Big[\frac{|\rho-\overline{\rho}|}{\overline{\rho}-\underline{\rho}}S(\underline{\rho}) + \frac{|\rho-\underline{\rho}|}{\overline{\rho}-\underline{\rho}}S(\overline{\rho})\Big]y \end{aligned} \tag{1.4}$$

où c_0 est le coefficient d'amortissement nominal de la suspension considérée. La loi de commande est donc paramétrée par $\rho \in [\underline{\rho};\overline{\rho}]$, qui varie en fonction d'une loi de séquencement définie par la fonction suivante:

$$\rho(\varepsilon) = 10\frac{\mu\varepsilon^4}{\mu\varepsilon^4 + 1/\mu} \tag{1.5}$$

où $\varepsilon = u - v$ représente la différence entre la force souhaitée et la force atteignable. μ est un paramètre permettant de régler cette loi de séquencement (pour plus de détails, voir Chapitre 6.

1.4.3 Validations et comparaison des résultats

De façon à valider l'approche proposée, la loi de commande synthétisée est appliquée sur le système quart de véhicule non linéaire. Le schéma est fourni en Figure 1.7.

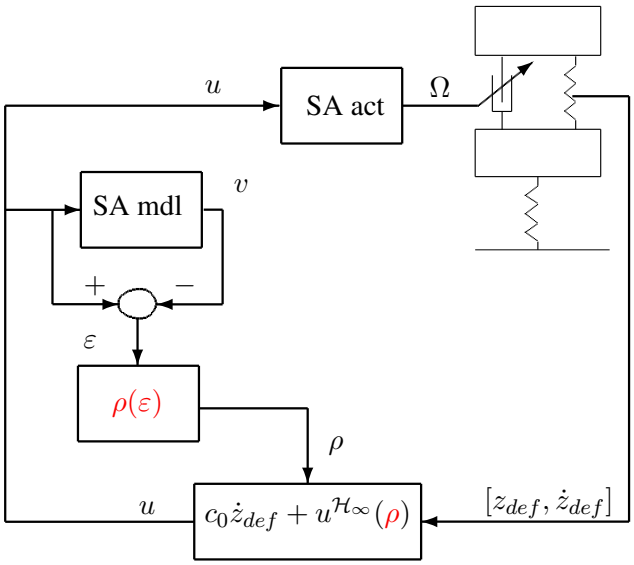

Figure 1.7: Schéma d'implementation.

L'approche proposée (appelée "LPV $\mathcal{H}_\infty$") est ici comparée à quelques approches intéressantes trouvées dans la littérature. Ainsi nous la comparons avec:

- Un contrôleur actif (sans limitation structurelle de dissipativité), appelé "Active $\mathcal{H}_\infty$ " synthétisé avec les mêmes fonctions de pondération que celles présentées ci-dessus et $\rho = \underline{\rho}$.

- Un contrôleur "Clipped $\mathcal{H}_\infty$ ", qui est le même que le contrôleur "Active $\mathcal{H}_\infty$ " mais saturé par $D(\dot{z}_{def})$, pour rendre la commande semi-active.

- La commande "mixed SH-ADD" proposée par Savaresi *et al.* (2005*a*):

$$u = c_{in}.\dot{z}_{def} \tag{1.6}$$

où c_{in} est défini par:

$$c_{in} = \begin{cases} c_{min} & \text{si } \left[(\ddot{z}_s^2 - \alpha^2 \dot{z}_s^2) \leq 0 \;\&\; \dot{z}_s \dot{z}_{def} > 0\right] \text{ OU } \left[(\ddot{z}_s^2 - \alpha^2 \dot{z}_s^2) > 0 \;\&\; \dot{z}_s \dot{z}_{def} > 0\right] \\ c_{max} & \text{si } \left[(\ddot{z}_s^2 - \alpha^2 \dot{z}_s^2) \leq 0 \;\&\; \dot{z}_s \dot{z}_{def} \leq 0\right] \text{ OU } \left[(\ddot{z}_s^2 - \alpha^2 \dot{z}_s^2) > 0 \;\&\; \dot{z}_s \dot{z}_{def} \leq 0\right] \end{cases} \tag{1.7}$$

avec $\alpha = 2\pi\sqrt{\frac{kt}{mus}}$, la fréquence de coupure de la commande, comme suggéré dans (Spelta, 2008).

- La commande "ADD" définie par:

$$u = c_{in}.\dot{z}_{def} \tag{1.8}$$

où c_{in} est définie par:

$$c_{in} = \begin{cases} c_{min} & \text{si } \ddot{z}_s \dot{z}_{def} \leq 0 \\ c_{max} & \text{si } \ddot{z}_s \dot{z}_{def} > 0 \end{cases} \tag{1.9}$$

- La suspension passive de la Renault Mégane Coupé. Cette suspension dénotée "Passive" est notre modèle de référence.

1.4.3.1 Résultats temporels

Dans un premier temps, pour valider l'approche et vérifier le fait que le contrôleur fournit bien une force atteignable pour l'actionneur semi-actif, une simulation classique de discontinuité de la route est réalisée. La Figure 1.8 montre la représentation Force / Vitesse de débattement ainsi que le paramètre de séquencement ρ.

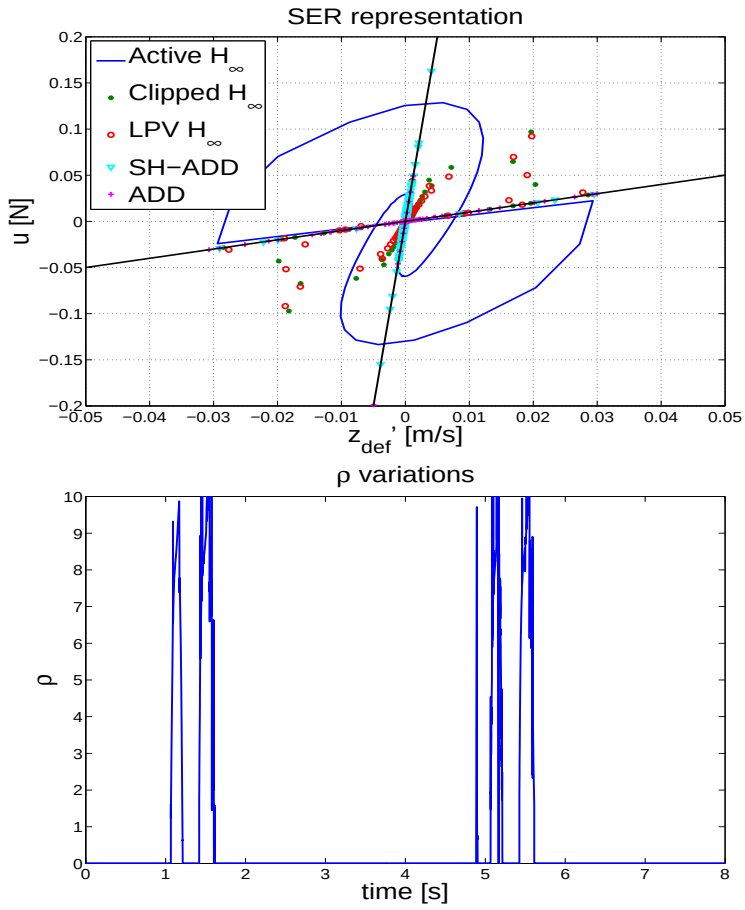

Figure 1.8: Diagramme Force / Vitesse de débattement en réponse à une perturbation de la route (haut). Variations de ρ (bas).

Il est important de noter que les forces fournies par le contrôleur respectent les contraintes de semi-activité. Ainsi, la structure proposée atteint bien le premier objectif fixé, à savoir fournir une commande dissipative. Par rapport aux autres approches (notamment ADD et Mixed SH-ADD) la commande proposée fournit des valeurs d'amortissements intermédiaires (alors que ADD et SH-ADD, commutent entre la valeur minimale et maximale d'amortissement, sans jamais prendre de valeurs intermédiaires). Le contrôleur actif, lui, entre dans tous les quadrants.

1.4.3.2 Résultats fréquentiels & Evaluation des performances

Cependant, l'étude temporelle ne permet pas de conclure sur l'efficacité de l'algorithme de contrôle. C'est pourquoi, pour l'analyse des performances des suspensions, nous réalisons une étude fréquentielle, couplée d'une analyse de densité spectrale sur des signaux particuliers. L'idée consiste à réaliser un pseudo-Bode du système bouclé (sur le modèle complet non-linéaire). Pour ce faire, un signal sinusoïdal (à différentes fréquences) est envoyé, et l'amplitude en sortie mesurée au bout de 10 périodes (afin d'atteindre un régime permanent). La Figure 1.9 fournit les résultats de ces pseudo-Bode pour les différentes stratégies de commande. Le choix de ces échelles de fréquences est justifié par des critères de performances mesurés (voir Poussot-Vassal *et al.*, 2009).

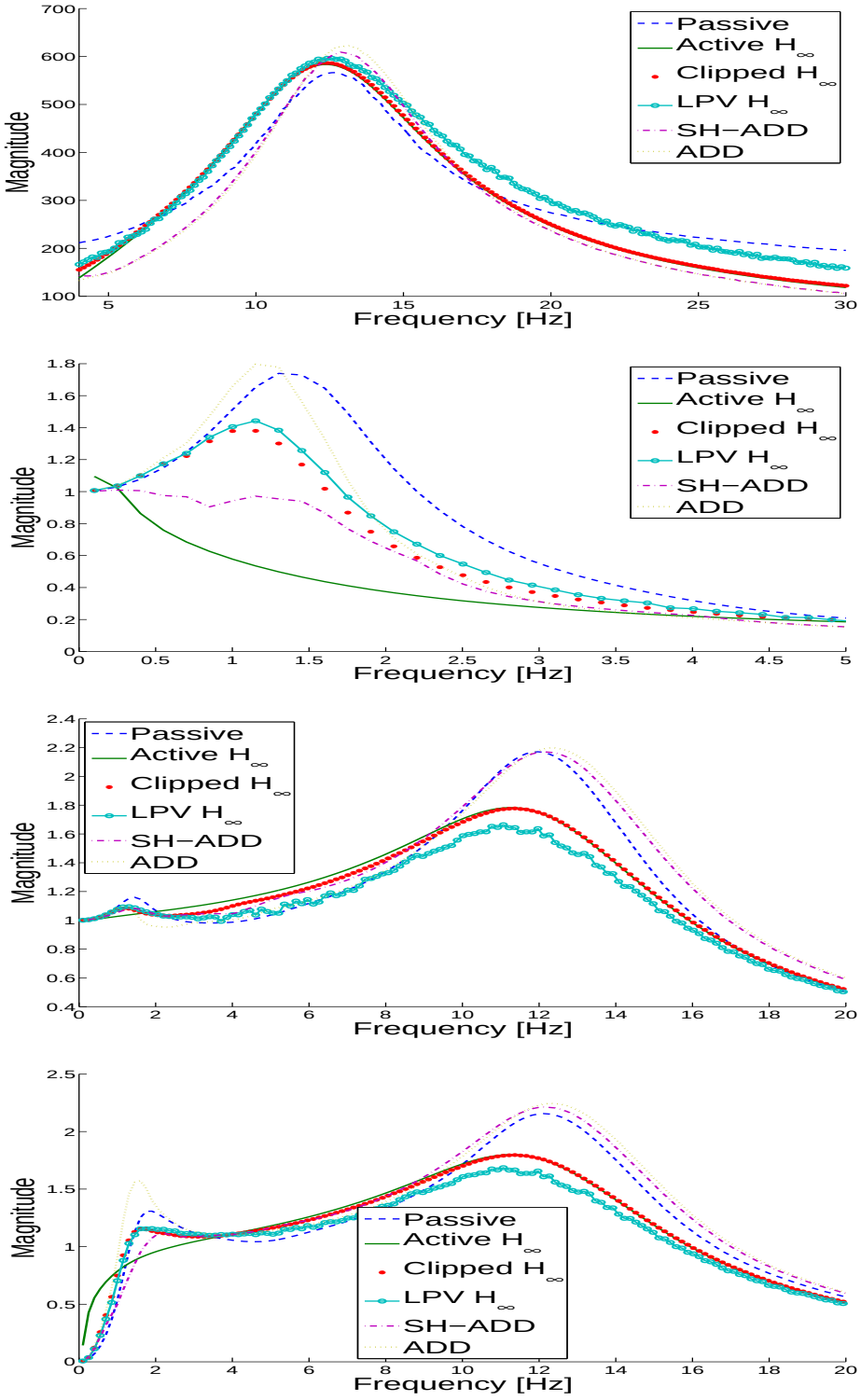

Figure 1.9: Réponses fréquentielles pour les différentes commandes semi-actives de $\ddot{z}_s/z_r$, z_s/z_r, z_{us}/z_r et z_{def}/z_r.

A partir des réponses fréquentielles fournies en Figure 1.9, nous calculons la densité spectrale de puissance des chacun de ces signaux par la formule suivante:

$$PSD_{f_1 \to f_2}(x) = \sqrt{\int_{f_1}^{f_2} x^2(f) df} \tag{1.10}$$

où f_1 et f_2 sont les bornes fréquentielles et x le signal étudié. Puis le gain est évalué par la fonction suivante:

$$\frac{\text{Passive PSD} - \text{Controlled PSD}}{\text{Passive PSD}} \tag{1.11}$$

Le tableau suivant résume les gains réalisé pour chaque approche:

Signal	Active $\mathcal{H}_\infty$	Clipped $\mathcal{H}_\infty$	LPV/$\mathcal{H}_\infty$	ADD	SH-ADD
$\ddot{z}_s/z_r$ $[4;30]$Hz	4.8%	3.8%	-4.4%	10%	10.8%
z_s/z_r $[0;5]$Hz	52.8%	23.5%	18.9%	16.9%	36.2%
z_{us}/z_r $[0;20]$Hz	3.2%	4.2%	9.9%	-4.9%	-5.8%
z_{def}/z_r $[0;20]$Hz	5.3%	5.7%	10.4%	-7.8%	-4.5%

Il est intéressant de noter que, bien que la solution Clipped semble la plus performante, aucune garantie de performance ni de stabilité ne peut être faite. Les approches ADD et mixed SH-ADD réalisent une amélioration notable des performances de confort mais dégradent la tenue de route. La solution proposée semble fournir a de bonnes performances en confort, mais également en tenue de route, ce qui en fait une solution intéressante.

1.4.4 Conclusions

De cette analyse, nous pouvons dresser les conclusions suivantes. La solution LPV $\mathcal{H}_\infty$ a les propriétés suivantes:

1. **Performances flexibles**: possibilité d'appliquer des critères $\mathcal{H}_\infty$, $\mathcal{H}_2$, placement de pôle, Multi-critère, etc (ici, nous ne présentons qu'un seul réglage mais d'autres peuvent être envisagés).
2. **Mesure**: seul le débattement et sa dérivée sont nécessaires pour réaliser ce contrôle (nul besoin de l'état).
3. **Calcul**: la synthèse mène à deux correcteurs LTI et une loi de séquencement, ce qui en fait une loi de commande simple à mettre en oeuvre (pas d'optimisation en ligne).
4. La **stabilité interne** est préservée (ce qui n'est pas le cas des approches Clipped).
5. **Mise en oeuvre**: cette approche est adaptable à n'importe quel type d'actionneurs.

1.5 Contrôle MIMO de la dynamique globale du véhicule

1.5.1 Motivations et problématiques associées

Sur les véhicules, la plupart des problèmes de contrôle commande sont résolus de manière locale et dissociée. La communication entre les différents organes de commande (capteurs, contrôleurs et

actionneurs) se fait a posteriori grâce aux connaissances des ingénieurs véhicule et au prix de coûteux temps de réglage. De plus, ce type d'approche ne permet pas d'utiliser de manière optimale les actionneurs disponibles et peut mener à des choix non appropriés dans le cas où le véhicule se trouve en situation critique.

Ainsi, la nouvelle tendance dans le secteur de l'analyse et du contrôle de la dynamique véhicule (que ce soit pour les véhicules de tourisme ou les camions), est de synthétiser des contrôleurs multi-variables, capables à la fois d'améliorer le confort et de garantir la sécurité des passagers en fonction de la situation dans laquelle le véhicule se trouve (normale, dangereuse ou critique), en utilisant tous les actionneurs disponibles et en les faisant collaborer dans toutes les situations. Quelques résultats fort intéressants, utilisant plusieurs actionneurs, ont été récemment proposés (voir e.g Andreasson and Bunte, 2006; Chou and d'Andréa Novel, 2005; Sampson and Cebon, 2003; Gáspár *et al.*, 2005; Falcone *et al.*, 2007*b*; Falcone *et al.*, 2007*c*). Les défis qui regroupent à la fois les secteurs industriels et académiques poussent à une investigation de plus en plus poussée dans ce sens (Shibahata, 2005).

Dans des travaux antérieurs de l'équipe (voir Gáspár *et al.*, 2007), nous avons présenté une solution utilisant les suspensions et le système de freinage différentiel pour améliorer le confort en situation de conduite normale et atténuer les accélérations latérales en cas de danger imminent, en supervisant le transfert de charge latéral.

Dans l'approche présentée, nous proposons un Contrôle Global de Châssis (CGC) qui utilise des actionneurs électromécaniques de freinage (EMB) et de direction active (AS) pour améliorer les propriétés de sécurité du véhicule dans les situations dangereuses et critiques. Afin d'obtenir un contrôleur dépendant de la situation dans laquelle le véhicule se trouve, la méthodologie robuste ($\mathcal{H}_\infty$) Linéaire à Paramètres Variants (LPV) est utilisée. De plus, afin de garantir un bon freinage (c.à.d. d'éviter le blocage des roues), un système d'anti-blocage des roues (ABS) récemment développé par Tanelli *et al.* (2007*a*), qui présente d'intéressantes propriétés de robustesse vis-à-vis des mesures et des actionneurs, est intégré dans la stratégie proposée. L'intérêt du CGC proposé réside dans le fait qu'il est plus qu'un simple contrôleur dans la mesure où il centralise les mesures et hiérarchise le contrôle global du véhicule et l'intervention des différents actionneurs: lorsqu'une situation dangereuse est détectée, le CGC fournit un couple de référence au système de freinage (qui, grâce au système d'ABS, permet d'éviter le glissement), et, si ce dernier n'est pas à même de garantir la sécurité en restabilisant le véhicule, le système de direction est activé pour aider, voire suppléer le freinage (e.g. en cas de faible adhérence de la route ou de défaillance du système de freinage). Comme la solution proposée ne nécessite pas de processus d'optimisation en-ligne, la structure du CGC proposé montre d'intéressantes propriétés d'implémentation sur tout type de véhicule, notamment ceux dotés d'un ABS (car fonctionne comme un "super" correcteur).

Dans les sous-sections suivantes, nous présentons tout d'abord la problématique, la description du modèle complet non linéaire du véhicule considéré ainsi que des actionneurs utilisés. Ensuite, la synthèse LPV/$\mathcal{H}_\infty$ appliquée à la structure CGC que nous proposons est décrite. De plus nous rappelons brièvement le contrôleur local d'ABS proposé dans (Tanelli, 2007). Afin de mettre en avant les avantages de la stratégie proposée, des simulations sur le modèle complet non linéaire sont réalisées, suivies d'une conclusion avec une discussion des résultats.

1.5.2 Notations et paramètres véhicule

Les notations suivantes sont employées: les indices $i = \{f, r\}$ et $j = \{l, r\}$ sont utilisés pour identifier respectivement les positions avant/arrière et gauche/droite du véhicule. Les indices $\{s, t\}$ identifient les forces provenant de la suspension ou du pneumatique. Les notations $\{x, y, z\}$ représentent les forces et dynamiques longitudinales, latérales et verticales. On notera ensuite la vitesse du

véhicule par $v = \sqrt{v_x^2 + v_y^2}$, le rayon effectif de chaque pneu par $R_{ij} = R - (z_{us_{ij}} - z_{r_{ij}})$, la masse totale du véhicule $m = m_s + m_{us_{fl}} + m_{us_{fr}} + m_{us_{rl}} + m_{us_{rr}}$, l'angle volant par $\delta = \delta_d + \delta^+$ (δ_d, étant l'angle fournit par le conducteur et δ^+, l'angle ajouté par le contrôleur) et $T_{b_{ij}}$ désigne le couple appliqué sur chaque roue, fournit par le contrôleur. Les paramètres utilisés, identifiés sur une Renault Mégane Coupé, véhicule initialement orienté sport, sont donnés en Annexe D.4 (voir aussi Zin, 2005).

1.5.3 Modèle du véhicule

1.5.3.1 Modèle Dynamique

Nous utilisons le modèle non linéaire complet du véhicle. Il permet de prendre en considération les dynamiques verticale (z_s), longitudinale (x), latérale (y), de roulis (θ), de tangage (ϕ) et de lacet (ψ) du châssis. Ce modèle restitue également les dynamiques verticales et de rotation des roues ($z_{us_{ij}}$ et ω_{ij}). Le modèle dynamique est défini par les équations données en (1.12), où $F_{tx_i} = F_{tx_{il}} + F_{tx_{ir}}$, $F_{ty_i} = F_{ty_{il}} + F_{ty_{ir}}$, $F_{tz_i} = F_{tz_{il}} + F_{tz_{ir}}$ and $F_{sz_i} = F_{sz_{il}} + F_{sz_{ir}}$, ($i = \{f, r\}$). Ces forces sont définies dans la suite.

$$
\left\{
\begin{array}{rcl}
\ddot{x}_s &=& \dot{x}_s + \dot{y}_s\dot{\psi} \\
&=& \big(-(F_{tx_{fr}} + F_{tx_{fl}})\cos(\delta) - (F_{tx_{rr}} + F_{tx_{rl}}) - (F_{ty_{fr}} + F_{ty_{fl}})\sin(\delta) - m\dot{\psi}\dot{y}_s \\
&& +F_{dx}\big)/m \\
\ddot{y}_s &=& \big(-(F_{tx_{fr}} + F_{tx_{fl}})\sin(\delta) + (F_{ty_{rr}} + F_{ty_{rl}}) + (F_{ty_{fr}} + F_{ty_{fl}})\cos(\delta) + m\dot{\psi}\dot{x}_s \\
&& +F_{dy}\big)/m \\
\ddot{z}_s &=& -\big(F_{sz_{fl}} + F_{sz_{fr}} + F_{sz_{rl}} + F_{sz_{rr}} + F_{dz}\big)/m_s \\
\ddot{z}_{us_{ij}} &=& \big(F_{sz_{ij}} - F_{tz_{ij}}\big)/m_{us_{ij}} \\
\ddot{\theta} &=& \big((F_{sz_{rl}} - F_{sz_{rr}})t_r + (F_{sz_{fl}} - F_{sz_{fr}})t_f + mh\ddot{y}_s + (I_y - I_z)\dot{\psi}\dot{\phi} + M_{dx}\big)/I_x \\
\ddot{\phi} &=& \big((F_{sz_{rr}} + F_{sz_{rl}})l_r - (F_{sz_{fr}} + F_{sz_{fl}})l_f - mh\ddot{x}_s + (I_z - I_x)\dot{\psi}\dot{\theta} + M_{dy}\big)/I_y \\
\ddot{\psi} &=& \big((F_{ty_{fr}} + F_{ty_{fl}})l_f\cos(\delta) - (F_{ty_{rr}} + F_{ty_{rl}})l_r - (F_{tx_{fr}} + F_{tx_{fl}})l_f\sin(\delta) \\
&& -(F_{tx_{rr}} - F_{tx_{rl}})t_r \\
&& +(F_{tx_{fr}} - F_{tx_{fl}})t_f\cos(\delta) - (F_{tx_{fr}} - F_{tx_{fl}})t_f\sin(\delta) \\
&& +(I_x - I_y)\dot{\theta}\dot{\phi} + M_{dz}\big)/I_z \\
\dot{\omega}_{ij} &=& (R_{ij}F_{tx_{ij}} - T_{b_{ij}})/I_w \\
\dot{\beta} &=& (F_{ty_f} + F_{ty_r})/(mv) + \dot{\psi}
\end{array}
\right. \tag{1.12}
$$

Ce modèle sera utilisé pour la validation de la méthode de commande. Il est à noter que le principal intérêt de travailler avec un modèle complet est qu'il permet de prendre en compte les transferts de charges non linéaires, qui influent les forces des pneumatiques, donc la dynamique globale du véhicule. Ces phénomènes sont d'autant plus importants que nous nous intéressons aux situations dangereuses (voir e.g. Shen and Yu, 2006).

1.5.3.2 Modèle des suspensions

Les suspensions sont souvent modélisées de la façon la plus simple, c.à.d. par un ressort et un amortisseur. En réalité, ces coefficients sont non linéaires et comportent des effets d'hystérésis (e.g. Zin *et al.*, 2008*b*; Poussot-Vassal *et al.*, 2007; Sammier *et al.*, 2003). Ici, comme nous nous attachons plus particulièrement aux comportements longitudinaux et latéraux, les coefficients de raideur et d'amortissement sont choisis linéaires. Ainsi, le modèle de suspension adopté est le suivant:

$$F_{sz_{ij}} = k_{ij}(z_{s_{ij}} - z_{us_{ij}}) + c_{ij}(\dot{z}_{s_{ij}} - \dot{z}_{us_{ij}}) \tag{1.13}$$

1.5.3.3 Modèle de pneumatique

Le contact pneu/chaussée est un domaine très actif où les travaux de recherche sont nombreux et variés (modélisation, identification...). Les modèles très largement adoptés sont complexes et fonction de nombreux paramètres (e.g. Botero *et al.*, 2007; Denny, 2005; Kiencke and Nielsen, 2000; Mammar and Koenig, 2002; Velenis *et al.*, 2005). A partir des résultats fournis dans Kiencke and Nielsen (2000) et Mammar and Koenig (2002), nous proposons le modèle de pneu suivant.

Modèle longitudinal: Le modèle longitudinal utilisé est celui de Burkhardt décrit par (1.14) (voir aussi Milliken and Milliken, 1995),

$$F_{tx_{ij}} = \big(\mu_1(1 - e^{-\lambda_{ij}\mu_2}) - \lambda_{ij}\mu_3\big)F_{n_{ij}} \tag{1.14}$$

où $\mu = [\mu_1, \mu_2, \mu_3]$ permet de définir la forme de la caractéristique de la force longitudinale de contact pneu/chaussée (voir Figure 1.10). $F_{n_{ij}} = g(m_{us_{ij}} + m_s/4) - (F_{tz_{ij}} + F_{sz_{ij}})$ définit la force normale s'appliquant sur chaque pneu.

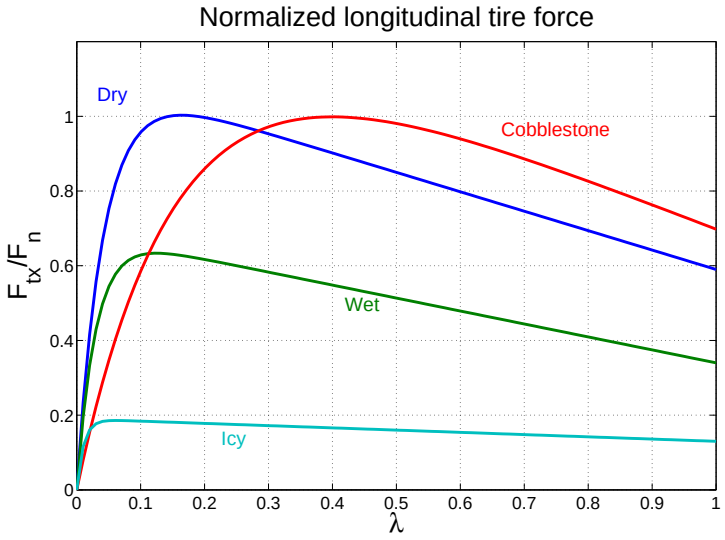

Figure 1.10: Force de contact normalisée $F_{tx_{ij}}/F_{n_{ij}}$ pour différents types de routes en fonction du coefficient de glissement longitudinal λ. $\mu_{sec} = [1.11, 23.99, 0.52]$, $\mu_{humide} = [0.687, 33.822, 0.347]$, $\mu_{pav} = [1.37, 6.46, 0.67]$, $\mu_{glace} = [0.19, 94.13, 0.06]$

Modèle latéral: La force latérale est définie par (1.15) et illustrée sur la Figure 1.11,

$$F_{ty_{ij}} = De^{-6|\lambda_{ij}|^5} \sin\big(C \arctan(B(1-E)\beta_{ij} + E\arctan(B\beta_{ij}))\big) \tag{1.15}$$

où, $\beta_{fj} = \beta_f = -\beta_{cog} - l_f\frac{\dot{\psi}}{v_x} + \delta$ et $\beta_{rj} = \beta_r = -\beta_{cog} + l_r\frac{\dot{\psi}}{v_x}$ sont les angles de glissements avant et arrière. De la même façon que pour le modèle longitudinal $B = (2-\mu)b_t$, $C = (5/4 - \mu/4)c_t$, $D = d_t\mu$ et $E = e_t$ représentent les paramètres qui caractérisent la forme de la force en fonction du coefficient d'adhérence $\mu \in [0; 1]$. De plus, le terme $e^{-6|\lambda_{ij}|^5}$ est ajouté au modèle conventionel pour modéliser le fait que les forces latérales diminuent quand les roues sont bloquées (e.g. quand le véhicule glisse, il n'est plus manœuvrable) ainsi, $\lim_{\lambda_{ij}\to|1|} F_{ty_{ij}} = 0$ (voir Figure 1.11).

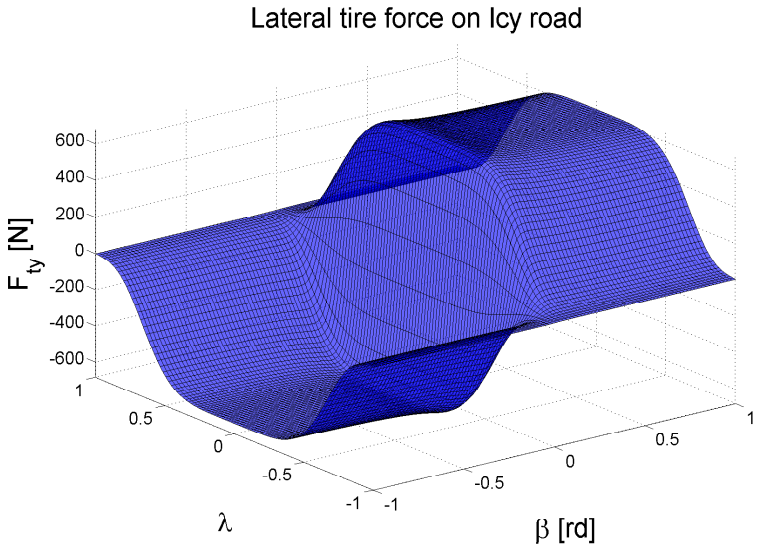

Figure 1.11: Force latérale de contact $F_{ty_{ij}}$ pour une route glacée ($\mu = 0.2$), en fonction de β, l'angle de glissement et de λ, le coefficient de glissement.

Modèle vertical: Finalement, les forces verticales sont décrites comme suit (1.16),

$$F_{tz_{ij}} = k_{t_{ij}}(z_{us_{ij}} - z_{r_{ij}}) + c_{t_{ij}}(\dot{z}_{us_{ij}} - \dot{z}_{r_{ij}}) \tag{1.16}$$

où $k_{t_{ij}}$ et $c_{t_{ij}}$ sont respectivement les raideur et amortissement verticaux du pneu.

1.5.3.4 Dynamique des actionneurs

Dans ce travail, nous considérons les actionneurs de freinage (EMB) et de direction (AS). Ces derniers sont modélisés par de simples filtres du premier ordre comme suit:

- L'actioneur EMB, fournit un couple de freinage, modélisé par,

$$\dot{T}_{b_{rj}} = \varpi(T^0_{b_{rj}} - T_{b_{rj}}) \tag{1.17}$$

  où, $\varpi = 70rd/s$ est la fréquence de coupure de l'actionneur, $T^0_{b_{ij}}$ et $T_{b_{ij}}$ sont respectivement les sorties du contrôleur et de l'actionneur. Il est à noter que ici, nous n'utilisons que les freins arrière dans la mesure où ils influencent d'avantage le lacet du véhicule que les freins avant.

- L'actionneur AS, qui fournit un angle de direction additif, est modélisé comme suit,

$$\dot{\delta}^+ = \kappa(\delta^0 - \delta^+) \tag{1.18}$$

  où, $\kappa = 10rd/s$ est la fréquence de coupure de l'actionneur, δ^0 et δ^+ sont les sorties angle additif issues du contrôleur et l'angle effectivement délivré par l'actionneur. De plus, cet angle est borné entre $[-5, +5]$ degrés.

1.5.4 Structure et synthèse du CGC LPV utilisant les freins et la direction

Cette partie a pour objectif de présenter le principal résultat de cette étude, à savoir la structure et la méthode de synthèse du contrôleur multivariable LPV de châssis, tolérant aux défauts, utilisant les actionneurs de freinage et de direction.

1.5.4.1 Structure et principe du Contrôle Global de Châssis

L'objectif est d'améliorer la tenue de route et la sécurité en utilisant les actionneurs de freinage arrière, et d'actionner le système de direction active si le freinage n'est pas à même de remplir la tâche demandée pour atteindre les objectifs de performance.

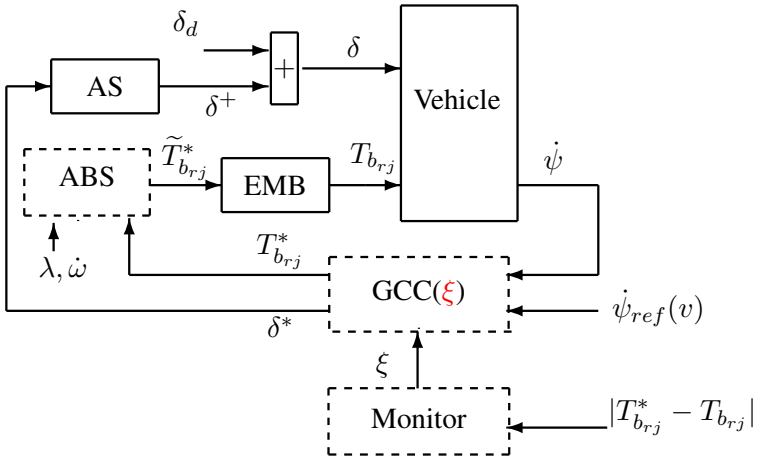

Figure 1.12: Structure globale de contrôle.

La Figure 1.12 présente la structure de contrôle proposée Les blocs sont énumérés puis décrits ci-après:

- **Vehicle & Actionneurs (AS & EMB)**: sont les modèles du véhicule et des actionneurs.
- **GCC(ξ)**: est le contrôleur global de châssis qui fournit le couple de référence ($T^*_{b_{rj}}$) et l'angle additif à fournir (δ^*). Il est séquencé par ξ, le paramètre issu du superviseur et qui modifie la commande.
- **ABS**: est le système d'antiblocage des roues implémenté localement sur chaque roue qui fournit $\widetilde{T}_{b_{rj}}$, le couple de freinage en fonction de la référence ($T^*_{b_{rj}}$) définie par CCG(ξ) (basé sur les résultats de Tanelli *et al.* (2007*a*))
- **Monitor**: est la stratégie de séquencement qui supervise GCC(ξ)

1.5.4.2 Système LPV et synthèse du CGC par approche LPV/$\mathcal{H}_\infty$

L'idée consiste à synthétiser un CGC qui génère un moment stabilisant M^*_{dz} pour atteindre les performances désirées et un angle volant additif δ^+ quand le freinage ne suffit pas.

Remarque 1: Pour convertir le moment stabilisant (M^*_{dz}) en couple de freinage, la transformation suivante est effectuée:

$$\begin{cases} T^*_{b_{rl}} &= \dfrac{RM^*_{dz}}{t_r} \\ T^*_{b_{rr}} &= -\dfrac{RM^*_{dz}}{t_r} \end{cases} \tag{1.19}$$

De plus, l'espace du couple de freinage est défini par $T_{b_{rj}} \in \mathcal{T}_b$ avec $\mathcal{T}_b := \{T_b \in \mathbb{R}\colon 0 \leq T_b \leq T_{b_{max}}\}$.

Par la suite, nous définissons le système généralisé utilisé pour la synthèse, puis la solution LPV/$\mathcal{H}_\infty$ pour la mise en place d'un retour de sortie dynamique est décrite sous forme d'inégalités matricielles linéaires (LMI).

Modèle généralisé LPV (pour la synthèse): Le modèle utilisé pour la synthèse du contrôleur est le modèle bicyclette étendu décrit par l'équation (1.20) et basé sur les équations de (1.12).

$$\begin{aligned} \begin{bmatrix} \dot{v}_y \\ \ddot{\psi} \\ \dot{\beta} \end{bmatrix} &= \begin{bmatrix} 0 & \frac{l_r C_{yr} - l_f C_{yf}}{mv} - v & \frac{C_{yr} - C_{yf}}{m} \\ 0 & -\frac{l_f^2 C_{yf} + l_r^2 C_{yr}}{I_z v} & \frac{l_r C_{yr} - l_f C_{yf}}{I_z} \\ 0 & -1 + \frac{l_r C_{yr} - l_f C_{yf}}{mv^2} & -\frac{C_{yf} + C_{yr}}{mv} \end{bmatrix} \begin{bmatrix} v_y \\ \dot{\psi} \\ \beta \end{bmatrix} + \begin{bmatrix} \frac{C_{yf}}{m} \\ \frac{-l_f C_{yf}}{I_z} \\ \frac{C_{yf}}{mv} \end{bmatrix} \delta^* \\ &+ \begin{bmatrix} 0 \\ \frac{1}{I_z} \\ 0 \end{bmatrix} M^*_{dz} + \begin{bmatrix} \frac{-1}{m} \\ 0 \\ \frac{1}{mv} \end{bmatrix} F_{dy} \end{aligned} \tag{1.20}$$

Ensuite, nous définissons les fonctions de pondérations afin de spécifier les performances souhaitées pour le système bouclé, et obtenir ainsi le système généralisé (voir la Figure 1.13):

- $W_{e_{\dot{\psi}}} = 10\frac{s/500+1}{s/50+1}$ est utilisé pour contraindre l'erreur sur la vitesse de lacet ($e_{\dot{\psi}} = \dot{\psi}_{ref} - \dot{\psi}$)
- $W_{\dot{v}_y} = 10^{-3}$ est utilisé pour atténuer les accélérations latérales
- $W_{M^*_{dz}} = 10^{-5}\frac{s/10\varpi+1}{s/100\varpi+1}$ permet de limiter la commande sur le moment stabilisant
- $W_{\delta^*}(\xi) = \xi\frac{s/\kappa+1}{s/10\kappa+1}$ limite la commande en angle volant en fonction de ξ

On remarquera que la pondération sur la commande de direction ($W_{\delta^*}(\xi)$) est linéairement dépendante du paramètre de séquencement $\xi(.) \in \mathcal{P}_\xi$, où $\mathcal{P}_\xi$ est défini par $\mathcal{P}_\xi := \{\xi \in \mathbb{R}\colon \underline{\xi} \leq \xi \leq \overline{\xi}\}$ ($\underline{\xi} = 0.1$ et $\overline{\xi} = 10$). Lorsque $\xi = \overline{\xi}$, la commande en direction est pénalisée, donc atténuée. Réciproquement, quand $\xi = \underline{\xi}$, elle ne l'est plus, et la commande sur la direction est activée.

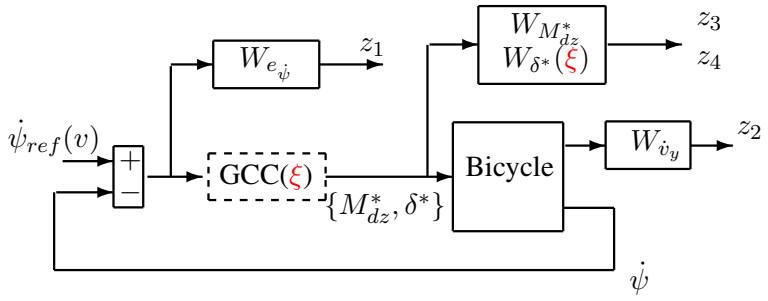

Figure 1.13: Système généralisé pour la synthèse.

Ainsi, le système généralisé peut être décrit par un système LPV

$$\Sigma(\xi): \left[\begin{array}{c} \dot{x} \\ \hline z \\ y \end{array}\right] = \left[\begin{array}{c|cc} A(\xi) & B_1(\xi) & B_2 \\ \hline C_1(\xi) & D_{11}(\xi) & D_{12} \\ C_2 & 0 & 0 \end{array}\right] \left[\begin{array}{c} x \\ \hline w \\ u \end{array}\right] \tag{1.21}$$

où x inclut les variables d'état du système et des pondérations, $w = F_{dy}$ et $u = [\delta^*, M^*_{dz}]$ sont respectivement les entrées exogènes et les commandes du système;

$$z = [z_1, z_2, z_3, z_4] = [W_{e_\psi} e_\psi, W_{\dot{v}_y} \dot{v}_y, W_{M^*_{dz}} M^*_{dz}, W_{\delta^0}(\xi)\delta^0] \tag{1.22}$$

définit les sorties contrôlées, et $y = \dot{\psi}_{ref}(v) - \dot{\psi}$ est la sortie mesurée ($\dot{\psi}_{ref}(v)$ étant fourni par un modèle bicyclette de référence, comme celui donné par l'équation (1.20)).

Finalement, pour la synthèse, le système (1.21) peut être mis sous forme polytopique, i.e. comme une combinaison convexe de chaque système défini à une extrémité du polytope formé par $\mathcal{P}_\xi$, en l'occurrence $\Sigma(\underline{\xi})$ et $\Sigma(\overline{\xi})$.

Solution polytopique du problème LPV/$\mathcal{H}_\infty$: Le problème consiste à trouver un contrôleur stabilisant, séquencé par ξ, de la forme,

$$S(\xi): \left[\begin{array}{c} \dot{x}_c \\ u \end{array}\right] = \left[\begin{array}{cc} A_c(\xi) & B_c(\xi) \\ C_c(\xi) & 0 \end{array}\right] \left[\begin{array}{c} x_c \\ y \end{array}\right] \tag{1.23}$$

qui minimise la norme $\mathcal{H}_\infty$ de la boucle fermée LPV formée par l'interconnexion de (1.21) et (1.23) à chaque extrémité du polytope. Ce problème mène au Lemme Réel Borné (BRL) pour les systèmes LPV. Une solution basée sur la résolution LMI peut être trouvée en appliquant la proposition suivante.

Solution LMI pour la synthèse LPV/$\mathcal{H}_\infty$: D'après la définition du système (1.21), et en utilisant le changement de base proposé dans (Scherer *et al.*, 1997), la LMI (1.24) non conservative peut être exprimée pour résoudre le BRL. Appliqué aux systèmes LPV polytopique, il consiste à résoudre la LMI (1.24) à chaque extrémité du polytope formé par le système, en conservant la même fonction de Lyapunov, i.e. le même $X > 0$ and $Y > 0$.

$$\left[\begin{array}{cccc} A\mathbf{X} + \mathbf{X}A^T + B_2\widetilde{\mathbf{C}} + \widetilde{\mathbf{C}}^T B_2^T & (*)^T & (*)^T & (*)^T \\ \widetilde{\mathbf{A}} + A^T & \mathbf{Y}A + A^T\mathbf{Y} + \widetilde{\mathbf{B}}C_2 + C_2^T\widetilde{\mathbf{B}}^T & (*)^T & (*)^T \\ B_1^T & B_1^T\mathbf{Y} + D_{21}^T\widetilde{\mathbf{B}}^T & -\gamma I_m & (*)^T \\ C_1\mathbf{X} + D_{12}\widetilde{\mathbf{C}} & C_1 & D_{11} & -\gamma I_q \end{array}\right] < 0$$
$$\left[\begin{array}{cc} \mathbf{X} & I_n \\ I_n & \mathbf{Y} \end{array}\right] > 0 \tag{1.24}$$

Ensuite, le problème consiste à trouver $\widetilde{A}$, $\widetilde{B}$ et $\widetilde{C}$ à chaque extrémité du polytope. La reconstruction du contrôleur se fait par les relations suivantes

$$\left\{\begin{array}{rcl} \widetilde{C} & = & C_c M^T \\ \widetilde{B} & = & N B_c \\ \widetilde{A} & = & YAX + NB_cC_2X + YB_2C_cM^T + NA_cM^T \end{array}\right.$$

où N et M sont définies t.q. $MN^T = I - XY$.

Adaptée à notre problème, la solution de (1.24), en utilisant l'interface Yalmip (Lofberg, 2004) et le solver Sedumi (Sturm, 1999), on obtient $\gamma = 2.48$ et le contrôleur donné sur le diagramme de Bode de la Figure 1.14.

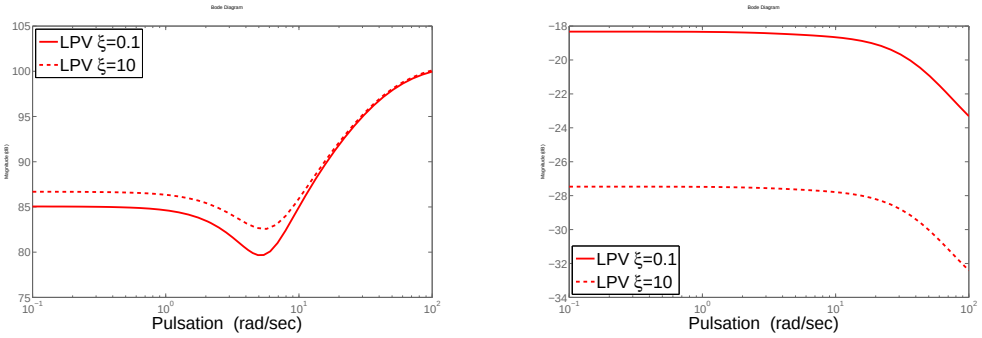

Figure 1.14: Diagrammes de Bode des sorties du correcteur δ^+ et M^*_{dz}.

Sur la Figure 1.14 les transferts de la mesure vers la direction et le freinage pour différente valeurs de ξ sont donnés. Comme la pondération sur la direction a été définie comme dépendant de ξ, on constate bien que lorsque $\xi = \overline{\xi}$, la commande en direction est atténuée, alors que lorsque $\xi = \underline{\xi}$, la commande en direction est plus importante. En conséquence, quand ξ est faible (resp. élevé), le contrôle de la direction est activé (resp. désactivé). Les valeurs intermédiaires donneront un comportement intermédiaire. Il est cependant important de noter que, tant que $\xi \in \mathcal{P}_\xi$, la boucle fermée reste stable, quelle que soit la valeur de ξ grâce à l'approche LPV.

1.5.4.3 Contrôleur d'ABS local

Comme énoncé précédemment (c.f. Figure 1.12), un contrôleur local d'ABS est utilisé pour éviter le glissement lors des phases de fort freinage. Comme la synthèse du CGC est faite sur un modèle linéaire, ce contrôleur local est essentiel pour le bon fonctionnement. Dans cet article, nous utilisons une stratégie ABS par mode glissant, récemment développée par Tanelli *et al.* (2007*a*), qui a montré de bonnes propriétés de robustesse par rapport au type d'actionneur, au changement de type de route et qui prends en considération le compromis entre l'estimation du glissement et la mesure de la décélération de la roue.

Cette stratégie, qui se base sur le concept de Mixed Slip and Deceleration (MSD) (Savaresi *et al.*, 2007), consiste à piloter ε, une combinaison barycentrique du coefficient de glissement λ et de la mesure de la décélération linéaire normalisée de la roue $\eta = -\frac{\dot{\omega} R}{g}$ autour d'une référence $\overline{\varepsilon}$, définie par le concepteur.

$$\varepsilon = \alpha\lambda - (1-\alpha)\eta \text{ avec } \alpha \in [0,1] \tag{1.25}$$

La loi de commande (ABS) pour chaque roue est alors définie par:

$$T_{b_{ABS}} = \begin{cases} T_{b_{max}} & \text{si } e = \overline{\varepsilon} - \varepsilon > \Delta \\ 0 & \text{si } e = \overline{\varepsilon} - \varepsilon < -\Delta \\ \dfrac{T_{b_{max}}}{2} & \text{si } e = \overline{\varepsilon} - \varepsilon = 0 \\ \dfrac{T_{b_{max}}}{2}(1 + e|e|^{-q}\Delta^{q-1}) & \text{sinon} \end{cases} \tag{1.26}$$

où $T_{b_{max}} = 1200Nm$ est le couple de freinage maximal, $q = 0.5$ est un facteur de lissage, $\Delta = 0.1$ est une zone morte définie pour éviter le broutage et $\overline{\varepsilon} = 0.2$ (pour plus d'informations, voir Tanelli, 2007; Poussot-Vassal, 2007).

Pour être adaptée au CGC que nous proposons, la modification suivante (de façon à ce que le freinage ne soit activé que lorsqu'on en a besoin):

$$T_{b_{rj}} = \min(T_{b_{ABS_{rj}}}, T^*_{b_{rj}}) \tag{1.27}$$

1.5.4.4 Superviseur: mesure de l'efficacité de freinage

Le but de ce superviseur est d'indiquer au CGC s'il doit activer ou non le contrôle de direction. Pour cela une mesure de l'efficacité du système de freinage est utilisée comme suit:

$$e = \max(|e_{T_{b_{rj}}}|)\,, j = \{l, r\} \tag{1.28}$$

où $e_{T_{b_{rj}}} = T_{b_{ABS_{rj}}} - T^*_{b_{rj}}$. De là, $\xi(e)$ est défini comme:

$$\xi := \begin{cases} \overline{\xi} & \text{si } e \leq \underline{\chi} \\ \dfrac{\overline{\chi} - e}{\overline{\chi} - \underline{\chi}}\overline{\xi} + \dfrac{e - \underline{\chi}}{\overline{\chi} - \underline{\chi}}\underline{\xi} & \text{si } \underline{\chi} < e < \overline{\chi} \\ \underline{\xi} & \text{si } e \geq \overline{\chi} \end{cases} \tag{1.29}$$

où $\underline{\chi} = \frac{30}{100}T_{b_{max}}$ et $\overline{\chi} = \frac{70}{100}T_{b_{max}}$ sont des valeurs définies par l'utilisateur, qui caractérisent le moment où le système de freinage n'est plus assez efficace. Il est important de noter que d'autres types de stratégies peuvent être aisément envisagées, sans pour autant affecter la méthode de synthèse (voir Ding *et al.*, 2005).

1.5.5 Validation sur le modèle non linéaire

Nous validons à présent la stratégie CGC proposée sur le modèle non linéaire précédement présenté, en simulant des situations critiques de conduite avec et sans défaillance sur l'actionneur de freinage. Ici nous considérons un véhicule roulant à une vitesse initiale de 100km/h qui effectue une manœuvre d'évitement diobstacle d'urgence sur route humide (test à l'élan).

1. Scenario 1: les actionneurs sont sains (Figures 1.15-haut et 1.16)

2. Scenario 2: l'actionneur de freinage arrière gauche est défaillant (Figures 1.15-bas et 1.17)

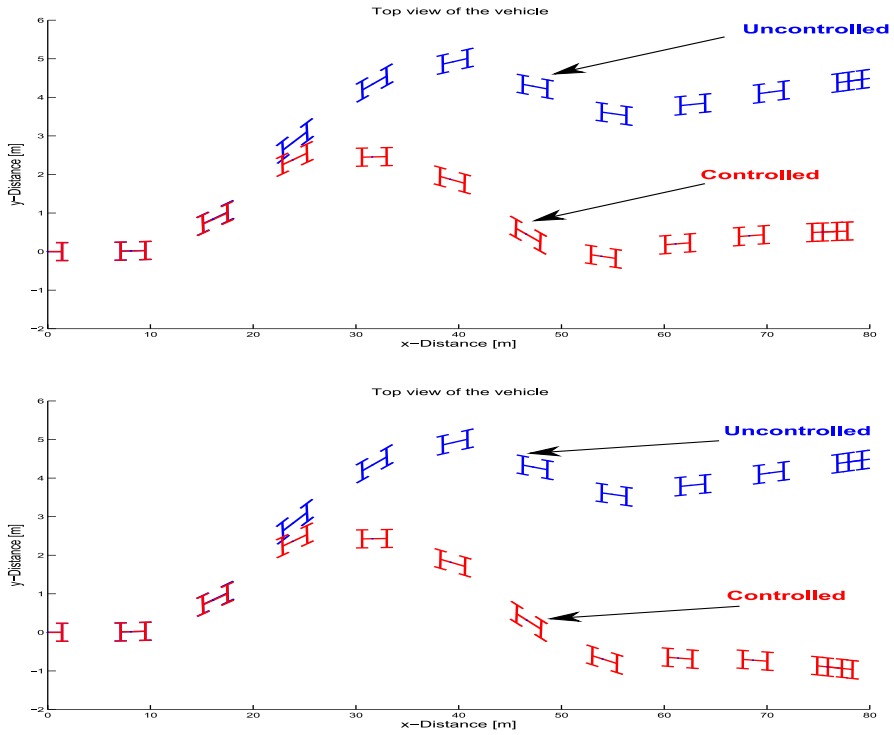

Figure 1.15: Chemin parcouru par le véhicule pour une vitesse initiale $v_0 = 100$km/h sans (avec) un actionneur défaillant, haut (bas).

1.5.5.1 Scénario 1

Comme la route est humide, le coefficient d'adhésion entre le pneu et la route est faible, ainsi, les forces longitudinales et latérales de réaction sont diminuées. En conséquence, pendant la manœuvre, le véhicule non contrôlé dévie fortement de sa trajectoire et ne peut pas se rabattre (Figure 1.15-haut).

En comparant les courbes de vitesse de lacet de la Figure 1.16-(a), on voit clairement que le contrôleur proposé améliore de manière considérable le suivi de trajectoire.

Ensuite, la Figure 1.16-(b) montre que le paramètre de séquencement ξ ne varie pas car le système de freinage suffit pour améliorer la tenue de route, l'actionneur étantassez efficace et fonctionnant correctement. En conséquence, seul le système de freinage est utilisé pour améliorer la dynamique du véhicule (Figure 1.16-(c)) et la commande de direction est quasi-nulle ($|\delta^0| < 10^{-3}$ degrés).

1.5.5.2 Scénario 2

Dans cette situation, le système de freinage arrière gauche est défaillant. La limitation du couple de freinage à 50Nm (1200N en comportement normal). La trajectoire du véhicule est donnée sur la Figure 1.15-bas.

Comme dans la situation précédente, la tenue de route est améliorée (voir la vitesse de lacet de la Figure 1.17-(a)). Comme le frein arrière gauche est défaillant, quand le système en a besoin, de

$t = 1.5s$ à $t = 2.1s$, le GCC détecte que le freinage ne peut pas garantir la sécurité. Ainsi le moniteur modifie le ξ et le CGC active le contrôle de direction pour prendre la main (Figure 1.17-(b,c)).

1.5.6 Conclusions

Dans ce travail, nous présentons une nouvelle méthodologie de contrôle global de châssis pour améliorer la sécurité active des véhicules en utilisant le système de freinage, et, si nécessaire (e.g. en cas de défaillance ou faible adhésion de la route), le système de direction active. Dans la mesure où la solution proposée s'intègre dans un schéma de gestion de la dynamique globale du véhicule, la solution proposée montre une bonne efficacité face aux situations extrêmes de conduite et aux défaillances soudaines des actionneurs grâce à l'approche LPV qui permet, via le paramètre de séquençage, de garantir la sécurité des passagers en toutes situations. Des simulations de scénarios de conduite critiques, réalisés sur un modèle complet de véhicule fortement non linéaire, montrent l'efficacité de la structure de commande robuste.

En terme d'intégration, l'intérêt de ce type de stratégie réside dans le fait qu'il n'utilise aucun processus d'optimisation en ligne et qu'il s'intègre facilement dans l'architecture déjà existante des véhicules.

1.6 Perspectives potentielles des travaux

Concernant les perspectives des ces travaux, il serait intéressant de poursuivre les recherches à la fois dans les directions théoriques et applicatives. Les points suivants semblent particulièrement intéressants à développer:

1. D'un point de vue théorique, les outils de synthèse de contrôleurs sur des systèmes LPV est toujours un sujet de recherche actif, cependant les résultats sont encore limités en ce qui concerne les systèmes avec entrée saturée. De plus, autant la commande LPV est un sujet très largement traité dans la littérature, autant la modélisation LPV l'est beaucoup moins. Ainsi de nombreux résultats (notamment méthodologiques), quant à la meilleure mise sous forme LPV, restent à traiter. La modélisation LPV et la comparaison de son domaine de validité par rapport au modèle non linéaire et LTI sont donc des sujets de grand intérêt où de nombreux développements restent à faire. De plus des investigations sur les méthodes de discrétisation des systèmes et contrôleurs LPV doivent être menées.

2. D'un point de vue applicatif, la mise en oeuvre et la validation des stratégies de CGC de contrôle de suspensions semi-actives, prenant en compte les problèmes de codage, de discrétisation et de limitations matérielles est un sujet très intéressant et stimulant (notamment pour valider la théorie). D'un point de vue applicatif, les méthodes LPV peuvent être utilisées afin de réaliser des stratégies tolérantes aux fautes et défauts. Ce dernier point est d'autant plus intéressant qu'il s'associe à d'autres domaines de la communauté automatique (e.g. la détection de faute et la reconfiguration) et qu'il est crucial dans le secteur automobile et industriel de manière générale.

C'est pourquoi il nous semble intéressant d'orienter les futures recherches vers ces domaines, où application et résultats théoriques sont extrêmement liés et où les résultats dépassent le domaine de l'automobile, et peuvent être appliqués à bien d'autres domaines comme les systèmes sous-marins, aérospatiaux, médicaux...

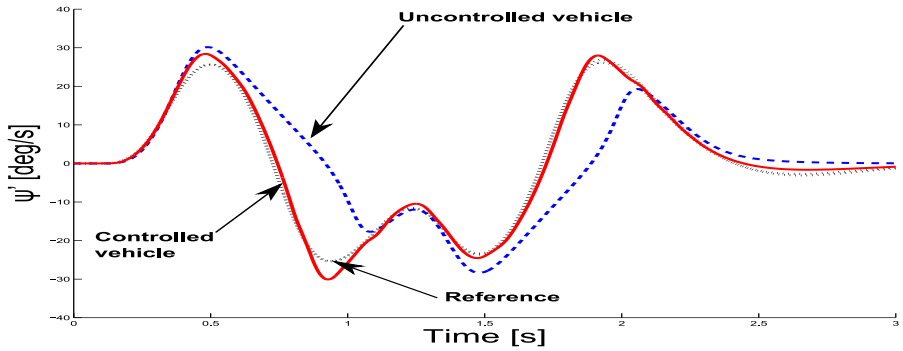

(a) Vitesse de lacet ($\dot{\psi}$).

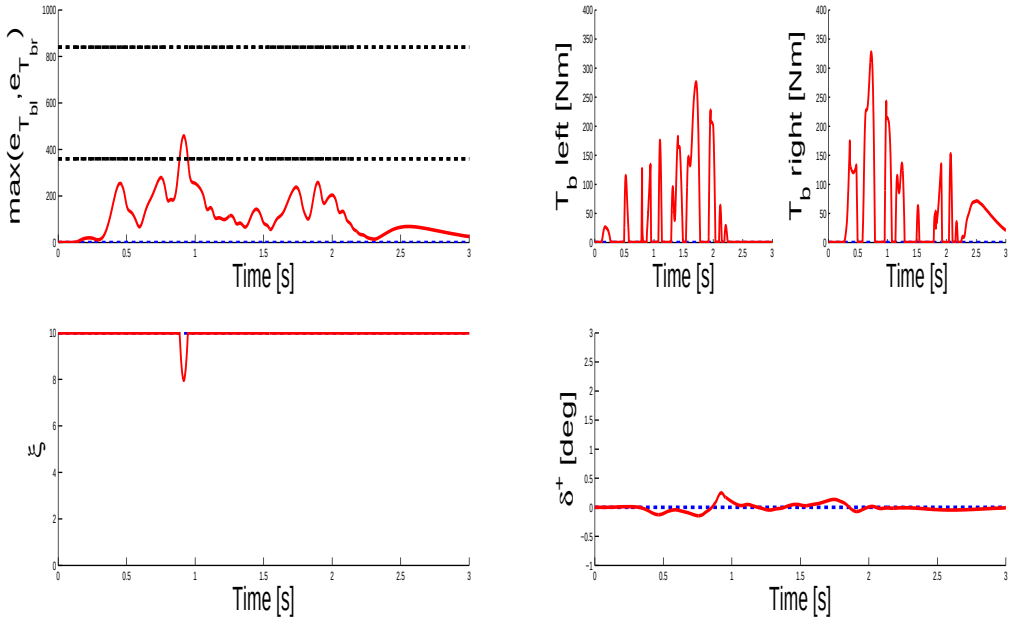

(b) Paramètre de séquencement (ξ), fonction de $\max(|e_{T_{b_{rj}}}|)$.

(c) Commandes (δ^0 et $T^0_{b_{rj}}$).

Figure 1.16: Scénario 1: manœuvre de dépassement pour une vitesse initiale de $v_0 = 100$km/h sur route HUMIDE avec des actionneurs SAIN.

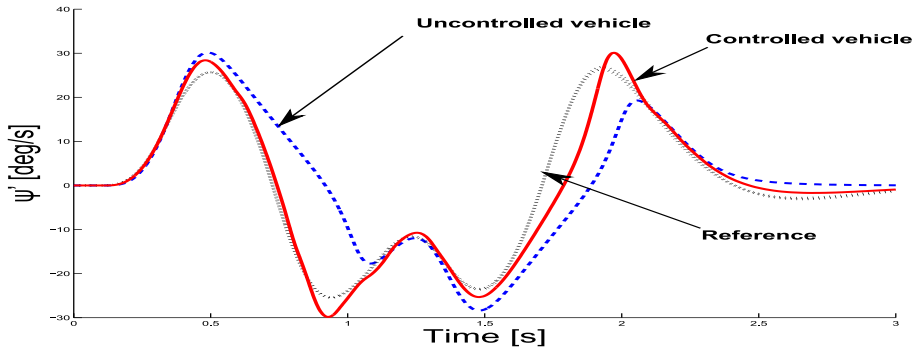

(a) Vitesse de lacet ($\dot{\psi}$).

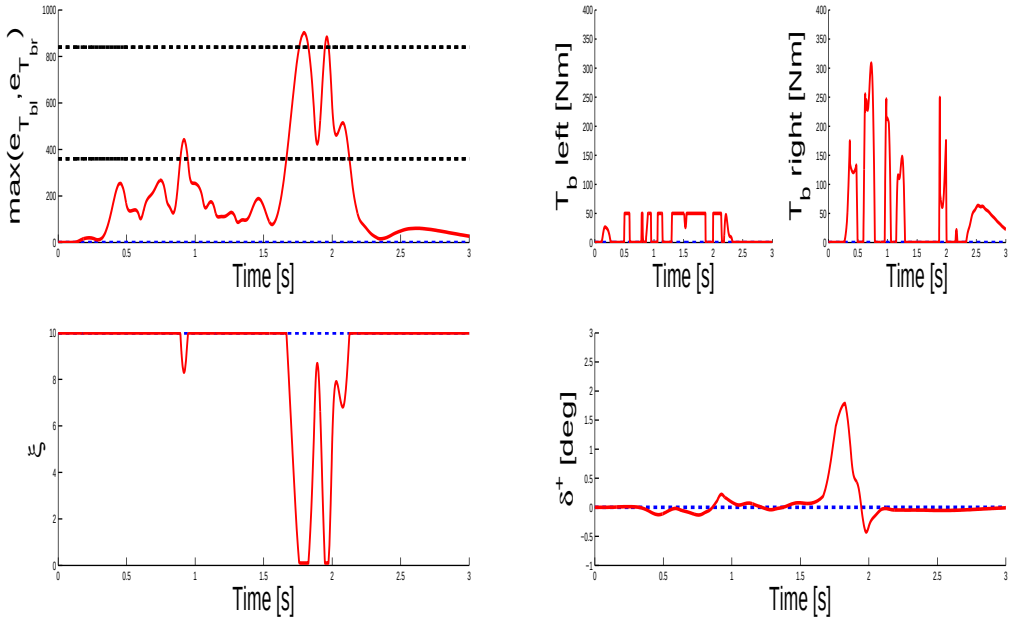

(b) Paramètre de séquencement (ξ), fonction de $\max(|e_{T_{b_{rj}}}|)$.

(c) Commandes (δ^0 et $T^0_{b_{rj}}$).

Figure 1.17: Scénario 2: manœuvre de dépassement pour une vitesse initiale de $v_0 = 100$km/h sur route HUMIDE avec un actionneur DEFAILLANT.

Chapter 2

Historical facts and state of the art

2.1 Introduction

This chapter provides a non exhaustive overview of some recent key historical events leading to the raising importance of the convex optimization and Linear Matrix Inequalities (LMIs) in the control community. It aims at introducing why and how robust control and convex optimization communities are so linked. Then, all "definitions" provided in this chapter may require mathematical and formal definitions given and explained in Chapter 3. The chapter gives an introduction to the importance of the LMI and Linear Parameter Varying (LPV) concepts, widely involved in this work. The actual automotive framework and challenges are introduced in order to present this thesis problematic. According to recent advances in the automotive control, we provide the general framework of this thesis summarizing interesting recent advances in the domain.

This thesis does not contain any theoretical contribution in robust control, and the state of the art in this field is mainly devoted to the "user" and might be non exhaustive. This chapter tries to give a summary of the robust and automotive fields. The robust part is mainly based on very complete papers and lecture notes such as (Boyd *et al.*, 1994; Scherer and Wieland, 2004; Scorletti, 2004; Arzelier, 2005).

The Chapter is structured as follows: Section 2.2 sketches some historical facts leading the control community to the extensive use of LMI tools in order to analyze and solve control problems. As the robust methodology was initially set for Linear Time Invariant (LTI) systems, Section 2.3 is devoted to recall some historical facts and contributive papers introducing gain-scheduling and especially LPV modeling and control, through the natural extension of robust control of LTI systems to LPV ones. Section 2.4 introduces the recent advances and perspectives of the main topic of the thesis, i.e. automotive control (focusing on suspension and global chassis control applications). Finally, Section 2.5 gives an outlook and some perspectives in automotive control and in LMI based control and analysis, providing some open research topics and problems encountered and analyzed in the thesis.

2.2 LMIs in (robust) control theory

In control design theory, a model derived from physical knowledge or identification, describing the real physical system, is often used to synthesize the controller that fulfills the closed-loop system performance specifications. As it is impossible to completely capture all the real physical plant dynamics, the control oriented model is always incomplete and is subject to modeling errors and uncertainties (e.g. stiffness of a spring, inertia of a rotational mass). Furthermore, even if the system

model is accurate, actuator and sensor disturbances may alter in an unpredictable way the closed-loop performances when the controller is implemented on the real application.

Robust control theory is developed to deal with model uncertainties and disturbances in order to ensure the closed-loop system performances (e.g. stability, $\mathcal{H}_\infty$ criterion, ...). Due to its properties (see next Chapter), the $\mathcal{H}_\infty$ control approach is one of the most widely used methodologies in robust control (it will be also extensively used in this thesis). In order to understand the reasons that have motivated to use LMI based robust control tools, let firstly and briefly recall some historical facts.

2.2.1 Historical facts

1890: Lyapunov theory. Analysis and control of dynamical systems through LMIs began in 1890, when Lyapunov showed that (known today as the Lyapunov inequality or theory) the following dynamical system (governed by differential equations):

$$\frac{d}{dt}x(t) = Ax(t)\ ,\ A \in \mathbb{R}^{n\times n} \tag{2.1}$$

is exponentially stable (i.e. all state trajectories converge to zero) if and only if there exists $P \in \mathbb{R}^{n\times n}$ such that $P = P^T \succ 0$ (a positive definite matrix) and:

$$A^T P + PA \prec 0 \tag{2.2}$$

At the same time, Lyapunov also showed that this first LMI (2.2) could be solved explicitly by introducing any $Q \in \mathbb{R}^{n\times n}$ such that $Q = Q^T \succ 0$ and solving the following set of equality:

$$A^T P + PA + Q = 0 \tag{2.3}$$

The 1930's: Feedback notion. Later, negative feedback stability properties were "discovered" thanks to Nyquist and Bode's results on amplifiers (earlier results were obtained by Black). More specifically, they introduced the notion of magnitude and phase in the frequency domain. Since then, open loop system transfer function has become a standard tool to determine the closed loop stability.

The 1940's: LMIs for control engineering problems. In the 1940's, Lur'e, Postnikov and others were among the first ones to apply the Lyapunov inequality to a real control engineering problem and to prove stability of a system containing a nonlinear actuator. The Lyapunov inequalities were analytically solved when problems solved are limited to low size. The Lyapunov theory has shown to be useful for real control engineering problems.

Note that today, the Lur'e problem is still widely studied when nonlinearities are included in the loop and stability is checked through Lur'e Lyapunov.

The 1960's: Graphical method and state space. In the 1960's, Kalman, Yakubovic and Popov solve the problem earlier expressed by Lur'e and Postnikov through the use of a graphical tool: it raises the celebrated Popov criterion. The LMI involved is what is called now the Positive Real Lemma (PRL). The problem of absolute stability is studied through the Lyapunov theory and the input-output stability is studied by Zames and Sandberg, with the apparition of the small gain theorem.

From this, the PRL and its extensions were more and more studied and concepts of passivity (related to the PRL), small-gain theorem, introduced by Zames (1966), now related to the Bounded Real Lemma (BRL), and quadratic optimal control were found to be related.

One of the most fundamental advances in control theory rose at this period with the state space representation which grew in importance and resulted in the Linear Quadratic Gaussian (LQG) control with the work of Wiener, Kalman, Bellman and others. This control procedure provides, among others, a unified approach to multi-variable control.

The 1970's: Riccati method. In the 1970's, Willems exposes another analytical solution to the PRL through the Algebraic Riccati Equation (ARE). Willems shows that the LMI:

$$\begin{bmatrix} A^TP + PA + Q & PB + C^T \\ B^TP + C & R \end{bmatrix} \succeq 0 \tag{2.4}$$

can be solved by the following ARE (with $R \neq 0$), where $Q = Q^T \succ 0$, $P = P^T \succ 0$, A is the system dynamical matrix and B the vector input:

$$A^TP + PA + Q - (PB + C^T)R^{-1}(B^TP + C) = 0 \tag{2.5}$$

But (hopefully), Willems did not exclude the fact that LMIs may be an interesting solution from the computational point of view.

The 1980's: Robust control and Convex optimization. In the eighties, thanks to spatial and aeronautical industries, robustness property appeared to be a new important challenge, more than a "simple" system stabilization and performance achievement. As a consequence, optimal and modal approaches appear to be limited in the sense that they were not able to guarantee this robustness.

A pioneering paper by Zames (1981), followed by Francis and Zames (1984) and Francis *et al.* (1984) introduced the robustness principle. The model uncertainty was expressed in the frequency domain and the disturbance rejection problem was treated. At that time, the dominating methodology was based on state space descriptions. Kimura (1984) introduced the mixed sensitivity $\mathcal{H}_\infty$ control problem (now widely spread in control engineering). However, the solution to Zames' $\mathcal{H}_\infty$ method for multi-variable systems turned out to be hard to be solved in the frequency domain. Then, Doyle and Stein (1984) developed a state-space technique for the solution of the general multi-input multi-output $\mathcal{H}_\infty$ control problem introducing the standard problem, which is now a key notion in robust control. Francis and Doyle (1987) then made a synthesis of the works on this topic and provided the unifying standard problem notion. The solution of the standard problem was greatly improved in (Glover and Doyle, 1988; Doyle *et al.*, 1989). Over the years, the $\mathcal{H}_\infty$ control theory has been extended to other well-known developments, as the loop shaping procedure presented in McFarlane and Glover (1992), which enables a more intuitive design for control engineers, and the structured singular value (μ_{ssv}) synthesis in Doyle (1982), which exploits the structure of the uncertainties in contrast to the uncertainties in $\mathcal{H}_\infty$ control which are unstructured.

However, the main drawback was the requirement to compute the solution of a high order Riccati equation. This difficulty was removed later, and a simplified solution to the $\mathcal{H}_\infty$ and $\mathcal{H}_2$ standard problem for MIMO systems was derived in the form of Algebraic Riccati Equation (ARE) in Doyle *et al.* (1989), which constitutes an important advance in robust control theory.

Until that time, only analytical solutions were proposed to solve these inequalities. But a radical breakthrough occurred when Pyatnitskii, Skorodinskii, Doyle and Boyd shown that many control problems could be solved using convex optimization tools, elaborating then the LMI approach (from the name of this class of problems). They reduced the Lur'e problem to a convex optimization problem involving LMIs, and solved it using ellipsoid algorithm. They have also formulated, in the same time, a new solution to find the Lyapunov function.

It is worth noting recalling the important fact that, at the same period, in the optimization community, Karmarkar developed the Interior Point (IP) method that allows to solve linear program (that includes LMIs ones) in a polynomial time, much more efficiently than ellipsoid algorithms, s.t.:

$$\begin{array}{rl} \max & c^T x \\ \text{s.t.} & Ax \leq b \end{array} \tag{2.6}$$

where x is the decision variable, c a known vector defining the function to minimize, A (resp. and b) a constant known matrix (resp. a vector) that defines the constraints. Later, Nesterov and Nemirovkii applied IP method to convex problem involving LMIs (see Nesterov and Nemirovskii, 1994). From this point, problems solved through analytical (e.g. by Riccati equations) or graphical (e.g. by Popov criterion) methods can now be efficiently numerically treated through optimization algorithms. From now on, (robust) control and optimization communities are strongly linked.

The 1990's: Growing importance of LMIs and Robust control. LMIs based techniques suggest to be a strong alternative to the Riccati equations to solve classical control problems, such as the $\mathcal{H}_\infty$, $\mathcal{H}_2$ and passivity ones. In Gahinet and Apkarian (1994) and Iwasaki and Skelton (1994), LMI formulations of these problems are given. These LMI based formulations show to be more flexible than Riccati formulations (see Doyle *et al.*, 1989) since they allow to avoid some structural hypotheses. The computational complexity of the LMI formulation is now of the same order as the available Riccati solvers. One of the culminating points of all these works is celebrated with the famous books of Boyd, El Ghaoui, Feron and Balakrishnan (Boyd *et al.*, 1994) and Zhou *et al.* (1996) where these notions are well explained and a complete literature reference list is given. Nowadays, robust control is being more and more used in the industry (e.g. aeronautic, automotive, process control) as well as in the university, either to control or to analyze controlled systems.

2.2.2 LMI and robust control perspectives

A control/optimization convergence: the LMI approach. The convergence between control theory (from Lyapunov to robust control synthesis, μ analysis) and convex optimization (from optimization to efficient convex methods and solvers) lead to a growing community that includes both optimization and control engineers. Nowadays, (convex) optimization, LMI and robust control communities are very close so that, challenges and results are linked.

From the optimization community, we can notice the recent apparition of efficient and mature numerical tools like semi-definite problem (SDP) solvers, able to solve LMI (see e.g. SeDuMi by Sturm (1999) and DSDP by Benson *et al.* (2000)) together with user friendly interface toolbox (e.g. YALMIP by Lofberg (2004)). These toolboxes, provide to the control research and control engineers efficient tools to work together with LMIs in an easy and efficient way. It certainly contributed to the extension of the LMI based control approaches in the recent years. Nowadays, LMIs show to be a powerful formulation and design tool for a large variety of linear control problems. Since solving LMI is a convex optimization problem, such an approach presents the advantage to get reliable numerical solutions where analytical solution may not be found. From that time, active researches around LMIs leads to the resolution of many control problems such as:

- **Pole placement**, proposed in Chilali *et al.* (1999) and Bambang *et al.* (1993) (through state feedback design)
- $\mathcal{H}_\infty$ **control**, well described in Gahinet and Apkarian (1994), Iwasaki and Skelton (1994) and Chilali *et al.* (1999)

- $\mathcal{H}_2$ **control** in Abedor *et al.* (1994) and Rotea (1993) (see also Masubuchi *et al.*, 1995; Scherer, 2000)
- **Robust regulation** introduced in Abedor *et al.* (1995)
- **Passivity** given in Sun *et al.* (1994)

Additionally, the Riccati based multiobjective design (e.g. the $\mathcal{H}_\infty/\mathcal{H}_2$) was more and more studied through the works of Bernstein and Haddad (1989). Then, Khargonekar and Rotea (1991), Doyle *et al.* (1994) Bambang *et al.* (1993) worked on this control design using LMI state feedback design, and where multiobjective, e.g. $\mathcal{H}_\infty$ and $\mathcal{H}_2$ criteria, were applied to the same controlled outputs. More recently, Campos-Delgado and Zhou (2003), Scherer *et al.* (1997) introduced dynamical output feedback multiobjective design, where objectives can be applied to different controlled outputs, then it allows to specify different objectives according to the output.

Some recent/new challenges... about LPV. Recent theoretical papers on (robust) control are concerned with challenging topics like:

- Relaxation methodologies; i.e. methods to turn a non convex problem into a convex one, tractable for SDP solvers such as Sum Of Square (SOS), $\mathcal{S}$-Procedure, Moment theory... and new analysis tools like Integral Quadratic Constraints (ICQ).
- Synthesis of controller with constrained structure such as fixed dimension or structure (see e.g. Bu and Sznaier, 2000) or handling a priori input saturations (see e.g. Henrion *et al.*, 1999; Henrion *et al.*, 2004; Scorletti *et al.*, 2001; Garcia and Tarbouriech, 2001).
- LMI based anti-windup synthesis: (see e.g. Grimm *et al.*, 2003; Wu and Lu, 2004; Hu *et al.*, 2003).
- Multiobjective control design through LMI tools (see e.g. Peaucelle and Arzelier, 2002; Arzelier and Peaucelle, 2004*b*) or coupled Riccati equation (see e.g. PhD Thesis of Jungers, 2006).

Consequently, LMI is now a central tool in the control community and its extension to LPV systems is one of the merging challenges in the recent years (especially concerning conservatism reduction). Now the robust control community is attached to the development of extensions of robust tools to "nonlinear" problems. A first step of this research is concerned with the extension of robust control modeling, analysis and control design to LPV systems.

2.3 Gain-scheduled (LPV) systems and controllers

Gain-scheduling is a very old notion in control theory that rose when control community wished to adapt the control mechanism according to some measured variable (e.g. in aerospace applications: the Mach or the altitude of the plane). Then the notion of gain-scheduling mainly started due to industrial or practical engineering requirements.

In the following, the gain scheduling method involved in this thesis, namely the LPV theory, is introduced. The main difference between this methodology and other gain scheduling approaches is the use of LPV systems instead of nonlinear systems or locally linearized ones. This section gives a short historical overview and describes the LPV general concepts and the gain scheduling approach used in this thesis. Since the literature in this field is very large, many papers that inspired the study,

are presented. If the reader is interested about this methodology, he is invited to refer to these works and the references therein.

Firstly, the LPV notions with some key contributive papers are introduced, then, a short introduction on the LPV modeling in done. Finally, some elements on the control of LPV system are given.

2.3.1 Gain-scheduling and LPV notions

The late 1980's - early 1990's: Gain-scheduling. As previously mentioned, advances in gain-scheduling started with industrial applications (e.g. aerospace systems) and process requirements (e.g. industrial chemical process).

During this period, the academic community started working on gain-scheduling control synthesis for nonlinear systems. Then, one of the earliest academical approach introducing the gain-scheduled concepts involved nonlinear approaches. This methodology, known today as the Adaptive Control is celebrated through the book of Åström and Wittenmark (1995). This large approach includes some widely known concepts such as: self-tuning control, model reference adaptive control and gain-scheduling... These approaches are "nonlinear" in the sense that they use nonlinear tools to synthesize controllers and analyze the closed-loop stability and performances, far away from LMIs...

The 1990's: Gain-scheduling and LPV. The guarantee of stability and theoretical validation for slowly varying scheduling parameters were presented in Shamma and Athans (1991). This paper contributes to the development of the LPV systems.

In the same time, a strong attention was paid on robust control, and thanks to LMI tools, the synthesis of LTI robust controllers are now extended to LPV systems. The LPV control synthesis allows to schedule the controller according to system measurements or external user defined parameters. Then, according to this varying property, LPV controllers may recover a higher performance level than the "classical" LTI controllers, but the price to pay is linked to the optimization process i.e. the conservatism introduced by the control problem formulation.

The need for a robust synthesis methodology for LPV systems has been exposed in Shamma and Athans (1991) and Dahleh and Shamma (1992) through Linear Differential Inclusions (LDI)[1]. A specific LDI, treated in this thesis is the Polytopic LDI (PLDI). As an illustration, considering the following LPV system (ρ begin the varying parameter and $\rho \in \mathcal{P}_\rho$, with $\mathcal{P}_\rho$ a clesed set),

$$\Sigma_{LPV} : \left\{ \begin{array}{rcl} \dot{x}(t) & = & A(\rho)x(t) + B(\rho)w(t) \\ z(t) & = & C(\rho)x(t) + D(\rho)w(t) \end{array} \right. \tag{2.7}$$

can be described by a convex combination of the systems defined at all vertices ω_i defined by the bounds of each varying parameter ρ_i. Then, the polytopic system is described as,

$$\Sigma_{LPV} \in \mathbf{Co}\Big\{ \begin{bmatrix} A_1 & B_1 \\ C_1 & D_1 \end{bmatrix}, \ldots, \begin{bmatrix} A_N & B_N \\ C_N & D_N \end{bmatrix} \Big\} = \mathbf{Co}\Big\{ \sum_{i=1}^{N} \alpha_i \begin{bmatrix} A(\omega_i) & B(\omega_i) \\ C(\omega_i) & D(\omega_i) \end{bmatrix} \Big\} \tag{2.8}$$

where

$$\sum_{i=1}^{N} \alpha_i = 1 \text{ and } \alpha_i \geq 0 \tag{2.9}$$

[1] A LDI is a describing family of linear time varying system.

where N is the number of vertices of the polytope (function of the number of varying parameters ρ). See Boyd *et al.* (1994) and references therein for further details on the analysis of nonlinear systems using differential inclusions.

Then, thanks to work results of Becker, Packard, Balas, Packard, Apkarian and Gahinet, the $\mathcal{H}_\infty$ control synthesis, among others, was extended to LPV systems with an exogenously varying parameter, using a single quadratic Lyapunov function and LMIs tools. Then, as an illustration, the Lyapunov inequality for LPV system turns to be, for all $P = P^T > 0$:

$$A(\rho)^T P + PA(\rho) < 0 \tag{2.10}$$

Then, if the LPV system is a polytopic parameter dependent model (where $A(\rho) \in Co\{A_1, \ldots, A_p\}$, for all $\rho \in \mathcal{P}_\rho$), the system is said to be quadratically stable if and only if:

$$A_i^T P + PA_i < 0, \forall i = 1, \ldots, N \tag{2.11}$$

Later, this work was extended by Fromion, Monaco and Normand-Cyrot for analysis and by Wu for synthesis, by incorporating a Parameter Dependent Lyapunov Function (PDLF), $P(\rho) = P(\rho)^T > 0$ resulting in a new Lyapunov inequality (for LPV systems) :

$$A(\rho)^T P(\rho) + P(\rho)A(\rho) + \frac{\partial P(\rho)}{\partial \rho}\dot{\rho} < 0 \tag{2.12}$$

where $\dot{\rho}$, the parameter time derivative, appears as a key notion in the stability analysis. The interest in incorporating such a PDLF was to reduce the introduced conservatism by the number and nature of the varying parameters.

Similarly, a polytopic model with parameter dependent Lyapunov function (where $A(\rho, \dot{\rho}) \in Co\{A_{11}, \ldots, A_{Nm}\}$, for all $\rho \in \mathcal{P}_\rho$ and $\dot{\rho} \in \mathcal{P}_{\dot{\rho}}$), is said to be quadratically stable if and only if:

$$A_i^T P(\rho_i) + P(\rho_i)A_i + \frac{\partial P(\rho)}{\partial \rho}\dot{\rho}_j < 0, \forall i = 1, \ldots, N \text{ and } j = 1, \ldots, m \tag{2.13}$$

In Biannic (1996) PhD Thesis, a summary of these points is well described. Nowadays, conservatism reduction is a challenging problem that requires academic works (see e.g. Briat *et al.*, 2008*b*). More theoretical details are given in Chapter 3.

LMI confirms (again) to be an appropriate tool to use in this thesis problematic, in order to synthesize robust multi-variable, multi-objective (LTI and) LPV controllers. Now, perspectives and outlook in LPV theory through LMI are both concerned with the conservatism reduction for control synthesis and problem formulation (e.g. modeling) from the application point of view. Concerning these perspectives, the following research fields are still under development:

- Gain-scheduling with uncertain parameters Apkarian and Adams (1998).
- Conservatism reduction through Affine PDLF, (see e.g. Gahinet *et al.*, 1996; de Souza and Trofino, 2005)
- Conservatism reduction through scaling use (see e.g. Scherer, 2004).
- Multiobjective for LPV systems (Scherer, 1996).
- Application of LPV techniques (Tuan and Apkarian, 1999; Balas *et al.*, 2003).
- Geometrical approaches (Bokor *et al.*, 2004).

- Application of LPV methods to time-delay systems (Briat *et al.*, 2007; Briat *et al.*, 2008*a*).

The LPV system based gain-scheduling approach (or LPV control design) can be divided in a two steps procedure, which are described thereafter:

- Formulation of an LPV model, for control (observation) purpose.
- Synthesis and reconstruction of the LPV controller.

2.3.2 LPV modeling

The first step of the LPV approach consists in "translating" (if necessary) the nonlinear model into a LPV one. This procedure is much more complex than simply linearizing the nonlinear system at many working points. The general idea consists in finding a transformation that turns the nonlinear model into a linear parameterized one. This parameterized (LPV) model should match the whole nonlinear system state space range.

A nonlinear system can be described, in a non unique way, as a LPV system. The LPV modeling is a very delicate step where a lot of research is still under development (see PhD Thesis of Bruzelius, 2004). Briefly, the general aim is to find $\rho = \sigma(x) \in \mathcal{P}_\rho$ such that the LPV model is equivalent to the nonlinear one, i.e.:

$$A(\sigma(x))x + B(\sigma(x))w = f(x, w) \tag{2.14}$$

where $f(x, w) = \dot{x}$ is the nonlinear dynamical system equation and $\rho = \sigma(x)$ is known and depends on the measured signal. The main problem is obviously to find such a $\sigma(.)$ function.

2.3.3 LPV control

The next step, which we focus on in this thesis, is, for a given LPV system, the synthesis of an LPV controller. As illustrated below, finding a Lyapunov function that ensures the stability of the parameter dependent closed-loop system results in an infinite set of LMIs (due to the infinite values of the ρ parameters). To relax this problem, different approaches to reduce this problem into a finite number of LMIs are commonly used (see Chapter 3 and Biannic, 1996):

1. Gridding parameter space (Apkarian and Adams, 1998).
2. Transforming the parameter dependent system into an uncertain system thanks to the Linear Fractional Transformation (LFT) (see e.g. (Apkarian and Gahinet, 1995)).
3. Transforming the system into a Polytopic system (Apkarian *et al.*, 1995; de Souza and Trofino, 2005).

Each approach has its own advantages and drawback. In this thesis, the polytopic approach is mostly used, which is appropriate when the parameter dependency enters in a linear way in the system definition, and when the number of varying parameters is limited (see e.g. Biannic, 1996; Zin *et al.*, 2006).

Such an approach basically consists in considering the LPV system as an LDI, therefore, the synthesis procedure is deeply simplified. This procedure consists in dividing a nonlinear problem into a set of local linear-like system problems. The nonlinear controller is obtained from the set of linear controllers of the sub-problems by changing the active linear controller according to the operating conditions of the nonlinear process. The parameters of the linear controllers are scheduled by the

operating conditions. This condition means that the varying parameters must be measured (or at least observed) on line in order to adapt the controller. Note that this can be viewed as a restriction from the implementation point of view.

However, the resulting controller shares the structure of a linear controller. As the parameters change continuously according to the operating conditions of the physical system, the LPV controller is no longer linear.

2.4 Automotive dynamical systems control

Due to the need for performance and safety improvements, automotive control requirements are increasing and leading to more and more complex control challenges. Problems encountered in this field of application are large and meet new challenges of the control research community. In order to enhance comfort, safety, reliability and energy consumption of road vehicle, the number of passive (e.g. air-bag, driving assistance, chassis structure, etc.), semi-active (e.g. suspension) and active (e.g. steering, braking, light, throttle, engine, energy monitoring, etc.) actuators and systems to be designed and controlled is increasing. Therefore, many works are studied in the automotive field, among other:

- Engine modeling and control (e.g. PhD Thesis of Gauthier (2007) on diesel engine).
- Passenger modeling.
- Energy consumption.
- Chassis modeling, control and observation.
- ...

For automotive systems engineers, this need for performance leads to an increasing number of systems and subsystems to be designed, controlled and monitored. As a consequence, the number of controllers to synthesize is increasing, and fault detections complexity is raising. Since now, active subsystems control design was done separately, therefore, each actuator was built in order to solve a local problem. Today, to reach high performance requirements in terms of security, comfort and reliability, vehicle controllers can no longer be designed separately but in a unified way, in order to solve a general vehicle objective and to account for actuator and dynamical coupling. Moreover, structural limitations of the new vehicle actuators have to be handled by the control solution in order to ensure optimal performances and guarantee safety. In this work, the main aim is to control suspension, braking and steering systems in order to enhance vehicle properties (see Figure 2.1); thus, this work is related to the Chassis modeling, control and observation field (with accent on control). Consequently, we will focus on these systems, where industrial challenges are strong.

Figure 2.1 shows the complexity of the vehicle architecture. Before introducing the state of the art on vehicle dynamical control, it is important to keep in mind that control is not the only purpose of interest in the dynamical automotive area. Dynamical modeling, estimation etc. are still active research fields where many advances are expected. Concerning these points, the reader can refer to the the very complete books of Gillespie (1992), Kiencke and Nielsen (2000) and Milliken and Milliken (1995) (the last reference is more race vehicle oriented) where mechanical, dynamical elements of modern automotive vehicle are fairly well described.

As automotive and control theory is a long time history, here we try to set a recent state of the art of advances in vehicle dynamical control. Since this thesis focuses on suspension and global chassis

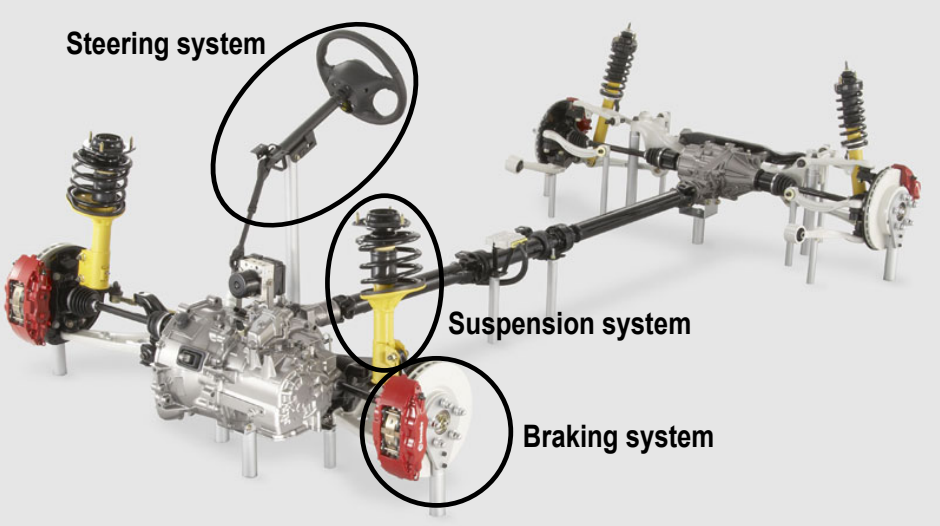

Figure 2.1: Vehicle chassis skeleton (& actuators).

control, accent will be given on problematic and solutions involving suspensions, braking and steering systems without any restriction on the control synthesis methodology.

In the following, a description of the recent developments on suspension, braking, steering and global chassis modeling and control is done. By the way, since the thesis contributions are mostly related to suspension and global chassis control, sections on suspension and global chassis approaches are more developed than the ones on steering and braking. For sake of clarity, actuators and models will be more precisely and formally derived and analyzed in Chapters 4 & 5.

2.4.1 Tire/Road interaction modeling & Braking control

Braking control is a very complex research field closely related with tire/road interaction modeling. Many works in this domain are still under development. Here a short historical recall and references to contributive papers in the following key domains are given:

- Tire/Road interaction.
- Braking control.

2.4.1.1 Tire/Road interaction modeling

One of the most problematic points in vehicle control resides in the difficulty of characterizing and describing the tire/road interaction. In this domain, the early works of Goodyear, Pacejka, Burckhardt and others have been essential in the understanding of the physical behavior, and provided results are well admitted in both academical and industrial fields for simulation and control validation. Thus, tire models are casted as follows (see also Figure 2.2):

- Longitudinal tire/road models, that defines the longitudinal friction force between the road and the tire contact path. Such a force is mainly characterized by the slip ratio which defines the

Figure 2.2: Tire/Road contact forces.

relative speed between the longitudinal speed of the wheel and the linear rotational speed of the wheel, defined as:

$$\lambda = \frac{v - R\omega\cos(\beta)}{\max\{v, R\omega\cos(\beta)\}} \tag{2.15}$$

where v is the vehicle speed vector norm, R is the radius of the wheel and ω is the rotational speed of the wheel. β is the side slip angle which characterizes the angle between the wheel axis and the vehicle speed vector.

- Lateral tire/road models, that define the lateral friction force between the road and the tire contact path. This force is mainly defined as a function of the side slip angle.
- Vertical tire/road models, that define the vertical force provided by the tire. This force is mainly given by the tire vertical stiffness.

More information on these models are given in Chapter 4. Concerning the vertical model, as it "simply" consists in a spring stiffness and as it is not a key element in vehicle dynamic, it is not under strong investigation. Conversely, the main challenges in tire area are concerned with identification and estimation of longitudinal and lateral models (see e.g. Ray, 1997; Savaresi *et al.*, 2006). Among the most famous longitudinal and lateral models and work we can quote:

- The Pacejka model (from the name of its author), which is a nonlinear static function of a large quantity of measures and parameters. This model is clearly the most largely used in the literature for both analysis and control (see e.g. Bakker *et al.*, 1989; Gillespie, 1992; Milliken and Milliken, 1995).
- The Burckhardt model (also from its author name), which is also a nonlinear static model (see e.g. Burckhardt, 1993; Gillespie, 1992; Milliken and Milliken, 1995).
- The LuGre model (based on the well known friction model), which is a nonlinear dynamical model (see e.g. Canudas *et al.*, 2003*a*; Velenis *et al.*, 2005; Canudas and Tsiotras, 1998; Svendenius and Gafvert, 2006).

2.4.1.2 Braking control

One of the main activities in the field of braking is concerned with the synthesis of Anti-locking Braking System (ABS) in order to control the longitudinal car behavior in emergency situations. The aim of the ABS is to avoid wheels to be locked when braking and to guarantee maximal braking force to minimize the braking distance (Denny, 2005; Gissinger *et al.*, 2003; Seron *et al.*, 2007). Moreover, ABS can also greatly improve the vehicle safety in dangerous situations (e.g. yaw stability). As a matter of fact, the main motivation of the increasing presence of ABS in vehicle is that it can provide improvement in safety performance, especially in the yaw, lateral and longitudinal directions. As an illustration, it is used in the Electronic Stability Control (ESC) systems. Nowadays, it is one of the mostly studied problems (see e.g. Kiencke and Nielsen, 2000) and references therein. Consequently, when braking control is to be studied, it is often done in the longitudinal framework.

As the braking system aims at avoiding slipping, it is related with the tire/road friction force knowledge. According to this, the design of automatic braking system is highly dependent on:

- The braking actuator.
- The road adhesion (and its knowledge).
- The available measurements (and their reliability).

Braking control research field has grown together with the recent technological developments in braking actuators. Recently, Electro-Mechanical Braking (EMB) systems, which allow a continuous modulation of the braking torque, have provided extensive possibilities to braking control, allowing to formulate classical regulation problems. Previously, hydraulic actuators were used, for which, only ON/OFF strategies where developed, leading to typical limit cycles. A nice work that synthesizes the control challenges is given in Tanelli (2007).

Since traction and braking problems are "somehow" reciprocal, treating the braking problem corresponds in some sense in finding a solution to the traction problem. Thereafter, some recent relevant results in braking control developed in the literature are given to illustrate some recently developed solutions. These results are cast in two parts; the first where the control is directly synthesized according to measures, then secondly, according to the tire friction force estimation. It is to remember that braking control is often related to slip and vehicle speed estimation.

Direct braking control. A recent interesting approach (Savaresi *et al.*, 2007; Tanelli *et al.*, 2007*b*; Tanelli *et al.*, 2007*a*), uses the mixed slip-deceleration (MSD), which consists in regulating ε, a convex combination of the wheel slip ratio (λ) and of the normalized linear wheel deceleration ($\eta = -\frac{\dot{\omega}R}{g}$) measurements, as given in equation (2.16).

$$\varepsilon = \alpha\lambda + (1-\alpha)\eta \tag{2.16}$$

where ω is the wheel angular velocity, R is the wheel radius, g the gravitational constant and α denotes the slip/deceleration repartition. The interest of this new regulated output variable ε, comes from the complementarity of the involved measurements. The wheel deceleration η is easy to measure thanks to encoders, but the control law cannot be implemented since it requires somehow the road quality estimation (because of the non-uniqueness of the solution). Hence, the regulation loop including this measurement requires road estimation heuristics. On the other hand, regulating only the slip ratio (λ) is efficient since it ensures uniqueness and the set point is easy to derive from basic tire knowledge, but this value, function of vehicle velocity, is hard to compute in practice, especially at low speed.

The MSD approach aims at overcoming poor slip measurement and deceleration efficiency. In this work, a variable structure control approach (namely sliding mode) is chosen to control the ε variable (according to a user defined set point $\overline{\varepsilon}$), making the control insensitive to actuator characteristics. As long as the sliding mode presents invariance properties, this choice is adapted to such a problem where the regulated variable is well defined and where many parameters are uncertain (e.g. the wheel radius and measurements). This strategy is involved in one of our contribution, presented in Section 7.4.

Botero *et al.* (2007) present a simple control structure using a new tire sensor that measures, among others, the tire longitudinal force. The proposed control logic, compared to already existing one, is thus completely different.

Other approaches have been recently developed such as constrained gain scheduled LQR control (see Johansen *et al.*, 2003) or Sliding mode (see Schinkel and Hunt, 2002) have also been recently developed.

Observer & Extremum seeking based control. Vehicle braking highly depends on the road type and on measurements quality. As an illustration, while wheel speed is accurately measured thanks to encoder, it is much more difficult for vehicle longitudinal speed to be measured, especially in braking manoeuver (Tanelli *et al.*, 2006). Even if these measures are known, friction forces (function of the road adhesion) are highly nonlinear and hard to observe. Another trend in braking control consists in designing an observer based controller. In Alvarez *et al.* (2002), an adaptive braking system for emergency situations based on a tire/road friction observer is designed. (see also Canudas *et al.*, 2003*b*; Gustafsson, 1997; Ono *et al.*, 2003; Yi *et al.*, 2003).

Since even observers are complex to design due to the highly nonlinear and uncertain wheel and road/tire model, other ABS designs are designed using optimum seeking and sliding mode control (see e.g. Drakunov *et al.*, 1995; Krstic and Wang, 2000; Tanelli and Savaresi, 2006).

2.4.2 Steering modeling and control

Steering modeling and control are a very important fields of investigation because of their deep influence on the vehicle dynamics and in the driver driving feelings. As a consequence, steering control is more and more studied since, in extremely dangerous situations, it may prevent the driver from accident and since it can provide varying driving feeling to the driver. As long as it is not one of the main points of the thesis, this section is reduced to short explanations.

2.4.2.1 Steering modeling and technology

The steering modeling is often represented as a double integrator that links the driver torque (applied on the steering wheel) and the wheel angle.

Nowadays, there is a growing interest in steer-by-wire (see Figure 2.3) which allows to remove the direction column, to reduce vehicle weight cost and improve safety. This leads to extensive researches on driver feeling. As a matter of fact, the main problem is to be able to reproduce to the driver the road irregularities (related to suspensions) and the wheel resistance when cornering (related to the tire modeling) (Canudas *et al.*, 2003*b*).

Figure 2.3: Steer by wire system.

2.4.2.2 Steering control

Steering control is widely explored in the literature. It can be divided in two categories, corresponding to the desired objectives:

- Lateral and yaw rate control that aims at responding very quickly, in order to prevent high yaw rate or lateral acceleration (e.g. in the case of the ESP) (see e.g. Ackermann and Bunte, 1996; Mammar and Koenig, 2002; Hsu and Gerdes, 2005; Falcone *et al.*, 2007*a*; Villagra *et al.*, 2007; Falcone *et al.*, 2007*b*).

- Lateral driver assistance to enhance line keeping and to assist the driver (see e.g. Raharijaona, 2004; Aubert and Mammar, 1996; Claeys, 2002)

2.4.3 Suspension control

Suspension modeling and control is a very active field of activity in control theory. The damper is a key element in automotive vehicle since it is the main element that "guarantee" good isolation of the passengers against to road irregularities (comfort specification) while ensuring vehicle road contact (road-holding specification). Then, it is now widely known from automotive engineers that soft (resp. stiff) suspensions provide good comfort (resp. road-holding) performances. When vehicle comfort and road holding in normal cruise situation (i.e. not in emergency case like over-steering or rolling situations) are studied, it is well admitted that (controlled) suspension systems can provide good passenger isolation from road unevenness while keeping the road holding performances admissible. The main question is: how to find the "optimal" trade-off between these two performances? Concerning suspension modeling, the recent main advances are related to:

- **Semi-active actuators** (or controlled dampers) modeling and characterization.

In terms of suspension control, two dominating areas are explored in the literature, corresponding to the two kinds of actuators:

- **Active suspension control**, where an actuator is located between the chassis and the wheel which is able to provide and dissipate energy.

- **Semi-active suspension control**, where the actuator is only able to dissipate energy in a variable way (i.e. modify the damping factor). Such actuators are more and more studied due to industrial and theoretical control challenges.

In the following, these three points are described at a fairly high level to provide the reader some elementary basis on suspension modeling and control. Later (see Chapter 4), these actuators are described and analyzed in a more precise manner.

2.4.3.1 Passive dampers

A first response element has been found by adjusting passive dampers, i.e. dampers which can provide a single damping coefficient according to its deflection speed. In other words, the damping factor is tuned mechanically in order to give a certain performance level to the suspension, hence to the car and its passengers. As an illustration, Figure 2.4 shows a Renault Mégane Coupé passive damper force w.r.t. the deflection speed (denoted $\dot{z}_{def}$). Such a representation is known as the Speed-Effort Rule (SER).

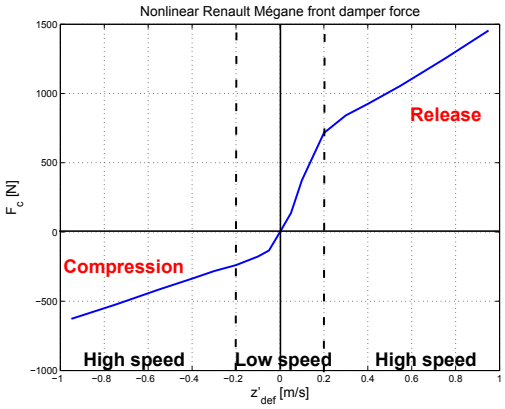

Figure 2.4: SER of the passive Renault Mégane Coupé damper.

By adjusting the shape of the SER, engineers are able to modify the damper performances, therefore, to orientate the vehicle toward comfort or road-holding. A general shape is to have a linear damping factor at low speed and a saturation like at high speeds. In this field of activity, the research is more mechatronics oriented, i.e. advances are more related to mechanical and hydraulic structures or material. In the control community, some results are concerned with the optimal passive dampers design (Giua and Usai, 1999; Jonasson and Roos, 2008), but these researches remains marginal. Nevertheless, it is still a very interesting area where optimization under constraint may be done. By the way, passive dampers are limitative since they can achieve only one single fixed performance.

2.4.3.2 Active suspension control

In order to improve the performances of the suspension, a first approach consists in adding (or replacing), to the usual damper, a controlled actuator that is able to provide a force whatever the deflection speed of the damper (e.g. the Hydractive suspension used in some Citroën cars). Active suspensions are subject to an extensive literature and many models (either nonlinear, LTI or LPV) are available and widely used. In the last decade, many different active suspension system control

approaches were developed. It is a domain where most of control design methodologies have been experimented. As an illustration, some recent control approaches are given here:

Linear Quadratic (LQ). The Linear Quadratic (LQ) control, which consists in synthesizing a control law that is optimal according to the considered criteria, is given by the solution of the following problem:

$$\min \int_0^{+\infty} \big(x(t)^T Q x(t) + u(t)^T R u(t)\big) dt \tag{2.17}$$

This control approach can provide both comfort and road holding improvements but requires the full state measurement or estimation. Concerning this control law, a very famous survey of Hrovat (1997) provides a general overview of LQ control on active suspensions.

The CRONE approach. This approach, widely known in the French control community, holds for Commande RObuste Non Entière (Robust Control methodology using Non Full Derivative). It has been implemented on Citroën BX experimental car active suspensions, and is based on the fractional derivative. The general idea consists in ensuring a constant open loop transfer phase around the frequency of the unitary gain. In other words, this approach consists in dealing with the open loop as a transmittance and shaping it thanks to a few number of parameters (Oustaloup and Mathieu, 1999). The ideal version of the CRONE controller is a controller with a constant phase such that:

$$C(s) = C_0 \Big(\frac{1 + s/w_b}{1 + s/w_h}\Big)^m, m \in \mathbb{R} \tag{2.18}$$

which is approximated by a product of constant transmittances s.t.,

$$\widetilde{C}(s) = C_0 \prod_{i=1}^{N} \Big(\frac{1 + s/w_i^b}{1 + s/w_i^h}\Big)^{k_i}, k_i \in \mathbb{N} \tag{2.19}$$

As N, the order of the controller, should be large enough to ensure $\widetilde{C}(s) \approx C(s)$, it results in a complex form where the size of the implemented controller and the number of parameters to find and "optimize" are large (due to the difficulty of the approximation) (see e.g. Oustaloup *et al.*, 1996; Oustaloup and Mathieu, 1999).

Skyhook control. The Skyhook control, introduced by Karnopp *et al.* (1974), is an approach specifically dedicated to suspension control. It consists in designing an ideal active suspension control law so that the chassis is "linked" to the sky in order to reduce the vertical oscillations of the chassis and to isolate the passenger from the wheel trepidations (see Figure 2.5). As it is not realizable, this behavior is approximated by equation,

$$u = -c_{sky} \dot{z}_{def} - c_{sky}(1 - \alpha) \dot{z}_{us} \tag{2.20}$$

where $\dot{z}_{def}$ is the deflection speed of the suspension and $\dot{z}_{us}$ the wheel speed. Analysis and applications of this control law are widely explored in the automotive literature (see e.g. Emura *et al.*, 1994; Autran *et al.*, 1995; Sammier *et al.*, 2003; Sammier *et al.*, 2000). As an illustration, Maserati implements this suspension strategy in some of their vehicle (maybe in a modified version).

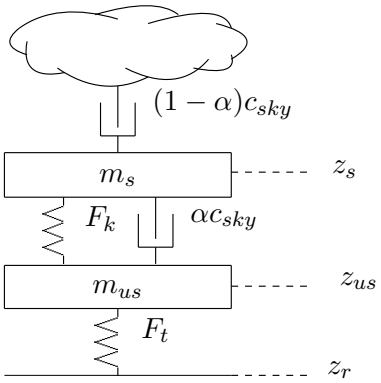

Figure 2.5: Skyhook suspension ideal control principle.

LTI robust control approaches. Since some years, robust control based active suspensions are being more and more studied. Due to the controller structure (that can be static or dynamic, output or state feedback), reached performances can greatly be enhanced.

As an illustration, the LTI/$\mathcal{H}_\infty$ control approach shows to achieve better results that simple Skyhook improving both comfort and road holding performances. Thanks to frequency based specifications, it is possible to shape sensitivity functions, which are well adapted to suspensions problematic where some specific frequencies are to be treated (see Rossi and Lucente, 2004; Sammier *et al.*, 2003; Zin *et al.*, 2005). Mixed LTI/$\mathcal{H}_\infty$/$\mathcal{H}_2$ control approaches, which extend the simple $\mathcal{H}_\infty$ performance objective, show to improve suspension performances reducing control signals energy (thanks to the $\mathcal{H}_2$ criteria) (see recent works of Gáspár *et al.*, 1998; Takahashi *et al.*, 1998; Abdellahi *et al.*, 2000; Tuan *et al.*, 2001; Lu and DePoyster, 2002; Lu, 2004) (see also Section 6.2).

LPV approaches. More recently, the use of LPV approaches lead to controllers that can either adapted their performances according to measured signals: e.g. road, deflection, etc. (see the very interesting results of Fialho and Balas, 2002; Gáspár *et al.*, 2004), or enhance closed-loop robustness, taking into account some model nonlinearities, (see Zin, 2005; Zin *et al.*, 2006). This approach is now of deep interest in the active suspension control topic and is largely used in this thesis.

Limitations. According to the author, this kind of research seems now to show some limitations since in all these cases, design is performed assuming that the actuator of the suspension is fully active, i.e. able to both dissipate and generate energy. Unfortunately such active actuators are not yet used on a wide range of vehicles because of their inherent cost (e.g. energy, weight, volume, price, etc.) and low performance (e.g. time response, reliability, etc.). As a matter of fact, the problem of energy consumption and low time response of such actuators suggests that the future of this technology is questionable. Even if recent results propose to bound the actuator force using time domain (e.g. Chen and Guo, 2005) or frequency domain (e.g. Gáspár *et al.*, 2004) constraints, the controller does not a priori fulfill the dissipative constraint of the semi-active actuator. It is why semi-active suspension modeling and control are more and more studied nowadays.

2.4.3.3 Toward controlled dampers

Since passive dampers can only provide a single SER, achieved performances are fixed and no control is possible. Since a decade, an increasing interest from both academic and industrial automotive communities is concerned with the so-called controlled dampers or semi-active suspensions. The main idea consists in building suspensions mounted with dampers where the damping factor is on-line adjustable. Therefore, the resulting SER can be said to be nearly infinite. As controlled dampers can provide different damping coefficients within a given range, vehicle performances can also vary.

Concerning controlled dampers, attention on this topic is increasing according to the growing demand for the industrial part to have damper that can modify the dissipative factor in real-time. According to this, different automotive suppliers now propose controlled dampers involving different kinds of technologies. It is why these dampers are increasingly studied from both mechanical and control communities (see Figure 2.6) and Spelta (2008) PhD Thesis:

- **Magneto-Rheological damper** (MR damper), is currently one of the most challenging shock absorber technology since it is low cost and presents a fast dynamic. Recently, they equipped the new Audi TT. MR dampers are composed by a magneto-rheological fluid, whose viscosity (hence the damping value) can vary according to a magnetic field, controlled by the current that flows in a self. Nowadays, many different car suppliers propose solutions based on MR fluid (see e.g. Sachs, 2008; Delphi, 2008; Lord, 2008).

- **Electro-Hydraulic damper** (ER damper), which is also on widely used in the automotive and motorcycle industry, due to its almost linear behavior. As an illustration, Volvo cars and top BMW motorcycles are equipped with this technology. The ER damper is based on the variable mechanical properties of the damper: the flowing oil is regulated by a valve that can be either continuously driven (providing an infinite set of damping coefficients) or "step by step" (providing a finite set of damping coefficients).

- **Air-Damping systems**, which is a recent technology where the damping is modified by the mean of a pressure pump. The damping is modified according to the resistance of the gas. This technology is hard to model since it is dependent on the air resistance.

- **Electro-Mechanical damper** (SOBEN principle), which consists in modifying the damping by mechanically modifying some section that allows the liquid to flow. By adjusting the section one modifies the flow rate, hence, the damping factor. An interest of this damper is that no special damping fluid is required and that compression and release damping can be independently modified (see Aubouet *et al.*, 2008).

Therefore, semi-active suspensions (or controlled dampers) are being more and more studied and modeled (in order to be controlled). As a reference, the following recent interesting works have been carried out (see also Section 4.2):

- MR damper modeling, (see e.g. Ahmadian and Song, 1999; Koo *et al.*, 2004; Savaresi *et al.*, 2005*b*).

- SOBEN modeling (see e.g. Aubouet *et al.*, 2008).

In a general way, it should be noticed that:

- Passive dampers can only dissipate energy in a single manner (provide a single SER).

Figure 2.6: From left to right: MR damper, ER damper and Air damper.

- Active dampers can provide and dissipate energy without any restriction.
- Semi-active dampers can dissipate energy in an infinite manner (provide an infinite set of SER).

More details on these dampers are given in Chapter 4

2.4.3.4 Semi-active suspension control for controlled dampers

Due to their low cost, low energy consumption and fast time response, semi-active suspensions (damper) are more and more used in the industry. But, due to their inherent structural limitations, adapted control strategies have to be derived. As far as the author knows, up to now, the following approaches are the main semi-active suspension control approaches.

New trends. One of the new trends in suspension control is concerned by semi-active control. As semi-active suspensions are only able to dissipate energy, effort on synthesizing control law that fulfills the dissipative constraint of the suspension is one of the actual key interests. In the last years, different kinds of strategies have been developed to tackle such limitations, but semi-active suspension control still remains an open research area where some solutions have already been found, as exposed thereafter. This problem is more deeply studied in Section 6.3, where a new approach developed in this thesis is compared with some semi-active suspension strategies.

First attempt: "Clipped" approaches. Karnopp (1983) and Margolis (1983) suggested a semi-active controller by passing the optimal active controller trough a limiter (saturation). This control law is now known as "clipped-optimal". The question that arises is: is optimal the clipped-optimal? If not, how far is it from the real optimal one? How would look like the optimal semi-active one? Clipped approaches lead to unpredictable behaviors and ensure neither closed-loop internal stability nor performances any longer. Active control applied on a semi-active damper, results in a "synthesize and try" method, without any performance guarantee (see e.g. Tseng and Hedrick, 1994; Canale *et al.*, 2006; Sammier *et al.*, 2003; Giorgetti *et al.*, 2006).

Quasi-linearization. The quasi-linearization control approach (see Kawabe *et al.*, 1998) consists in a two-step design. The first step is a quasi-linearization on the basis of the oscillating properties of the suspension system. The second one is a frequency loop-shaping. The first step is aimed at attenuating the oscillation in the lower frequency region, and the second step at attenuating the oscillation in the higher-frequency region.

Skyhook two-state control. The two-state Skyhook control is an on/off strategy that switches between high and low damping coefficients in order to achieve body comfort specifications. This control law consists in changing the damping factor c_{in} of the damper (i.e. its fluid viscosity, air resistance, etc.) according to the chassis velocity ($\dot{z}_s$) and the suspension deflection velocity ($\dot{z}_{def}$) using a logical rule as:

$$c_{in} = \begin{cases} c_{min} & \text{if } \dot{z}_s \dot{z}_{def} \leq 0 \\ c_{max} & \text{if } \dot{z}_s \dot{z}_{def} > 0 \end{cases} \tag{2.21}$$

where c_{min} and c_{max} are the minimal and maximal damping factors achievable by the considered controlled damper respectively. Then, basically, this control law consists in a switching controller which deactivates the controlled damper when the body speed and suspension deflection speed have opposite signs. The controlled damper only needs to have two damping coefficient states. This control strategy presents the advantage to be simple but requires two sensors.

Skyhook linear approximation control. The linear approximation of the Skyhook control algorithm, adapted to semi-active suspension actuators, consists in changing the damping factor c_{in} as a function of the chassis speed ($\dot{z}_s$) and the suspension deflection (z_{def}) s.t.:

$$c_{in} = \begin{cases} c_{min} & \text{if } \dot{z}_s z_{def} \leq 0 \\ sat\Big(\dfrac{\alpha c_{max}(\dot{z}_{def} + (1-\alpha)c_{max}\dot{z}_s}{\dot{z}_{def}}\Big) & \text{if } \dot{z}_s z_{def} > 0 \end{cases} \tag{2.22}$$

where c_{min} and c_{max} are the minimal and maximal damping factors achievable by the considered controlled damper respectively. The $\alpha \in [0, 1]$ parameter provides a tuning parameter that modifies the closed-loop performances. As the two-state control, the linear approximation consists in a switching controller which modifies the damping factor according to the body speed and suspension deflection speed. According to the second expression (when $\dot{z}_s z_{def} > 0$), such a control provides an infinite number of damping coefficients, then it requires a continuously variable controlled damper (e.g. an MR dampers). From the computational point of view, this control law also requires two measurements and is simple to implement.

Acceleration Driven Damper (ADD). The ADD control is a semi-active control law described in (Savaresi *et al.*, 2005*a*; Savaresi *et al.*, 2004), which consists in changing the damping factor c_{in} as:

$$c_{in} = \begin{cases} c_{min} & \text{if } \ddot{z}_s \dot{z}_{def} \leq 0 \\ c_{max} & \text{if } \ddot{z}_s \dot{z}_{def} > 0 \end{cases} \tag{2.23}$$

where c_{min} and c_{max} are the minimal and maximal damping factors achievable by the considered controlled damper respectively.

This strategy shows to be optimal in the sense that it minimizes the vertical body acceleration when no road information is available (therefore, this control law is a comfort oriented one). Since it requires the same number of sensors as the Skyhook two-state and the linear approximations control law, this control law is simple from the implementation point of view. Note that the control law is very similar to the two-state approximation of the Skyhook algorithm, with the difference that the switching law depends on the body acceleration ($\ddot{z}_s$), instead of the body speed (which is easier to practically measure). It is also to note that the ADD design is well adapted to comfort improvement but not to road-holding. Moreover, the "switching dynamic" may influences the closed loop performances.

Mixed Skyhook - ADD. The mixed Skyhook - ADD control is a semi-active control law described in (Savaresi and Spelta, 2007; Savaresi and Spelta, 2008), where the damping factor c_{in} is adjusted as:

$$c_{in} = \begin{cases} c_{min} & \text{if } \left[(\ddot{z}_s^2 - \alpha^2 \dot{z}_s^2) \leq 0 \;\&\; \dot{z}_s \dot{z}_{def} > 0\right] \text{ OR } \left[(\ddot{z}_s^2 - \alpha^2 \dot{z}_s^2) > 0 \;\&\; \dot{z}_s \dot{z}_{def} > 0\right] \\ c_{max} & \text{if } \left[(\ddot{z}_s^2 - \alpha^2 \dot{z}_s^2) \leq 0 \;\&\; \dot{z}_s \dot{z}_{def} \leq 0\right] \text{ OR } \left[(\ddot{z}_s^2 - \alpha^2 \dot{z}_s^2) > 0 \;\&\; \dot{z}_s \dot{z}_{def} \leq 0\right] \end{cases} \tag{2.24}$$

where c_{min} and c_{max} are the minimal and maximal damping factors achievable by the considered controlled damper respectively. The control law is characterized by the additional design parameter α which represents the desired crossover frequency (in rad/s) between Skyhook and ADD. Hence, for a standard automotive suspension, α can be chosen around 11 rad/s (1.8 Hz) which is a natural peak frequency to handle in comfort oriented suspensions. This algorithm is comfort oriented (since it tries to minimize the vertical acceleration) and results in a quasi optimal solution for that purpose (theoretically, because, of course, the performance will be related to the switch speed of the actuator). As the previous one, this strategy also results to be very simple, and provides an additional tuning parameter (α), which from the implementation point of view, is very convenient. But as this strategy is comfort oriented, road-holding performances (related to safety criteria) should be decreased, which can be problematic if suspensions are involved in a global chassis control framework (see Chapter 7).

Hybrid-Model Predictive Control (MPC). Giorgetti *et al.* (2006) introduce an hybrid model predictive optimal controller (using receding horizon). They solve an off-line optimization process which is a finite horizon optimal regulation problem s.t.:

$$\min_{\xi} J(\xi, x(k)) = \min_{\xi} \left[x^T(N) Q_N x(N) + \sum_{k=1}^{N-1} x^T(k) Q x(k) + y^2(k) \right] \tag{2.25}$$

subject to,

$$\begin{cases} x(k+1) &= Ax(k) + Bu(k) \\ y(k) &= Cx(k) + Du(k) \\ 0 &\leq u(k)\dot{z}_{def}(k) \\ |u(k)| &\leq \Lambda \end{cases} \tag{2.26}$$

where Q is a performance index and Q_N is the final weight, as in the optimal control theory. Matrices A, B, C and D in (2.26) define the LTI quarter car model, Λ is the maximal force allowed by the considered controlled damper and $u(k)\dot{z}_{def}(k) \geq 0$. ξ is a vector composed by the sequence of control signals (from 0 to $N-1$) to be applied. Finally, N is the prediction horizon. Giorgetti *et al.* (2006) show that choosing $N = 1$ leads to identical performances as the clipped-optimal approach, and by increasing N (e.g. until 40) performances should be significantly improved. The implemented control law does not involve any optimization procedure since the control algorithm provides a collection of affine gains over a polyhedral partition of the system states x (here $x \in \mathbb{R}^4$) (see also Borrelli *et al.*, 2003). By the way, this approach exhibits notable drawbacks:

- The receding horizon control law has to commute between a collection of affine gains. Then, the hybrid controller has to switch between a large number of controllers (function of the prediction horizon). As an illustration for $N = 1$, the control has to switch between 8 regions. For $N = 2$, 62 regions are obtained (which may lead to complex implementation or at least heavy test computation).

- The control law requires the full state measurement, which is somehow difficult to obtain in an acceptable way, then, an observer has to be introduced. Consequently, as long as the control law is nonlinear, stability and performances should be checked again.

Model Predictive Control (MPC). Thanks to improvements in optimization algorithms, MPC control is being more and more used in the automotive applications. Canale *et al.* (2006) introduce another MPC semi-active suspension which results in good performances compared to the Skyhook and LQ-Clipped approaches. The control algorithm consists in a receding horizon strategy given by the following algorithm steps:

1. Measure $x(k)$, the system state.
2. Solve
$$\min_{\xi} J(\xi, x(k), N_p, N_c) \tag{2.27}$$
such that semi-active and performance constraints are fulfilled and where N_p is the prediction horizon, N_c, the control horizon and ξ the sequence of control signals.
3. Apply the first element of the solution sequence ξ to the optimization problem as the actual control action.
4. Repeat the whole procedure at time $k + 1$.

Results provided in the paper are interesting and deserve a deep interest, but the main drawbacks here, are that:

- It requires an on-line "fast" optimization procedure in the control loop.
- It involves (again) optimal control, full state measurement and a good knowledge of the model parameters is necessary (see also Giua *et al.*, 2004).

2.4.4 Global chassis control

As previously exposed, in most vehicle control design approaches, suspension, steering and braking control systems are synthesized independently to solve local problems. The global communication and collaboration between each control structure (sensors, controllers and actuators) are achieved using empirical rules, derived thanks to the global knowledge of automotive engineers. But this kind of approach may lead to conflicting or inappropriate control objectives. Then, the new trend consists in providing control methodologies in order to make them collaborate.

This is why most of the recent studies in vehicle safety enhancement are concerned with the so-called Global Chassis Control (GCC). As many active systems are involved in cars to guarantee both security (e.g. ABS, ESC, etc.) and comfort (e.g. Suspensions, ABC, etc.), the whole control architecture is becoming even more and more complex. As a consequence global vehicle control is now an important issue in the future of vehicle control technology in order to improve comfort and safety (see Shibahata, 2005). While different approaches are being developed, the underling idea is to control the global vehicle dynamical behavior, and, to consider the vehicle as an object (position & orientation) moving in a (constrained) space, with (constrained) actuators (see Figure 2.7).

The new trend in vehicle dynamics control (either commercial or heavy) is to synthesize multivariable controllers that are able to improve both comfort and safety properties according to the vehicle situation (e.g. normal, dangerous or critical), and to enhance performances, supervising the vehicle state and using all the available actuators. The objective is to make actuators collaborate toward the same objective, according to the vehicle situation. Today, only few interesting results concerning these points are available.

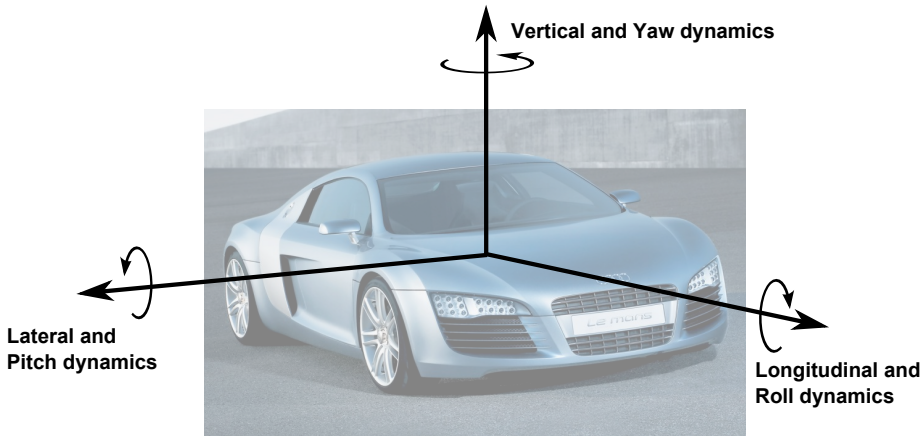

Figure 2.7: Vehicle main dynamics, toward Global Chassis Analysis and Control.

Nonlinear approaches. In Andreasson and Bunte (2006), an inverse model based control, involving an optimization procedure, is proposed. A control strategy is added to compensate for modeling error due to the inversion. According to the authors, this kind of approach presents important drawbacks such as non robustness of the control law and algorithm complexity since it requires an on-line inversion.

In Chou and d'Andréa Novel (2005), the authors present an interesting nonlinear control law involving suspension and braking actuators for commercial cars. The authors design a nonlinear control law that allows the vehicle to follow a desired yaw rate and longitudinal acceleration predefined trajectories while stabilizing the roll rate, pitch rate and vertical velocity using both braking and (active) suspension actuators. This approach consists in dividing the global control into two subproblems according to the considered actuator i.e. the horizontal dynamics is treated through the braking control and the vertical dynamics through the suspension forces. The proposed solution regulates the pitch rate, roll rate, vertical velocity and yaw rate by adapting a constrained optimal control algorithm. The control law results in a quite simple architecture and provides significant results but involves an optimization procedure, that may be costly for implementation.

MPC approach. A nice LTV model predictive approach is proposed in (Falcone *et al.*, 2007*b*; Falcone *et al.*, 2007*c*) involving active differential braking and steering actuators. It results in an optimization problem that is solved on-line and where the system model is linearized at each step in order to handle the nonlinearities of the vehicle model (especially tires). The considered system is described as:

$$x(k+1) = f(x(k), u(k)) \tag{2.28}$$

and the nonlinear control problem is defined (and solved on-line) as:

$$\begin{array}{ll} \min\limits_{U} & V_N(x_k, U_k, X_{ref}) \\ \text{s.t.} & x(k+1) = A_k x(k) + B_k u(k) \\ & x(k) \in \mathcal{X} \\ & u(k) \in \mathcal{U} \end{array} \tag{2.29}$$

where V is a cost function, $\mathcal{X}, \mathcal{U}$ are the system state and control input sets respectively and matrices A_k, B_k are the linearization of $x(k+1) = f(x(k), u(k))$ at each period. The proposed algorithm results in a good performance but seems quite complex for an embedded application where timing constraints are important.

LPV approach. In Gáspár *et al.* (2005), a heavy vehicle Linear Parameter Varying (LPV) model is introduced together with an integrated control structure with individual active control mechanisms, i.e. active anti-roll bars, active suspensions, and an active brake mechanism. The control takes into account both required performances, modeling uncertainties and fault detection. The design of the control law is based on LPV/$\mathcal{H}_\infty$ methods. A very interesting point in this paper is that the performances of the controlled system are enhanced thanks to a prediction procedure achieved thanks an observer. The interest in this design, compared to other existing approaches, is that no on-line optimization has to be performed, which consequently simplifies the implementation step.

2.5 Perspectives

As emphasized to this chapter, LMI is a very useful and powerful tool for MIMO controller synthesis. Thanks to the recent extension of LTI robust control methods to LPV systems (thanks to the LMI approach), it seems to be a very interesting issue for further theoretical investigations, but also for applicative ones where many problems are still under development. In this framework, one of the automotive new challenges lies on both Global Chassis Control (GCC) and semi-active suspension control where LPV methods are not widely explored yet.

Some open research topics and potential extensions. Potential topics that should be explored in the next years (in the LMI, the robust and the LPV control domains), may be:

- The development of solvers that allow control synthesis and analysis for large scale systems. As an illustration, if a problem is too large (i.e. large dimension of the system), the number of variables increases, then, optimal solution may not be founded (even if the problem is convex).

- The development of Bilinear Matrix Inequalities (BMI) solvers. Today such solvers exist but global optimum is not ensured. Their developments should be of great interest for practical problems.

Moreover, concerning vehicle control (and estimation), potential issue are related with:

- The synthesis of fault tolerant controllers, that handle an actuator failure, thus which are able to handle the vehicle dynamical problem by using an other actuator. This problem is related with fault detection problems, reconfiguration, etc. which are close to observation, switch, LPV theories (see e.g. Seron *et al.*, 2008; Gáspár *et al.*, 2005).

- The new developments of semi-active suspension strategies that can improve comfort and road-holding (see Section 6.3).

- The collaboration between the different vehicle actuators, to enhance performances or handle faulty actuators (see Chapter 7).

Perspective "explored" in this thesis (in the automotive framework). In this thesis, LPV robust tools are used in order to build new control methodologies for automotive control focusing on: firstly active and semi-active suspension control, and secondly, on Global Chassis Control involving different actuators at the same time to make them collaborate in all driving situations.

Chapter 3

Theoretical background on control theory

3.1 Introduction

This chapter is devoted to the introduction of the definitions, theoretical notions and tools for advanced control design and analysis. The main question is: how to formulate and calculate a(n) (adaptive) controller that satisfies closed-loop system performances? In order to answer this question, we will proceed in two steps:

1. Firstly, we present the notion of robustness using dissipative approach, mainly inspired from Boyd *et al.* (1994) and Scherer and Wieland (2004). The concepts of dissipativity, $\mathcal{H}_\infty$, $\mathcal{H}_2$ criteria and the LMI and convexity notions are introduced.

2. Secondly, a description of the robust controller synthesis with a quadratic supply function for LTI and LPV systems is given using LMIs. The LMI formalism advantages (compared to other optimization problems), and the controller synthesis as an LMI problem (tractable for SDP solvers), are both introduced.

It should be kept in mind that the problems of dissipativity, robust control, LMI, etc. have been and are still widely developed in the literature. This Chapter is largely inspired from works published by authors such as C.W. Scherer, S. Wieland, L. El-Ghaoui, P. Apkarian, P. Gahinet, F. Doyle, D. Arzelier, J. Bokor and many others, already cited in the previous state of art chapter. They contribute at different periods to diffusion of these approaches through courses (Scherer and Wieland, 2004; Scorletti, 2004), books (Boyd *et al.*, 1994; Alazard *et al.*, 1999; El-Ghaoui, 1997; Arzelier, 2005), and journal papers (Scherer *et al.*, 1997; Apkarian and Adams, 1998).

As the theoretical formulation is not the core contribution of the thesis, this chapter's vocation is to provide a summary of the tools involved in this work. For a mature reader in LMI and LPV approaches, this chapter may be viewed as short and uncomplete, but our intention is to present the main ideas and concepts. Conversely, an unfamiliar reader should also refer to the bibliography provided in this domain (see also previous Chapter). As a matter of fact, the material provided in this Chapter gives the fundamental mathematical elements.

This chapter is structured as follows: in Section 3.2, definitions of dynamical systems are given to make the reader familiar with the notations and representations chosen in this thesis, as well as mathematical background to understand the control approach. Section 3.3 introduces the notions of

robustness together with the dissipativity theory. Then, according to the dissipative properties, the $\mathcal{H}_\infty$, $\mathcal{H}_2$, passivity and multi-objective performance criteria of LTI systems are presented in Section 3.4. Section 3.5 gives LMI based solutions of the classical quadratic performance objectives for LTI systems, i.e. it provides a solution to the controller synthesis with quadratic performance. The extension to LPV systems is described in section 3.6. It is worth noting that all definitions are given for continuous time problems[1].

3.2 Dynamical system, norm and LMI definitions

In this Section, the basic elements and notations concerning dynamical systems and their associated norms are introduced. Then definitions of tools such as LMIs and convexity are given.

3.2.1 Dynamical system definitions

In control theory, dynamical systems are mostly modeled and analyzed thanks to the use of a set of Ordinary Differential Equations (ODE)[2]. We provide general definitions of different dynamical system modelings.

3.2.1.1 Nonlinear dynamical systems

Nonlinear dynamical system modeling is the "most" representative model of a given system. Generally this model is derived thanks to system knowledge, physical equations etc. Nonlinear dynamical systems are described by nonlinear ODEs.

Definition 3.2.1 (*Nonlinear dynamical system*)

For given functions $f : \mathbb{R}^n \times \mathbb{R}^{n_w} \mapsto \mathbb{R}^n$ and $g : \mathbb{R}^n \times \mathbb{R}^{n_w} \mapsto \mathbb{R}^{n_z}$, a nonlinear dynamical system ($\Sigma_{\mathcal{NL}}$) can be described as:

$$\Sigma_{\mathcal{NL}} : \begin{cases} \dot{x}(t) &= f(x(t), w(t)) \\ z(t) &= g(x(t), w(t)) \end{cases} \tag{3.1}$$

where $x(t)$ is the state which takes values in a state space $X \in \mathbb{R}^n$, $w(t)$ is the input taking values in the input space $W \in \mathbb{R}^{n_w}$ and $z(t)$ is the output that belongs to the output space $Z \in \mathbb{R}^{n_z}$.

The main advantage of nonlinear dynamical modeling is that (if it is correctly described) it catches most of the real system phenomena. On the other side, the main drawback is that there is a lack of mathematical and methodological tools; e.g. parameter identification, control and observation synthesis and analysis are complex and non systematic (especially for MIMO systems). In this field, notions of robustness, observability, controllability, closed loop performance etc. are not so obvious. In particular, complex nonlinear problems often need to be reduced in order to become tractable for nonlinear theory, or to apply input-output linearization approaches (e.g. in robot control applications).

In the context of global automotive chassis control, such a nonlinear modeling appears to be nice and very useful for simulation and performance analysis but not for control synthesis purposes (or at

[1] Discrete time formulation is very similar but still requires a particular attention (see e.g. (Åström and Wittenmark, 1997; Robert, 2007)).

[2] Partial Differential Equations (PDEs) may be used for some applications such as irrigation channels, traffic flow, etc. but methodologies involved are more complex compared to the ones for ODEs. Anyway, it is still an interesting field of research (see e.g. PhD Thesis of Jacquet, 2007).

least, not for a multivariable approach). It should be noticed that, for local control (e.g. braking), it would become a powerful tool. Some of these points are developed later.

3.2.1.2 LTI dynamical systems

As nonlinear modeling seems to lead to complex problems, especially for MIMO systems control, the LTI dynamical modeling is often adopted for control and observation purposes. The LTI dynamical modeling consists in describing the system through linear ODEs. According to the previous nonlinear dynamical system definition, LTI modeling leads to a local description of the nonlinear behavior (e.g. it locally describes, around a linearizing point, the real system behavior).

Definition 3.2.2 (*LTI dynamical system*)

Given matrices $A \in \mathbb{R}^{n\times n}$, $B \in \mathbb{R}^{n\times n_w}$, $C \in \mathbb{R}^{n_z\times n}$ and $D \in \mathbb{R}^{n_z\times n_w}$, a Linear Time Invariant (LTI) dynamical system (Σ_{LTI}) can be described as:

$$\Sigma_{LTI} : \left\{ \begin{array}{rcl} \dot{x}(t) & = & Ax(t) + Bw(t) \\ z(t) & = & Cx(t) + Dw(t) \end{array} \right. \tag{3.2}$$

where $x(t)$ is the state which takes values in a state space $X \in \mathbb{R}^n$, $w(t)$ is the input taking values in the input space $W \in \mathbb{R}^{n_w}$ and $z(t)$ is the output that belongs to the output space $Z \in \mathbb{R}^{n_z}$.

The LTI system locally describes the real system under consideration and the linearization procedure allows to treat a linear problem instead of a nonlinear one. For this class of problem, many mathematical and control theory tools can be applied like closed loop stability, controllability, observability, performance, robust analysis, etc. for both SISO and MIMO systems. However, the main restriction is that LTI models only describe the system locally, then, compared to nonlinear models, they lack of information and, as a consequence, are incomplete and may not provide global stabilization.

3.2.1.3 LPV dynamical systems

According to the previous nonlinear and LTI dynamical system definitions, a natural extension of the LTI definition lies in the LPV system description which gives somehow a tradeoff between nonlinear and LTI formulations, as described thereafter.

Definition 3.2.3 (*LPV dynamical system*)

Given the linear matrix functions $A \in \mathbb{R}^{n\times n}$, $B \in \mathbb{R}^{n\times n_w}$, $C \in \mathbb{R}^{n_z\times n}$ and $D \in \mathbb{R}^{n_z\times n_w}$, a Linear Parameter Varying (LPV) dynamical system (Σ_{LPV}) can be described as:

$$\Sigma_{LPV} : \left\{ \begin{array}{rcl} \dot{x}(t) & = & A(\rho(.))x(t) + B(\rho(.))w(t) \\ z(t) & = & C(\rho(.))x(t) + D(\rho(.))w(t) \end{array} \right. \tag{3.3}$$

where $x(t)$ is the state which takes values in a state space $X \in \mathbb{R}^n$, $w(t)$ is the input taking values in the input space $W \in \mathbb{R}^{n_w}$ and $z(t)$ is the output that belongs to the output space $Z \in \mathbb{R}^{n_z}$. Then, $\rho(.)$ is a varying parameter vector that takes values in the parameter space $\mathcal{P}_\rho$ (a convex set) such that,

$$\mathcal{P}_\rho := \{\rho(.) := \left[\begin{array}{ccc} \rho_1(.) & \dots & \rho_l(.) \end{array} \right]^T \in \mathbb{R}^l \text{ and } \rho_i \in \left[\begin{array}{cc} \underline{\rho}_i & \overline{\rho}_i \end{array} \right] \forall i = 1, \dots, l\} \tag{3.4}$$

where l is the number of varying parameters. For sake of readability, $\rho(.)$ will be denoted as ρ. Then, from a general viewpoint,

- *$\rho(.) = \rho$, a constant value, (3.3) is a Linear Time Invariant (LTI) system.*
- *$\rho(.) = \rho(t)$, (3.3) is a Linear Time Varying (LTV) system, where the parameter is a priori known.*
- *$\rho(.) = \rho(x(t))$, (3.3) is a quasi-Linear Parameter Varying (qLPV) system.*
- *$\rho(.) = \rho(t)$ and an external parameter, (3.3) is an LPV system.*

An LPV system has a linear state space representation but the matrices are dependent on the varying parameters. Then, a LPV system can be viewed as a combination of LTI systems, or, in some specific cases as a Linear Differential Inclusion (LDI).

In this sense, an LPV model can be viewed as a linear system linearized along the varying parameters trajectories, characterized by $\rho \in \mathcal{P}_\rho$. The advantage of such a representation, among others, is that it allows to model nonlinear parameters description, while keeping the linear structure. Then it allows the use of tools of the linear control theory (with some slight modifications). In other words, LPV systems can model nonlinear plants through the linearization of these nonlinear models along the trajectories of ρ. In this thesis, the polytopic LPV model is employed Zin (2005) PhD Thesis.

Definition 3.2.4 (*Polytopic LPV dynamical system*)

An LPV system is said to be polytopic if it can be expressed as:

$$\left[\begin{array}{c|c} A(\rho) & B(\rho) \\ \hline C(\rho) & D(\rho) \end{array}\right] = \sum_{i=1}^{N} \alpha_i(\rho) \left[\begin{array}{c|c} A(\omega_i) & B(\omega_i) \\ \hline C(\omega_i) & D(\omega_i) \end{array}\right] \in \mathbf{Co}\left\{ \left[\begin{array}{c|c} A_1 & B_1 \\ \hline C_1 & D_1 \end{array}\right], \ldots, \left[\begin{array}{c|c} A_N & B_N \\ \hline C_N & D_N \end{array}\right] \right\} \tag{3.5}$$

where ω_i are the vertices of the polytope formed by all the extremities of each varying parameter $\rho \in \mathcal{P}_\rho$, and where $\alpha_i(\rho)$ are defined as,

$$\alpha_i(\rho) := \frac{\prod_{k=1}^{l} |\rho_k - \mathcal{C}(\omega_i)_k|}{\prod_{k=1}^{l} (\overline{\rho}_k - \underline{\rho}_k)} \, , i = 1, \ldots, N \tag{3.6}$$

$$\alpha_i(\rho) \geq 0 \text{ and } \sum_{i=1}^{N} \alpha_i(\rho) = 1 \tag{3.7}$$

where $\mathcal{C}(\omega_i)_k$ is the k^{th} component of the vector $\mathcal{C}(\omega_i)$ defined as,

$$\mathcal{C}(\omega_i)_k := \{\rho_k | \rho_k = \overline{\rho}_k \text{ if } (\omega_i)_k = \underline{\rho}_k \text{ or } \rho_k = \underline{\rho}_k \text{ otherwise}\} \tag{3.8}$$

Then, $N = 2^l$ is the number of vertices of the polytope formed by the extremum of each varying parameter ρ_i and A_i, B_i, C_i and D_i are constant known matrices (that represent the system evaluated at each vertex).

According to this formulation, the polytopic LPV system is defined as a convex combination of the systems defined at each bound of the varying parameters. This convexity gives an interesting framework for control synthesis since this step will be deeply simplified (see section 3.5).

Let notice that the polytopic representation of LPV systems is not often straightforward since parameters are not linearly entering in the system representation. Then generally, a transformation is required, in order to have a state space representation affinely dependent on the parameters as presented below.

Example: LPV modeling with 2 parameters. Let consider a 2 parameter affinely dependent LPV system (parameters $\rho_1(.)$ and $\rho_2(.)$, $l = 2$). Then,

$$\rho = [\rho_1(.), \rho_2(.)] \in \mathcal{P}_\rho = \mathbf{Co}\{(\underline{\rho_1}, \underline{\rho_2}), (\overline{\rho_1}, \underline{\rho_2}), (\underline{\rho_1}, \overline{\rho_2}), (\overline{\rho_1}, \overline{\rho_2})\} = \mathbf{Co}\{\omega_1, \omega_2, \omega_3, \omega_4\} \tag{3.9}$$

The polytope $\mathcal{P}_\rho$ is formed of $N = 4$ vertices and

$$\Sigma_{LPV} \in \mathbf{Co}\{\Sigma(\omega_1), \Sigma(\omega_2), \Sigma(\omega_3), \Sigma(\omega_4)\} \tag{3.10}$$

The polytopic coordinates are given by (see also Figure 3.1):

$$\omega = \begin{bmatrix} \omega_1 \\ \omega_2 \\ \omega_3 \\ \omega_4 \end{bmatrix} = \begin{bmatrix} \underline{\rho}_1 & \underline{\rho}_2 \\ \underline{\rho}_1 & \overline{\rho}_2 \\ \overline{\rho}_1 & \underline{\rho}_2 \\ \overline{\rho}_1 & \overline{\rho}_2 \end{bmatrix} \text{ and } \mathcal{C}(\omega) := \begin{bmatrix} \overline{\rho}_1 & \overline{\rho}_2 \\ \overline{\rho}_1 & \underline{\rho}_2 \\ \underline{\rho}_1 & \overline{\rho}_2 \\ \underline{\rho}_1 & \underline{\rho}_2 \end{bmatrix} \tag{3.11}$$

As an illustration, by applying (3.8), to

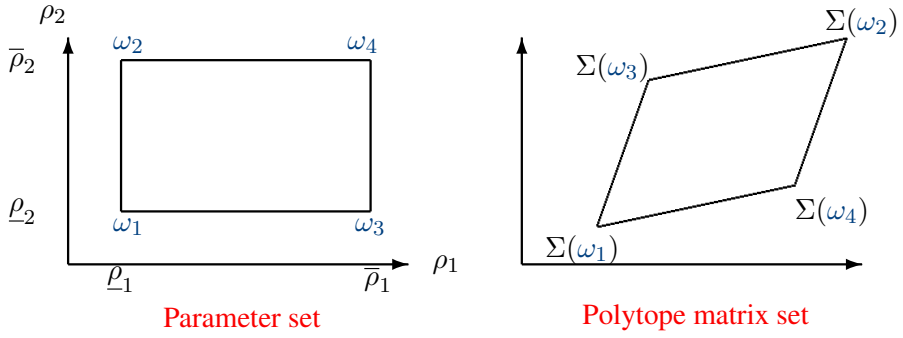

Figure 3.1: Illustration of the polytopic parameter and system representation.

- $i = 1$ and $k = 2$, i.e.,

$$\mathcal{C}(\omega_1)_2 := \{\rho_2 | \rho_2 = \overline{\rho}_2 \text{ if } (\omega_1)_2 = \underline{\rho}_2 \text{ or } \rho_2 = \underline{\rho}_2 \text{ otherwise}\} \tag{3.12}$$

  we obtain, $\mathcal{C}(\omega_1)_2 = \overline{\rho}_2$

- $i = 3$ and $k = 1$, i.e.,

$$\mathcal{C}(\omega_3)_1 := \{\rho_1 | \rho_1 = \overline{\rho}_1 \text{ if } (\omega_3)_1 = \underline{\rho}_1 \text{ or } \rho_1 = \underline{\rho}_1 \text{ otherwise}\} \tag{3.13}$$

  we obtain, $\mathcal{C}(\omega_3)_1 = \overline{\rho}_1$

Then we have,

$$\begin{aligned}
\omega_1 &= [\underline{\rho}_1, \underline{\rho}_2] \quad \alpha_1(\rho) = \frac{|\rho_1 - \overline{\rho}_1||\rho_2 - \overline{\rho}_2|}{(\overline{\rho}_1 - \underline{\rho}_1)(\overline{\rho}_2 - \underline{\rho}_2)} \\
\omega_2 &= [\overline{\rho}_1, \underline{\rho}_2] \quad \alpha_2(\rho) = \frac{|\rho_1 - \underline{\rho}_1||\rho_2 - \overline{\rho}_2|}{(\overline{\rho}_1 - \underline{\rho}_1)(\overline{\rho}_2 - \underline{\rho}_2)} \\
\omega_3 &= [\underline{\rho}_1, \overline{\rho}_2] \quad \alpha_3(\rho) = \frac{|\rho_1 - \overline{\rho}_1||\rho_2 - \underline{\rho}_2|}{(\overline{\rho}_1 - \underline{\rho}_1)(\overline{\rho}_2 - \underline{\rho}_2)} \\
\omega_4 &= [\overline{\rho}_1, \overline{\rho}_2] \quad \alpha_4(\rho) = \frac{|\rho_1 - \underline{\rho}_1||\rho_2 - \underline{\rho}_2|}{(\overline{\rho}_1 - \underline{\rho}_1)(\overline{\rho}_2 - \underline{\rho}_2)}
\end{aligned} \tag{3.14}$$

The polytopic system is defined as:

$$\begin{aligned}
\left[\begin{array}{c|c} A(\rho) & B(\rho) \\ \hline C(\rho) & D(\rho) \end{array}\right] &= \alpha_1(\rho) \left[\begin{array}{c|c} A(\omega_1) & B(\omega_1) \\ \hline C(\omega_1) & D(\omega_1) \end{array}\right] + \alpha_2(\rho) \left[\begin{array}{c|c} A(\omega_2) & B(\omega_2) \\ \hline C(\omega_2) & D(\omega_2) \end{array}\right] \\
&+ \alpha_3(\rho) \left[\begin{array}{c|c} A(\omega_3) & B(\omega_3) \\ \hline C(\omega_3) & D(\omega_3) \end{array}\right] + \alpha_4(\rho) \left[\begin{array}{c|c} A(\omega_4) & B(\omega_4) \\ \hline C(\omega_4) & D(\omega_4) \end{array}\right]
\end{aligned} \tag{3.15}$$

$\Diamond$

3.2.2 LTI/LPV systems and signals norms

Before introducing the mathematical background on systems, norm and control synthesis, basic notions and definition on topology are recalled to provide the reader all the elements to understand the notations and concepts that are used in some definitions. These definitions are somehow the elementary notions of the tools involved in this thesis. Reader is also invited to refer to the famous book of Zhou *et al.* (1996), where all the following definitions and additional information are given.

3.2.2.1 Signals norm

All the following definitions are given assuming signals $x(t) \in \mathbb{C}$, then they will involve the conjugate (denoted as $x^*(t)$). When signals are real (i.e. $x(t) \in \mathbb{R}$), $x^*(t) = x^T(t)$.

Definition 3.2.5 (*Norm and Normed vector space*)

- *Let V be a finite dimension space. Then $\forall\ p \geq 1$, the application $||.||_p$ is a norm, defined as,*

$$||v||_p = \big(\sum_i |v_i|^p\big)^{1/p} \tag{3.16}$$

- *Let V be a vector space over $\mathbb{C}$ (or $\mathbb{R}$) and let $\|.\|$ be a norm defined on V. Then V is a normed space.*

Definition 3.2.6 (*$\mathcal{L}_1$, $\mathcal{L}_2$, $\mathcal{L}_\infty$ norms*)

- *The 1-Norm of a function $x(t)$ is given by,*

$$\|x(t)\|_1 = \int_0^{+\infty} |x(t)|dt \tag{3.17}$$

- *The 2-Norm (that introduces the energy norm) is given by,*

$$\begin{aligned} \|x(t)\|_2 &= \sqrt{\int_0^{+\infty} x^*(t)x(t)dt} \\ &= \sqrt{\frac{1}{2\pi}\int_{-\infty}^{+\infty} X^*(j\omega)X(j\omega)d\omega} \end{aligned} \tag{3.18}$$

  The second equality is obtained by using the Parseval identity.

- *The ∞-Norm is given by,*

$$\|x(t)\|_\infty = \sup_t |x(t)| \tag{3.19}$$

$$\|X\|_\infty = \sup_{Re(s)\geq 0} \|X(s)\| = \sup_\omega \|X(j\omega)\| \tag{3.20}$$

  if the signals that admit the Laplace transform, analytic in $Re(s) \geq 0$ (i.e. $\in \mathcal{H}_\infty$).

3.2.2.2 Some topological spaces recalls

Definition 3.2.7 (*Banach, Hilbert, Hardy and $\mathcal{L}_p$ spaces*)

- *A Banach space is a (real or complex) complete (i.e. all Cauchy sequences, of points in K have a limit that is also in K) normed vector space B (with norm $\|.\|_p$).*
- *A Hilbert space is a (real or complex) vector space H with an inner product $< ., . >$ that is complete under the norm defined by the inner product. The norm of $f \in H$ is then defined by,*

$$\|f\| = \sqrt{< f, f >} \tag{3.21}$$

  Every Hilbert space is a Banach since a Hilbert space is complete with respect to the norm associated with its inner product.
- *The Hardy spaces ($\mathcal{H}_p$) are certain spaces of holomorphic functions (functions defined on an open subset of the complex number plane $\mathbb{C}$ with values in $\mathbb{C}$ that are complex-differentiable at every point) on the unit disk or upper half plane.*
- *The $\mathcal{L}_p$ space are spaces of p-power integrable functions (function whose integral exists, generally called Lebesgue integral), and corresponding sequence spaces.*

For example, $\mathbb{R}^n$ and $\mathbb{C}^n$ with the usual spatial p-norm, $\|.\|_p$ for $1 \leq p < \infty$, are Banach spaces. This means that a Banach space is a vector space B over the real or complex numbers with a norm $\|.\|_p$ such that every Cauchy sequence (with respect to the metric $d(x, y) = ||x - y||$) in B has a limit in B.

Definition 3.2.8 (*$\mathcal{L}_2$ space*)

$\mathcal{L}_2$ is a Hilbert space of matrix-valued (or scalar-valued) functions on $\mathbb{C}$ and consists of all complex matrix functions $f(j\omega)$, $\forall \omega \in \mathbb{R}$, such that,

$$||f||_2 = \sqrt{\frac{1}{2\pi} \int_{-\infty}^{+\infty} \mathbf{Tr}[f^*(j\omega) f(j\omega)] d\omega} < \infty \tag{3.22}$$

The inner product for this Hilbert space is defined as (for $f, g \in \mathcal{L}_2$)

$$< f, g >= \sqrt{\frac{1}{2\pi} \int_{-\infty}^{+\infty} \mathbf{Tr}[f^*(j\omega) g(j\omega)] d\omega} \tag{3.23}$$

Definition 3.2.9 (*$\mathcal{H}_2$ and $\mathcal{RH}_2$ spaces*)

$\mathcal{H}_2$ is a subspace (Hardy space) of $\mathcal{L}_2$ with matrix functions $f(j\omega)$, $\forall \omega \in \mathbb{R}$, analytic in $Re(s) > 0$ (functions that are locally given by a convergent power series and differentiable on each point of its definition set). In particular, the real rational subspace of $\mathcal{H}_2$, which consists of all strictly proper and real rational stable transfer matrices, is denoted by $\mathcal{RH}_2$.

Example: In control theory

$$\begin{aligned} \frac{s+1}{(s+10)(s+6)} &\in \mathcal{RH}_2 \\ \frac{s+1}{(s-10)(s+6)} &\notin \mathcal{RH}_2 \\ \frac{s+1}{(s+10)} &\notin \mathcal{RH}_2 \end{aligned} \tag{3.24}$$

$\Diamond$

Definition 3.2.10 ($\mathcal{L}_\infty$ *space*)

$\mathcal{L}_\infty$ is a Banach space of matrix-valued (or scalar-valued) functions on $\mathbb{C}$ and consists of all complex bounded matrix functions $f(j\omega)$, $\forall\omega \in \mathbb{R}$, such that,

$$\sup_{\omega\in\mathbb{R}} \overline{\sigma}[f(j\omega)] < \infty \tag{3.25}$$

Definition 3.2.11 ($\mathcal{H}_\infty$ *and* $\mathcal{RH}_\infty$ *spaces*)

$\mathcal{H}_\infty$ is a (closed) subspace in $\mathcal{L}_\infty$ with matrix functions $f(j\omega)$, $\forall\omega \in \mathbb{R}$, analytic in $Re(s) > 0$ (open right-half plane). The real rational subspace of $\mathcal{H}_\infty$ which consists of all proper and real rational stable transfer matrices, is denoted by $\mathcal{RH}_\infty$.

Example: In control theory

$$\begin{aligned} \frac{s+1}{(s+10)(s+6)} &\in \mathcal{RH}_\infty \\ \frac{s+1}{(s-10)(s+6)} &\notin \mathcal{RH}_\infty \\ \frac{s+1}{(s+10)} &\in \mathcal{RH}_\infty \end{aligned} \tag{3.26}$$

$\Diamond$

3.2.2.3 System norms

Definition 3.2.12 ($\mathcal{H}_2$ *norm*)

The $\mathcal{H}_2$ norm of a strictly proper LTI system defined as on (3.2.2) from input $w(t)$ to output $z(t)$ and which belongs to $\mathcal{RH}_2$, is the energy ($\mathcal{L}_2$ norm) of the impulse response $g(t)$ defined as,

$$\begin{aligned} \|G(j\omega)\|_2 &= \sqrt{\int_{-\infty}^{+\infty} g^*(t)g(t)dt} \\ &= \sqrt{\frac{1}{2\pi}\int_{-\infty}^{+\infty} \mathbf{Tr}[G^*(j\omega)G(j\omega)]d\omega} \\ &= \sup_{w(s)\in\mathcal{H}_2} \frac{||z(s)||_\infty}{||u(s)||_2} \end{aligned} \tag{3.27}$$

The norm $\mathcal{H}_2$ is finite if and only if $G(s)$ is strictly proper (i.e. $G(s) \in \mathcal{RH}_2$).

Remark: $\mathcal{H}_2$ physical interpretations and remarks

- For SISO systems, it represents the area located below the so called Bode diagram.
- For MIMO systems, the $\mathcal{H}_2$ norm is the impulse-to-energy gain of $z(t)$ in response to a white noise input $w(t)$ (satisfying $W^*(j\omega)W(j\omega) = I$, i.e. uniform spectral density).
- The $\mathcal{H}_2$ norm can be computed analytically (through the use of the controllability and observability Grammians) or numerically (through LMIs).

Definition 3.2.13 ($\mathcal{H}_\infty$ *norm*)

The $\mathcal{H}_\infty$ norm of a proper LTI system defined as on (3.2.2) from input $w(t)$ to output $z(t)$ and which belongs to $\mathcal{RH}_\infty$, is the induced energy-to-energy gain ($\mathcal{L}_2$ to $\mathcal{L}_2$ norm) defined as,

$$\begin{aligned} \|G(j\omega)\|_\infty &= \sup_{\omega\in\mathbb{R}} \overline{\sigma}\left(G(j\omega)\right) \\ &= \sup_{w(s)\in\mathcal{H}_2} \frac{\|z(s)\|_2}{\|w(s)\|_2} \\ &= \max_{w(t)\in\mathcal{L}_2} \frac{\|z\|_2}{\|w\|_2} \end{aligned} \tag{3.28}$$

Remark: $\mathcal{H}_\infty$ physical interpretations

- This norm represents the maximal gain of the frequency response of the system. It is also called the worst case attenuation level in the sense that it measures the maximum amplification that the system can deliver on the whole frequency set.
- For SISO (resp. MIMO) systems, it represents the maximal peak value on the Bode magnitude (resp. singular value) plot of $G(j\omega)$, in other words, it is the largest gain if the system is fed by harmonic input signal.
- Unlike $\mathcal{H}_2$, the $\mathcal{H}_\infty$ norm cannot be computed analytically. Only numerical solutions can be obtained (e.g. Bisection algorithm, or LMI resolution).

3.2.3 LMI and convexity

As exposed in Chapter 2, the convexity notion is crucial since it dramatically simplifies the optimization problem (global optimum achievable in polynomial time). As long as the thesis is not focussed on optimization, no theoretical results are given. By the way, since the $\mathcal{H}_\infty$ and $\mathcal{H}_2$ control solutions involved in this thesis are based on optimization under LMIs constraints, we introduce this tool and its properties, as well as some elements on optimization. Optimization introduction can be found in e.g. (Bergounioux, 2001; Scorletti, 2004; Ciarlet, 1998; Bonnans, 2006).

Definition 3.2.14 (*Convex function*)

A function $f : \mathbb{R}^m \to \mathbb{R}$ is convex if and only if for all $x, y \in \mathbb{R}^m$ and $\lambda \in [0\ 1]$,

$$f(\lambda x + (1-\lambda)y) \leq \lambda f(x) + (1-\lambda)f(y) \tag{3.29}$$

Equivalently, f is convex if and only if its epigraph,

$$\textbf{\textit{epi}}(f) = \{(x, \lambda) | f(x) \leq \lambda\} \tag{3.30}$$

is convex.

The convexity provides a framework where optimization results are now well established and where efficient and robust tools are available. Then a particular category of convex functions is concerned by the Linear Matrix Inequalities (LMIs) which are defined as follows.

Definition 3.2.15 (*(Strict) LMI constraint*)

A Linear Matrix Inequality constraint on a vector $x \in \mathbb{R}^m$ is defined as,

$$F(x) = F_0 + \sum_{i=1}^{m} F_i x_i \succeq 0 (\succ 0) \tag{3.31}$$

where $F_0 = F_0^T$ and $F_i = F_i^T \in \mathbb{R}^{n \times n}$ are given, and symbol $F \succeq 0 (\succ 0)$ means that F is symmetric and positive semi-definite ($\succeq 0$) or positive definite ($\succ 0$), i.e. $\{\forall u | u^T F u (>) \geq 0\}$.

Example: Lyapunov equation. A very famous LMI constraint is the Lyapunov inequality of an autonomous system $\dot{x} = Ax$. Then the stability LMI associated is given by,

$$\begin{array}{rcl} x^T K x & > & 0 \\ x^T (A^T K + K A) x & < & 0 \end{array} \tag{3.32}$$

which is equivalent to,

$$F(K) = \left[\begin{array}{cc} -K & 0 \\ 0 & A^T K + K A \end{array} \right] \prec 0 \tag{3.33}$$

where $K = K^T$ is the decision variable. Then, the inequality $F(K) \prec 0$ is linear in K.
$\Diamond$

LMI constraints $F(x) \succeq 0$ are convex in x, i.e. the set $\{x | F(x) \succeq 0\}$ is convex. Then LMI based optimization falls in the convex optimization. This property is fundamental because it guarantees that the global (or optimal) solution x^* of the the minimization problem under LMI constraints can be found efficiently, in a polynomial time (by optimization algorithms like e.g. Ellipsoid, Interior Point methods).

3.2.4 Semi-Definite Programming (SDP) Problem

The optimization problem involved in this thesis is called LMI optimization. In terms of mathematical programming, this means semi-definite programming (SDP). In optimization, LMI programming is a generalization of the Linear Programming (LP) to cone positive semi-definite matrices, which is defined as the set of all symmetric positive semi-definite matrices of particular dimension.

Note that the name of cone comes from the geometrical shape of the solution conic problems (see e.g. 3D Lorentz cone or "Ice-cream cone").

Definition 3.2.16 (*SDP problem*)

A SDP problem is defined as,

$$\begin{array}{rl} \min & c^T x \\ \text{under constraint } F(x) & \succeq 0 \end{array} \tag{3.34}$$

where $F(x)$ is an affine symmetric matrix function of $x \in \mathbb{R}^m$ (e.g. LMI) and $c \in \mathbb{R}^m$ is a given real vector, that defines the problem objective.

From the control engineer point of view, if we can end to this problem formulation, then we can consider that the problem is solved. SDP problems are theoretically tractable and practically:

- They have a polynomial complexity, i.e. there exists an algorithm able to find the global minimum (for a given a priori fixed precision) in a time polynomial in the size of the problem (given by m, the number of variables and n, the size of the LMI).

- SDP can be practically and efficiently solved for LMIs of size up to 100×100 and $m \leq 1000$ (see El-Ghaoui, 1997). Note that today, due to extensive developments in this area, it may be even larger.

3.2.5 Some useful lemmas

These lemmas are widely used in control theory for LMI relaxations. They are given for sake of completeness since they are used in the following sections.

Lemma 3.2.1 (*Schur lemma*)

Let $Q = Q^T$ and $R = R^T$ be affine matrices of compatible size, then the condition

$$\begin{bmatrix} Q & S \\ S^T & R \end{bmatrix} \succeq 0 \tag{3.35}$$

is equivalent to

$$\begin{array}{rl} R & \succ 0 \\ Q - SR^{-1}S^T & \succeq 0 \end{array} \tag{3.36}$$

The Schur lemma allows to a convert a quadratic constraint (ellipsoidal constraint) into an LMI constraint.

Lemma 3.2.2 (*Kalman-Yakubovich-Popov lemma*)

For any triple of matrices $A \in \mathbb{R}^{n\times n}$, $B \in \mathbb{R}^{n\times m}$, $M \in \mathbb{R}^{(n+m)\times(n+m)} = \begin{bmatrix} M_{11} & M_{12} \\ M_{21} & M_{22} \end{bmatrix}$, the following assessments are equivalent:

1. *There exists a symmetric $K = K^T \succ 0$ s.t.*

$$\begin{bmatrix} I & 0 \\ A & B \end{bmatrix}^T \begin{bmatrix} 0 & K \\ K & 0 \end{bmatrix} \begin{bmatrix} I & 0 \\ A & B \end{bmatrix} + M < 0$$

2. *$M_{22} < 0$ and for all $\omega \in \mathbb{R}$ and complex vectors $col(x, w) \neq 0$*

$$\begin{bmatrix} A - j\omega I & B \end{bmatrix} \begin{bmatrix} x \\ w \end{bmatrix} = 0 \Rightarrow \begin{bmatrix} x \\ w \end{bmatrix}^T M \begin{bmatrix} x \\ w \end{bmatrix} < 0$$

3. *If $M = -\begin{bmatrix} I & 0 \\ A & B \end{bmatrix}^T \begin{bmatrix} 0 & K \\ K & 0 \end{bmatrix} \begin{bmatrix} I & 0 \\ A & B \end{bmatrix}$ then the second statement is equivalent to the condition that, for all $\omega \in \mathbb{R}$ with $\det(j\omega I - A) \neq 0$,*

$$\begin{bmatrix} I \\ C(j\omega I - A)^{-1}B + D \end{bmatrix}^* \begin{bmatrix} Q & S \\ S^T & R \end{bmatrix} \begin{bmatrix} I \\ C(j\omega I - A)^{-1}B + D \end{bmatrix} > 0$$

This lemma is used to convert frequency inequalities into Linear Matrix Inequalities. It will be used in Section 3.4 to illustrate the quadratic performances.

Lemma 3.2.3 (*Projection Lemma*)

For given matrices $W = W^T$, M and N, of appropriate size, there exists a real matrix $K = K^T$ such that,

$$W + MKN^T + NK^TM^T \prec 0 \tag{3.37}$$

if and only if there exist matrices U and V such that,

$$\begin{array}{rcl} W + MU + U^TM^T & \prec & 0 \\ W + NV + V^TN^T & \prec & 0 \end{array} \tag{3.38}$$

or, equivalently, if and only if there exists a scalar $\epsilon > 0$ such that,

$$\begin{array}{rcl} W & \prec & \epsilon MM^T \\ W & \prec & \epsilon NN^T \end{array} \tag{3.39}$$

or, equivalently, if and only if,

$$\begin{array}{rcl} M_\perp^T W M_\perp & \prec & 0 \\ N_\perp^T W N_\perp & \prec & 0 \end{array} \tag{3.40}$$

where $M_\perp$ and $N_\perp$ are the orthogonal complements of M, N respectively (i.e. $M_\perp^T M = 0$).

The projection lemma is also widely used in control theory. It allows to eliminate variable by a change of basis (projection in the kernel basis). It is involved in one of the $\mathcal{H}_\infty$ solutions (see e.g.

Doyle *et al.*, 1989).

Lemma 3.2.4 (*Completion Lemma*)

Let $X = X^T, Y = Y^T \in \mathbb{R}^{n\times n}$ such that $X > 0$ and $Y > 0$. The three following statements are equivalent:

1. *There exist matrices $X_2, Y_2 \in \mathbb{R}^{n\times r}$ and $X_3, Y_3 \in \mathbb{R}^{r\times r}$ such that,*

$$\begin{bmatrix} X & X_2 \\ X_2^T & X_3 \end{bmatrix} \succ 0 \text{ and } \begin{bmatrix} X & X_2 \\ X_2^T & X_3 \end{bmatrix}^{-1} = \begin{bmatrix} Y & Y_2 \\ Y_2^T & Y_3 \end{bmatrix} \tag{3.41}$$

2. $\begin{bmatrix} X & I \\ I & Y \end{bmatrix} \succeq 0$ *and* **rank** $\begin{bmatrix} X & I \\ I & Y \end{bmatrix} \leq n + r$

3. $\begin{bmatrix} X & I \\ I & Y \end{bmatrix} \succeq 0$ *and* **rank** $[XY - I] \leq r$

This lemma is useful for solving LMIs. It allow to simplify the number of variables when a matrix and its inverse enter in a LMI.

3.3 Notion of robustness and dissipativity

In control theory, the robustness means that, for a given controller, the closed loop system remains stable (robust stability) or maintains a certain level of performance (robust performance) for a given level of uncertainties. The notion of robustness is very large and often misused since it is often related to the $\mathcal{H}_\infty$ control design. Even if this approach has some interesting properties concerning robustness, it is not the only one and other design approaches are also robust if they are well designed (e.g. pole placement). Usually, $\mathcal{H}_\infty$ design approach is introduced, thanks to the small gain theorem (see e.g. Zhou *et al.*, 1996). By the way, in this section, we aim at introducing the LMI approach to $\mathcal{H}_\infty$, $\mathcal{H}_2$ and other control designs through the dissipative approach (inspired from (Scherer and Wieland, 2004; Scherer, 2000)).

3.3.1 Feedback(forward) framework

In the control synthesis problem, the control laws are mainly of two types:

- The "open loop" control, known as feedforward, which does not use any system measured information, and which is of the form:

$$u_{ff} = C_{ff} w_{ref} \tag{3.42}$$

  where u_{ff} is the feedforward control, w_{ref} the reference signal and C_{ff} the feedforward compensator (either static or dynamic).

- The "closed loop" control, known as feedback, which involves measurements of the system variables (denoted as y), and which is of the form:

$$u_{fb} = C_{fb} y \tag{3.43}$$

where u_{fb} is the feedback control, y the measured variable and C_{fb} the feedback controller (either static or dynamic).

Then generally, we can write,

$$u = u_{ff} + u_{fb} = \begin{bmatrix} C_{ff} \\ C_{fb} \end{bmatrix} \begin{bmatrix} w_{ref} \\ y \end{bmatrix} = C \begin{bmatrix} w_{ref} \\ y \end{bmatrix} \tag{3.44}$$

By assuming that w_{ref} is part of the "measured signal", we can write $u = Cy$. Figure 3.2 gives the general framework of the study, known as the standard problem, where:

- $\Sigma(s)$ is the system model, that can be either LTI, LPV, switched, nonlinear... Usually $\Sigma(s)$ includes both actuators and sensors models.
- $C(s)$ is the controller, that controls the system $\Sigma(s)$ (it can be LTI, LPV, nonlinear...)
- $w(t)$ represents the exogenous system inputs (reference, disturbances, noise, etc.).
- $y(t)$ is the output (or measured) signal, provided by a sensor on the system, and used by the controller.
- $u(t)$ is the control signal, provided by the controller $C(s)$, that feeds the system $\Sigma(s)$.
- $z(t)$ is the controlled output.

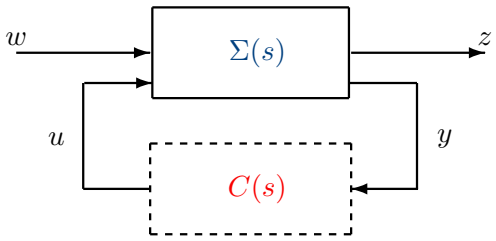

Figure 3.2: Standard Problem.

3.3.2 Feedback and performance specifications

The feedback control problem consists in finding a controller that:

- Stabilizes the closed-loop system.
- Provides performance to the specified controlled output.
- Ensures these properties in presence of uncertainties (if possible).

A classical approach consists in synthesizing a controller $C(s)$ and in studying the frequency shape of the loop transfer defined as $L(s) = \Sigma(s)C(s)$. The aim is then to shape such $L(s)$ to guarantee some performances, e.g., high gain in low frequencies and low gain in high frequencies. This approach is known as loop shaping (see e.g. (McFarlane and Glover, 1992)). Another widely used approach is the so called Standard Problem Formulation as shown on Figure 3.2. This formalism present the advantage to be easy to derive practically.

The extension of the Standard Problem through the interconnection of the input (W_i) and output (W_o) weighting functions allows to select and shape some specific controlled output in the frequency domain (as illustrated on Figure 3.3).

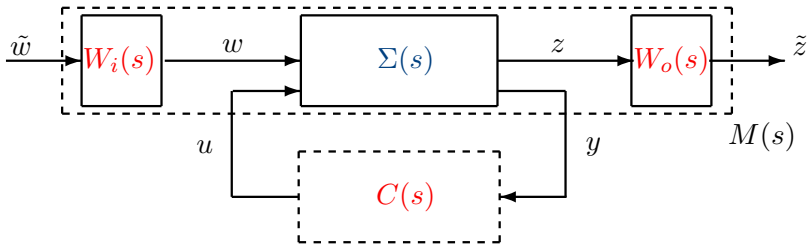

Figure 3.3: Generalized control scheme.

Remark: About performance and stability From the mathematical point of view, all performance problems can be viewed as a stabilization problem under constraints (e.g. $\mathcal{H}_\infty$).

3.3.3 Dissipative dynamical systems

Dissipativity is a fundamental property of physical systems. It is closely related to the intuitive phenomena of loss or dissipation of energy, which is a good starting point to understand the notions of $\mathcal{H}_\infty$, $\mathcal{H}_2$, passivity, used is this thesis. To mathematically define such a property, we consider the general nonlinear system definition (3.1) and introduce two functions:

- $V(x(t))$, the storage function which measures the amount of energy stored inside the system, and defined as:

$$V : X \to \mathbb{R} \tag{3.45}$$

  Note that the storage function generalizes the notion of energy function for a dissipative system and is linked with the Lyapunov function.

- $s(w(t), z(t))$, the supply rate which defines the rate at which energy flows into the system, and defined as:

$$s : W \times Z \to \mathbb{R} \tag{3.46}$$

  where $w \in W$ and $z \in Z$. Then, assume that for all $t_0 < t_1 \in \mathbb{R}$, the supply function $s(w(t), z(t))$ (or supply rate), which represents the supply delivered to the system, is locally absolutely integrable.

These functions are related to the dissipativity inequality, defined thereafter.

Definition 3.3.1 (*Dissipativity*)

The nonlinear system defined by

$$\Sigma_{\mathcal{NL}} : \begin{cases} \dot{x}(t) &= f(x(t), w(t)) \\ z(t) &= g(x(t), w(t)) \end{cases} \tag{3.47}$$

with the supply function $s(w(t), z(t))$, or simply $s(w, z)$, is said to be dissipative if there exists a storage function $V(x(t))$ such that for all $t_0 \leq t_1$,

$$\begin{aligned} & V(x(t_0)) + \int_{t_0}^{t_1} s(w(t), z(t))dt \geq V(x(t_1)) \\ \Leftrightarrow \quad & V(x(t_1)) - V(x(t_0)) - \int_{t_0}^{t_1} s(w(t), z(t))dt \leq 0 \\ \Leftrightarrow \quad & \int_{t_0}^{t_1} \big[\frac{\partial V(x(t))}{\partial t} - s(w(t), z(t))\big]dt \leq 0 \end{aligned} \tag{3.48}$$

where all signals ($w(t) \in W$, $x(t) \in X$ and $z(t) \in Z$) satisfy the nonlinear system dynamical equations. The pair $(\Sigma_{\mathcal{NL}}, s(w, z))$ is said to be

- *Conservative, if equality holds for all $t_0 \leq t_1$.*
- *Strictly dissipative, if the strict inequality holds in (3.48).*

This definition states that along the time trajectories of a dissipative system, the supply rate is not less than its increase in storage. A dissipative system cannot store more energy than the supply amount fed from the outside.

There is no particular assumption made on $s(w, z)$ or its integral. The supply function can be interpreted as the supply delivered to the system, so it represents the rate at which supply flows into the system. Note also that the storage function does not have to be strictly positive.

Property 3.3.1 (*Local dissipativity*)

If $V(x(t))$ is differentiable, by taking the time derivative, the last statement of (3.48) is equivalent to:

$$\frac{\partial V(x(t))}{\partial x} f(x(t), w(t)) \leq s\big(w(t), g(x(t), z(t))\big) \tag{3.49}$$

for all $\{x(t), w(t), z(t)\}$ solution of $\Sigma_{\mathcal{NL}}$. According to this property, it comes out that the dissipativity of dynamical systems is a local property.

3.4 Linear systems with quadratic supply functions

Up to now, the dissipativity has been introduced and defined in a very general way, considering general (nonlinear) systems and supply function. In this section the considered systems are LTI systems, and supply and storage functions are quadratic:

LTI system. According to definition (3.2.2), the system is defined as,

$$\Sigma_{LTI} : \begin{cases} \dot{x}(t) &= Ax(t) + Bw(t) \\ z(t) &= Cx(t) + Dw(t) \end{cases} \tag{3.50}$$

and $T(j\omega)$ is the corresponding transfer matrix, associated to Σ_{LTI}.

Quadratic supply function. Consider the supply function as a quadratic function, defined by:

$$\begin{aligned} s(w,z) &= \begin{bmatrix} w \\ z \end{bmatrix}^T \begin{bmatrix} Q & S \\ S^T & R \end{bmatrix} \begin{bmatrix} w \\ z \end{bmatrix} \\ &= \begin{bmatrix} x \\ w \end{bmatrix}^T \begin{bmatrix} 0 & I \\ C & D \end{bmatrix}^T \begin{bmatrix} Q & S \\ S^T & R \end{bmatrix} \begin{bmatrix} 0 & I \\ C & D \end{bmatrix} \begin{bmatrix} x \\ w \end{bmatrix} \\ &= w^TQw + w^TSz + z^TS^Tw + z^TRz \end{aligned} \tag{3.51}$$

Let us define P as:

$$P := \begin{bmatrix} Q & S \\ S^T & R \end{bmatrix} \in \mathbb{R}^{n_w+n_z} \tag{3.52}$$

a real symmetric matrix where no a priori assumptions are made.

Quadratic storage function. Consider now quadratic storage functions defined as:

$$V(x(t)) = x(t)^TKx(t) \text{ and } V(x(0)) = 0 \tag{3.53}$$

Note that this quadratic storage function is a Lyapunov function.

3.4.1 General quadratic performances

Proposition 3.4.1 (*Linear system with quadratic supply rate dissipativity*)

Suppose that the system Σ_{LTI} defined in (3.2) is controllable. Let choose a quadratic supply function $s(w,z) = w^TQw + w^TSz + z^TS^Tw + z^TRz$, then the following statements are equivalent:

- *(Σ_{LTI}, s) is (strictly) dissipative*
- *(Σ_{LTI}, s) admits a quadratic storage function $V(x) = x^TKx$, with $K = K^T \succ 0$*
- *There exists a $K = K^T \succ 0$ such that the following LMI is feasible*

$$\begin{aligned} F(K) &= \begin{bmatrix} A^TK + KA & KB \\ B^TK & 0 \end{bmatrix} - \begin{bmatrix} 0 & I \\ C & D \end{bmatrix}^T \underbrace{\begin{bmatrix} Q & S \\ S^T & R \end{bmatrix}}_{P} \begin{bmatrix} 0 & I \\ C & D \end{bmatrix} (\prec) \preceq 0 \\ &= \left[\begin{array}{cc} I & 0 \\ A & B \\ \hline 0 & I \\ C & D \end{array}\right]^T \left[\begin{array}{cc|cc} 0 & K & 0 & 0 \\ K & 0 & 0 & 0 \\ \hline 0 & 0 & -Q & -S \\ 0 & 0 & -S^T & -R \end{array}\right] \left[\begin{array}{cc} I & 0 \\ A & B \\ \hline 0 & I \\ C & D \end{array}\right] (\prec) \preceq 0 \end{aligned} \tag{3.54}$$

- *$\forall \omega \in \mathbb{R}$ with $\det(j\omega I - A) \neq 0$, the transfer function $T(j\omega) = C(j\omega I - A)^{-1}B + D$ satisfies (Kalman-Yakubovich-Popov lemma)*

$$\begin{bmatrix} I \\ T(j\omega) \end{bmatrix}^* \begin{bmatrix} Q & S \\ S^T & R \end{bmatrix} \begin{bmatrix} I \\ T(j\omega) \end{bmatrix} (>) \geq 0 \tag{3.55}$$

From the Linear (strict) dissipative definition expressed above, we can derive the general quadratic constraints as the following inequality:

$$\begin{aligned} &\left[\begin{array}{cc|cc} I & 0 & & \\ A & B & & \\ \hline 0 & I & & \\ C & D & & \end{array}\right]^T \left[\begin{array}{cc|cc} 0 & K & 0 & 0 \\ K & 0 & 0 & 0 \\ \hline 0 & 0 & -Q & -S \\ 0 & 0 & -S^T & -R \end{array}\right] \left[\begin{array}{cc|cc} I & 0 & & \\ A & B & & \\ \hline 0 & I & & \\ C & D & & \end{array}\right] (\prec) \preceq 0 \\ \Leftrightarrow \quad &\left[\begin{array}{cc} A^TK + KA - C^TRC & KB - C^TRD - C^TS^T \\ B^TK - D^TRC - SC & D^TRD - SD - D^TS^T - Q \end{array}\right] (\prec) \preceq 0 \end{aligned} \tag{3.56}$$

The structure of P (3.52) will express the way the input/output energy flows into the system. According to this matrix, we will then be able to define different performance criteria, with different properties e.g. (see also previous sections and the system norm definitions):

- The passivity performance is used to enforce dissipative properties of the closed loop (this property is widely used in e.g. electrical systems or networked control systems). This property ensures that the introduced energy is dissipated into the system. This approach is linked with the passivity theory.

- The $\mathcal{H}_\infty$ performance is used to enforce robustness to model uncertainties and to express frequency-domain performance specifications. Note that this approach is expressed here as a dissipative property, but is often introduced in the literature with the small gain theorem (the link between the two approaches is presented later in this chapter).

- The $\mathcal{H}_2$ performance can be used to handle stochastic aspects (noise, random disturbance). It is also used to reduce output signal energy.

- Time-domain constraints are used to tune transient responses and peak amplitudes, overshoots, etc.

- Pole placement can be useful to avoid fast dynamics and high frequencies in the controller (to facilitate digital implementation).

In the following, we derive examples of some well known quadratic supply functions, and give some physical interpretation. These quadratic functions are fundamental in order to introduce the control synthesis approach used in this thesis (Scherer *et al.*, 1997; Scherer and Wieland, 2004).

3.4.2 Passivity performances

Proposition 3.4.2 (*Passivity as LMIs*)

Suppose that the system Σ_{LTI} defined in (3.2) is controllable. Let us consider the quadratic supply function $s(w,z) = z^T w + w^T z$, then the following statements are equivalent:

- *(Σ_{LTI}, s) is dissipative.*
- *There exist $K = K^T \succ 0$ such that the following LMI is feasible,*

$$\left[\begin{array}{cc} I & 0 \\ A & B \\ \hline 0 & I \\ C & D \end{array}\right]^T \left[\begin{array}{cc|cc} 0 & K & 0 & 0 \\ K & 0 & 0 & 0 \\ \hline 0 & 0 & 0 & -I \\ 0 & 0 & -I & 0 \end{array}\right] \left[\begin{array}{cc} I & 0 \\ A & B \\ \hline 0 & I \\ C & D \end{array}\right] \preceq 0 \tag{3.57}$$

- *$\forall \omega \in \mathbb{R}$ with $\det(j\omega I - A) \neq 0$, the transfer function $T(j\omega) = C(j\omega I - A)^{-1}B + D$ satisfies (Kalman-Yakubovich-Popov lemma),*

$$T(j\omega)^* + T(j\omega) \geq 0 \tag{3.58}$$

The corresponding dissipative function is given by,

$$x^T(t)Kx(t) - \int_0^t \big(z^T(\tau)w(\tau) + w^T(\tau)z(\tau)\big)d\tau \tag{3.59}$$

and the he quadratic form is:

$$P = \left[\begin{array}{cc} 0 & I \\ I & 0 \end{array}\right] \tag{3.60}$$

This proposition is also known as the Positive Real Lemma (PRL). This lemma played an important role in the history of LMIs, since it was one of the first problems related to the stability of controlled systems (see Chapter 2). Note that for SISO systems, positive realness of the transfer function means that its Nyquist plot entirely lies in the right half complex plane.

3.4.3 $\mathcal{H}_\infty$ performances

The $\mathcal{H}_\infty$ problem consists in minimizing, or bounding to a given γ_∞ level, the system gain between $||w||_2$ and $||z||_2$ ($\mathcal{L}_2$ to $\mathcal{L}_2$ induced norm).

Proposition 3.4.3 ($\mathcal{H}_\infty$ *as LMIs*)

Suppose that the system Σ_{LTI} defined in (3.2) is controllable. Let us consider the quadratic supply function $s(w,z) = \gamma_\infty^2 w^T w - z^T z$, then the following statements are equivalent:

- *(Σ_{LTI}, s) is dissipative.*
- *There exists $K = K^T \succ 0$ such that the following LMI is feasible,*

$$\left[\begin{array}{cc} I & 0 \\ A & B \\ \hline 0 & I \\ C & D \end{array}\right]^T \left[\begin{array}{cc|cc} 0 & K & 0 & 0 \\ K & 0 & 0 & 0 \\ \hline 0 & 0 & -\gamma_\infty^2 I & 0 \\ 0 & 0 & 0 & I \end{array}\right] \left[\begin{array}{cc} I & 0 \\ A & B \\ \hline 0 & I \\ C & D \end{array}\right] \prec 0 \tag{3.61}$$

- *$\forall \omega \in \mathbb{R}$ with $\det(j\omega I - A) \neq 0$, the transfer function $T(i\omega) = C(j\omega I - A)^{-1}B + D$ satisfies (Kalman-Yakubovich-Popov lemma),*

$$T^*(j\omega) \times T(j\omega) < \gamma_\infty^2 I \tag{3.62}$$

Then, it follows

$$\begin{array}{rl} & \dfrac{z^*(j\omega)z(j\omega)}{w(j\omega)^* w(j\omega)} < \gamma_\infty^2 \\ \Leftrightarrow & \dfrac{||z||_2^2}{||w||_2^2} < \gamma_\infty^2 \\ \Leftrightarrow & ||T(j\omega)||_\infty = \sup\limits_{\omega \in \mathbb{R}} \sigma_{max}(T(j\omega)) < \gamma_\infty^2 \end{array} \tag{3.63}$$

The corresponding dissipative function is given by,

$$x^T(t)Kx(t) - \int_0^t \left(\gamma_\infty^2 w^T(\tau)w(\tau) - z^T(\tau)z(\tau)\right)d\tau \tag{3.64}$$

and the quadratic form is:

$$P = \left[\begin{array}{cc} \gamma_\infty^2 I & 0 \\ 0 & -I \end{array}\right] \tag{3.65}$$

The $\mathcal{L}_2$-norm of the output z of a system Σ_{LTI} is uniformly bounded by γ_∞^2 times the $\mathcal{L}_2$-norm of the input w (initial condition $x(0) = 0$). This property is the basis of the $\mathcal{H}_\infty$ control, later used in this thesis. Then the well known Bounded Real Lemma (BRL), that leads to the LMI approach of the

$\mathcal{H}_\infty$ control is derived as follows:

$$
\begin{aligned}
& \left[\begin{array}{cc|cc} I & 0 & & \\ A & B & & \\ \hline 0 & I & & \\ C & D & & \end{array}\right]^T \left[\begin{array}{cc|cc} 0 & K & 0 & 0 \\ K & 0 & 0 & 0 \\ \hline 0 & 0 & -\gamma^2 I & 0 \\ 0 & 0 & 0 & I \end{array}\right] \left[\begin{array}{cc|cc} I & 0 & & \\ A & B & & \\ \hline 0 & I & & \\ C & D & & \end{array}\right] \prec 0 \\
\Leftrightarrow & \left[\begin{array}{cc} A^TK + KA + C^TC & KB + C^TD \\ B^TK + D^TC & D^TD - \gamma^2 I \end{array}\right] \prec 0 \\
\Leftrightarrow & \left[\begin{array}{cc} A^TK + KA & KB \\ B^TK & -\gamma^2 I \end{array}\right] + \left[\begin{array}{cc} C^TC & C^TD \\ D^TC & D^TD \end{array}\right] \prec 0 \\
\Leftrightarrow & \left[\begin{array}{cc} A^TK + KA & KB \\ B^TK & -\gamma^2 I \end{array}\right] + \left[\begin{array}{c} C^T \\ D^T \end{array}\right] I \left[\begin{array}{cc} C & D \end{array}\right] \prec 0 \\
\Leftrightarrow & \left[\begin{array}{ccc} A^TK + KA & KB & C^T \\ B^TK & -\gamma^2 I & D^T \\ C & D & -I \end{array}\right] \prec 0
\end{aligned}
\tag{3.66}
$$

Note that the BRL is an LMI if the only unknown (decision variables) are K and γ^2. In the case of the control synthesis, this BRL is no longer an LMI but a Bilinear Matrix Inequality (BMI). In the next section, we will illustrate this problem through the dynamical output feedback control synthesis. In this case, relaxation techniques have to be applied in order to turn it into a LMI, tractable for LMI solver. For that purpose, the Completion lemma or Projection lemma are commonly used (see e.g. Scherer *et al.*, 1997; Clement and Duc, 2000; Arzelier and Peaucelle, 2004*a*; Iwasaki and Skelton, 1994).

3.4.4 Relation with the small gain theorem

Theorem: Small gain (first version). Let consider the control loop given on Figure 3.4 where Σ is a stable system (Bounded Input Bounded Output). The loop is internally stable iff. (Zhou *et al.*, 1996),

$$\forall x(t), y(t) \in \mathcal{L}_2, ||\Sigma(x(t)) - \Sigma(y(t))||_2 \leq \alpha ||x(t) - y(t)||_2 \tag{3.67}$$

where $0 < \alpha < 1$. Then if Σ is a linear system, this condition is equivalent to,

$$||\Sigma||_\infty < 1 \tag{3.68}$$

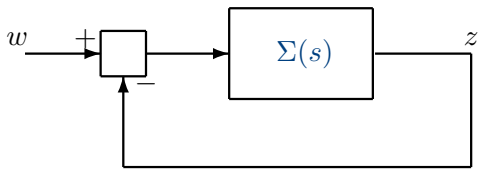

Figure 3.4: Small gain theorem (first version).

△

Theorem: Small gain (second version). Let consider the control loop given on Figure 3.5 where Σ is a LTI nominally stable system (i.e. $\in \mathcal{RH}_\infty$), $\gamma > 0$. The interconnected system on Figure 3.5 is well-posed and internally stable for all $\Delta \in \mathcal{RH}_\infty$ with, (Zhou *et al.*, 1996).

$$||\Delta||_\infty \leq \frac{1}{\gamma} \text{ iff. } ||M||_\infty \leq \frac{1}{\gamma} \tag{3.69}$$

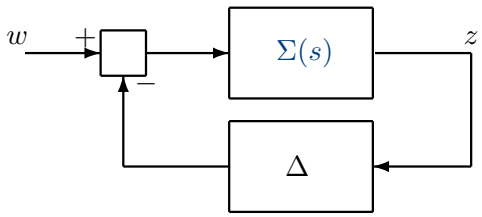

Figure 3.5: Small gain theorem (second version).

△

3.4.5 $\mathcal{H}_2$ performances

Proposition 3.4.4 ($\mathcal{H}_2$ *as LMIs*)

Suppose that the system Σ_{LTI} defined in (3.2) asymptotically stable and strictly proper, e.g. $D = 0$ with $T(j\omega)$ is the corresponding transfer function. Let us consider the quadratic supply function $s(w, z) = w^T w$, then the following statements are equivalent:

1. $||T(j\omega)||_2 < \gamma_2$
2. *There exists a $X = X^T \succ 0$ such that,*

$$\begin{array}{rcl} AX + XA^T + BB^T & \prec & 0 \\ \mathbf{Tr}(CXC^T) < \gamma_2^2 & & \end{array} \tag{3.70}$$

3. *There exists a $Y = Y^T \succ 0$ such that,*

$$\begin{array}{rcl} AY + YA^T + C^T C & \prec & 0 \\ \mathbf{Tr}(B^T Y B) < \gamma_2^2 & & \end{array} \tag{3.71}$$

4. *There exists a $K = K^T \succ 0$ and Z such that the following LMIs are feasible,*

$$\begin{array}{rcl} \begin{bmatrix} A^T K + KA & KB \\ B^T K & -I \end{bmatrix} & < & 0 \\ \begin{bmatrix} K & C^T \\ C & Z \end{bmatrix} & > & 0 \\ \mathbf{Tr}(Z) & < & \gamma_2^2 \end{array} \tag{3.72}$$

5. *There exists a $K = K^T \succ 0$ and Z such that the following LMIs are feasible,*

$$\begin{array}{rcl} \begin{bmatrix} A^T K + KA & KC^T \\ CK & -I \end{bmatrix} & < & 0 \\ \begin{bmatrix} K & B \\ B^T & Z \end{bmatrix} & > & 0 \\ \mathbf{Tr}(Z) & < & \gamma_2^2 \end{array} \tag{3.73}$$

The corresponding dissipative function is given by (according to first inequality),

$$x^T(t)Kx(t) - \int_0^t \big(w^T(\tau)w(\tau)\big)d\tau \tag{3.74}$$

and (thanks to second inequality),

$$\frac{1}{\alpha}C^T C < K \tag{3.75}$$

and the the quadratic form is given by,

$$P = \begin{bmatrix} 0 & I \\ I & 0 \end{bmatrix} \tag{3.76}$$

3.4.6 Generalized $\mathcal{H}_2$ performances

The Generalized $\mathcal{H}_2$ norm consists in keeping the peak amplitude of the output z under a certain value to avoid e.g. actuator saturations.

Proposition 3.4.5 (*Generalized $\mathcal{H}_2$ as LMIs*)

Consider a system Σ_{LTI} asymptotically stable and strictly proper, e.g. $D = 0$ ($T(j\omega)$ is the corresponding transfer function). Let consider the quadratic supply function $s(w, z) = w^T w$, then the following statements are equivalent:

1. *(Σ_{LTI}, s) is dissipative.*
2. *There exists a $K = K^T \succ 0$ such that the following LMIs are feasible,*

$$\begin{array}{rcl} \left[\begin{array}{cc} A^T K + KA & KB \\ B^T K & -I \end{array} \right] & \prec & 0 \\ \left[\begin{array}{cc} K & C^T \\ C & \gamma_2^2 I \end{array} \right] & \succ & 0 \end{array} \tag{3.77}$$

The corresponding dissipative function is (according to first inequality),

$$x^T(t) K x(t) - \int_0^t \big(w(\tau)^T w(\tau)\big) d\tau \leq 0 \tag{3.78}$$

and (thanks to second inequality),

$$\frac{1}{\gamma_2^2} C^T C < K \tag{3.79}$$

The quadratic form is given by,

$$P = \left[\begin{array}{cc} 0 & I \\ I & 0 \end{array} \right] \tag{3.80}$$

It yields also to,

$$\begin{array}{rcl} z(t)^T z(t) = x(t)^T C^T C x(t) & < & \gamma_2^2 K \\ & < & \gamma_2^2 \displaystyle\int_0^t \big(w^T(\tau) w(\tau)\big) d\tau \end{array} \tag{3.81}$$

and taking the supremum leads to ($\forall w \in \mathcal{L}_2$),

$$||z||_\infty^2 < \gamma_2^2 ||w||_2^2 \tag{3.82}$$

3.5 LMI based LTI control synthesis

In this Section, $\mathcal{H}_\infty$, $\mathcal{H}_2$ and mixed $\mathcal{H}_\infty$ /$\mathcal{H}_2$ controller synthesis results are given using LMIs, since they are widely used in this thesis. First the general formulation is recalled in order to define the generalized problem, then LMIs solutions are derived in the LTI framework.

3.5.1 General problem formulation (LTI case)

In order to introduce the LMI based solution for controller synthesis, first the definition of the generalized problem is recalled. Now, let consider the following description of the generalized LTI system M as,

$$M : \left[\begin{array}{c} \dot{x} \\ \hline z \\ y \end{array}\right] = \left[\begin{array}{c|cc} A & B_1 & B_2 \\ \hline C_1 & D_{11} & D_{12} \\ C_2 & D_{21} & D_{22} \end{array}\right] \left[\begin{array}{c} x \\ \hline w \\ u \end{array}\right] \tag{3.83}$$

where x is the state vector of the system plus the state vector of the weighting functions, z holds for the controlled output of the system (i.e. the variables we aim at controlling with a performance criteria), y are the measured values (that will feed the controller), w holds for the exogenous signals and u, the control input signal. Now we will assume $x \in X \subset \mathbb{R}^n$, $z \in Z \subset \mathbb{R}^{n_z}$, $y \in Y \subset \mathbb{R}^{n_y}$, $w \in W \subset \mathbb{R}^{n_w}$ and $u \in U \subset \mathbb{R}^{n_u}$.

Then, according to this general formulation, the controller C is defined as,

$$\left[\begin{array}{c} \dot{x}_c \\ u \end{array}\right] = \left[\begin{array}{cc} A_c & B_c \\ C_c & D_c \end{array}\right] \left[\begin{array}{c} x_c \\ y \end{array}\right] \tag{3.84}$$

where $x_c \in X_c \subset \mathbb{R}^n$, $u \in U \subset \mathbb{R}^{n_u}$, $y \in Y \subset \mathbb{R}^{n_y}$.

Remark: Dynamical Output Feedback. In this thesis only Dynamical Output Feedback controller are used. Then all approaches are done in order to synthesize a controller C of the form (3.84).

Then, the resulting closed-loop system in Figure 3.2, also denoted through the lower Linear Fractional Representation (LFR) is given by (see also Appendix C.3),

$$\mathcal{F}_l(M, C) : \left[\begin{array}{c} \dot{\xi} \\ z \end{array}\right] = \left[\begin{array}{cc} \mathcal{A} & \mathcal{B} \\ \mathcal{C} & \mathcal{D} \end{array}\right] \left[\begin{array}{c} \xi \\ w \end{array}\right] \tag{3.85}$$

where,

$$\begin{array}{rcl} \mathcal{A} & = & \left[\begin{array}{cc} A + B_2(I - D_cD_{22})^{-1}D_cC_2 & B_2(I - D_cD_{22})^{-1}C_c \\ B_c(I - D_cD_{22})^{-1}C_2 & A_c + B_c(I - D_cD_{22})^{-1}D_{22}C_c \end{array}\right] \\ \mathcal{B} & = & \left[\begin{array}{c} B_1 + B_2(I - D_cD_{22})^{-1}D_cD_{21} \\ B_c(I - D_cD_{22})^{-1}D_{21} \end{array}\right] \\ \mathcal{C} & = & \left[\begin{array}{cc} C_1 + D_{12}(I - D_cD_{22})^{-1}D_cC_2 & D_{12}(I - D_cD_{22})^{-1}C_c \end{array}\right] \\ \mathcal{D} & = & D_{11} + D_{12}(I - D_cD_{22})^{-1}D_cD_{21} \end{array} \tag{3.86}$$

For sake of simplicity, we will often consider $D_{22} = 0$ (i.e. no direct feed-through from input to output, hence, strictly proper transfer function). The resulting closed-loop system is then given as,

$$\begin{array}{rcl} \mathcal{A} & = & \left[\begin{array}{cc} A + B_2D_cC_2 & B_2C_c \\ B_cC_2 & A_c \end{array}\right] \\ \mathcal{B} & = & \left[\begin{array}{c} B_1 + B_2D_cD_{21} \\ B_cD_{21} \end{array}\right] \\ \mathcal{C} & = & \left[\begin{array}{cc} C_1 + D_{12}D_cC_2 & D_{12}C_c \end{array}\right] \\ \mathcal{D} & = & D_{11} + D_{12}D_cD_{21} \end{array} \tag{3.87}$$

where $\xi = [x^T \; x_c^T]^T \in \mathbb{R}^{2n}$, $z \in \mathbb{R}^{n_z}$, $w \in \mathbb{R}^{n_w}$.

The objective of a controller is to make $\mathcal{A}$ Hurwitz (i.e. render the closed loop system stable) and to achieve some performance specification on the transfer from exogenous input w to controlled outputs z. It is worth noting that all control problems can be viewed as a stabilization problem (with or without constraint, like $\mathcal{H}_2$, $\mathcal{H}_\infty$, etc.).

3.5.2 Hurwitz condition and α-stability

3.5.2.1 Hurwitz condition

The main role of a controller is to ensure the internal stability of the closed-loop system. The aim is to find a Lyapunov function K that satisfies,

$$V(\xi) = \xi^T K \xi \text{ where } K = K^T \succ 0 \tag{3.88}$$

such that,

$$\dot{V}(\xi) = \xi^T \big(\mathcal{A}^T K + K\mathcal{A}\big)\xi < 0 \tag{3.89}$$

For stability, solving such LMIs in K proves the closed-loop stability. But, finding a controller ensuring stability is generally not obvious according to the controller structure. As a matter of fact, when the stabilizing controller has to be found, (3.89) is a BMI since $\mathcal{A}$ is composed of unknown elements (e.g. the controller matrices A_c, C_c, C_c and D_c) coupled with the unknown Lyapunov matrix K. Then relaxations techniques have to be applied to "convexify" the problem.

Thereafter, relaxation of some problems are given since they are used for control purpose later in the thesis.

3.5.2.2 α-stability

The α-stability is closely related to the Hurwitz condition since it consists in a slight modification. For control synthesis, it consists in placing poles in a certain region (e.g. $\left[\begin{array}{cc} \underline{\alpha} & \overline{\alpha} \end{array}\right]$). Let consider the following Lyapunov functions:

$$\begin{array}{rcl} V_1 & = & \xi^T K e^{2\underline{\alpha}t} \xi > 0 \\ V_2 & = & \xi^T K e^{2\overline{\alpha}t} \xi > 0 \end{array} \tag{3.90}$$

where $\underline{\alpha}$ (respectively $\overline{\alpha}$) is the desired lowest (respectively highest) pole of the closed loop. The derivative of this function leads to the following inequalities to be satisfied:

$$\begin{array}{rcl} \dot{V} & = & \xi^T e^{2\underline{\alpha}t} (\mathcal{A}^T K + K\mathcal{A} + 2\underline{\alpha} K)\xi < 0 \\ \dot{V} & = & \xi^T e^{2\underline{\alpha}t} (\mathcal{A}^T K + K\mathcal{A} + 2\overline{\alpha} K)\xi > 0 \end{array} \tag{3.91}$$

These LMI conditions ensure that the poles of the closed loop are located within the region defined between $\left[\begin{array}{cc} \underline{\alpha} & \overline{\alpha} \end{array}\right]$.

Remark: About the Lyapunov function. Note that this formulation is only a change of basis. Instead of guaranteeing that the Lyapunov equation derivative ($\dot{V}$) is negative (i.e. $\dot{V} < 0$, one guarantees that its derivative, i.e. the convergence dynamic is lower that $\underline{\alpha}$. The same remark holds for $\overline{\alpha}$.

3.5.3 $\mathcal{H}_\infty$ design

For any system, the $\mathcal{H}_\infty$ control synthesis is a disturbance attenuation problem. It consists in finding a stabilizing controller that minimizes the impact of the input disturbances $w(t)$ on the controlled output $z(t)$. In the case of the $\mathcal{H}_\infty$ control, this impact is measured thanks to the induced $\mathcal{L}_2$ norm. This problem is represented on Figure 3.6.

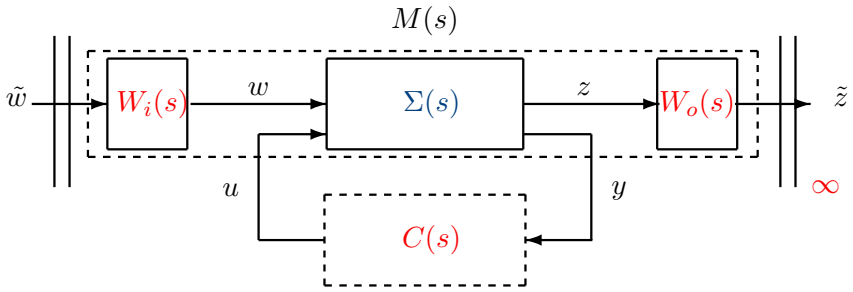

Figure 3.6: Generalized $\mathcal{H}_\infty$ problem.

A more formal way to formulate this problem can be written as: minimize the $\mathcal{H}_\infty$ norm of the interconnection of M and C on the set of internally stabilizing controllers so that the $\mathcal{H}_\infty$ norm of the transfer functions $T_{zw}(s)$, from input w to output z satisfies,

$$\begin{array}{rcl} ||T_{zw}(s)||_\infty & = & ||\mathcal{C}(sI-\mathcal{A})^{-1}\mathcal{B}+\mathcal{D}||_\infty < \gamma_\infty \\ & = & ||\mathcal{F}_l(M,C)||_\infty < \gamma_\infty \end{array} \tag{3.92}$$

Now, when we refer to the $\mathcal{H}_\infty$ control problem, we mean: Find a controller C for system M such that, given γ_∞,

$$||\mathcal{F}_l(M,C)||_\infty < \gamma_\infty \tag{3.93}$$

The minimum of this norm is denoted as γ_∞^* and is called the optimal $\mathcal{H}_\infty$ gain. Hence, it comes,

$$\gamma_\infty^* = \min_{(A_c,B_c,C_c,D_c) s.t. \sigma\mathcal{A}\subset\mathbb{C}^-} \|T_{zw}(s)\|_\infty \tag{3.94}$$

As presented in the previous sections, this condition is fulfilled thanks to the BRL. As a matter of fact, the system is internally stable and meets the quadratic $\mathcal{H}_\infty$ performances iff. $\exists\ K = K^T \succ 0$ such that (see Proposition 3.4.3),

$$\begin{bmatrix} \mathcal{A}^T K + K\mathcal{A} & K\mathcal{B} & \mathcal{C}^T \\ \mathcal{B}^T K & -\gamma_2^2 I & \mathcal{D}^T \\ \mathcal{C} & \mathcal{D} & -I \end{bmatrix} \prec 0 \tag{3.95}$$

where $\mathcal{A}$, $\mathcal{B}$, $\mathcal{C}$, $\mathcal{D}$ are given in (3.86). Then, as an illustration,

$$\mathcal{B}K = \begin{bmatrix} B_1 + B_2 D_c D_{21} \\ B_c D_{21} \end{bmatrix} \begin{bmatrix} K_1 \\ K_2 \end{bmatrix} = \begin{bmatrix} B_1 K_1 + B_2 D_c D_{21} K_1 \\ B_c D_{21} K_2 \end{bmatrix} \tag{3.96}$$

where K_1, K_2, B_c and D_c are unknown and coupled. Since this inequality is not an LMI and not tractable for SDP solver, relaxations have to be performed (indeed it is a BMI). In the following, we provide the LMI solution of such a problem for the Dynamical Output Feedback case (DOF) (interested reader also can refer to the proof given in Appendix A.1).

Remark: About state and static output feedback. Note that the state feedback solution is even simpler to derive. However, the static output feedback remains an open research area since it is not possible to turn it into an LMI (for the pole placement problem, it has been shown to be NP hard (see e.g. Fu, 2004)). Therefore, this field of research remains one of the open problems, that is very interesting since, if a solution can be found, the controller to be implemented can drastically be improved.

Result 3.5.1 (*LTI/$\mathcal{H}_\infty$ solution (Scherer* et al., *1997)*)

A dynamical output feedback controller of the form $C(s) = \left[\begin{array}{c|c} A_c & B_c \\ \hline C_c & D_c \end{array}\right]$ *that solves the* $\mathcal{H}_\infty$ *control problem, is obtained by solving the following LMIs in (*$\boldsymbol{X}$, $\boldsymbol{Y}$, $\widetilde{\boldsymbol{A}}$, $\widetilde{\boldsymbol{B}}$, $\widetilde{\boldsymbol{C}}$ *and* $\widetilde{\boldsymbol{D}}$*), while minimizing* γ_∞*,*

$$\begin{array}{l} \left[\begin{array}{cccc} M_{11} & (*)^T & (*)^T & (*)^T \\ M_{21} & M_{22} & (*)^T & (*)^T \\ M_{31} & M_{32} & M_{33} & (*)^T \\ M_{41} & M_{42} & M_{43} & M_{44} \end{array}\right] \prec 0 \\ \left[\begin{array}{cc} \boldsymbol{X} & I_n \\ I_n & \boldsymbol{Y} \end{array}\right] \succ 0 \end{array} \tag{3.97}$$

where,

$$\begin{array}{rcl} M_{11} & = & A\boldsymbol{X} + \boldsymbol{X}A^T + B_2\widetilde{\boldsymbol{C}} + \widetilde{\boldsymbol{C}}^T B_2^T \\ M_{21} & = & \widetilde{\boldsymbol{A}} + A^T + C_2^T\widetilde{\boldsymbol{D}}^T B_2^T \\ M_{22} & = & \boldsymbol{Y}A + A^T\boldsymbol{Y} + \widetilde{\boldsymbol{B}}C_2 + C_2^T\widetilde{\boldsymbol{B}}^T \\ M_{31} & = & B_1^T + D_{21}^T\widetilde{\boldsymbol{D}}^T B_2^T \\ M_{32} & = & B_1^T\boldsymbol{Y} + D_{21}^T\widetilde{\boldsymbol{B}}^T \\ M_{33} & = & -\gamma_\infty I_{n_u} \\ M_{41} & = & C_1\boldsymbol{X} + D_{12}\widetilde{\boldsymbol{C}} \\ M_{42} & = & C_1 + D_{12}\widetilde{\boldsymbol{D}}C_2 \\ M_{43} & = & D_{11} + D_{12}\widetilde{\boldsymbol{D}}D_{21} \\ M_{44} & = & -\gamma_\infty I_{n_y} \end{array} \tag{3.98}$$

Then, the reconstruction of the controller C *is obtained by the following equivalent transformation,*

$$\left\{\begin{array}{rcl} D_c & = & \widetilde{\boldsymbol{D}} \\ C_c & = & (\widetilde{\boldsymbol{C}} - D_cC_2\boldsymbol{X})M^{-T} \\ B_c & = & N^{-1}(\widetilde{\boldsymbol{B}} - \boldsymbol{Y}B_2D_c) \\ A_c & = & N^{-1}(\widetilde{\boldsymbol{A}} - \boldsymbol{Y}A\boldsymbol{X} - \boldsymbol{Y}B_2D_cC_2\boldsymbol{X} - NB_cC_2\boldsymbol{X} - \boldsymbol{Y}B_2C_cM^T)M^{-T} \end{array}\right. \tag{3.99}$$

where M *and* N *are defined such that* $MN^T = I_n - XY$ *(that can be solved through a singular value decomposition plus a Cholesky factorization).*

Remark: Numerical issues. Note that for practical issues, LMI (3.97) is solved a first time to find γ_∞^*, the optimal bound solution. Then, we will often play the LMI resolution with a fixed attenuation level $\gamma_\infty = \gamma_\infty^*(1+\nu)$, ($\nu$ being a percentage). In this second step, the second statement of (3.97) is

replaced by,

$$\begin{bmatrix} X & \alpha I_n \\ \alpha I_n & Y \end{bmatrix} > 0 \tag{3.100}$$

where $\alpha > 0$, and the optimization to be done consists in maximizing α. This procedure maximizes the minimal eigenvalue of XY, and hence pushes it away from I_n, and avoid bad conditioning when inverting M and N in the controller reconstruction step (3.99).

Algorithm 3.5.1 (*LMI based DOF $\mathcal{H}_\infty$ control synthesis*)

The LMI based solution of the $\mathcal{H}_\infty$ control synthesis problem is given by the following steps:

1. *Problem solution: minimize γ_∞ subject to LMIs (3.97) and find γ_∞^*, the optimal $\mathcal{H}_\infty$ bound (optimization step).*
2. *Conditioning improvement: set $\gamma_\infty > \gamma_\infty^*$, and solve LMIs (3.97) for this fixed γ_∞ value (feasibility step).*
3. *Find the appropriate M and N (e.g. by Singular values decomposition plus Cholesky factorization).*
4. *Controller reconstruction: Reconstruct the controller according to (3.99).*

Remark: Controller order. Note that the controller is of the same order as the generalized system M that includes the plant model and the weighting functions, which may be of high order (see Chapters 6 and 7). Reduced order controller (i.e. controller dimension $<$ system dimension) should be imagined by introducing a constraint as $\dim A_c \leq k < \dim A$. But such a constraint involves rank constraint and current optimization techniques do not hold for those kinds of problems. Some techniques are now under development (see e.g. Malik *et al.*, 2006; Bu and Sznaier, 2000).

3.5.4 $\mathcal{H}_2$ design

The $\mathcal{H}_\infty$ norm considered above gives the system gain when input and output are measured using the $\mathcal{L}_2$ norm. Rather than bounding the output energy, it may be desirable to keep the peak amplitude of the controlled output below a certain level, e.g. to avoid actuator saturations.

Now, when we refer to the $\mathcal{H}_2$ control problem, we mean: Find a controller C for system M such that, given γ_∞,

$$||\mathcal{F}_l(M, C)||_2 < \gamma_2 \tag{3.101}$$

The $\mathcal{H}_2$ problem can be expressed as follow (see Proposition 3.4.4),

$$\begin{bmatrix} \mathcal{A}^T K + K\mathcal{A} & K\mathcal{B} \\ \mathcal{B}^T K & -I \end{bmatrix} \prec 0\,, \begin{bmatrix} K & \mathcal{C}^T \\ \mathcal{C} & Z \end{bmatrix} \succ 0\,, \mathbf{Tr}(Z) < \gamma_2 \tag{3.102}$$

where $\mathcal{A}$, $\mathcal{B}$, $\mathcal{C}$, $\mathcal{D}$ are given in (3.86). By applying the same transformations as before (on the $\mathcal{H}_\infty$ problem) we obtain,

Result 3.5.2 (*LMI-based LTI/$\mathcal{H}_2$ solution (Scherer* et al., *1997)*)

A dynamical output feedback controller of the form $C(s) = \left[\begin{array}{c|c} A_c & B_c \\ \hline C_c & D_c \end{array}\right]$ *that solves the* $\mathcal{H}_2$ *control problem is obtained by solving the following LMIs in (*$\boldsymbol{X}$, $\boldsymbol{Y}$, $\widetilde{\boldsymbol{A}}$, $\widetilde{\boldsymbol{B}}$, $\widetilde{\boldsymbol{C}}$ *and* $\widetilde{\boldsymbol{D}}$*) while minimizing* γ_2*,*

$$\begin{array}{l} \left[\begin{array}{ccc} M_{11} & (*)^T & (*)^T \\ M_{21} & M_{22} & (*)^T \\ M_{31} & M_{32} & M_{33} \end{array}\right] \prec 0 \\ \left[\begin{array}{ccc} N_{11} & (*)^T & (*)^T \\ N_{21} & N_{22} & (*)^T \\ N_{31} & N_{32} & N_{33} \end{array}\right] \succ 0 \\ \boldsymbol{Tr}(\boldsymbol{Z}) < \gamma_2 \end{array} \tag{3.103}$$

where,

$$\begin{array}{rcl} M_{11} & = & A\boldsymbol{X} + \boldsymbol{X}A^T + B_2\widetilde{\boldsymbol{C}} + \widetilde{\boldsymbol{C}}^T B_2^T \\ M_{21} & = & \widetilde{\boldsymbol{A}} + A^T + C_2^T\widetilde{\boldsymbol{D}}^T B_2^T \\ M_{22} & = & \boldsymbol{Y}A + A^T\boldsymbol{Y} + \widetilde{\boldsymbol{B}}C_2 + C_2^T\widetilde{\boldsymbol{B}}^T \\ M_{31} & = & B_1^T + D_{21}^T\widetilde{\boldsymbol{D}}^T B_2^T \\ M_{32} & = & B_1^T\boldsymbol{Y} + D_{21}^T\widetilde{\boldsymbol{B}}^T \\ M_{33} & = & -I_{n_u} \\ N_{11} & = & X \\ N_{21} & = & I_n \\ N_{22} & = & Y \\ N_{31} & = & C_1\boldsymbol{X} + D_{12}\widetilde{\boldsymbol{C}} \\ N_{32} & = & C_1 + D_{12}\widetilde{\boldsymbol{D}}C_2 \\ N_{33} & = & \boldsymbol{Z} \end{array} \tag{3.104}$$

Then, the reconstruction of the controller C *is obtained by the following equivalent transformation,*

$$\left\{\begin{array}{rcl} D_c & = & \widetilde{\boldsymbol{D}} \\ C_c & = & (\widetilde{\boldsymbol{C}} - D_cC_2\boldsymbol{X})M^{-T} \\ B_c & = & N^{-1}(\widetilde{\boldsymbol{B}} - \boldsymbol{Y}B_2D_c) \\ A_c & = & N^{-1}(\widetilde{\boldsymbol{A}} - \boldsymbol{Y}A\boldsymbol{X} - \boldsymbol{Y}B_2D_cC_2\boldsymbol{X} - NB_cC_2\boldsymbol{X} - \boldsymbol{Y}B_2C_cM^T)M^{-T} \end{array}\right. \tag{3.105}$$

where M *and* N *are defined such that* $MN^T = I_n - XY$ *(that can be solved through a singular value decomposition plus a Cholesky factorization).*

3.5.5 Multi-objectives design ($\mathcal{H}_\infty/\mathcal{H}_2$ case)

Multi-objective control problem consists in designing a controller that achieves different closed-loop objectives (e.g. pole placement and $\mathcal{H}_\infty$ performance etc.). The interest of a multi-objective problem is that, according to the considered system, different performances can be specified to different controlled channels. The problem formulation is an extension of the simple $\mathcal{H}_\infty$ or $\mathcal{H}_2$ problem. Hence, the way to solve it is also very similar, but as exposed in Chapter 2, it leads to other problems (especially from the computational viewpoint).

3.5.5.1 General problem formulation

The multi-objective (or mixed) synthesis consists in giving different constraints on the controlled system outputs. In other words, each channel defined as a transfer between input w_i to output z_i is associated with a performance criteria (i being the applied performance criterion, that can be $\mathcal{H}_\infty$, $\mathcal{H}_2$, pole placement, peak to peak, etc.). Mathematically, it comes the following extended formulation:

$$\left[\begin{array}{c} \dot{x} \\ \hline z_1 \\ \vdots \\ z_n \\ \hline y \end{array}\right] = \left[\begin{array}{c|ccc|c} A & B_1 & \dots & B_n & B_u \\ \hline C_1 & D_{11} & \dots & D_{1n} & D_{1u} \\ \vdots & \vdots & \ddots & \vdots & \vdots \\ C_n & D_{1n} & \dots & D_{nn} & D_{nu} \\ \hline C & D_1 & \dots & D_n & D_{ny} \end{array}\right] \left[\begin{array}{c} x \\ \hline z_1 \\ \vdots \\ z_n \\ \hline u \end{array}\right] \tag{3.106}$$

By considering the following controller,

$$\left[\begin{array}{c} \dot{x}_c \\ u \end{array}\right] = \left[\begin{array}{cc} A_c & B_c \\ C_c & D_c \end{array}\right] \left[\begin{array}{c} x \\ y \end{array}\right] \tag{3.107}$$

the corresponding closed-loop representation is given by,

$$\left[\begin{array}{c} \dot{\xi} \\ \hline z_1 \\ \vdots \\ z_n \end{array}\right] = \left[\begin{array}{c|ccc} \mathcal{A} & \mathcal{B}_1 & \dots & \mathcal{B}_n \\ \hline \mathcal{C}_1 & \mathcal{D}_{11} & \dots & \mathcal{D}_{1n} \\ \vdots & \vdots & \ddots & \vdots \\ \mathcal{C}_n & \mathcal{D}_{1n} & \dots & \mathcal{D}_{nn} \end{array}\right] \left[\begin{array}{c} \xi \\ \hline w_1 \\ \vdots \\ w_n \end{array}\right] \tag{3.108}$$

where each channel $T_{z_i w_i} = \dfrac{z_i}{w_i}$ is subject to a control performance index i. According to this formulation, the extension of the previously control criteria can be applied to solve a multi-objective control. Thanks to the LMI formulation, mixed approaches can be either applied to the same or different outputs. Thereafter, the mixed $\mathcal{H}_\infty$/$\mathcal{H}_2$ is described as an illustration.

3.5.5.2 $\mathcal{H}_\infty$/$\mathcal{H}_2$ problem formulation

A widely explored mixed control design is $\mathcal{H}_\infty$/$\mathcal{H}_2$ that ensures robustness (using the $\mathcal{H}_\infty$ property) while minimizing the signal energy ($\mathcal{H}_2$ property). The $\mathcal{H}_\infty$ approach is essentially based on the worst case performance analysis, then it provides low performances with high robustness margin. On the other hand, the $\mathcal{H}_2$ performance criterion reflects a mean performance, but provides low robustness margin. Then, since both approaches share the same formalism, a natural idea is to associate them in a unified synthesis. Figure 3.7 gives the representation of the mixed approach for the $\mathcal{H}_\infty$/$\mathcal{H}_2$ problem.

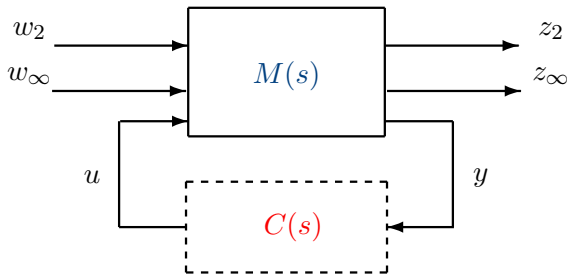

Figure 3.7: Multi-objective $\mathcal{H}_\infty/\mathcal{H}_2$ generalized plant.

Result 3.5.3 (*LTI/$\mathcal{H}_\infty$/$\mathcal{H}_2$*)

The $\mathcal{H}_\infty/\mathcal{H}_2$ synthesis consists in imposing:

$$T_\infty = \left\| \frac{z_\infty}{w_\infty} \right\|_\infty < \gamma_\infty \text{ and } T_2 = \left\| \frac{z_2}{w_2} \right\|_2 < \gamma_2 \tag{3.109}$$

The resulting LMI based problem formulation consists in solving the following problem subject to $K = K^T \succ 0$ (note that to obtain LMIs, the same change of variable as introduced in the $\mathcal{H}_\infty$ and $\mathcal{H}_2$ problems can be applied).

$$\begin{cases} \begin{bmatrix} \mathcal{A}^T K + K\mathcal{A} & K\mathcal{B}_\infty & \mathcal{C}_\infty^T \\ \mathcal{B}_\infty^T K & -\gamma_\infty^2 I & \mathcal{D}_{\infty 1}^T \\ \mathcal{C}_\infty & \mathcal{D}_{\infty 1} & -I \end{bmatrix} \prec 0 \\ \begin{bmatrix} \mathcal{A}^T K + K\mathcal{A} & K\mathcal{B}_2 \\ \mathcal{B}_2^T K & -I \end{bmatrix} \prec 0 \,, \begin{bmatrix} K & \mathcal{C}_2^T \\ \mathcal{C}_2 & Z \end{bmatrix} \succ 0 \,, \mathbf{Tr}(Z) < \gamma_2 \end{cases} \tag{3.110}$$

Even after the change of basis, it is impossible (non convex problem) to minimize simultaneously the $\mathcal{H}_\infty$ and $\mathcal{H}_2$ criteria. As a consequence, the problem is usually reformulated as one of the problems below:

- A linear combination of γ_∞ and γ_2, e.g.:

$$\gamma_{mix} = \alpha\gamma_\infty + (1-\alpha)\gamma_2 \text{ , where } \alpha \in [0\ 1] \tag{3.111}$$

- Minimize γ_∞ (resp. γ_2) while fixing γ_2 (resp. γ_∞).

Remark: Pareto optimality. In the mixed approach, it is impossible to both minimize the $\mathcal{H}_\infty$ and $\mathcal{H}_2$ performance criteria. Then a compromise has to be done. Such a compromise, well known in economy, game theory and engineering, is also called the Pareto optimality (from the name of it "inventor", Vilfredo Pareto[3]). In game theory, the Pareto optimum corresponds to a situation where the gain of one player can only be improved by reducing the one of the other. Transposing this notion to the mixed approach in control theory, a player situation (e.g. γ_∞, $\mathcal{H}_\infty$ performance level) cannot be improved (diminished) without reducing (increasing) the one of the other (e.g. γ_2, $\mathcal{H}_2$ performance level). Then, for a Pareto optimum solution, the improvement in one objective requires the degradation

[3]Italian economist who used the concept in his studies of economic efficiency and income distribution.

of another. Multiobjective optimization is, therefore, concerned with the generation and selection of non inferior solution points.

In Section 6, an illustration of this problem will be given, exhibiting the Pareto optimal curve (trade-off). For more detail on Pareto and game theory, the reader is invited to refer to recent work of Jungers (2006) PhD Thesis.

3.6 Extension to LPV control

In this section, the extension of the results presented in previous section is done to LPV systems. More particularly we will focus on polytopic LPV systems. We first recall the general formulation, then provide the LMI based results for $\mathcal{H}_\infty$, $\mathcal{H}_2$ and mixed $\mathcal{H}_\infty/\mathcal{H}_2$ LPV controller synthesis.

3.6.1 General problem formulation (LPV case)

The LPV system under consideration is defined as in Definition (3.3) i.e.:

$$\Sigma_{LPV} : \left\{ \begin{array}{rcl} \dot{x}(t) & = & A(\rho(.))x(t) + B(\rho(.))w(t) \\ z(t) & = & C(\rho(.))x(t) + D(\rho(.))w(t) \end{array} \right. \tag{3.112}$$

where matrices are parameter dependent. Let us consider the following description of the generalized LPV system $M(\rho)$ as (including the performance weighting functions),

$$\left[\begin{array}{c} \dot{x} \\ \hline z \\ y \end{array} \right] = \left[\begin{array}{c|cc} A(\rho) & B_1(\rho) & B_2(\rho) \\ \hline C_1(\rho) & D_{11}(\rho) & D_{12}(\rho) \\ C_2(\rho) & D_{21}(\rho) & 0 \end{array} \right] \left[\begin{array}{c} x \\ \hline w \\ u \end{array} \right] \tag{3.113}$$

where x is the state vector of the system plus the state vector of the weighting functions, z holds for the controlled output of the system (i.e. the variables we aim at controlling or giving a performance criteria), y are the measured values (that will feed the controller), w holds for the exogenous signals and u, the control input signal. Let assume that $x \in X \in \mathbb{R}^n$, $z \in Z \in \mathbb{R}^{n_z}$, $y \in Y \in \mathbb{R}^{n_y}$, $w \in W \in \mathbb{R}^{n_w}$ and $u \in U \in \mathbb{R}^{n_u}$. Moreover $\rho \in \mathcal{P}_\rho$. According to this general formulation, the controller $C(\rho)$ to be designed is defined as,

$$\left[\begin{array}{c} \dot{x_c} \\ u \end{array} \right] = \left[\begin{array}{cc} A_c(\rho) & B_c(\rho) \\ C_c(\rho) & D_c(\rho) \end{array} \right] \left[\begin{array}{c} x \\ y \end{array} \right] \tag{3.114}$$

where $x_c \in X_c \in \mathbb{R}^n$, $u \in U \in \mathbb{R}^{n_u}$, $y \in Y \in \mathbb{R}^{n_y}$. Then, $\rho \in \mathcal{P}_\rho$, s.t.

$$\rho_i \in \left[\begin{array}{cc} \underline{\rho}_i & \overline{\rho}_i \end{array} \right] , \forall i = 1, \ldots, p \tag{3.115}$$

The resulting closed loop, also denoted through the Linear Fractional Transformation (LFT) $\mathcal{F}_l(M(\rho), C(\rho))$ is given by,

$$\left[\begin{array}{c} \dot{\xi} \\ z \end{array} \right] = \left[\begin{array}{cc} \mathcal{A}(\rho) & \mathcal{B}(\rho) \\ \mathcal{C}(\rho) & \mathcal{D}(\rho) \end{array} \right] \left[\begin{array}{c} \xi \\ w \end{array} \right] \tag{3.116}$$

where,

$$\begin{array}{rcl} \mathcal{A} & = & \begin{bmatrix} A(\rho)+B_2(\rho)D_c(\rho)C_2(\rho) & B_2(\rho)C_c(\rho) \\ B_c(\rho)C_2(\rho) & A_c(\rho) \end{bmatrix} \\ \mathcal{B} & = & \begin{bmatrix} B_1(\rho)+B_2(\rho)D_c(\rho)D_{21}(\rho) \\ B_c(\rho)D_{21}(\rho) \end{bmatrix} \\ \mathcal{C} & = & \begin{bmatrix} C_1(\rho)+D_{12}(\rho)D_c(\rho)C_2(\rho) & D_{12}(\rho)C_c(\rho) \end{bmatrix} \\ \mathcal{D} & = & D_{11}(\rho)+D_{12}(\rho)D_c(\rho)D_{21}(\rho) \end{array} \tag{3.117}$$

where $\xi = [x^T \; x_c^T]^T \in \mathbb{R}^{2n}$, $z \in \mathbb{R}^{n_z}$, $w \in \mathbb{R}^{n_w}$. Then, the generalized system and its controller are represented as on Figure 3.6.1

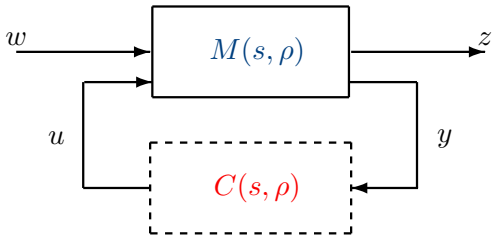

Figure 3.8: Generalized LPV plant & Controller.

Thereafter, the LPV results for $\mathcal{H}_\infty$, $\mathcal{H}_2$ and mixed design are given.

3.6.2 LPV control design

The LPV control design approaches developed thereafter stand for general LPV problems.

3.6.2.1 LPV/$\mathcal{H}_\infty$ control

The $\mathcal{H}_\infty$ control synthesis solution for LPV systems is extended from the LTI one as follows.

Result 3.6.1 (*LMI-based LPV/$\mathcal{H}_\infty$ solution*)

A dynamical output feedback controller of the form $C(s,\rho) = \left[\begin{array}{c|c} A_c(\rho) & B_c(\rho) \\ \hline C_c(\rho) & D_c(\rho) \end{array}\right]$ *that solves the* $\mathcal{H}_\infty$ *control problem is obtained by solving the following LMIs in (*$\boldsymbol{X}(\rho)$, $\boldsymbol{Y}(\rho)$, $\widetilde{\boldsymbol{A}}(\rho)$, $\widetilde{\boldsymbol{B}}(\rho)$, $\widetilde{\boldsymbol{C}}(\rho)$ *and* $\widetilde{\boldsymbol{D}}(\rho)$*) while minimizing* γ_∞*,*

$$\begin{array}{c} \left[\begin{array}{cccc} M_{11} & (*)^T & (*)^T & (*)^T \\ M_{21} & M_{22} & (*)^T & (*)^T \\ M_{31} & M_{32} & M_{33} & (*)^T \\ M_{41} & M_{42} & M_{43} & M_{44} \end{array}\right] \prec 0 \\ \left[\begin{array}{cc} \boldsymbol{X}(\rho) & I_n \\ I_n & \boldsymbol{Y}(\rho) \end{array}\right] \succ 0 \end{array} \tag{3.118}$$

where,

$$\begin{array}{rcl} M_{11} & = & A(\rho)\boldsymbol{X}(\rho) + \boldsymbol{X}(\rho)A(\rho)^T + \dfrac{\partial X(\rho)}{\partial \rho}\dot{\rho} + B_2\widetilde{\boldsymbol{C}}(\rho) + \widetilde{\boldsymbol{C}}(\rho)^T B_2^T \\ M_{21} & = & \widetilde{\boldsymbol{A}}(\rho) + A(\rho)^T + C_2^T\widetilde{\boldsymbol{D}}(\rho)^T B_2^T \\ M_{22} & = & \boldsymbol{Y}(\rho)A(\rho) + A(\rho)^T\boldsymbol{Y}(\rho) + \dfrac{\partial Y(\rho)}{\partial \rho}\dot{\rho} + \widetilde{\boldsymbol{B}}(\rho)C_2 + C_2^T\widetilde{\boldsymbol{B}}(\rho)^T \\ M_{31} & = & B_1(\rho)^T + D_{21}(\rho)^T\widetilde{\boldsymbol{D}}(\rho)^T B_2^T \\ M_{32} & = & B_1(\rho)^T\boldsymbol{Y}(\rho) + D_{21}(\rho)^T\widetilde{\boldsymbol{B}}(\rho)^T \\ M_{33} & = & -\gamma I_{n_u} \\ M_{41} & = & C_1(\rho)\boldsymbol{X}(\rho) + D_{12}(\rho)\widetilde{\boldsymbol{C}}(\rho) \\ M_{42} & = & C_1(\rho) + D_{12}(\rho)\widetilde{\boldsymbol{D}}(\rho)C_2 \\ M_{43} & = & D_{11}(\rho) + D_{12}(\rho)\widetilde{\boldsymbol{D}}(\rho)D_{21}(\rho) \\ M_{44} & = & -\gamma I_{n_y} \end{array} \tag{3.119}$$

Then, the reconstruction of the controller C *is obtained by the following equivalent transformation (for* $\dfrac{\partial X(\rho)}{\partial \rho}\dot{\rho} = 0$*),*

$$\left\{\begin{array}{rcl} D_c(\rho) & = & \widetilde{\boldsymbol{D}}(\rho) \\ C_c(\rho) & = & (\widetilde{\boldsymbol{C}}(\rho) - D_c(\rho)C_2(\rho)\boldsymbol{X}(\rho))M(\rho)^{-T} \\ B_c(\rho) & = & N(\rho)^{-1}(\widetilde{\boldsymbol{B}}(\rho) - \boldsymbol{Y}(\rho)B_2(\rho)D_c(\rho)) \\ A_c(\rho) & = & N(\rho)^{-1}(\widetilde{\boldsymbol{A}}(\rho) - \boldsymbol{Y}(\rho)A(\rho)\boldsymbol{X}(\rho) - \boldsymbol{Y}(\rho)B_2(\rho)D_c(\rho)C_2(\rho)\boldsymbol{X}(\rho) \\ & - & N(\rho)B_c(\rho)C_2(\rho)\boldsymbol{X}(\rho) - \boldsymbol{Y}(\rho)B_2(\rho)C_c(\rho)M(\rho)^T)M(\rho)^{-T} \end{array}\right. \tag{3.120}$$

where $M(\rho)$ *and* $N(\rho)$ *are defined such that* $M(\rho)N(\rho)^T = I_n - X(\rho)Y(\rho)$ *(that can be solved through a singular value decomposition plus a Cholesky factorization).*

3.6.2.2 LPV/$\mathcal{H}_2$ control

Result 3.6.2 (*LMI-based LPV/$\mathcal{H}_2$ solution*)

A dynamical output feedback controller of the form $C(s,\rho) = \left[\begin{array}{c|c} A_c(\rho) & B_c(\rho) \\ \hline C_c(\rho) & D_c(\rho) \end{array}\right]$ *that solves the* $\mathcal{H}_2$ *control problem is obtained by solving the following LMIs in* ($\boldsymbol{X}(\rho)$, $\boldsymbol{Y}(\rho)$, $\widetilde{\boldsymbol{A}}(\rho)$, $\widetilde{\boldsymbol{B}}(\rho)$, $\widetilde{\boldsymbol{C}}(\rho)$ *and* $\widetilde{\boldsymbol{D}}(\rho)$) *while minimizing* γ_2,

$$\begin{array}{l} \left[\begin{array}{ccc} M_{11} & (*)^T & (*)^T \\ M_{21} & M_{22} & (*)^T \\ M_{31} & M_{32} & M_{33} \end{array}\right] \prec 0 \\ \left[\begin{array}{ccc} N_{11} & (*)^T & (*)^T \\ N_{21} & N_{22} & (*)^T \\ N_{31} & N_{32} & N_{33} \end{array}\right] \succ 0 \\ \boldsymbol{Tr}(\boldsymbol{Z}) < \gamma_2 \end{array} \tag{3.121}$$

where,

$$\begin{array}{rcl} M_{11} & = & A(\rho)\boldsymbol{X}(\rho) + \boldsymbol{X}(\rho)A(\rho)^T + \dfrac{\partial X(\rho)}{\partial \rho}\dot{\rho} + B_2\widetilde{\boldsymbol{C}}(\rho) + \widetilde{\boldsymbol{C}}(\rho)^T B_2^T \\ M_{21} & = & \widetilde{\boldsymbol{A}}(\rho) + A^T(\rho) + C_2^T\widetilde{\boldsymbol{D}}(\rho)^T B_2^T \\ M_{22} & = & \boldsymbol{Y}(\rho)A(\rho) + A(\rho)^T\boldsymbol{Y}(\rho) + \dfrac{\partial Y(\rho)}{\partial \rho}\dot{\rho} + \widetilde{\boldsymbol{B}}(\rho)C_2 + C_2^T\widetilde{\boldsymbol{B}}^T(\rho) \\ M_{31} & = & B_1(\rho)^T + D_{21}(\rho)^T\widetilde{\boldsymbol{D}}(\rho)^T B_2^T \\ M_{32} & = & B_1(\rho)^T\boldsymbol{Y}(\rho) + D_{21}(\rho)^T\widetilde{\boldsymbol{B}}(\rho)^T \\ M_{33} & = & -I_{n_u} \\ N_{11} & = & X(\rho) \\ N_{21} & = & I_n \\ N_{22} & = & Y(\rho) \\ N_{31} & = & C_1(\rho)\boldsymbol{X}(\rho) + D_{12}(\rho)\widetilde{\boldsymbol{C}}(\rho) \\ N_{32} & = & C_1(\rho) + D_{12}(\rho)\widetilde{\boldsymbol{D}}(\rho)C_2 \\ N_{33} & = & \boldsymbol{Z} \end{array} \tag{3.122}$$

Then, the reconstruction of the controller C *is obtained by the following equivalent transformation (for* $\dfrac{\partial X(\rho)}{\partial \rho}\dot{\rho} = 0$*),*

$$\left\{\begin{array}{rcl} D_c(\rho) & = & \widetilde{\boldsymbol{D}}(\rho) \\ C_c(\rho) & = & (\widetilde{\boldsymbol{C}}(\rho) - D_c(\rho)C_2(\rho)\boldsymbol{X}(\rho))M(\rho)^{-T} \\ B_c(\rho) & = & N(\rho)^{-1}(\widetilde{\boldsymbol{B}}(\rho) - \boldsymbol{Y}(\rho)B_2(\rho)D_c(\rho)) \\ A_c(\rho) & = & N(\rho)^{-1}(\widetilde{\boldsymbol{A}}(\rho) - \boldsymbol{Y}(\rho)A(\rho)\boldsymbol{X}(\rho) - \boldsymbol{Y}(\rho)B_2(\rho)D_c(\rho)C_2(\rho)\boldsymbol{X}(\rho) \\ & - & N(\rho)B_c(\rho)C_2(\rho)\boldsymbol{X}(\rho) - \boldsymbol{Y}(\rho)B_2(\rho)C_c(\rho)M(\rho)^T)M(\rho)^{-T} \end{array}\right. \tag{3.123}$$

where $M(\rho)$ *and* $N(\rho)$ *are defined such that* $M(\rho)N(\rho)^T = I_n - X(\rho)Y(\rho)$ *(that can be solved through a singular value decomposition plus a Cholesky factorization).*

3.6.2.3 LPV/$\mathcal{H}_\infty$/$\mathcal{H}_2$ control

Result 3.6.3 (*LMI-based LPV/$\mathcal{H}_\infty$/$\mathcal{H}_2$ solution*)

The $\mathcal{H}_\infty$/$\mathcal{H}_2$ synthesis consists in imposing:

$$T_\infty = \left\| \frac{z_\infty}{w_\infty} \right\|_\infty < \gamma_\infty \; T_2 = \left\| \frac{z_2}{w_2} \right\|_2 < \gamma_2 \tag{3.124}$$

Hence the LMI based problem formulation is the following: minimize a combination of γ_2 and γ_∞ subject to $K(\rho) = K(\rho)^T \succ 0$ and Z (Chilali and Gahinet, 1996; Scherer et al., *1997).*

$$\begin{cases} \begin{bmatrix} \mathcal{A}(\rho)^T K(\rho) + K(\rho)\mathcal{A}(\rho) + \frac{\partial K(\rho)}{\partial \rho}\dot{\rho} & K(\rho)\mathcal{B}_\infty(\rho) & \mathcal{C}_\infty(\rho)^T \\ \mathcal{B}_\infty(\rho)^T K(\rho) & -\gamma_\infty^2 I & \mathcal{D}_{\infty 1}(\rho)^T \\ \mathcal{C}_\infty(\rho) & \mathcal{D}_{\infty 1}(\rho) & -I \end{bmatrix} \prec 0 \\ \begin{bmatrix} \mathcal{A}(\rho)^T K(\rho) + K(\rho)\mathcal{A}(\rho) + \frac{\partial K(\rho)}{\partial \rho}\dot{\rho} & K(\rho)\mathcal{B}_2(\rho) \\ \mathcal{B}_2(\rho)^T K(\rho) & -I \end{bmatrix} \prec 0 \, , \; \begin{bmatrix} K(\rho) & \mathcal{C}_2(\rho)^T \\ \mathcal{C}_2(\rho) & Z \end{bmatrix} \\ \mathbf{Tr}(Z) < \gamma_2 \end{cases} \tag{3.125}$$

3.6.2.4 Parameters variations and Lyapunov function

As the LPV version of the LMI based solution of the control synthesis depends on the derivative of the varying parameter, one can notice that (due to the Lyapunov function):

- By choosing $K(\rho) = K_0$ constant, then, $\dfrac{\partial K(\rho)}{\partial \rho} = 0$, means that ρ can vary arbitrarily fast. This assumption is conservative since we miss decision variables, but may be justified in some cases where no information on the parameter is available. Moreover, it greatly simplifies the solution. Later in this thesis, this solution will used (see Chapters 6 and 7).

- By choosing $K(\rho) = K_0 + \rho_1 K_1 + \cdots + \rho_n K_n$ then, $\dfrac{\partial K(\rho)}{\partial \rho}$ is linear, and depends on the parameter variation rate. This solution shows to reduce the conservatism of the solution. As an illustration, de Souza and Trofino (2005) made a very interesting study on this parameter dependency through the state feedback control synthesis under $\mathcal{H}_2$ constraint.

3.6.3 LPV control design: Polytopic approach

Note first that the previous three results depend on the parameter ρ (whatever the chosen Lyapunov function). Therefore, the solution relies in an infinite number of LMIs (in the LTI case, the number of LMIs was fixed).

As these problems turn to be of infinite dimension, due to infinite values of ρ, it results in an infinite dimension problem. Then to relax it into finite dimension problems, three different kind of approaches are commonly found in the literature:

1. The polytopic approach (used in this thesis).

2. The gridding approach.

3. The Linear Fractional Representation (LFR) approach.

Since it simplifies the computation and programming design, the polytopic approach is used in this thesis. Note that this approach is also well adapted when parameters dependency is decoupled (e.g. $\rho_1 \neq f(\rho_2)$, i.e. parameters are independent from each other) and when they enter in a linear way in the system description (see PhD Thesis of Biannic, 1996; Bruzelius, 2004).

The polytopic control design approach consists in describing the LPV model as a Linear Differential Inclusion (LDI) in order to form a polytope with each bound of the varying parameter. To design such a controller, the following steps have to be followed (together with requirements to be fulfilled) as presented in Apkarian *et al.* (1995).

3.6.3.1 First step - Parameter varying set description

The first step consists in defining the parameter varying set, according to the nonlinear model, i.e. $\mathcal{P}_\rho$. This description can be simple but may introduce conservatism in the solution of the controller, then it has to be done carefully. The aim is to end with:

$$\mathcal{P}_\rho := \mathbf{Co}\{\omega_1, \ldots, \omega_N\} \tag{3.126}$$

where N is the number of vertices of the parameter set ($N = 2^l$, with l the number of varying parameters). ω_i, which denotes the i^{th} vertices is a vector composed of a combination of the upper and lower bound of the varying parameters (see Definition 3.2.4).

Remark: Conservatism reduction. Conservatism of a polytopic model can be measured by calculating the volume of the parameter polytope (see e.g. Kwiatkowski *et al.*, 2007). Then, a way to reduce the solution conservatism is to reduce the size of the polytope, if it is possible (see example thereafter).

Example: Illustration of a polytope reduction. Let consider a nonlinear system with the following dynamical equation, affinely function of v and v^2.

$$\dot{x} = f(v, v^2) = v \left[\begin{array}{c|c} A_1 & B_1 \\ \hline C_1 & D_1 \end{array}\right] + v^2 \left[\begin{array}{c|c} A_2 & B_2 \\ \hline C_2 & D_2 \end{array}\right] \tag{3.127}$$

Then by choosing $\rho_1 = v$ and $\rho_2 = v^2$, the parameter set becomes $\mathcal{P}_\rho = \left[\begin{array}{cc} \underline{\rho}_1 & \overline{\rho}_1 \end{array}\right] \times \left[\begin{array}{cc} \underline{\rho}_2 & \overline{\rho}_2 \end{array}\right]$, as illustrated on Figure 3.9

By reconsidering the polytope, and taking into account the parameter link: if $\rho_1 = v$, then $\rho_2 = v^2 = \rho_1^2$, the following polytope reduction can be easily applied (see Figure 3.10)

The second polytope clearly shows to be less conservative than the first one. Indeed, instead of 4 vertices, we end with only 3, and we obtain a polytope closer to the real parameter variation. This method has been considered in (Robert *et al.*, 2006).
$\Diamond$

3.6.3.2 Second step - Construction of the polytopic system

Then, one needs to construct the polytopic system to guarantee the following requirements:

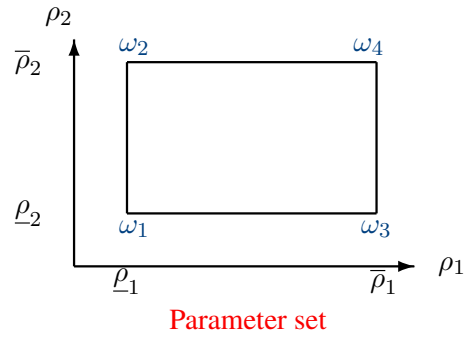

Figure 3.9: Original parameter set.

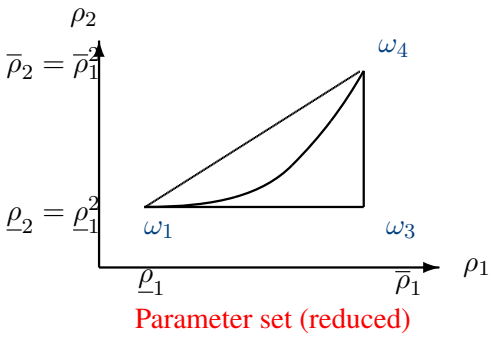

Figure 3.10: Reduced parameter set.

R1 - First requirement: No direct transfer between the input and the output. The generalized plant must be strictly proper, i.e. $D_{22}(\rho) = 0$.

$$M(\rho) = \left[\begin{array}{c} \dot{x} \\ \hline z \\ y \end{array}\right] = \left[\begin{array}{c|cc} A(\rho) & B_1(\rho) & B_2(\rho) \\ \hline C_1(\rho) & D_{11}(\rho) & D_{12}(\rho) \\ C_2(\rho) & D_{21}(\rho) & 0 \end{array}\right] \left[\begin{array}{c} x \\ \hline w \\ u \end{array}\right] \tag{3.128}$$

R2 - Second requirement: Parameter independent of the input and output matrices. In order to allow for application of the polytopic approach, matrices $\left[\begin{array}{cc} B_2(\rho) & D_{12}(\rho) \end{array}\right]^T$ and $\left[\begin{array}{cc} C_2(\rho) & D_{21}(\rho) \end{array}\right]$ must be constant (i.e. independent of ρ). Then the polytopic systems under consideration must have the following form:

$$M(\rho) = \left[\begin{array}{c} \dot{x} \\ \hline z \\ y \end{array}\right] = \left[\begin{array}{c|cc} A(\rho) & B_1(\rho) & B_2 \\ \hline C_1(\rho) & D_{11}(\rho) & D_{12} \\ C_2 & D_{21} & 0 \end{array}\right] \left[\begin{array}{c} x \\ \hline w \\ u \end{array}\right] \tag{3.129}$$

If this requirement is not fulfilled, a simple solution consists in filtering the input and/or the output through strictly proper transfer functions (see the example given thereafter, for input matrix parameter dependent).

Example: Render input matrices ρ independent. Consider the following generalized system:

$$M(\rho): \quad \left[\begin{array}{c} \dot{x} \\ \hline z \\ y \end{array}\right] = \left[\begin{array}{c|cc} A(\rho) & B_1(\rho) & B_2(\rho) \\ \hline C_1(\rho) & D_{11}(\rho) & D_{12}(\rho) \\ C_2 & D_{21} & 0 \end{array}\right] \left[\begin{array}{c} x \\ \hline w \\ u_f \end{array}\right] \tag{3.130}$$

where $\left[\begin{array}{cc} B_2(\rho) & D_{12}(\rho) \end{array}\right]^T$ are ρ dependent. Then, consider the following strictly proper filter:

$$\mathcal{F}: \quad \left[\begin{array}{c} \dot{x}_f \\ u_f \end{array}\right] = \left[\begin{array}{c|c} A_f & B_f \\ \hline C_f & 0 \end{array}\right] \left[\begin{array}{c} x_f \\ u \end{array}\right] \tag{3.131}$$

By interconnecting these two systems, one obtains,

$$\mathcal{F}+M(\rho): \quad \left[\begin{array}{c} \dot{x} \\ \dot{x}_f \\ \hline z \\ \hline y \end{array}\right] = \left[\begin{array}{cc|c|c} A(\rho) & C_f B_2(\rho) & B_1(\rho) & 0 \\ 0 & A_f & 0 & B_f \\ \hline C_1(\rho) & C_f D_{12}(\rho) & D_{11}(\rho) & 0 \\ \hline C_2 & 0 & D_{21} & 0 \end{array}\right] \left[\begin{array}{c} x \\ x_f \\ \hline w \\ \hline u \end{array}\right] \tag{3.132}$$

Then, in the new extended system, the input matrix is ρ independent.
$\Diamond$

Construction of the Polytopic system. According to the number of parameters given by $\rho(.) \in \mathcal{P}_\rho \in \mathbb{R}^l$, the polytopic system is composed by N vertices and can be expressed as:

$$\left[\begin{array}{c|c} A(\rho) & B(\rho) \\ \hline C(\rho) & D(\rho) \end{array}\right] = \sum_{i=1}^{N} \alpha_i(\rho) \left[\begin{array}{c|c} A(\omega_i) & B(\omega_i) \\ \hline C(\omega_i) & D(\omega_i) \end{array}\right] \in \mathbf{Co}\left\{ \left[\begin{array}{c|c} A_1 & B_1 \\ \hline C_1 & D_1 \end{array}\right], \ldots, \left[\begin{array}{c|c} A_N & B_N \\ \hline C_N & D_N \end{array}\right] \right\} \tag{3.133}$$

where ω_i define each vertex of the parameter polytope.

3.6.3.3 Third step - Controller solution

Considering the polytopic system defined below, the polytopic controller is achieved by synthesizing a controller at each vertex of the polytopic system. In order to ensure the global stability, each of these controllers must share the same Lyapunov function (quadratic stability), that is, if we consider the LMI presented below, the same $K(\rho)$. This means that the controllers found are stabilizing for the entire set formed by the system polytope.

After this step, one ends with a set of N controllers such that:

$$\left\{ \left[\begin{array}{c|c} A_{c_1} & B_{c_1} \\ \hline C_{c_1} & D_{c_1} \end{array}\right], \ldots, \left[\begin{array}{c|c} A_{c_N} & B_{c_N} \\ \hline C_{c_N} & D_{c_N} \end{array}\right] \right\} \tag{3.134}$$

Remark: About the implementation. From that point, one can clearly sees how the polytopic approach can be heavy from the implementation point of view. As the number of controllers increases with the number of varying parameters ($N = 2^l$), it is of great importance not to have too many varying parameters (this remark is left at the reader appreciation).

Remark: About the conservatism. Conservatism reduction is a big challenge in both optimization and control theory. In the polytopic control design, the conservatism appears due to many factors, like, among others:

- The increasing number of parameters ($N = 2^l$).
- The increasing range of variation of the parameters ($\rho \in \left[\begin{array}{cc} \underline{\rho} & \overline{\rho} \end{array} \right]$). Note that this point is illustrated through an example in Chapter 6, with the half vehicle model.
- The considered Lyapunov function $K(\rho)$ that can be constant ($K(\rho) = K$), parameter dependent ($K(\rho) = K_0 + \sum_{i=1}^{l} K_i \rho_i$), etc.

In this thesis, the constant Lyapunov function is mostly considered.

3.6.3.4 Fourth step - Polytopic control reconstruction

The reconstruction of the LPV polytopic controller, is given as:

$$C(\rho) = \sum_{i=1}^{N} \alpha_i \left[\begin{array}{cc} A_{c_i} & B_{c_i} \\ C_{c_i} & D_{c_i} \end{array} \right] \tag{3.135}$$

where,

$$\alpha_i(\rho) := \frac{\prod_{k=1}^{l} |\rho_k - \mathcal{C}(\omega_i)_k|}{\prod_{k=1}^{l} (\overline{\rho}_k - \underline{\rho}_k)} \, , i = 1, \ldots, N \tag{3.136}$$

$$\alpha_i(\rho) \geq 0 \text{ and } \sum_{i=1}^{N} \alpha_i(\rho) = 1 \tag{3.137}$$

Then, as illustrated on Figure 3.11, the controller "evolves" in a controller set according to the parameter variation.

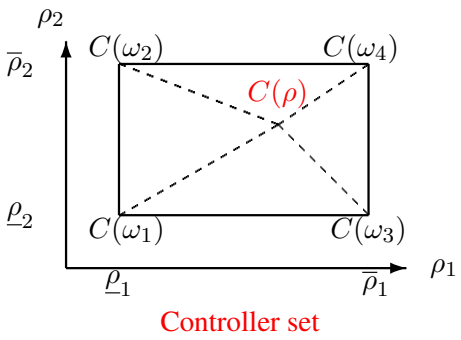

Figure 3.11: Illustration (for two parameters) of the polytopic controller reconstruction.

3.7 Concluding remarks

In this chapter, we have introduced the $\mathcal{H}_\infty$, $\mathcal{H}_2$ and mixed concepts through the dissipative theory, introducing in the same time, the LMI tools involved in this thesis. Then, a solution to the dynamical controller feedback synthesis of the $\mathcal{H}_\infty$, $\mathcal{H}_2$ and mixed objectives for both LTI and polytopic LPV problems are given. The author stresses that there is no particular contribution in this chapter. The aim is simply at introducing the tools used in this thesis for automotive controller synthesis.

We basically see that the robust formalism, together with the LMI approach leads to a simple and flexible control synthesis method. According to this, numerical tools can be efficiently implemented to control complex systems.

In these two first chapters, a general introduction and mathematical background were given to unfamiliar reader. In the following chapter, the automotive actuators and physical phenomena mostly involved in our study are described. These elements will be the basis for vehicle modeling purpose.

Chapter 4

Automotive systems and actuators

4.1 Introduction

Automotive vehicles are complex systems composed of many different elements (e.g. throttle, engine, clutch, anti-roll bar, steering, brakes, suspensions, wheels, etc.) with complex and nonlinear dynamical behaviors, especially in critical driving situations (see e.g. Kiencke and Nielsen, 2000; Gillespie, 1992; Milliken and Milliken, 1995). As this thesis is concerned by analyzing and controlling the global chassis behavior through suspension, braking and steering actuators, this Chapter is devoted to the introduction of these main elements that are of crucial importance in the global vehicle dynamics. More attention is given to suspensions and tires in this thesis. The steering system is also involved, but the complexity of this actuator is not studied. For more details on this point, the reader is invited to refer to a nice recent work on lateral driving assistance involving the steering system (Raharijaona, 2004) PhD Thesis.

In this chapter, the elements of the vehicle (e.g. suspension, tire, steering and chassis) are viewed as independent actuators, body structure or phenomenon, providing (or subject to) a force or a moment. These models will be the basis of the vehicle models, introduced in Chapter 5. This chapter aims at introducing actuators and physical phenomena and emphasize the challenging points, the nonlinear behaviors to be handled, and some of the technological solutions proposed in the literature.

The Chapter is structured as follows: Section 4.2 is devoted to the description and analysis of the suspension systems (both active and semi-active). Due to their high performances and low cost, semi-active suspensions are of a growing interest. Illustrations through examples of two different semi-active dampers technologies are given, namely: a Delphi MR damper (available at the Tecnologico de Monterrey, Mexico) and a SOBEN damper (available in SOBEN, Alès, France). In Section 4.3, the tire modeling is described and analyzed in order to stress the main critical points related to this physical component. Finally, Section 4.4 provides some elements on steering and direction column.

4.2 Suspension systems

4.2.1 General presentation

The main role of the suspension system, which is the link between the wheels and the chassis structure, is to ensure two main objectives:

- Isolate the vehicle chassis from an uneven ground in order to improve passenger comfort (ability of the chassis to be unsensitive to uncomfortable irregularities of the road).

- Provide good road-holding properties in order to ensure passenger safety (ability of the wheel to stay in contact with the road in presence of irregularities and load transfer).

Suspension system constitutes one of the main actuators that influence the vehicle vertical attitude behavior i.e. vertical, roll and pitch dynamics. These are crucial for car manufacturers since they are related to comfort feeling, which is one of the main customer choice criteria (see IPSOS[1] web site). Moreover, as we will see in Chapters 5 and 7, these dynamics influence the load transfer and are important also for safety improvements (longitudinal, lateral and yaw dynamics).

From the mechanical point of view, the suspension system is a vehicle organ (composed of dynamical and structural elements) that provides a force depending on the load of the vehicle and on the force provided by the wheel due to road irregularities (see Figure 4.1). There exist many different kinds of suspensions where the geometry mainly varies according to the location (front or rear) and to the type of vehicle (commercial, sport or heavy). From a dynamical point of view, classical passive suspension systems are composed of a spring and a damping element. According to Figure 4.1, the

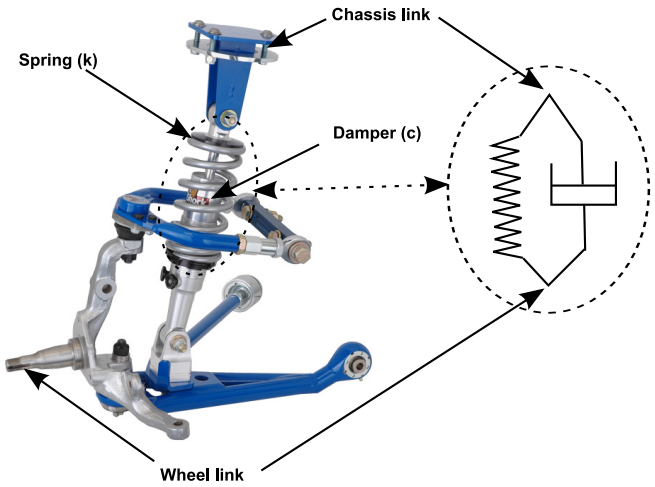

Figure 4.1: A whole suspension system: suspension actuator (spring & damper) and structures (link to the chassis & to the wheel).

suspension system denotes the set of elements that link the wheel and the chassis. In our framework, as we are mostly interested in the dynamical behavior, the model presented thereafter will not involve the suspension geometry.

Remark: About suspension geometry Note that the suspension geometry and kinematic effects have been studied and compared using the ADAMS Car software. It is a vehicle multi-body modeling dedicated software that allows to easily model the efforts, the moments and the vehicle geometry. Moreover, it allows co-simulation between MATLAB and ADAMS. In (Poussot-Vassal *et al.*, 2008*a*), have we validated an LPV/$\mathcal{H}_\infty$ control law on an accurate suspension model developed in ADAMS (by the Tecnologico de Monterrey).

[1] Polling national French agency.

4.2.2 Different kinds of suspension systems

Without loss of generality we define the different kinds of suspensions as illustrated on Figure 4.2. Let notice that the spring element of the suspension system is always considered as passive since no "real" controlled spring stiffness is today used and developed in the industry. In fact, this element is not deeply studied in this thesis; by the way, interested reader can refer to (Jonasson and Roos, 2008), where authors optimize both damping and stiffness factors.

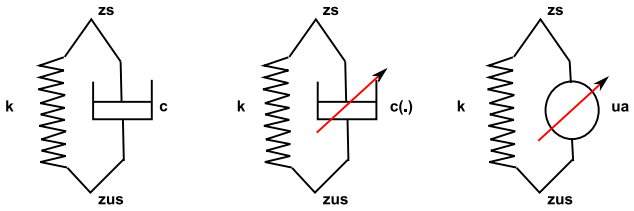

Figure 4.2: Different kinds of suspension systems (from left to right): passive, semi-active and active.

According to Figure 4.2, suspension systems can be cast into three categories with the following properties and limitations:

- Passive suspensions, which always dissipate energy through a fixed flow rate (fixed by the value of the damping factor).
- Semi-active suspensions, which dissipate energy, but with a varying flow rate (adjustable by a control unit that modifies the damping factor).
- Active suspensions, which can both dissipate and generate energy with a varying flow rate (defined by the dynamical characteristics of the actuator, e.g. electrical motor).

A commonly used representation to illustrate the different kinds of suspensions is the Speed/Effort Rule (SER) of the damping element. This representation describes the achievable damper force w.r.t. the deflection speed of the damper, i.e., the difference between the chassis and the wheel velocities (respectively denoted $\dot{z}_s$ and $\dot{z}_{us}$). Figure 4.3 gives an illustration of the main differences between passive, semi-active and active dampers involved in suspension systems.

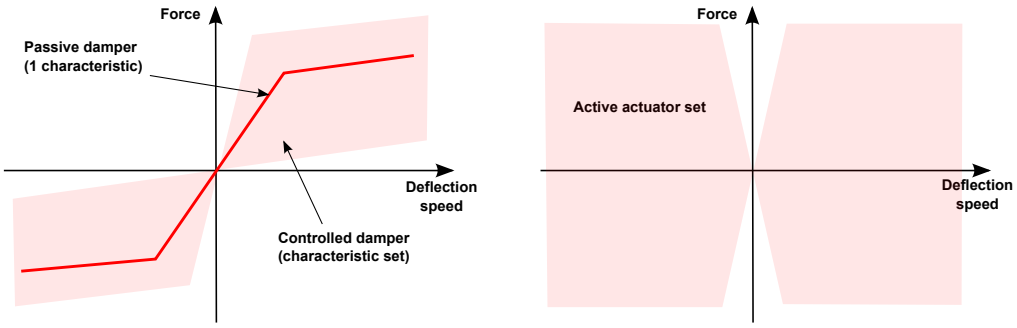

Figure 4.3: SER of a passive, semi-active (left) and active (right) suspension system.

4.2.3 Mathematical modeling

As introduced in Figure 4.1, a suspension system can be simply modeled with a spring and a damper element (or, an active actuator). Then, in our study, the force (effort) F_s provided by the suspension system is defined as (by convention, the force is positive for positive suspension deflection):

$$F_s = F_k(.) + u \tag{4.1}$$

where $F_k(.)$ is a (nonlinear) function that defines the force provided by the spring, and u, the force provided by the considered damping element that characterizes the kind of suspension (i.e. passive, semi-active or active). According to this general representation, many different mathematical expressions have been developed in the literature in order to characterize the kind of suspension. Before introducing these models, and since the spring is not the key element in the study, it will be assumed that the spring force $F_k(.)$ is either:

- Linear: $F_k = kz_{def}$, where $z_{def} = z_s - z_{us}$ is the deflection of the spring, and k the linearized spring constant stiffness coefficient.
- Nonlinear: $F_k = k\big(z_{def}\big)$ is a nonlinear static function of the deflection as defined on Figure 4.4.

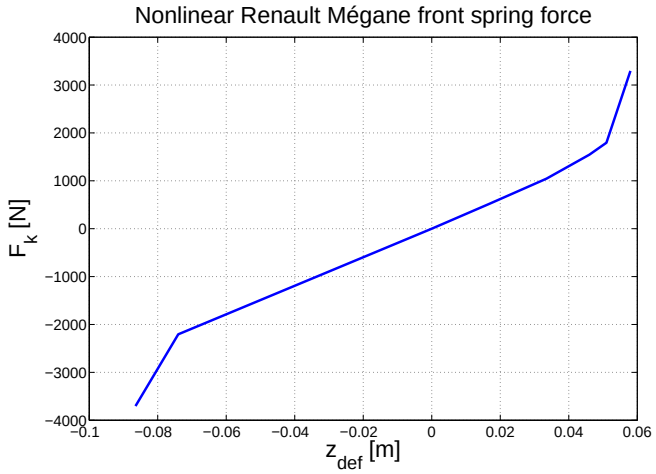

Figure 4.4: Nonlinear stiffness of a Renault Mégane Coupé (front suspension).

Remark: Spring modeling Other models are available in the literature (e.g. $F_k = kz_{def} + k^{nl}z_{def}^3$ in (Gáspár *et al.*, 2008*a*)), which results in similar curves.

The different mathematical dampers models (i.e. passive, semi-active or active), describing the kind of suspension, are characterized by the definition of the u force.

4.2.3.1 Passive suspension (passive damper case)

Since they are only able to dissipate energy, passive suspensions are dissipative actuators. Hence, the equivalent mathematical model is dissipative and the admitted models for study are:

- Linear: in this case, the damping factor is linear, and the dissipative force linearly depends on the deflection speed as,

$$u = c\dot{z}_{def} \tag{4.2}$$

where $\dot{z}_{def} = \dot{z}_s - \dot{z}_{us}$ is the deflection speed and c, the linear damping coefficient of the suspension.

- Nonlinear: in this case, $F_c(\dot{z}_{def})$ is a nonlinear function.

$$u = F_c(\dot{z}_{def}) \tag{4.3}$$

where $F_c(\dot{z}_{def})$ is either described with static maps (see e.g. Figure 4.5), or by nonlinear functions such as (Gáspár *et al.*, 2008*a*):

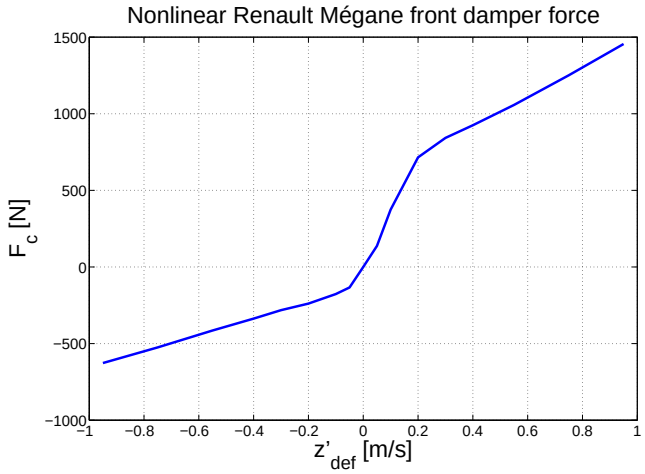

Figure 4.5: Nonlinear damping force of a Renault Mégane Coupé (front suspension).

$$u = c\dot{z}_{def} - c^{sym}|\dot{z}_{def}| + c^{nl}\sqrt{|\dot{z}_{def}|}sgn(\dot{z}_{def}) \tag{4.4}$$

Remark: Shape of the damping force. Shaping of the damping force (such as the one on Figure 4.5) is a very complex step usually carried out by the car manufacturer or the supplier. It is determinant for the vehicle dynamic and driver feeling. In fact, when the control performance is evaluated, the reference model, i.e. the normal car to be compared with, is given by this damping force (from a Renault Mégane Coupé car).

Note that more complex models (including hysteresis phenomena) such as dynamical ones can be used, but are not widely explored in the literature since they are not of a great interest for passive suspension modeling and analysis. As a matter of fact, "complex" models are involved in semi-active damper modeling.

4.2.3.2 Active suspension

According to Figure 4.2, active suspensions denote suspensions containing a spring and an additional actuator that is able to both dissipate and to generate energy. Then, if we consider the suspension

model model given on (4.1), the active part is given by,

$$\dot{u} = \varpi(u - u^0) \tag{4.5}$$

where u is the effective force provided by the actuator, u^0 the required force, and ϖ the cut-off frequency of the actuator.

4.2.3.3 Semi-active suspension (controlled damper)

According to the model given in (4.1), a general controlled damper formulation is given by,

$$u = F_c(., \Omega) \tag{4.6}$$

where $F_c(.)$ is the (nonlinear) function that characterizes the family of damping factors within the achievable area (see Figure 4.3). Then, Ω is the parameter, or the control input, that modifies the suspension damping factor (and therefore the SER). As a matter of fact, $F_c(.)$ depends on the achievable performance of the considered controlled damper, and Ω depends on the type of controlled damper.

As an illustration, if the controlled damper is magneto-rheologic, Ω is the current feeding the self which modifies the magnetic field. Then, as for passive dampers, many controlled damper models exist. From a general viewpoint, we can cast them as follows:

- Linear like model: these models consist is describing the force as a linear function on the deflection speed.

  $$F_c(., \Omega) = c(\Omega)\dot{z}_{def} \tag{4.7}$$

  where $c(\Omega)$ is the linearized damping coefficient, parameterized by Ω. As far as the author knows, this model formulation is not commonly used in the literature, but can be interesting, especially for LPV modeling.

- Nonlinear models: nonlinear damper models are widely studied. Most of them are related to a specific technology. Roughly speaking, damper models can be cast into two categories: static models (which are described as a static function of the deflection, deflection velocity and/or acceleration, etc.), and dynamical models which include an additional internal dynamical state. Here, these models are illustrated through examples found in the literature and which are of real interest.

  – Static models (Shuqui *et al.*, 2006):

  $$F_c(., \Omega) = A_1(\Omega)\tanh\left(A_2(\Omega)\dot{z}_{def}\right) + A_3(\Omega)\dot{z}_{def} \tag{4.8}$$

  where $\{A_1, A_2, A_3\}$ are model parameters that are dependent on the input (Ω parameter).

  $$F_c = A_1(\Omega)\tanh\left[A_3(\Omega)\left(\dot{z}_{def} + \frac{V_0(\Omega)}{X_0(\Omega)}z_{def}\right)\right] + A_2(\Omega)\left(\dot{z}_{def} + \frac{V_0(\Omega)}{X_0(\Omega)}z_{def}\right) \tag{4.9}$$

  where $\{A_0, A_1, A_2, V_0, X_0\}$ are model parameters.
  Note that the first model is a function of the deflection speed, then it models the dampers as a bijective function in the space $\{F_c, \dot{z}_{def}\}$ since the second formulation proposes a damping force function of both deflection and deflection speed, and allows then to model hysteresis phenomena.

– Dynamical nonlinear models (Ahmadian and Song, 1999; Koo *et al.*, 2004): they introduce a dynamical state in the model description. One of the well known dynamical damper models was developed by Bouc-Wen:

$$\begin{cases} F_c &= c_0(\Omega)\dot{z}_{def} + k_0(\Omega)(z_{def} - z^0_{def}) + \gamma(\Omega)z \\ \dot{z} &= -\beta(\Omega)|\dot{z}_{def}|z|z|^{n-1} - \delta(\Omega)\dot{z}_{def}|z|^n + A(\Omega)\dot{z}_{def} \end{cases} \tag{4.10}$$

where $\{c_0, k_0, A, z^0_{def}, \gamma, \beta, \delta, A, n\}$ are model parameters (dependent on Ω) and z is the internal state that introduces some dynamic in the model and models hysteresis phenomena.

In the following, we present two different semi-active suspensions (or controlled dampers) in order to illustrate the models introduced. These studies are in reality much more complex and require many experimental tests and theoretical investigations. As a matter of fact, they stand as examples to illustrate the application of some of the previous models.

4.2.4 Study cases - MR damper & SOBEN damper

Since semi-active dampers are an increasing research area involving chemical, mechanical, and control communities, many companies are involved in the development of (new) semi-active technologies. Note that the automotive industry is not the only one to be involved in semi-active actuator. Among others, the civil engineering domain is also largely involved in semi-active dampers in order to compensate building oscillations during earthquakes.

During this thesis, the collaboration projects with the Tecnologico de Monterrey and SOBEN, allows me to "study" two different kinds of Semi-Active dampers:

- A Magneto-Rheological damper, built by DELPHI[2], studied within the collaboration with the Tecnologico de Monterrey.
- A mechanical damper, involving a new technology, built by SOBEN[3], studied during the Master Thesis of Aubouet (2007).

Since the damper study is very complex and is not the main purpose of this thesis, the case studies presented below are given as illustrative examples. The possibilities of such actuators are illustrated through experimental results.

4.2.4.1 Magneto-Rheological dampers (MRD)

In automotive industry, MRD are increasingly used to design semi-active suspension systems. This class of dampers provides a fast, smooth and continuously variable damping coefficient with a wide range of available forces preserving low power consumption (Delphi, 2005). The range of adjustability is virtually infinite within the SER space, making the MRD technology an excellent replacement for conventional suspension dampers. The MRD working principle consists in adjusting the fluid viscosity contained in the compression and release chambers by adjusting the magnetic field intensity provided by a self inductance located at the extremity of the piston. When a magnetic field is created, the fluid particles are aligned and oppose themselves to the fluid movement, increasing the damping coefficient.

[2] Automotive supplier

[3] Young innovative damper company.

During the collaboration with the Tecnologico de Monterrey, a MRD has been bought to the DELPHI company for study purpose. On Figures 4.6 and 4.7, both displacement/force and speed/force diagrams are given for two different current input values. The experiments have been first carried out in Monterrey in order to evaluate the achievable forces of the damper.

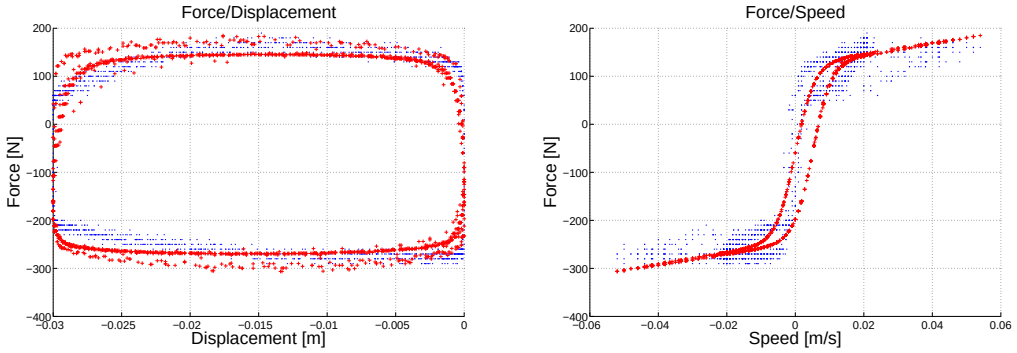

Figure 4.6: MRD study case: 2A current input (red dot: real experimental values; green crosses: model result).

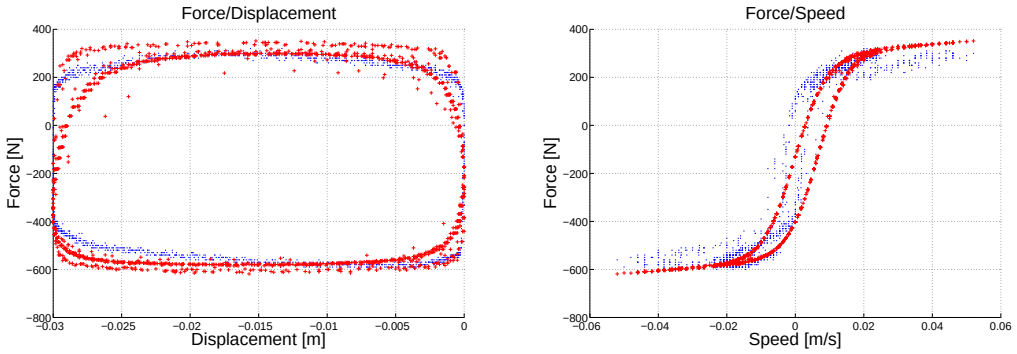

Figure 4.7: MRD study case: 3A current input (red dot: real experimental values; green crosses: model result).

In order to illustrate the previous semi-active damper model presentation, here we aim at fitting the experimental values with one of the models presented below. This is described here but a more complete study is available in the Master Thesis of Kern (2008) and Zolnierczyk (2008). The model identified is given by:

$$F_c = A_1(\Omega)\tanh\left[A_3(\Omega)\left(\dot{z}_{def} + \frac{V_0(\Omega)}{X_0(\Omega)}z_{def}\right)\right] + A_2(\Omega)\left(\dot{z}_{def} + \frac{V_0(\Omega)}{X_0(\Omega)}z_{def}\right) \tag{4.11}$$

where Ω is the current value (as the system is current controlled). In the two cases presented below, the parameter set $\{A_1(\Omega), A_2(\Omega), A_3(\Omega), V_0(\Omega), X_0(\Omega)\}$ has been considered as constant, i.e. as $\{A_1, A_2, A_3, V_0, X_0\}$, and identification performed for each input current value independently. On Figures 4.6 and 4.7 parameter identification results are plotted (red crosses) and compared to real experimental values (blue points).

Remark: About the identification. Here, the identification has been performed for fixed values of the parameters, i.e. avoiding the Ω dependency, but an internal study report done by Zolnierczyk (2008) and Kern (2008) (Master students in the laboratory) has been carried out in order to study and parameterize the previous models according to the current. Roughly speaking, this study provides an extended model where the parameters are current dependent (described as polynomial functions of the current), i.e.

$$F_c = A_1(I)\tanh\left[A_3(I)\left(\dot{z}_{def} + \frac{V_0(I)}{X_0(I)}z_{def}\right)\right] + A_2(I)\left(\dot{z}_{def} + \frac{V_0(I)}{X_0(I)}z_{def}\right) \tag{4.12}$$

Results are not given in this thesis, but are accessible under request through (Zolnierczyk, 2008) Master Thesis. Further works are still under investigation but not reported in this thesis.

4.2.4.2 SOBEN damper

The SOBEN damper is a mechanical based semi-active damper whose working principle is kept confidential (patented). Basically, it consists in adjusting flow section, thanks to screw adjustments, in order to modify the damping factor. The interest of such a technology is that these adjustments make possible to independently modify the damping factor in compression and release. Figures 4.8 and 4.9 show experimental results for different screw adjustments (experiments data provided by S. Aubouet[4]).

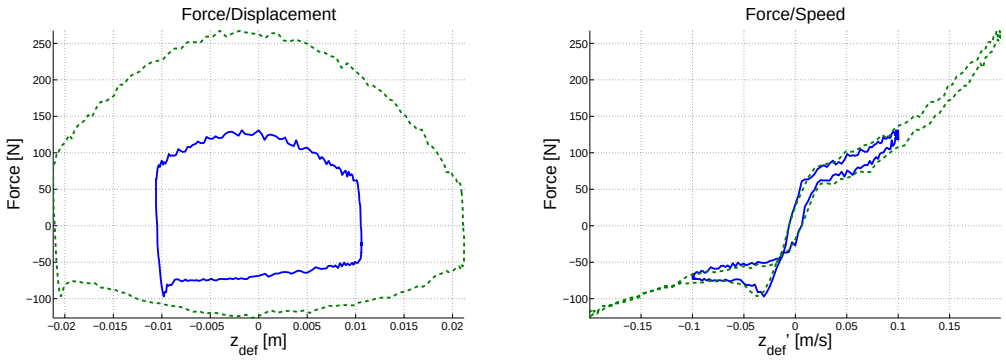

Figure 4.8: SOBEN study case: screw adjustment for low damping (green dashed: $2cm$ of solicitation; solid blue: $1cm$ of solicitation).

Here, Figures 4.8 and 4.9 only provide several damper characteristics for different deflection solicitations and different screw adjustments. For more detail on the modeling, (see Aubouet, 2007; Aubouet *et al.*, 2008).

Remark: Discussion on the damper models MRD vs. SOBEN concept. An interesting remark about MRD concerns the shape of the SER plot. Indeed, results exhibit a certain symmetry: at low speed the slope is almost identical in compression and release (same remark at high speed). Then, this symmetry is cleverly exploited in the models previously exposed. On the contrary, the SOBEN damper does not have a symmetrical behavior, then identification should be done in two steps (one

[4]PhD. student in GIPSA-lab granted by the SOBEN company.

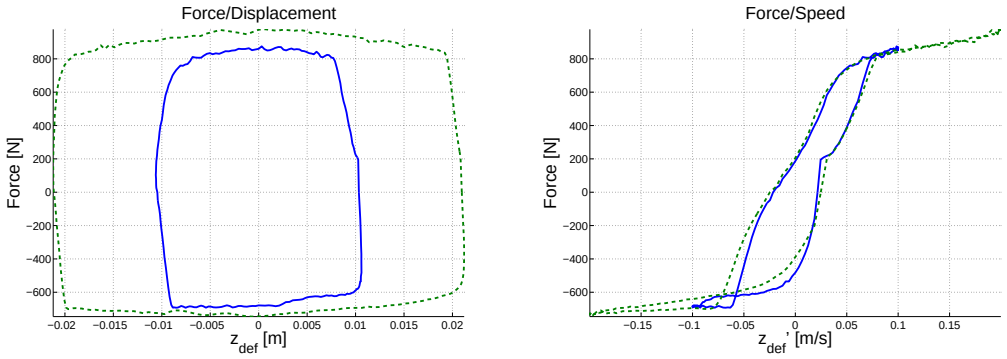

Figure 4.9: SOBEN study case: screw adjustment for high damping (green dashed: $2cm$ of solicitation; solid blue: $1cm$ of solicitation).

for positive speeds, and one for negative ones). The identification work is thus much harder for the SOBEN example and a new model has to be invented to fit the experimental values, but it provides some additional degree of freedom, which, from the control point of view, can be an advantage.

4.3 Tire systems & Road friction phenomena

The tire is the interface between the road and the vehicle. The way of transmitting efforts from the road irregularities to the vehicle is then crucial for the global vehicle dynamic. From a physical modeling viewpoint, the road/tire interaction depends on the tribology theory. Then the contact modeling is a very particular and complex task; much work has been and is still performed (see e.g. Bakker *et al.*, 1989; Canudas *et al.*, 2003*a*; Velenis *et al.*, 2005; Svendenius and Gafvert, 2006; Yi *et al.*, 2003; Ono *et al.*, 2003; Gustafsson, 1997) works. In the sequel, we briefly present the tire longitudinal, lateral and vertical models used for study and control purpose. The author stresses that the models presented here are not the most complete ones, but believes that they are accurate enough for full vehicle modeling.

First the typical variables that characterize the tire forces and moments are introduced. Then longitudinal, lateral and vertical forces and moments involved in the study are described.

4.3.1 Slip angle & Slip ratio

The slip ratio and slip angle are two values that are essential for the tire characterization (see also PhD Thesis of Ramirez-Mendoza, 1997; Sammier, 2001).

- The slip angle defines the angle between the wheel direction and the wheel speed vector $\overrightarrow{v_{ij}}$ (where $i = \{\text{front,rear}\}$ and $j = \{\text{left,right}\}$). Then, for 4 wheels vehicles, where only front

wheels are steerable, β_{ij} is defined as (and illustrated on Figure 4.10):

$$\begin{aligned}
\beta_{fl} &= -\arctan\left(\frac{\dot{y}_s + l_f\dot{\psi}}{\dot{x}_s - t_f\dot{\psi}}\right) + \delta \\
\beta_{fr} &= -\arctan\left(\frac{\dot{y}_s + l_f\dot{\psi}}{\dot{x}_s + t_f\dot{\psi}}\right) + \delta \\
\beta_{rl} &= -\arctan\left(\frac{\dot{y}_s - l_r\dot{\psi}}{\dot{x}_s - t_r\dot{\psi}}\right) \\
\beta_{rr} &= -\arctan\left(\frac{\dot{y}_s - l_r\dot{\psi}}{\dot{x}_s + t_r\dot{\psi}}\right)
\end{aligned} \tag{4.13}$$

where $\dot{x}_s$ and $\dot{y}_s$ are the longitudinal and lateral vehicle velocities respectively, $\dot{\psi}$ is the vehicle COG yaw rate and δ the steering angle. The vehicle dimensions are characterized by l_f, l_r, t_f and t_r (see Appendix D.4 and Figure 4.11).

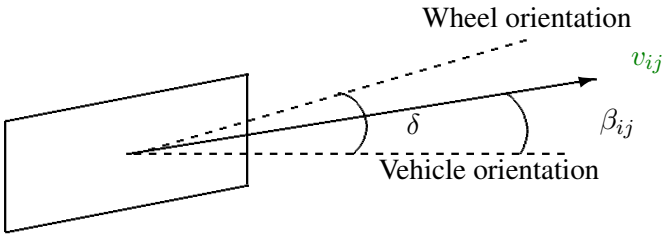

Figure 4.10: Illustration of the slip angle β_{ij} (top view of the wheel).

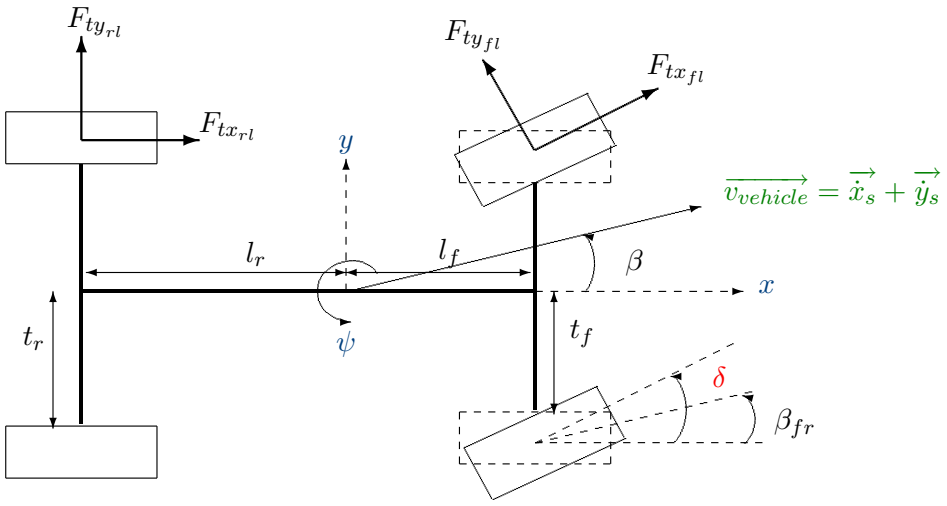

Figure 4.11: Vehicle geometry and β_{ij} (top view of the vehicle).

- The slip ratio λ_{ij} is a dimensionless value defined for each wheels as,

$$\lambda_{ij} = \frac{v_{ij} - R_{ij}\omega_{ij}\cos(\beta_{ij})}{\max\{v_{ij}, R_{ij}\omega_{ij}\cos(\beta_{ij})\}} \text{ where } i = \{f, r\} \text{ and } j = \{l, r\} \tag{4.14}$$

where $v_{ij} = ||\overrightarrow{v}_{ij}||$ is the ij^{th} wheel vehicle speed, R_{ij} holds for the wheel radius, ω_{ij} the wheel rotational speed and β_{ij} the slip angle as defined above. Physically, from this λ definition, it comes that,

- If $\lambda = 0 \Leftrightarrow v = R\omega$, there is no friction, then the vehicle runs at constant speed.
- If $\lambda > 0 \Leftrightarrow v > R\omega\cos(\beta)$, then vehicle is braking.
- If $\lambda < 0 \Leftrightarrow v < R\omega\cos(\beta)$, then vehicle is accelerating.

Moreover, $\lambda = 1$ means that the wheel is locked. Reciprocally, $\lambda = -1$ means that the wheel skates.

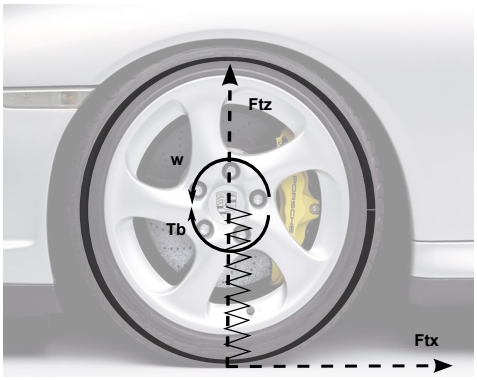

Figure 4.12: Wheel longitudinal dynamic.

According to these value definitions, the longitudinal and lateral tire forces and moments can be derived. It is to note that these two variables are very hard to measure (or compute on line) (see e.g. Caroux *et al.*, 2007; Gustafsson, 1997)

4.3.2 Longitudinal tire force

The longitudinal tire force F_{tx} is a nonlinear function of the slip ratio, parameterized by the road condition. A commonly admitted model is the Burckhardt (1993) model, given in (Kiencke and Nielsen, 2000; Sammier, 2001):

$$F_{tx} = \big(\mu_1(1 - e^{-\lambda\mu_2}) - \lambda\mu_3\big)F_n \tag{4.15}$$

where $F_n = -F_{tz} + g(m_{us} + m_s/4)$ (g is the gravitational constant) holds for the normal load applied to the considered wheel. Then, $\mu = [\mu_1, \mu_2, \mu_3]$ is the longitudinal parameters vector that defines the road friction shape according to the considered road condition. On Figure 4.13, typical curves for different road conditions w.r.t. the slip ratio are shown (see also (Kiencke and Nielsen, 2000; Tanelli, 2007)). On this Figure, only forces for $\lambda \in \left[\begin{array}{cc} 0 & 1 \end{array}\right]$ are given. Between, $\left[\begin{array}{cc} -1 & 0 \end{array}\right]$, the curve is obtained by applying a symmetry w.r.t. $(0, 0)$.

As shown on Figure 4.14, the remarkable point of the these curves is that they present a linear part (for low λ), then, the friction curve shows a maximum peak value (F^*_{tx} at λ^*) and a decreasing slope until $\lambda = 1$. Physically, from this tire/road friction definition, it comes that, to get a maximal braking force, locked wheel does not appear as a good solution. In fact, it will be shown that locking wheel is a very bad situation for vehicle stability. On Figure 4.14, three zone are defined:

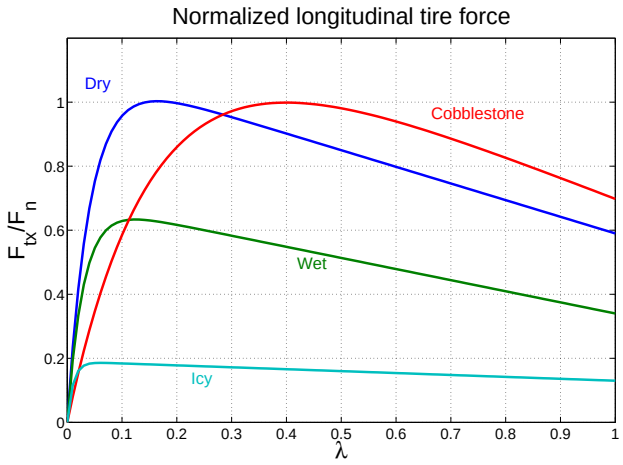

Figure 4.13: Longitudinal normalized tire friction force $F_{tx_{ij}}/F_{n_{ij}}$ for different kinds of road adhesion as a function of λ, the slip ratio. $\mu_{dry} = [1.11, 23.99, 0.52]$, $\mu_{wet} = [0.687, 33.822, 0.347]$, $\mu_{cobblestone} = [1.37, 6.46, 0.67]$, $\mu_{ice} = [0.19, 94.13, 0.06]$

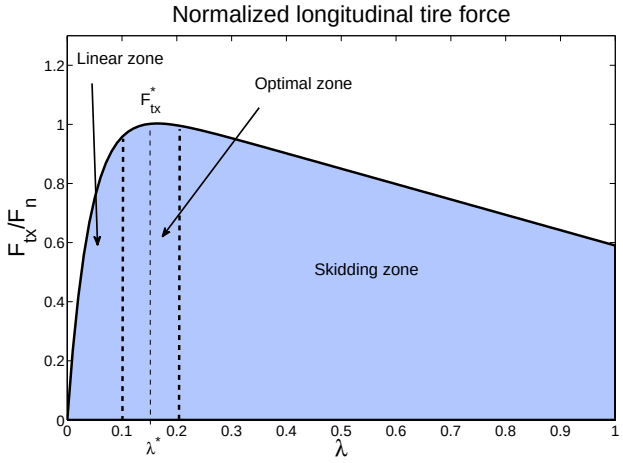

Figure 4.14: Illustration of the different braking zone.

- The linear zone where the tire friction is proportional to the slip ratio λ. Note that remaining in this zone is nice for control purpose since it is kept advantage of the linear structure, i.e.

$$\frac{F_{tx}}{F_n} = C_x \lambda \tag{4.16}$$

  where C_x is the slope of the linear part (also known as the longitudinal tire stiffness). Moreover, by considering F_n as constant, i.e. no load transfer, the longitudinal force description is considerably simplified.

- The optimal zone where the tire friction is almost maximal. This zone corresponds to a λ^* where the ABS aims at regulating the λ (note that it is not so simple since it require the λ measure and since λ^* varies according to the road surface) (Denny, 2005).

- The skidding zone (also known as the unstable zone) where the friction decreases and leads the wheels to be locked (the first aim of the ABS is to avoid this zone).

4.3.3 Lateral tire force

As for longitudinal force, many models are available in the literature for the lateral force. We have chosen to model the lateral force by formulae (4.17), illustrated on Figure 4.15 (Bakker *et al.*, 1989; Kiencke and Nielsen, 2000; Mammar and Koenig, 2002),

$$F_{ty} = D_y \sin\Big(C_y \arctan\big(B_y(1-E_y)\beta + E_y \arctan(B_y\beta)\big)\Big)e^{-6|\lambda|^5} \tag{4.17}$$

where, $B_y = (2-\mu)b_y$, $C_y = (5/4-\mu/4)c_y$, $D_y = d_y\mu$ and $E_y = e_y$ are the lateral tire parameters, function of $\mu \in [0;1]$, the tire/road adhesion coefficient (see D.4). Additionally, the term "$e^{-6|\lambda_{ij}|^5}$" is used to model the lateral friction forces dependency w.r.t. the slip ratio: when slipping occurs on a wheel, lateral forces are reduced, i.e., $\lim_{\lambda\to|1|} F_{ty} = 0$ (see also Figure 4.15).

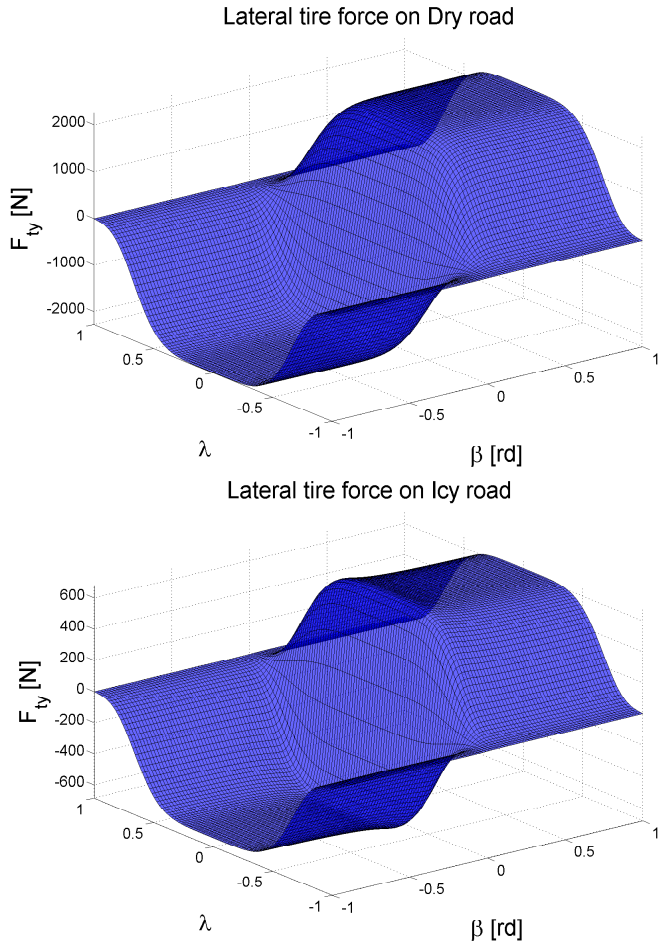

Figure 4.15: Lateral tire friction force $F_{ty_{ij}}$ for different kinds of roads as a function of β, the side slip angle and λ, the slip ratio.

Remark: About $e^{-6|\lambda_{ij}|^5}$ scaling factor. This scaling factor has been added by the author to model the loss of manoeuvrability. We stress that no experimental test have been carried out. Thus, the parameters have been arbitrarily chosen; but as the friction is diminished when from $|\lambda| = 0.5$ author believe that in classical driving situations, this term will not affect the vehicle dynamic (see Figure 4.15).

4.3.4 Vertical tire force

The vertical force is linearly described by (4.18),

$$F_{tz} = k_t(z_{us} - z_r) + c_t(\dot{z}_{us} - \dot{z}_r) \tag{4.18}$$

where $k_{t_{ij}}$ and $c_{t_{ij}}$ are the tire vertical stiffness and damping constant respectively. Note that since the c_t parameter is very small and k_t very high, c_t is often neglected in the vertical modeling. However, this damping physically exists since tire dissipates energy. This force is not a contact force, thus it is applied at the center of gravity of the wheel.

4.3.5 Vertical tire (auto-aligning) moment

The auto-aligning moment represents the moment applied on the vertical axis of the tire. This moment describes the physical fact that wheels naturally align with the vehicle speed vector. It is modeled as (Kiencke and Nielsen, 2000):

$$M_{tz} = D_z \sin\Big[C_z \arctan\Big(B_z\big((1-E_z)\beta + (\frac{E_z}{B_z}\arctan(B_z\beta))\big)\Big)\Big]F_n \tag{4.19}$$

where $\{B_z, C_z, D_z, E_z\}$ are the auto-aligning model parameters and where β is the slip angle as described above.

This moment plays an important role when the steering control is involved. Indeed, when the steering modeling and control are treated, this moment is very important as it models a part of the force that that the driver feels when the steering torque is applied.

4.3.6 Braking actuators

Electro-Mechanical Braking (EMB) systems have been recently more and more studied. They replace the Hydraulic actuators that were only able to deliver an on/off control torque (see PhD Thesis of Tanelli, 2007). EMB systems allow to provide a continuously variable modulation braking torque. Then EMB actuators will be modeled as a first order low-pass transfer function:

$$\dot{T}_b = \varpi(T_b^0 - T_b) \tag{4.20}$$

where $\varpi = 70rd/s$ is the actuator cut-off frequency, $\dot{T}_b$ is the applied braking torque and $\dot{T}_b^0$ the desired torque.

4.3.7 Discussion on tire modeling & on related challenges

This section introduces the tire element, and more specifically, the tire/road interaction phenomena description and modeling. It is not exhaustive and the interested reader may refer to works quoted in

this section and in the state of the art given in Chapter 2. The main purpose here is to present the models involved in our study.

Then according to these models, it is important to notice some challenging points related to tire friction modeling, value estimation and measurements.

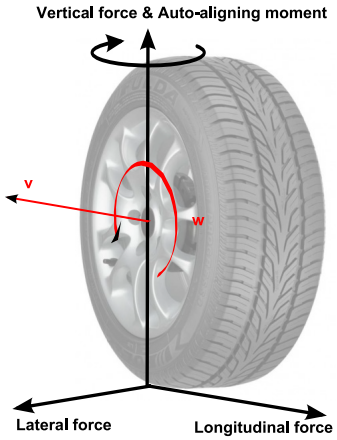

Figure 4.16: Tire forces and moments.

Some challenging points. The main challenge in braking control is to guarantee maximal braking force, i.e. to guarantee a slip ratio λ around the optimal value λ^*. For more information, the reader can refer to a very recent PhD Thesis of Tanelli (2007) where these problems are more deeply treated.

4.4 Steering system & Direction column

In this section, some elements on the steering system (and direction column) are briefly presented.

4.4.1 Remarks on the direction column

When one aims at modeling the vehicle in a manoeuver, or at controlling the steering wheels (e.g. for driver assistance), the angle applied on the directional wheels (here, the front wheels), two choices may be done:

- The model input is the wheel angle. This solution is widely used in the literature but suggests that the direction column already has an inner controller.
- The model input is the steering wheel torque. This solution is much more realistic since in reality, the driver steers the vehicle by applying a torque on the steering wheel, and feels the feedback force (coming from the auto-aligning moments).

As this thesis is more focused on the global chassis control, the column direction will not be taken into account. But for sake of clarity and completeness, the general model is given thereafter.

4.4.2 Direction column model

The direction column system which relates the driving angle δ applied to the directional wheels to the applied torque T on the steering wheel, is modeled as follows:

$$\ddot{\delta} = \frac{1}{R_s} T \tag{4.21}$$

where R_s is the reduction factor. Then T is given by:

$$T = T_d + T_v + T_c \tag{4.22}$$

where T_d is the driver torque, T_v is a function of the auto-aligning torque M_{tz} described above, coming from the vehicle and tire dynamics, and T_c the controlled torque, provided by the steering controller.

Note that the interest in working with the direction column is to take into account the auto-aligning moment, which represents a nonlinear disturbance, for steering control synthesis. In the PhD Thesis of Raharijaona (2004), an interesting illustration of the steering control is presented (for driver lateral assistance).

4.5 Concluding remarks

In this chapter, we principally introduced the suspension modeling and characteristics, together with mathematical models (with industrial illustrative examples) and the tire/road friction phenomena that are adopted in this thesis for simulation and control purpose. The main issue in this chapter is to introduce the complex forces that enter into consideration when global chassis is studied. The next chapter is devoted to the vehicle models involved in the literature and in this thesis for control and simulation purposes; they are based on these actuators and sub-systems.

In this chapter, we pointed out also some challenging points and some problems that occur for control purpose.

Chapter 5

Vehicle modeling and analysis

5.1 Introduction

According to the previously introduced elements, namely, suspension, tire and steering subsystems, many different vehicle models have been developed and are available in the literature. This chapter details the models involved in this thesis, together with their structural limitations. These models are mainly based on well known results nicely exposed in (Gillespie, 1992; Milliken and Milliken, 1995; Kiencke and Nielsen, 2000). Additionally, performance specifications, related to driver feelings, vehicle limitations and safety requirements, are given. These specifications will play an important role in the next chapters, for control synthesis and evaluation. In this chapter, we provide a library of vehicle models, relevant for our work and for analysis and control synthesis purpose.

Automotive expert may consider the given models as limitative for simulation purpose (especially from the mechanical point of view), but we stress that the models involved here are developed for control purpose, and to simulate and describe the main vehicle dynamical behaviors (see Figure 5.1).

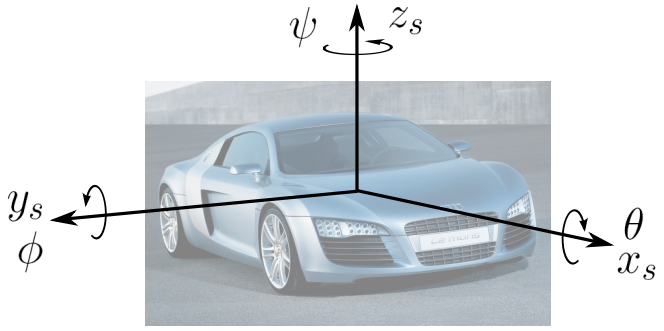

Figure 5.1: Vehicle dynamics.

Other ways of modeling could be done using specific software (as CarSim, ADAMS Car, Modelica, etc. but are not described here), and may be used in co-simulation with Matlab/Simulink, as shown in (Poussot-Vassal *et al.*, 2008*a*).

The main contributions presented in this chapter concern the definition of the full vehicle dynamics. More precisely:

- The extension of the full nonlinear vehicle model presented in Zin (2005). The model defined in

this work includes additional dynamics (such as slip ratio, wheel speed) and force descriptions (such as longitudinal and extended lateral tire forces). This extension is very important when the braking control is to be studied (see also Chapter 7).

- The validation of this extended model structure and parameters done using experimental results obtained on a Renault Mégane Coupé car. This step has been carried thanks to a collaboration with G.L. Gissinger, M. Basset and C. Lamy from the MIAM laboratory (Mulhouse, France).

The Chapter is structured as follows: Section 5.2 introduces the quarter car models (vertical and/or longitudinal), which are widely used in the literature and in the thesis, for suspension and braking control purposes. Then, half car models (vertical and lateral), involved in suspension and steering control are given in Section 5.3. Section 5.4 introduces the full vehicle nonlinear model that will be extensively used for control validation (see Chapter 7) and that has been validated through experimental tests thanks to a collaborative work with the MIAM research team, Mulhouse, France (see also Zin *et al.*, 2004). Finally, Section 5.5 describes the performance specifications and the metrics that are used to quantify and evaluate the control performances.

5.2 Quarter vehicle models

In this section, the quarter car models (both vertical and longitudinal) are introduced. The dynamical equations and some descriptions of the challenges related to these models are presented in order to give some background to the reader before reading the Chapter 6.

5.2.1 Vertical quarter car model

When suspension modeling and control are considered, the vertical quarter car model is often used. This model allows to study the vertical behavior of a vehicle according to the suspension characteristic (passive or controlled). Figure 5.2 shows what is the so-called vertical quarter car and where it comes from.

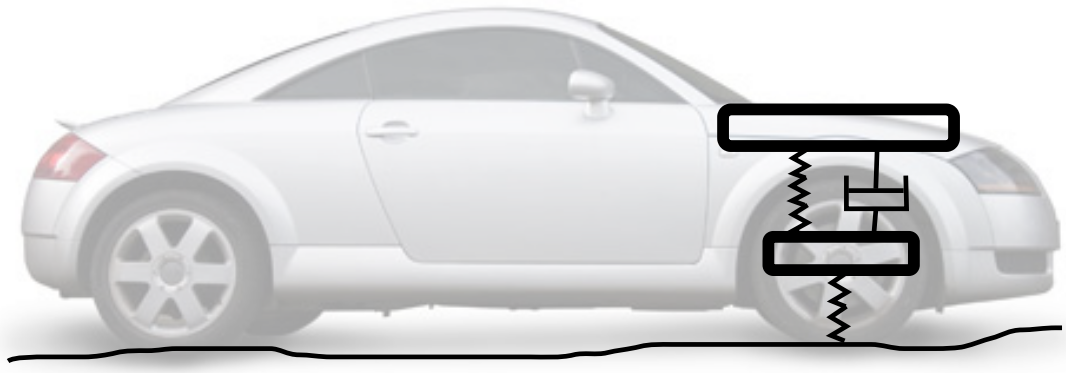

Figure 5.2: Quarter car of a vehicle.

On Figure 5.3, the passive and controlled quarter car models, as they are treated in the literature, are shown. As illustrated on Figure 5.3, and according to Section 4.2, when controlled suspension is considered, the passive damper F_c is removed and replaced by an actuator that provides a force u either active or semi-active (depending on the chosen actuator).

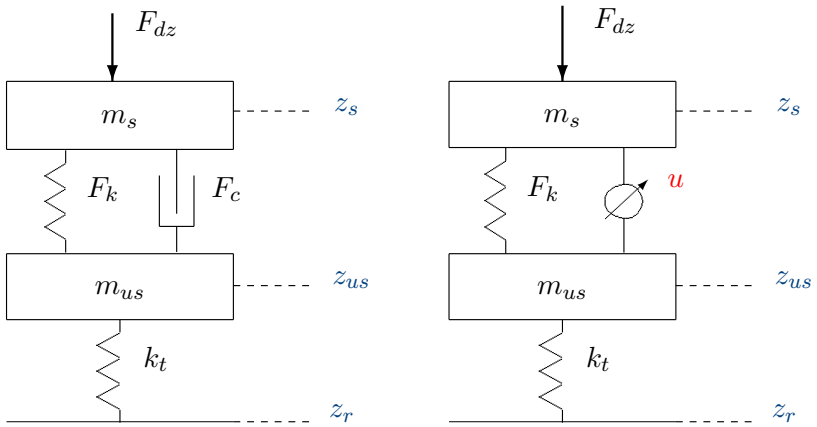

Figure 5.3: Passive (left) and Controlled (right) quarter car model.

The nonlinear, LTI and LPV dynamical models of the vertical quarter car are given thereafter.

Nonlinear model. Vertical efforts generated by the suspension and tire elements are nonlinear (see Chapter 4). Let recall that:

$$\left\{\begin{array}{lcll} F_{tz} & = & k_t(z_{us}-z_r)+c_t(\dot{z}_{us}-\dot{z}_r) & \\ F_{sz} & = & F_k(z_s-z_{us})+F_c(\dot{z}_s-\dot{z}_{us}) & \text{(passive suspension case)} \\ F_{sz} & = & F_k(z_s-z_{us})+u & \text{(controlled suspension case)} \end{array}\right. \tag{5.1}$$

where k_t and c_t are the linear tire stiffness and damping factors. Then, the vertical quarter car model is given by the following dynamical equations,

$$\left\{\begin{array}{rcl} m_s\ddot{z}_s & = & -(F_{sz}+F_{dz}) \\ m_{us}\ddot{z}_{us} & = & F_{sz}-F_{tz} \end{array}\right. \tag{5.2}$$

where $F_k(.)$ is a nonlinear function of the suspension deflection $z_{def}=(z_s-z_{us})$, $F_k(.)$ a nonlinear function of the deflection velocity, m_s and m_{us} are known as sprung and unsprung masses respectively. z_s and z_{us} are the chassis and unsprung masses bounce. Then, F_{dz} describes a vertical disturbance force (that can be caused by a load transfer, e.g. steering situation). Finally, according to the suspension model chosen, different kinds of quarter car models may be obtained. The characterization is done through the input u (see Section 4.2):

- If $u=F_c(\dot{z}_s-\dot{z}_{us})$, the suspension is passive.
- If $u=F_c(\dot{z}_s-\dot{z}_{us},\Omega)$, the suspension is semi-active, where Ω is input parameter of the controlled damper that modifies the damping factor.
- If u is an independent function, the quarter car is said to be active.

In this model, the nonlinear phenomena come from the force description of the suspension elements and not from the equation structure. Therefore, the vertical quarter vehicle model can "easily" be set as a LPV model (as shown thereafter).

Remark: Unsprung mass. The unsprung mass m_{us} corresponds to the set of elements that compose the wheel, the suspension system, and multiple links from the chassis to the "road". Without loss of generality, we will often refer to as the wheel since z_{us} is the center of the wheel (see also Figure 5.3).

Property 5.2.1 (*Invariant points*)

The model (5.2) has remarkable properties: the system exhibits some invariant points. They are called invariant since they characterize points and behaviors in the frequency domain that will not change, whatever the applied control law is. This means that some variables are uncontrollable at some specific frequencies (Moreau, 1995).

1. *From (5.2), by adding the two equalities, one obtains (with $F_{dz} = 0$),*

$$\begin{array}{rl} & m_s\ddot{z}_s + m_{us}\ddot{z}_{us} = k_t(z_r - z_{us}) \\ \Leftrightarrow & m_s(j\omega)^2 Z_s(j\omega) + (m_{us}(j\omega)^2 + k_t)Z_{us}(j\omega) = k_t Z_r(j\omega) \end{array} \tag{5.3}$$

if $\omega = \omega_1 = \sqrt{\frac{k_t}{m_{us}}}$, then,

$$\left.\frac{Z_s(j\omega)}{Z_r(j\omega)}\right|_{\omega_1} = \frac{m_{us}}{m_s} \tag{5.4}$$

2. *Similarly,*

$$\begin{array}{rl} & k_t(z_r - z_{us}) + k_t(z_{us} - z_r) = 0 \\ \Leftrightarrow & k_t(z_r - z_{us}) + m_{us}\ddot{z}_s - m_{us}\ddot{z}_s + k_t z_s - k_t z_s + k_t z_{us} - k_t z_r = 0 \\ \Leftrightarrow & m_s\ddot{z}_s + m_{us}\ddot{z}_{us} + m_{us}\ddot{z}_s - m_{us}\ddot{z}_s + k_t z_s - k_t z_s + k_t z_{us} = k_t z_r \\ \Leftrightarrow & \Big((m_s + m_{us})(j\omega)^2 + k_t\Big) Z_s(j\omega) + (m_{us}(j\omega)^2 + k_t)(Z_s(j\omega) - Z_{us}(j\omega)) = k_t Z_r(j\omega) \end{array} \tag{5.5}$$

if $\omega = \omega_2 = \sqrt{\frac{k_t}{m_s + m_{us}}}$, then,

$$\left.\frac{Z_{def}(j\omega)}{Z_r(j\omega)}\right|_{\omega_2} = \left.\frac{Z_s(j\omega) - Z_{us}(j\omega)}{Z_r(j\omega)}\right|_{\omega_2} = \frac{m_s + m_{us}}{m_s} \tag{5.6}$$

So, whatever the designed control law, these points are not modified. These properties have to be kept in mind during the suspension control design step.

Figure 5.4 shows the frequency response (pseudo-Bode diagram) of $\ddot{z}_s/z_r$, z_s/z_r, z_{us}/z_r and z_{def}/z_r of the nonlinear vertical quarter car model with the Renault Mégane Coupé nonlinear parameters; i.e. nonlinear spring and passive damper forces (given in Figures 4.4 and 4.5) and parameters given in Table 5.1.

Remark: About the pseudo-Bode. The "pseudo-Bode" concept is largely used in this thesis and aims at plotting Bode-like diagram of nonlinear models. The pseudo-Bode computation method is given in Appendix B.2.

Note that these transfers ($\ddot{z}_s/z_r$, z_s/z_r, z_{us}/z_r and z_{def}/z_r) are widely used in the suspension community in order to evaluate performances of the proposed control laws. The same outputs with

Symbol	Value	Unit	Signification
m_s	315	kg	sprung mass
m_{us}	37.5	kg	unsprung mass
k	29500	N/m	suspension linearized stiffness
c	1500	$N/m/s$	suspension linearized damping
k_t	208000	N/m	tire stiffness
z_{def}	$[-0.09; 0.05]$	m	suspension bound (stroke limit)

Table 5.1: Linearized Renault Mégane Coupé parameters of the quarter vertical model (front suspension).

respect to the external load F_{dz} are also involved when the load transfer is under consideration but the quarter car behavior w.r.t. road irregularities remains mostly treated (Zin, 2005).

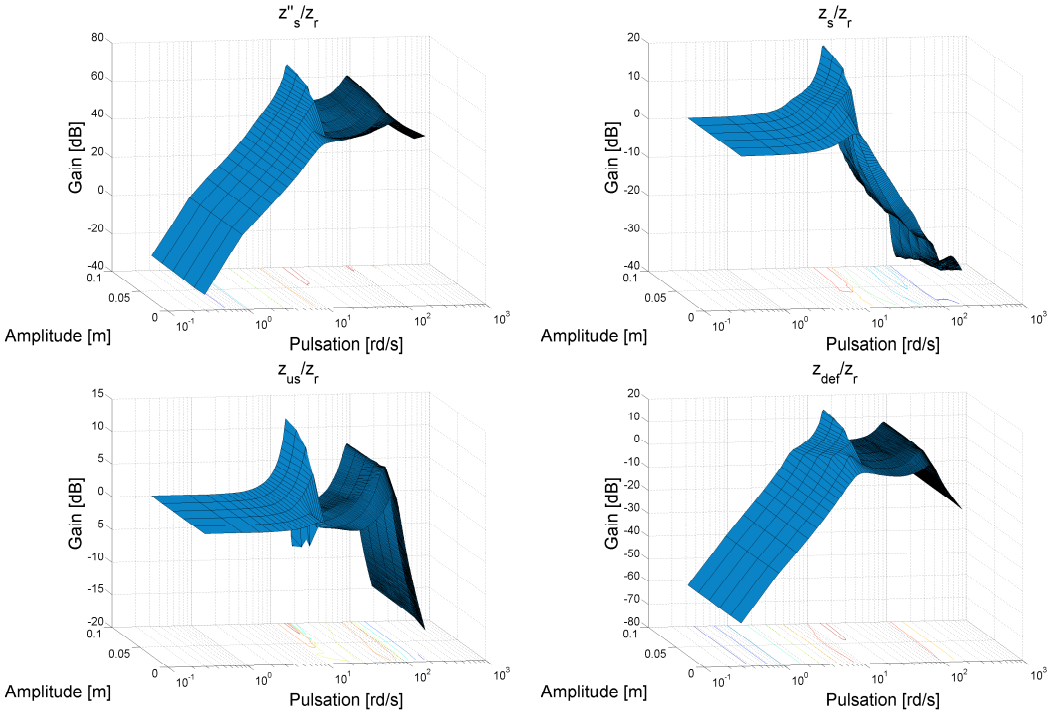

Figure 5.4: Pseudo-Bode diagrams of $\ddot{z}_s/z_r$, z_s/z_r, z_{us}/z_r and z_{def}/z_r for various input magnitude and frequencies.

Figure 5.4 shows interesting phenomena: for low input amplitude ($z_r < 3cm$) the quarter car behavior remains in the linear zone of the suspension (small deflection and deflection speed, see Figures 4.4 and 4.5), then the behavior is very similar to the linear one (see after), but when the road disturbances become larger, the suspensions enter the nonlinearities and the peak values increase. Then the suspension frequency behavior is deeply affected. Note that in Chapter 6, this problem is handled by an LPV control design.

LTI model. The LTI quarter car model is obtained by choosing a linear suspension model (or by linearizing the nonlinear model) i.e. $F_k = k(z_s - z_{us})$ and $F_c = c(\dot{z}_s - \dot{z}_{us})$ where k and c are the linear stiffness and damping coefficients. Then, equations (5.1) and (5.2) become:

$$\left\{ \begin{array}{rcl} m_s\ddot{z}_s & = & -k(z_s - z_{us}) - c(\dot{z}_s - \dot{z}_{us}) - u - F_{dz} \\ m_{us}\ddot{z}_{us} & = & k(z_s - z_{us}) + c(\dot{z}_s - \dot{z}_{us}) + u - k_t(z_{us} - z_r) \end{array} \right. \tag{5.7}$$

and as an illustration, the associated state space representation can be derived as:

$$\begin{bmatrix} \dot{z}_s \\ \ddot{z}_s \\ \dot{z}_{us} \\ \ddot{z}_{us} \end{bmatrix} = \begin{bmatrix} 0 & 1 & 0 & 0 \\ \frac{-k}{m_s} & \frac{-c}{m_s} & \frac{k}{m_s} & \frac{c}{m_s} \\ 0 & 0 & 0 & 1 \\ \frac{k}{m_{us}} & \frac{c}{m_{us}} & \frac{-k-k_t}{m_{us}} & \frac{-c}{m_{us}} \end{bmatrix} \begin{bmatrix} z_s \\ \dot{z}_s \\ z_{us} \\ \dot{z}_{us} \end{bmatrix} + \begin{bmatrix} 0 \\ \frac{-1}{m_s} \\ 0 \\ \frac{1}{m_{us}} \end{bmatrix} u + \begin{bmatrix} 0 \\ 0 \\ 0 \\ \frac{k_t}{m_{us}} \end{bmatrix} z_r + \begin{bmatrix} 0 \\ \frac{-1}{m_s} \\ 0 \\ 0 \end{bmatrix} F_{dz} \tag{5.8}$$

LPV model. As previously exposed, the nonlinearities of the nonlinear model (5.2) are caused by the suspension forces. Then, the LPV formulation can be derived by selecting as the varying parameters, the nonlinearity of the stiffness and damping coefficients of the suspension, as done in (Zin *et al.*, 2008*a*). Then, the LPV model can be given as,

$$\left\{ \begin{array}{rcl} m_s\ddot{z}_s & = & -k(.)(z_s - z_{us}) - c(.)(\dot{z}_s - \dot{z}_{us}) - u - F_{dz} \\ m_{us}\ddot{z}_{us} & = & k(.)(z_s - z_{us}) + c(.)(\dot{z}_s - \dot{z}_{us}) + u - k_t(z_{us} - z_r) \end{array} \right. \tag{5.9}$$

where $k(.)$ and $c(.)$ are the varying nonlinear stiffness and damping coefficients given on Figure 5.5 and obtained by taking the tangent on each points of Figures 4.4 and 4.5.

Consequently, the LPV associated model is given by:

$$\begin{bmatrix} \dot{z}_s \\ \ddot{z}_s \\ \dot{z}_{us} \\ \ddot{z}_{us} \end{bmatrix} = \begin{bmatrix} 0 & 1 & 0 & 0 \\ \frac{-k(.)}{m_s} & \frac{-c(.)}{m_s} & \frac{k(.)}{m_s} & \frac{c(.)}{m_s} \\ 0 & 0 & 0 & 1 \\ \frac{k(.)}{m_{us}} & \frac{c(.)}{m_{us}} & \frac{-k(.)-k_t}{m_{us}} & \frac{-c(.)}{m_{us}} \end{bmatrix} \begin{bmatrix} z_s \\ \dot{z}_s \\ z_{us} \\ \dot{z}_{us} \end{bmatrix} + \begin{bmatrix} 0 \\ \frac{-1}{m_s} \\ 0 \\ \frac{1}{m_{us}} \end{bmatrix} u + \begin{bmatrix} 0 \\ 0 \\ 0 \\ \frac{k_t}{m_{us}} \end{bmatrix} z_r + \begin{bmatrix} 0 \\ \frac{-1}{m_s} \\ 0 \\ 0 \end{bmatrix} F_{dz} \tag{5.10}$$

Remark: Parameter properties. In this case, note that:

- The parameter dependency enters in a linear way in the dynamical state matrix.
- The parameters are function of the state variables, i.e. $k(.)$ is function of $z_{def} = z_s - z_{us}$ and $c(.)$ is a function of $\dot{z}_{def} = \dot{z}_s - \dot{z}_{us}$.

The model is therefore said to be qLPV.

Different criteria can be used to evaluate a suspension performance. In Section 5.5, a performance criterion, based on industrial specifications is given. Before further reading and introduction of more complex models, for sake of clarity, the reader should keep in mind that the frequency analysis of the chassis displacement and acceleration (upper pseudo-Bode diagrams on Figure 5.4) are related to comfort specifications, and the evaluation of wheel displacement and suspension deflection (lower pseudo-Bode diagrams on Figure 5.4) is related to road-holding performances.

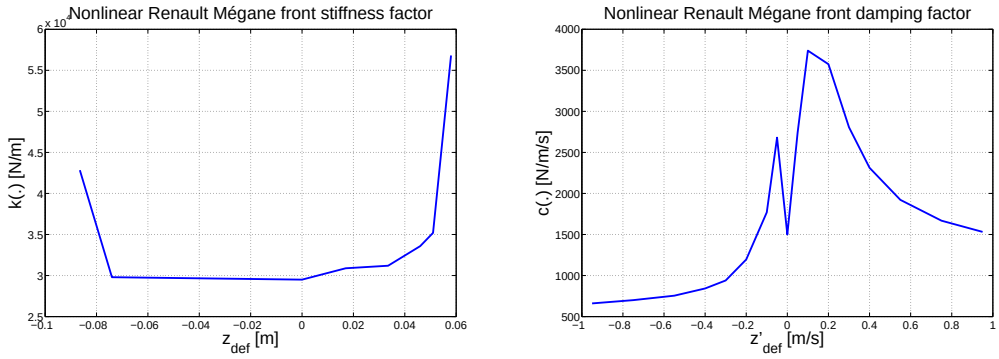

Figure 5.5: Spring ($k(.)$) and damping ($c(.)$) coefficients as a function of the suspension deflection and deflection speed respectively.

5.2.2 Extended quarter car model

The classical vertical quarter car model allows to model only the vertical bounce of the chassis and of the wheel. A natural extension consists in adding the longitudinal dimension, i.e. the wheel dynamic as shown on Figure 5.6.

Figure 5.6: Extended quarter car model.

Remark: Longitudinal quarter car model. Usually, when braking control and ABS are studied, a widely expanded model is the longitudinal quarter car model that only involves λ, ω and v.

Nonlinear model. The nonlinear model of the extended vertical longitudinal quarter vehicle model is given by the following equation set (involving new dynamics; namely λ, ω and v) and shown on

Figure 5.7:

$$\begin{cases} m_s\ddot{z}_s &= -(F_{sz}+F_{dz}) \\ m_{us}\ddot{z}_{us} &= F_{sz}-F_{tz} \\ \dot{\lambda} &= -\frac{1}{v}\left(\frac{1-\lambda}{m}-\frac{R^2}{I_w}\right)F_{tx}(\mu,\lambda,F_n)+\frac{R}{vI_w}T_b \\ I_w\dot{\omega} &= RF_{tx}(\mu,\lambda,F_n)-T_b \\ m\dot{v} &= -F_{tx}(\mu,\lambda,F_n) \end{cases} \tag{5.11}$$

where λ, ω and v are the longitudinal slip ratio, the rotational wheel speed and the longitudinal vehicle speed respectively, $m = m_s + m_{us}$ is the quarter car total mass, R characterizes the wheel radius, I_w is the wheel inertia, $F_{tx}(\mu,\lambda,F_n)$ is the longitudinal tire/road friction force (as described in Chapter 4, with μ the road adhesion and F_n the normal tire force) and T_b is the braking torque, applied at the center of the wheel (see also Figure 5.7).

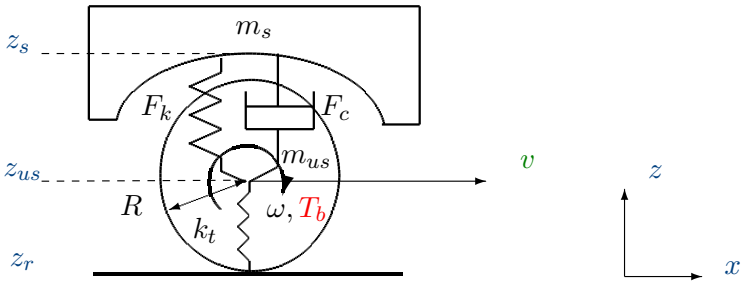

Figure 5.7: Extended quarter car model.

Symbol	Value	Unit	Signification
m_s	315	kg	sprung mass
m_{us}	37.5	kg	unsprung mass
k	29500	N/m	suspension linearized stiffness
c	1500	$N/m/s$	suspension linearized damping
k_t	208000	N/m	tire stiffness
z_{def}	$[-0.09; 0.05]$	m	suspension bound (stroke limit)
R	0.3	m	tire radius

Table 5.2: Linearized Renault Mégane Coupé parameters of the extended quarter vertical model (front suspension).

The coupling phenomenon, between (z_s, z_{us}) and (λ, ω, v), is the normal load F_n which is function of the suspension force and defined as:

$$F_n = -mg + F_{tz} - F_{sz} \tag{5.12}$$

where g is the gravitational constant. This model is being more and more studied since it can connect the work of both brake and suspension control communities. Before, vertical and longitudinal dynamics were often studied separately; but, due to the need for performances in emergency situations, they are studied together to synthesize braking controller handling normal load (since a normal load modifies the slip dynamics, hence the longitudinal force, and the vehicle and wheel dynamics).

The main point to remember, concerning this model, is that the new involved slip dynamics, λ is highly nonlinear and fast compared to the vehicle bounce.

As an illustration, on Figure 5.8 the model (5.11) is simulated on a straight road. The slip dynamics is shown w.r.t. the vehicle speed for an initial state of $\lambda_0 = 1$ (i.e. wheel locked). This simulation stands to illustrate the slip dynamic from wheel locked to free wheel.

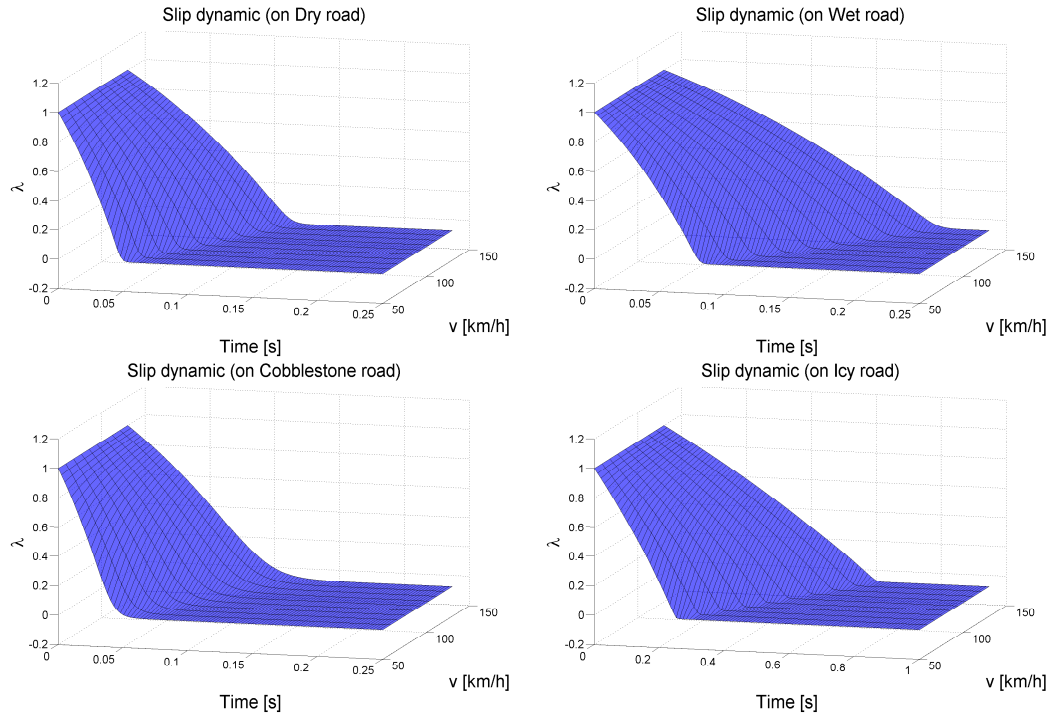

Figure 5.8: Slip dynamic according to the vehicle initial speed for an initial slip of $\lambda_0 = 1$ (i.e. wheel locked), for different road adhesion types: from top left to bottom right: dry, wet, cobblestone and icy.

Moreover, Figure 5.9 shows the slip dynamics with respect to the vehicle speed for an initial state of $\lambda_0 = 0$ (i.e. wheel not locked) with a braking torque of $T_b = 1200Nm$ (maximal torque available). Thus, this simulation shows how fast the slip goes from 0 to 1 when a braking torque is applied.

These two illustrative examples are mainly introduced to underline the slipping problematic. This point will be studied and recalled later in Chapter 7 where the braking strategies are involved. It mainly shows that the slipping situation, which leads the vehicle to instability and loss of manoeuvrability (lateral forces fall to 0), occurs very quickly. This motivates an extensive research in the field of the ABS. Moreover, the careful reader can note, especially on Figure 5.9 (top left), that the slip surface exhibits three dynamical behaviors:

- Firstly, a stiff increasing slope (from $\lambda = 0$ to $\lambda = 0.2$, between $t = 0$ to $t = 0.1$s), which corresponds to the stiff slope value of the longitudinal tire force given on Figure 4.14 (linear stable force zone, "Linear zone").

- Secondly, a low slope or inflection zone (from $\lambda = 0.2$ to $\lambda = 0.3$, between $t = 0.05$ to $t = 0.5$s) which corresponds to the maximal peak value of the longitudinal tire force of Figure 4.14 ("Optimal" braking zone).

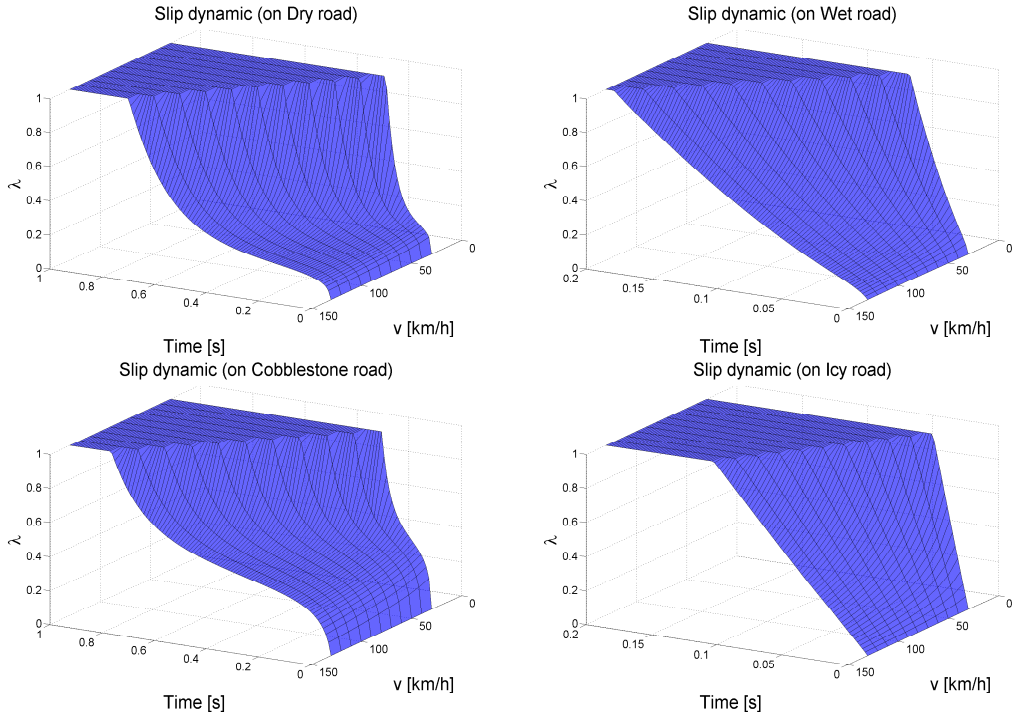

Figure 5.9: Slip dynamic according to the vehicle initial speed for an initial slip of $\lambda_0 = 0$ (i.e. wheel not locked) and for a braking torque $T_b = T_b^{max} = 1200Nm$, for different road adhesion types: from top left to bottom right: dry, wet, cobblestone and icy.

- Thirdly, a higher slope (from $\lambda = 0.3$ to $\lambda = 1$, between $t = 0.5$ to $t = 0.7$s), which corresponds to the falling slope of Figure 4.14 ("Skidding zone" of the tire, unstable zone).

This last remark illustrates what was pointed in Section 4.3 i.e. during a braking phase, the slip value increases very quickly. As a consequence, the wheel is locked very quickly too, and, according to the lateral tire modeling (see equation (4.17) and Figure 4.15) the vehicle is no longer manoeuvrable in less than $1s$. This illustrates how essential the ABS control unit is (see also Figure 5.10).

5.3 Half vehicle models

From now, all the parameters involved in the equations are defined in Appendix D.4.

5.3.1 Vertical half vehicle models

Vertical half vehicle models are the natural extension of the vertical quarter car model. It simply involves an additional dynamic: the pitch (ϕ) or roll (θ) motion.

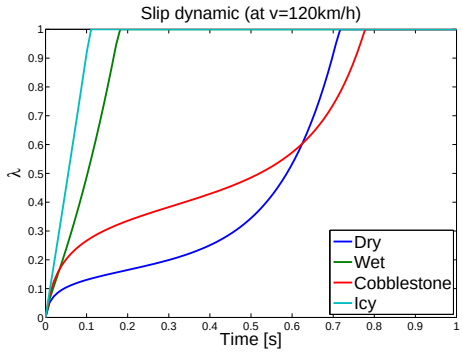

Figure 5.10: Slip dynamic according for an initial slip of $\lambda_0 = 0$ (i.e. wheel not locked), $v = 120km/h$ and for a braking torque $T_b = T_b^{max} = 1200Nm$, for different road adhesion types: dry, wet, cobblestone and icy.

Nonlinear roll oriented model. The nonlinear model involving roll dynamic is simply given by equation (5.13) and Figure 5.11,

$$\left\{\begin{array}{rcl} m_s\ddot{z}_s & = & -(F_{sz_l} + F_{tz_r} + F_{dz}) \\ m_{us_l}\ddot{z}_{us_f} & = & F_{sz_l} - F_{tz_r} \\ m_{us_r}\ddot{z}_{us_r} & = & F_{sz_l} - F_{tz_r} \\ I_x\ddot{\theta} & = & F_{sz_l}t_f - F_{tz_r}t_f + M_{dx} \end{array}\right. \tag{5.13}$$

where the index $\{l, r\}$ holds for {left,right}, F_{sz_j} are the suspension forces, F_{tz_j} are the tire forces, I_x is the roll inertia and M_{dx} is the disturbance moment on the x axis (i.e. on the roll axis). t_f denotes the front axle length as shown on Figure 5.11. z_s and ϕ are the chassis bounce and pitch at the center of gravity; z_{us_f} and z_{us_r} are the front and rear unsprung masses bounce respectively.

As an illustration, Figure 5.12 shows the frequency response (pseudo-Bode diagram) of $\ddot{z}_s/z_{r_l}$, z_s/z_{r_l}, z_{us_l}/z_{r_l}, z_{def_l}/z_{r_l} and θ/z_{r_l} of the nonlinear vertical half car model (roll oriented) with the Renault Mégane Coupé nonlinear suspensions parameters.

Remark: Models and extensions. The frequency responses are likely similar to the quarter car model and the remarks for the quarter model hold for this one:

- Both LPV (w.r.t. the spring stiffness) and LTI models can easily be derived from these equations.
- As for the vertical quarter car model, the main nonlinearities are introduced by the suspension elements. However, kinematic relations are also involved in these models (for more information, see the full model given thereafter).
- As for the quarter vertical mode, the extended model (involving the longitudinal dimension) can easily be derived.

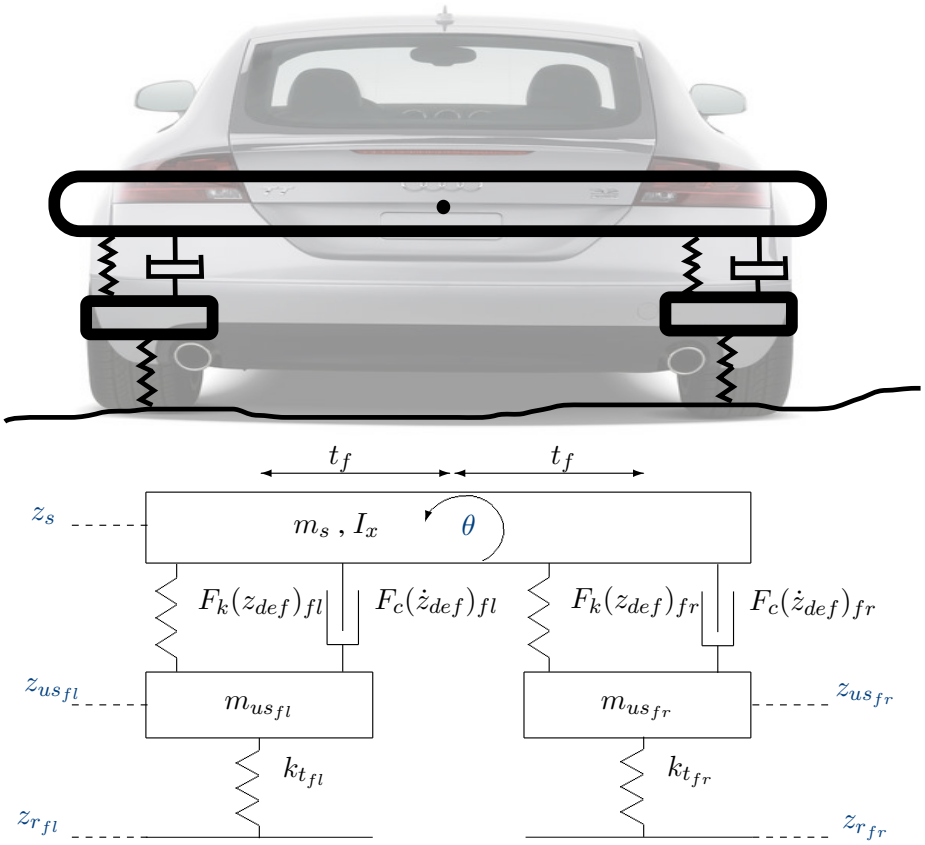

Figure 5.11: Half car model (roll oriented).

Nonlinear pitch oriented model. The nonlinear model involving the pitch dynamic is simply given by equation (5.14) (see also Figure 5.13),

$$\left\{\begin{array}{rcl} m_s\ddot{z}_s & = & -(F_{sz_f}+F_{tz_r}+F_{dz}) \\ m_{us_f}\ddot{z}_{us_f} & = & F_{sz_f}-F_{tz_r} \\ m_{us_r}\ddot{z}_{us_r} & = & F_{sz_f}-F_{tz_r} \\ I_y\ddot{\phi} & = & F_{sz_f}l_f - F_{tz_r}l_r + M_{dy} \end{array}\right. \tag{5.14}$$

where the index $\{f, r\}$ holds for {front,rear}, I_y is the pitch inertia and M_{dy} is the disturbance moment on the y axis (i.e. in the pitch axis). l_f and l_r denote the front and rear distance from the center of gravity. z_s and ϕ are the chassis bounce and pitch at the center of gravity; z_{us_f} and z_{us_r} are the front and rear unsprung masses bounce respectively.

5.3.2 Lateral vehicle model

The bicycle model is widely widespread in the automotive literature. It allows to treat the lateral and yaw dynamics and is mainly involved when steering control or Electronic Stability Control (ESC) are studied. Modified versions exist for braking control synthesis (e.g. yaw stability). Note that it is also involved in platooning problems (see e.g. Martinez, 2005).

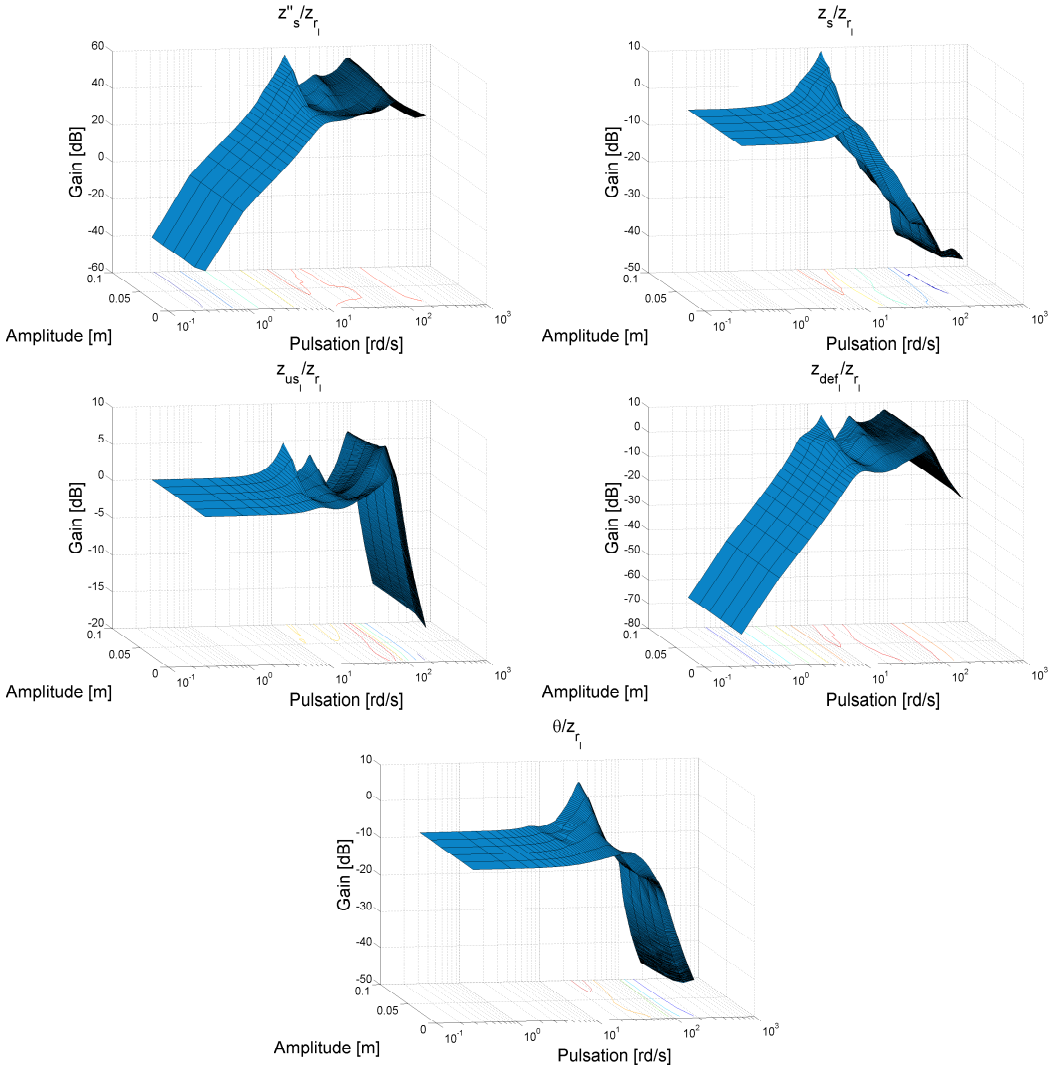

Figure 5.12: Pseudo-Bode diagrams $\ddot{z}_s/z_{r_l}$, z_s/z_{r_l}, z_{us_l}/z_{r_l}, z_{def_l}/z_{r_l} and θ/z_r for various input magnitudes and frequencies.

Nonlinear bicycle model. One of the most widely known model is the bicycle vehicle models (see Figure 5.14). It is described as in (see Ackermann and Bunte, 1996):

$$\begin{cases} mv(\dot{\beta}+\psi) &= F_{ty_f}+F_{ty_r}+F_{dy} \\ I_z\ddot{\psi} &= l_f F_{ty_f}-l_r F_{ty_r}+M_{dz} \end{cases} \tag{5.15}$$

where F_{ty_f} and F_{ty_r} are the lateral tire forces of the front and the rear wheels respectively. Disturbance moment and lateral forces are modeled by M_{dz} and F_{dy} respectively. β denotes the side slip angle at the vehicle center of gravity. This model is highly nonlinear since it involves nonlinear lateral tire forces and depends on the vehicle velocity v.

In our study (see Chapter 7), this model is used to generate a yaw rate reference when ESC strategies are designed.

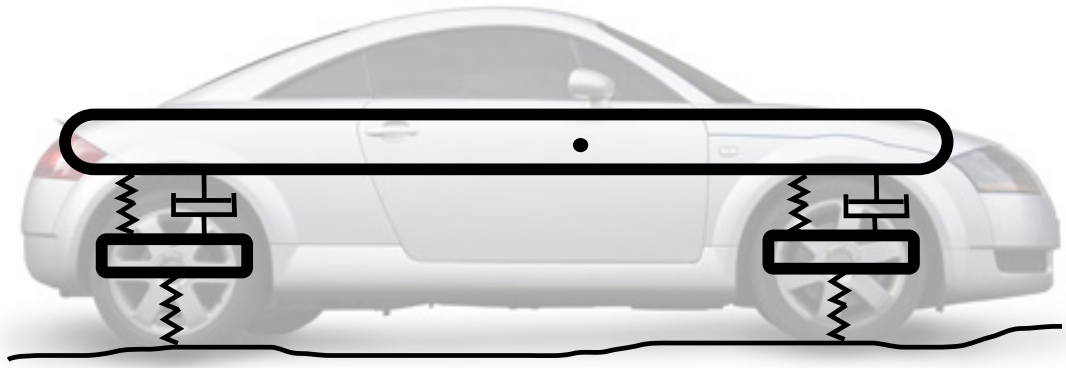

Figure 5.13: Half car model (pitch oriented).

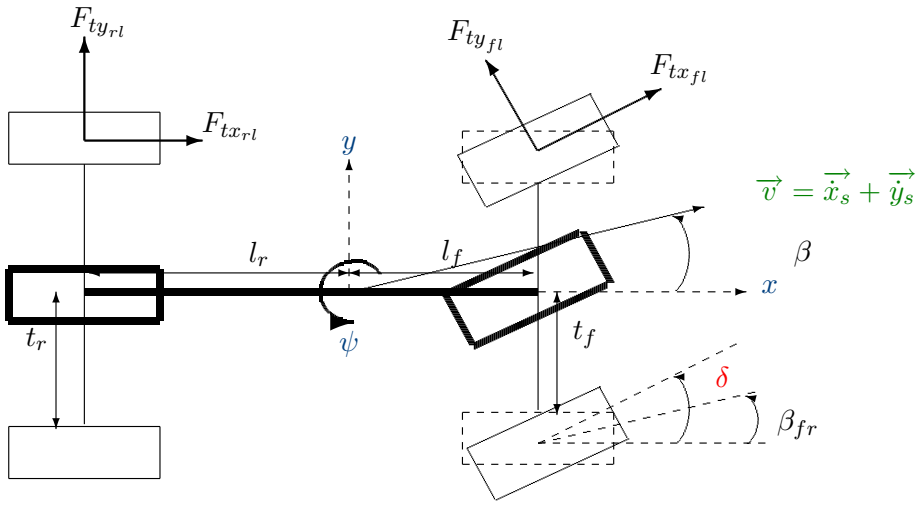

Figure 5.14: Bicycle model.

Linear bicycle model. As the bicycle model given in (5.15) presents high nonlinearities, it is often studied in its linear form. One assumes that:

- Linear lateral tire friction curve i.e.:

$$\begin{cases} F_{ty_f} &= C_{yf}\beta_f \\ F_{ty_r} &= C_{yr}\beta_r \end{cases} \tag{5.16}$$

where C_{yf} and C_{yr} are the linear stiffness of the lateral tire characteristics at the front and rear respectively.

- Small slip angles (β_f and β_r):

$$\left\{ \begin{array}{rcl} \beta_f & = & \delta - \beta - \dfrac{l_f \dot{\psi}}{v} \\ \beta_r & = & \beta + \dfrac{l_r \dot{\psi}}{v} \end{array} \right. \tag{5.17}$$

  where ψ denotes the vehicle yawn β_f and β_r denote the side slip angle at the front and rear. δ is the steering angle of the front wheel.

Then, under these considerations, the linearized model is given by (where v is a model parameter):

$$\begin{bmatrix} \ddot{\psi} \\ \dot{\beta} \end{bmatrix} = \begin{bmatrix} -\dfrac{l_f^2 C_{yf} + l_r^2 C_{yr}}{I_z v} & \dfrac{l_r C_{yr} - l_f C_{yf}}{I_z} \\ -1 + \dfrac{l_r C_{yr} - l_f C_{yf}}{m v^2} & -\dfrac{C_{yf} + C_{yr}}{mv} \end{bmatrix} \begin{bmatrix} \dot{\psi} \\ \beta \end{bmatrix} + \begin{bmatrix} \dfrac{-l_f C_{yf}}{I_z} \\ \dfrac{C_{yf}}{mv} \end{bmatrix} \delta + \begin{bmatrix} \dfrac{1}{I_z} \\ 0 \end{bmatrix} M_{dz} + \begin{bmatrix} 0 \\ \dfrac{1}{mv} \end{bmatrix} F_{dy} \tag{5.18}$$

On Figure 5.15, Bode diagrams of β/δ and $\dot{\psi}/\delta$ are given for different value of v.

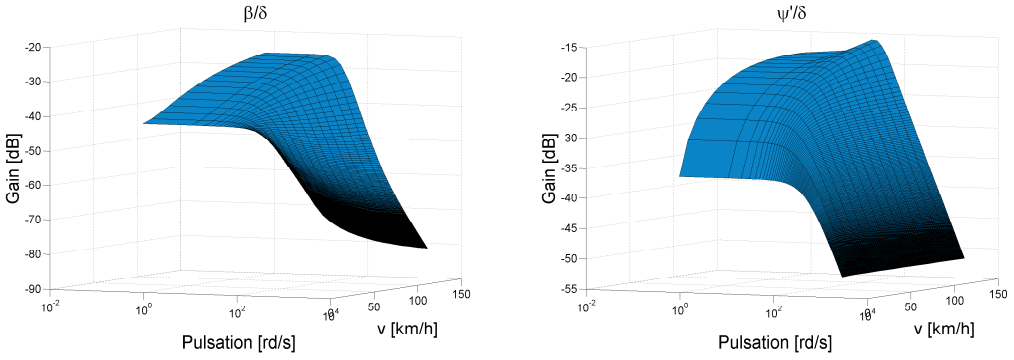

Figure 5.15: Bode diagrams of β/δ and $\dot{\psi}/\delta$ for different values of the vehicle speed v.

These diagrams show the dependency of the model w.r.t. the vehicle speed v. This explains why many works involving this model use now an LPV version of the bicycle model (see e.g. Gáspár *et al.*, 2007; Raharijaona, 2004).

Remark: About an LPV bicycle model. We point out that, for control purpose, a LPV bicycle model may be more appropriate, since the speed v deeply influences the dynamical behavior. Moreover, compared to the LPV quarter vertical model (5.9), the parameter is not state dependent, then the model should be LPV and not qLPV. Additionally, in this case, the v parameter does not directly enter linearly in the system description, but as $\frac{1}{v}$ and $\frac{1}{v^2}$. Then, if a polytopic approach is chosen for control synthesis, the LPV model would be of the form:

$$\begin{bmatrix} \ddot{\psi} \\ \dot{\beta} \end{bmatrix} = \Big(A_0 + \rho_1 A_1 + \rho_2 A_2\Big) \begin{bmatrix} \dot{\psi} \\ \beta \end{bmatrix} + \Big(B_0 + \rho_1 B_1\Big) \begin{bmatrix} \delta \\ M_{dz} \\ F_{dy} \end{bmatrix} \tag{5.19}$$

where $\rho_1 = \frac{1}{v}$ and $\rho_2 = \frac{1}{v^2}$. Note that this example has been illustrated in Section 3.6 (but without being studied).

5.4 Full vehicle model (for analysis)

Here, attention is given to the full vehicle model description. It is based on the model developed by Zin (2005), in collaboration with the MIAM laboratory in Mulhouse, France (see also (Zin *et al.*, 2004)). In some sense, it is the concatenation of the previously introduced models. According to our studies and control designs, the full vehicle model can be classified into to two categories:

1. First, the vertical full car model, which is the study of the vehicle attitude, where vertical (z_s and z_{us}), pitch (ϕ) and roll (θ) dynamics are involved (see top of Figure 5.16). This model considers the suspension, and vertical tire subsystems.

2. Secondly, the full vehicle model, which is used to analyze all the vehicle dynamical variables (i.e. attitude (z_s, z_{us}, θ and ϕ) plus longitudinal (x_s), lateral (y_s), yaw (ψ), slip (λ), wheel (ω) and sideslip (β) dynamics); see Figure 5.16. This model involves suspension and full tire (longitudinal, lateral and vertical) sub-systems.

As the full vertical model is simply a simplified version of the complete one, here we only introduce the full vehicle model. First, assumptions under which the model is described are introduced, then, kinematic equations (due to the vehicle geometry) are provided, and finally, the dynamical equations are listed. This complete model will be the one used in simulation for validation of the proposed GCC control structures (see Chapter 7).

5.4.1 Assumptions

Full vehicle modeling is not a simple task since it involves many subsystems and coupled nonlinear fast and slow dynamics. Thus, in our study, some modeling assumption have been done:

- The direction column is not considered (i.e. in the model, an angle δ applied to the steering wheel results in the same angle δ on the front wheels).

- The auto-aligning moments are neglected (i.e. they do not disturb the vehicle dynamic by bringing back the steering wheel to the initial position).

- The kinematic effects due to suspension geometry are neglected (i.e. the suspensions only provide a vertical force to the chassis).

- The gyroscopic effects of the sprung masses are neglected (i.e. wheels only generate longitudinal, lateral and vertical forces).

- The tire cambering is neglected (in cornering situation, usually cambering of the wheels is applied and controlled). In Lamy and Basset (2008), authors describe this dimension on more precise wheel and tire models.

- The anti-roll bars are not considered (note that they play an important role for heavy vehicles).

- The vehicle chassis plane is considered parallel to the road (usually, cars are bent over to improve air penetration and reduce aerodynamical resistance).

- The aerodynamical and wheel resistive effects are neglected e.g.:

– The air resistance can be modeled as: $F_{air} = \varrho(v, .)$, where $\varrho(.)$ is a nonlinear function of the speed and of the vehicle geometry. Note that simple models exist but in this work, this study is not of great interest.

– The wheels rolling resistance moment, caused by the inclination of the wheel axis in the longitudinal plane is neglected.

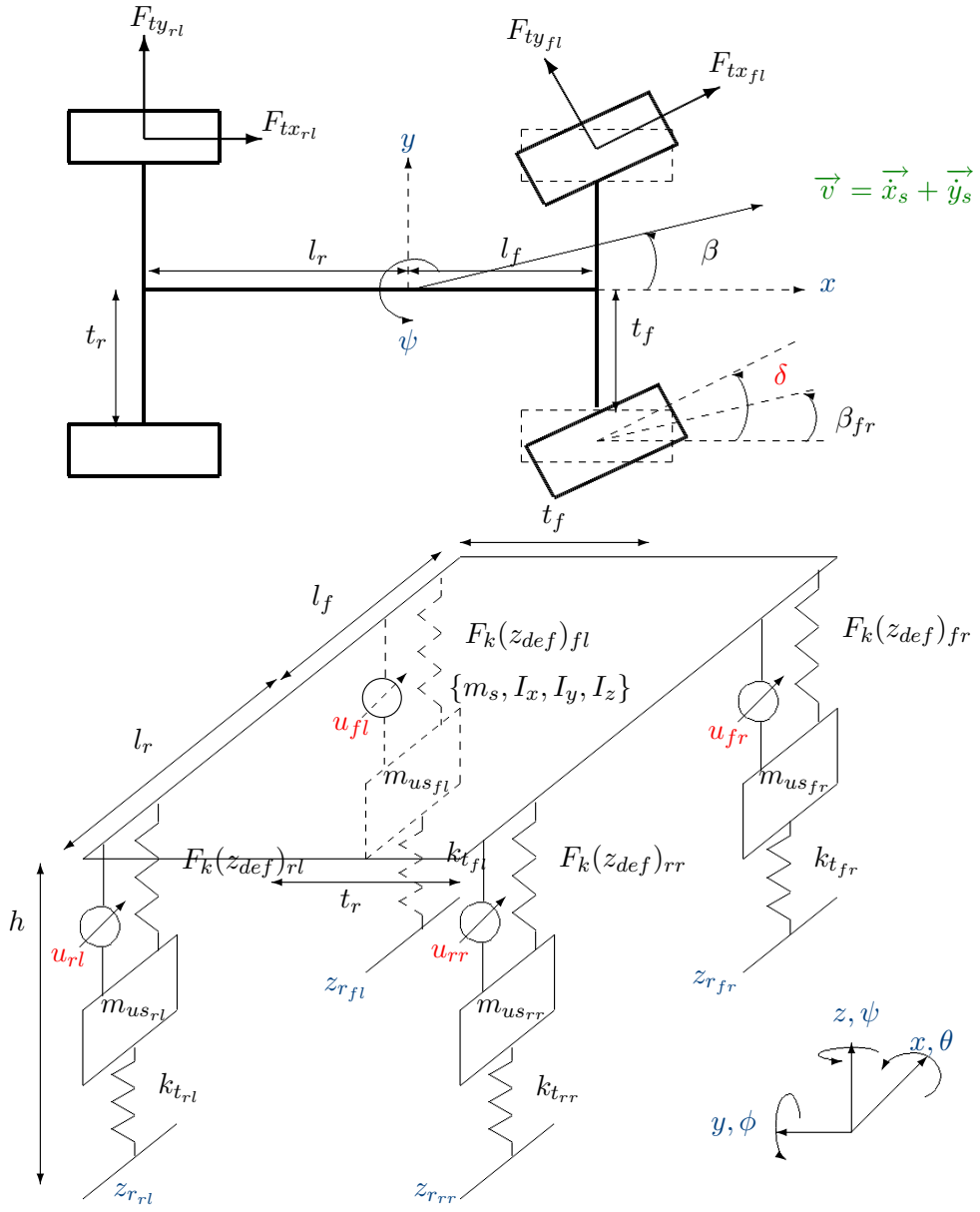

Figure 5.16: Full vehicle model, lateral & Longitudinal (top) and vertical (bottom).

5.4.2 Kinematic equations

The kinematic equations are mainly due to the vehicle geometry (and to the assumption done). Each corner of the vehicle is identified with $\{i, j\}$ index, where $i = \{f, r\}$ holds for front/rear and $j = \{l, r\}$ for left/right. The chassis corners (i.e. positions and velocities of the dynamical part) are described by,

$$\left\{\begin{array}{rcl} z_{s_{fl}} & = & z_s + l_f \sin(\phi) - t_f \sin(\theta) \\ z_{s_{fr}} & = & z_s + l_f \sin(\phi) + t_f \sin(\theta) \\ z_{s_{rl}} & = & z_s - l_r \sin(\phi) - t_r \sin(\theta) \\ z_{s_{rr}} & = & z_s - l_r \sin(\phi) + t_r \sin(\theta) \\ \dot{z}_{s_{fl}} & = & \dot{z}_s + \dot{\phi} l_f \cos(\phi) - \dot{\theta} t_f \cos(\theta) \\ \dot{z}_{s_{fr}} & = & \dot{z}_s + \dot{\phi} l_f \cos(\phi) + \dot{\theta} t_f \cos(\theta) \\ \dot{z}_{s_{rl}} & = & \dot{z}_s - \dot{\phi} l_r \cos(\phi) - \dot{\theta} t_r \cos(\theta) \\ \dot{z}_{s_{rr}} & = & \dot{z}_s - \dot{\phi} l_r \cos(\phi) + \dot{\theta} t_r \cos(\theta) \end{array}\right. \tag{5.20}$$

where z_s is the center of gravity of the sprung mass, ϕ (resp. θ) is the pitch (resp. roll) angle of the chassis. l_f, l_r, t_f and t_r hold for the vehicle geometry (see Figure 5.16). The height from the ground to the center of gravity is denoted by h.

5.4.3 Dynamical equations

The full vehicle model is defined by the following nonlinear dynamical equations (5.21).

$$\left\{\begin{array}{rcl} \ddot{x}_s & = & \dot{x}_s + \dot{y}_s \dot{\psi} \\ & = & \big(-(F_{tx_{fr}} + F_{tx_{fl}}) \cos(\delta) - (F_{tx_{rr}} + F_{tx_{rl}}) - (F_{ty_{fr}} + F_{ty_{fl}}) \sin(\delta) - m\dot{\psi}\dot{y}_s \\ & & + F_{dx} \big)/m \\ \ddot{y}_s & = & \big(-(F_{tx_{fr}} + F_{tx_{fl}}) \sin(\delta) + (F_{ty_{rr}} + F_{ty_{rl}}) + (F_{ty_{fr}} + F_{ty_{fl}}) \cos(\delta) + m\dot{\psi}\dot{x}_s \\ & & + F_{dy} \big)/m \\ \ddot{z}_s & = & -\big(F_{sz_{fl}} + F_{sz_{fr}} + F_{sz_{rl}} + F_{sz_{rr}} + F_{dz} \big)/m_s \\ \ddot{z}_{us_{ij}} & = & \big(F_{sz_{ij}} - F_{tz_{ij}} \big)/m_{us_{ij}} \\ \ddot{\theta} & = & \big((F_{sz_{rl}} - F_{sz_{rr}}) t_r + (F_{sz_{fl}} - F_{sz_{fr}}) t_f + mh\ddot{y}_s + (I_y - I_z)\dot{\psi}\dot{\phi} + M_{dx} \big)/I_x \\ \ddot{\phi} & = & \big((F_{sz_{rr}} + F_{sz_{rl}}) l_r - (F_{sz_{fr}} + F_{sz_{fl}}) l_f - mh\ddot{x}_s + (I_z - I_x)\dot{\psi}\dot{\theta} + M_{dy} \big)/I_y \\ \ddot{\psi} & = & \big((F_{ty_{fr}} + F_{ty_{fl}}) l_f \cos(\delta) - (F_{ty_{rr}} + F_{ty_{rl}}) l_r - (F_{tx_{fr}} + F_{tx_{fl}}) l_f \sin(\delta) \\ & & - (F_{tx_{rr}} - F_{tx_{rl}}) t_r \\ & & + (F_{tx_{fr}} - F_{tx_{fl}}) t_f \cos(\delta) - (F_{tx_{fr}} - F_{tx_{fl}}) t_f \sin(\delta) \\ & & + (I_x - I_y)\dot{\theta}\dot{\phi} + M_{dz} \big)/I_z \\ \dot{\omega}_{ij} & = & (R_{ij} F_{tx_{ij}} - T_{b_{ij}})/I_w \\ \dot{\beta} & = & (F_{ty_f} + F_{ty_r})/(mv) + \dot{\psi} \end{array}\right. \tag{5.21}$$

where the forces are given (following the description done in Chapter 5),

$$\begin{array}{rl} \text{Tires:} & \left\{\begin{array}{rcl} F_{tx_{ij}} & = & F_{tx}(\mu_{ij}, \lambda_{ij}, F_{n_{ij}}) \\ F_{ty_{ij}} & = & F_{ty}(\mu_{ij}, \beta_{ij}) \\ F_{tz_{ij}} & = & F_{tz}(z_{us} - z_r) \end{array}\right. \\ \text{Suspensions:} & \left\{ F_{sz_{ij}} = F_k(z_{s_{ij}} - z_{us_{ij}}) + u_{ij} \right. \end{array} \tag{5.22}$$

where m_s and $m_{us_{ij}}$ hold for the chassis and sprung masses respectively; m is the total mass of the vehicle. The vehicle inertia in the x-axis (resp. y-axis, z-axis) is denoted as I_x (resp. I_y, I_z).

$\{F_{dx}, F_{dy}, F_{dz}\}$ (resp. $\{M_{dx}, M_{dy}, M_{dz}\}$) are external forces (resp. moments) disturbances on the $\{x, y, z\}$ axes. ω_{ij} are the wheel rotational velocities and λ_{ij} the wheel slip ratio. β is the slip angle at the center of gravity. δ holds for the front wheel angle. $F_{tx_{ij}}$ (resp. $F_{ty_{ij}}$ and $F_{tz_{ij}}$) represents the longitudinal (resp. lateral and vertical) tire forces and $F_{sz_{ij}}$ are the vertical forces provided by the suspension system. Finally, h denotes the vehicle height at the center of gravity. The general synopsis of this model is summarized on Figure 5.17.

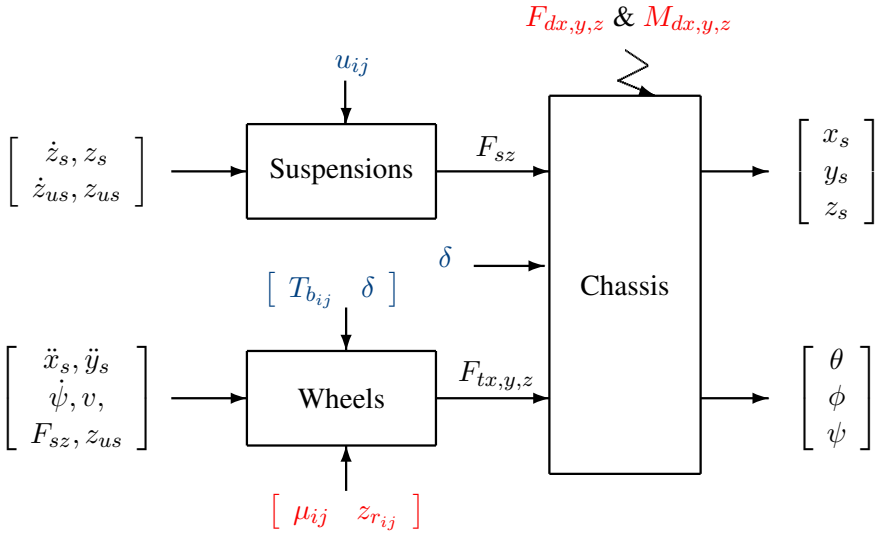

Figure 5.17: Full vehicle model synopsis.

5.4.4 Some experimental validations

In Mulhouse, the MIAM research team (expert in vehicle dynamics, identification and estimation), has performed experimental tests on a real Renault Mégane Coupé. They provided us experimental data and vehicle parameters for model validation[1] (see also a collaborative work Zin *et al.*, 2004). Note that other experiments (together with the MIAM team in Mulhouse, France) have been carried out during the thesis of Zin (2005), to validate the model. The model introduced in this thesis in an extension of the one proposed by A. Zin. Among other, we add:

- The wheel dynamics (ω, λ) (based on (Denny, 2005) and (Canudas *et al.*, 2003*a*; Velenis *et al.*, 2005)).
- More accurate longitudinal (F_{tx}) and lateral (F_{ty}) tire formulae (based on (Tanelli *et al.*, 2007*a*) and (Koenig and Mammar, 2003)), handling the loss of manoeuvrability.
- Additional chassis coupling phenomena between pitch, roll and yaw dynamics (based on (Chou and d'Andréa Novel, 2005)).

The measured signals are: $\ddot{x}_s$, $\ddot{y}_s$, $\dot{x}_s$, $\dot{y}_s$, $\dot{\psi}$, $\dot{\theta}$. They are compared with the simulated ones, using as input values v, the vehicle speed and δ, the steering wheel angle, with the full vehicle model described below. Thereafter, different simulations are performed.

[1] Acknowledgements to G.L. Gissinger, M. Basset, C. Lamy and G. Pouly who provided us the data.

5.4.4.1 Sine wave test ($v = 60km/h$)

In this experiment, the vehicle is subject to "sinusoidal" steering input signals with varying frequencies (vehicle speed of $v = 60km/h$). The input signals are the steering angle δ and the vehicle longitudinal velocity v; they are shown on Figure 5.18. Results and comparison between the nonlinear model and the experimental results are shown on Figure 5.19.

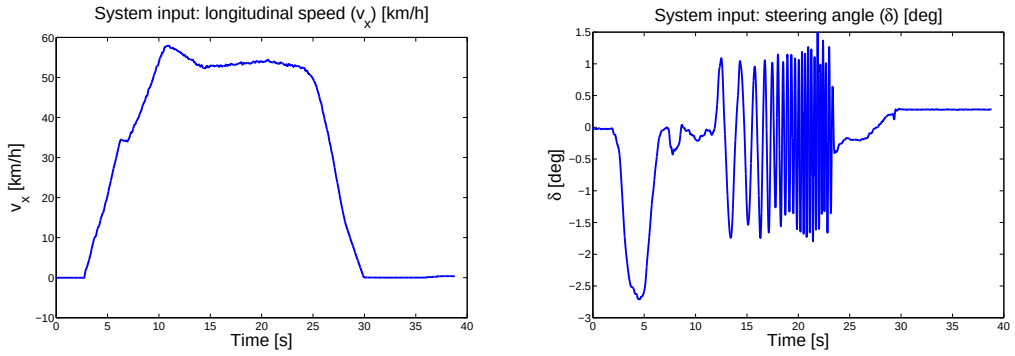

Figure 5.18: Input signals of the sine wave test ($v = 60km/h$): vehicle speed (left) and steering angle of the front wheels (right).

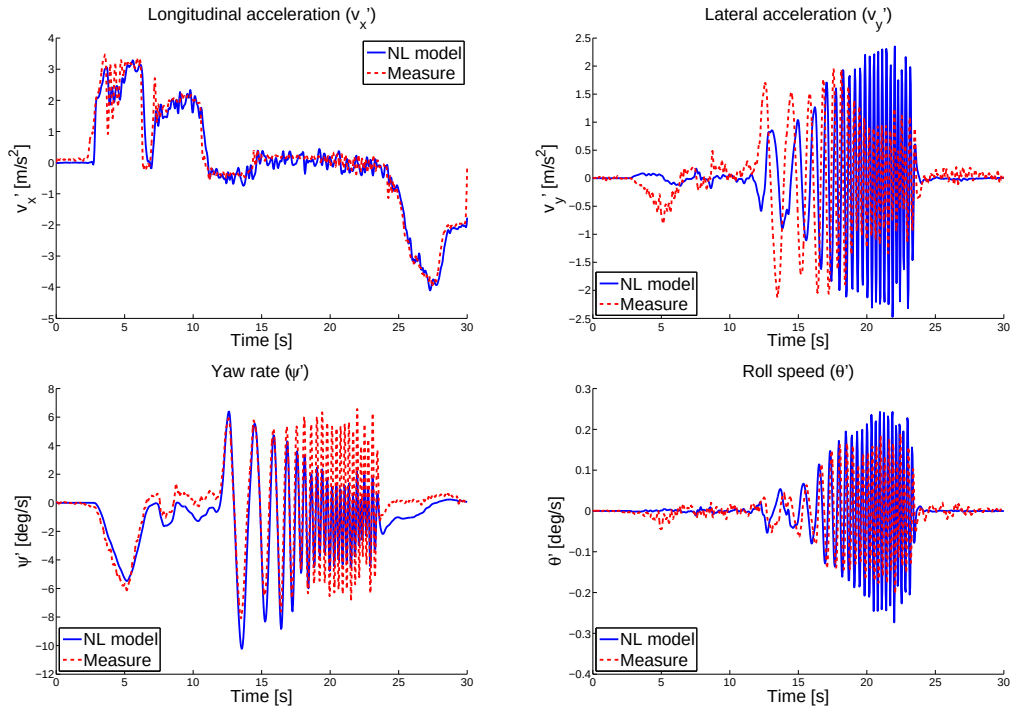

Figure 5.19: Output signals of the sine wave test ($v = 60km/h$) (from top left to bottom right): longitudinal acceleration ($\ddot{x}_s$), lateral acceleration ($\ddot{y}_s$), yaw rate ($\dot{\psi}$) and roll velocity ($\dot{\theta}$).

5.4.4.2 Sine wave test ($v = 40km/h$)

In this experiment, the vehicle is subject to sinusoidal steering input signals with varying frequencies (vehicle speed of $v = 40km/h$). The input signals are the steering angle δ and the vehicle longitudinal velocity v; they are shown on Figure 5.20. Results and comparison between the nonlinear model and the experimental results are shown on Figure 5.21.

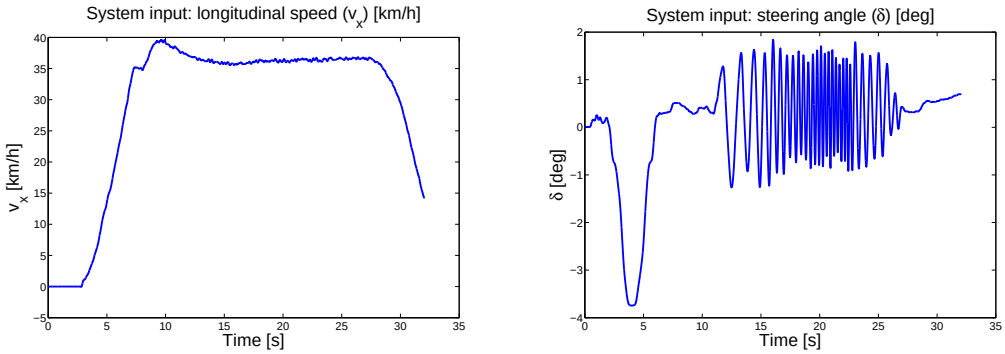

Figure 5.20: Input signals of the sine wave test ($v = 40km/h$): vehicle speed (left) and steering angle of the front wheels (right).

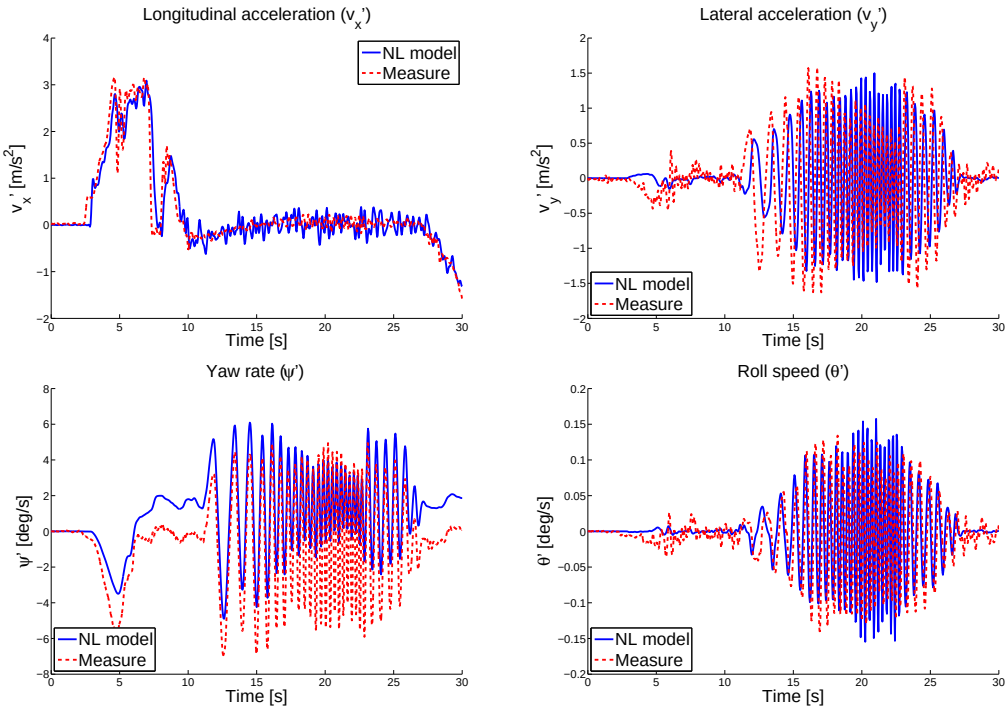

Figure 5.21: Output signals of the sine wave test ($v = 40km/h$) (from top left to bottom right): longitudinal acceleration ($\ddot{x}_s$), lateral acceleration ($\ddot{y}_s$), yaw rate ($\dot{\psi}$) and roll velocity ($\dot{\theta}$).

5.4.4.3 Obstacle avoidance test at $v = 80km/h$ ("Moose" test)

In this experiment, the vehicle runs in straight line and performs an emergency obstacle avoidance. The input signals are the steering angle δ and the vehicle longitudinal velocity v; they are shown on Figure 5.23. Results and comparison between the nonlinear model and the experimental results are shown on Figure 5.24.

This test is widely used in the automotive industry, especially for ESC validation. Usually, tests have to be performed on different road conditions to validate the ESC strategy (see e.g. Falcone *et al.*, 2007*b*) (see also Chapter 7). Here we only have experiment on dry road.

Remark: Why the "Moose" test? This test, is also known as the "Moose" test. As in the Scandinavian and American countries, such animals use to across the road, when it occurs, driver has to perform a quick avoidance manoeuver that may destabilize the vehicle, and cause a car accident. It is why today, car manufacturer use this "Moose test" to study the vehicle stability (or ESC strategies). Figure 5.22 shows the Moose in his natural environment.

Figure 5.22: Moose in his natural environment.

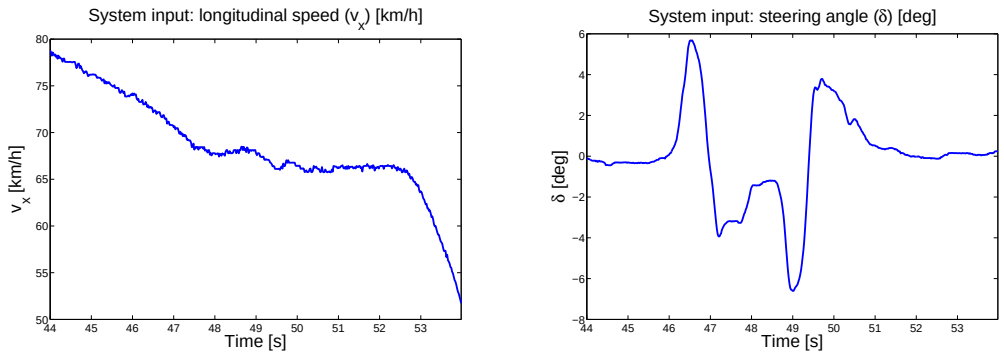

Figure 5.23: Input signals of the "Moose" test ($v = 80km/h$): vehicle speed (left) and steering angle of the front wheels (right).

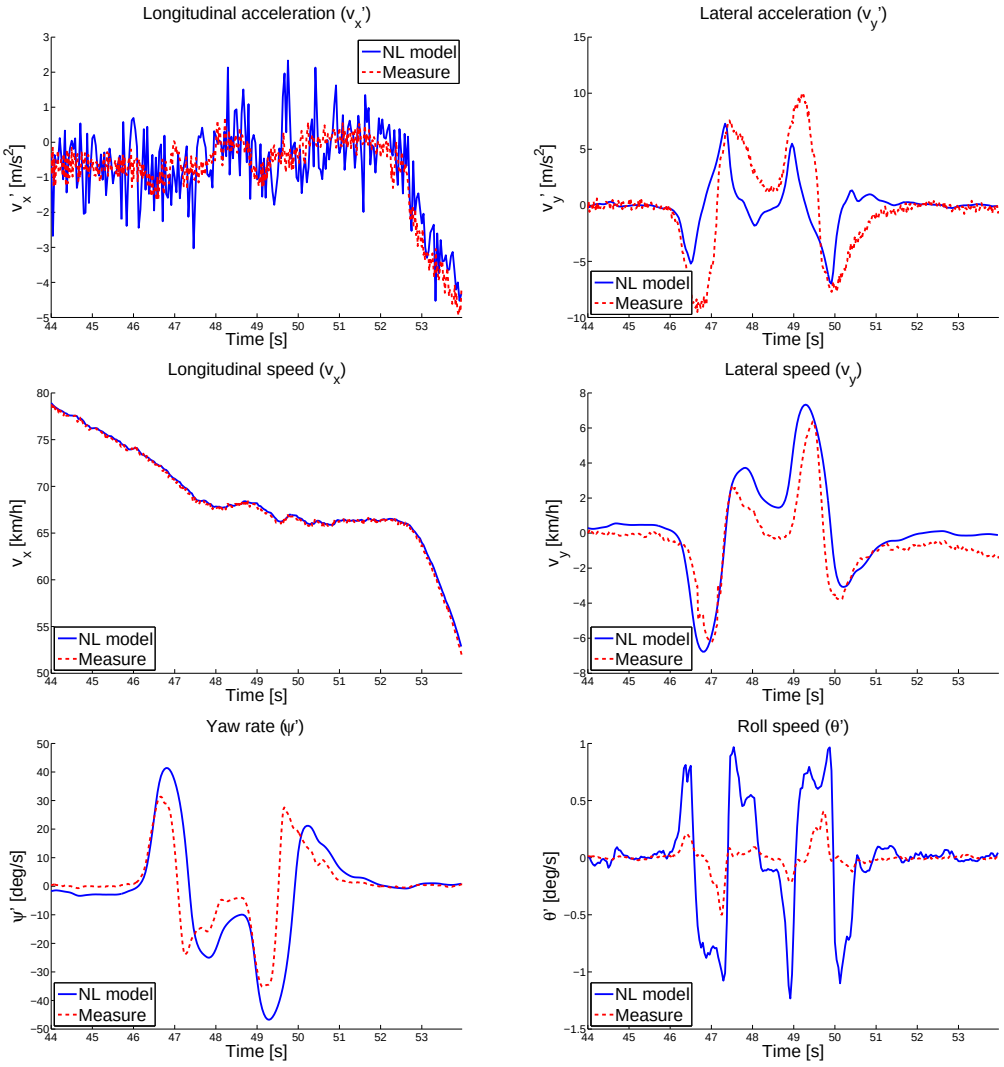

Figure 5.24: Output signals of the "Moose" test ($v = 80km/h$), from top left to bottom right: longitudinal acceleration ($\ddot{x}_s$), lateral acceleration ($\ddot{y}_s$), longitudinal speed ($\dot{x}_s$), lateral speed ($\dot{y}_s$), yaw rate ($\dot{\psi}$) and roll velocity ($\dot{\theta}$) .

5.4.4.4 Obstacle avoidance test at $v = 60km/h$ ("Moose" test)

In this experiment, the vehicle runs in straight line and performs an emergency obstacle avoidance. The input signals are the steering angle δ and the vehicle longitudinal velocity v; they are shown on Figure 5.25. Results and comparison between the nonlinear model and the experimental results are shown on Figure 5.26.

5.4.4.5 Some remarks about the experiments and obtained results

Let notice that, even if the model and experimental results do not perfectly match each other, differences are mainly due to the difficulty to have consistent tire parameters and vehicle exact data. In fact, these parameters depend on the road condition, the temperature, the humidity, the pressure,

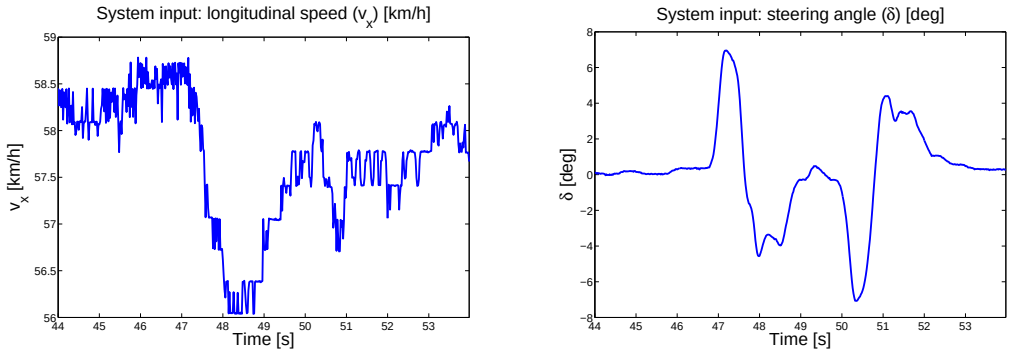

Figure 5.25: Input signals of the "Moose" test ($v = 60km/h$): vehicle speed (left) and steering angle of the front wheels (right).

the wear, etc. Moreover, the driving situations simulated are very complex since they all enter in the lateral tire nonlinearities, thus in the model limitations. The objective of this simulation test is not to validate the full vehicle model (which requires more than four tests), but to show to the reader that the described model is consistent with the real phenomena.

As a consequence, we can admit that the behavior described by the nonlinear model proposed is "correct" for our purpose and describes the vehicle dynamics in a good manner. Therefore, it will be acceptable for control strategy validations (done in simulations). Of course, the parameters identification improvements should be necessary by require more work and additional tests, and should be considered in the future.

According to the author, an interesting issue for control achievement, should be to identify and quantify the uncertain parameters to build an uncertain vehicle model, and, then a robust controller w.r.t. these uncertainties.

5.5 Performance specifications

In the automotive field, the performance specification is a whole subject where many works have been published. Briefly speaking, to define performances, the automotive engineer has first to formulate requirements in classical "words", then to turn them into mathematical expressions and introduce consistent metrics to quantify them. Usually, the first step is "straightforward" since it comes from driver feelings and expectative. The second step is much harder and also non unique since it should be non representative to all drivers. In this thesis, we have chosen some metrics for performance evaluations. These metrics are based either on our general observations and discussions with automotive experts and on criteria given by PSA Peugeot-Citroën car manufacturer (collaboration carried out during the Thesis of Sammier, 2001). By the way the author stresses that more representative other metrics should also be used.

Here we introduce some performance specifications and their metric (if any). First vertical performances are given, then, attitude ones. Finally, some specifications regarding the longitudinal, lateral and pitch dynamics are described, based on recent results led in collaboration with a car manufacturer (Chou and d'Andréa Novel, 2005; Giorgetti *et al.*, 2006; Falcone *et al.*, 2007*a*; Falcone *et al.*, 2007*b*; Falcone *et al.*, 2007*c*; Canale *et al.*, 2007).

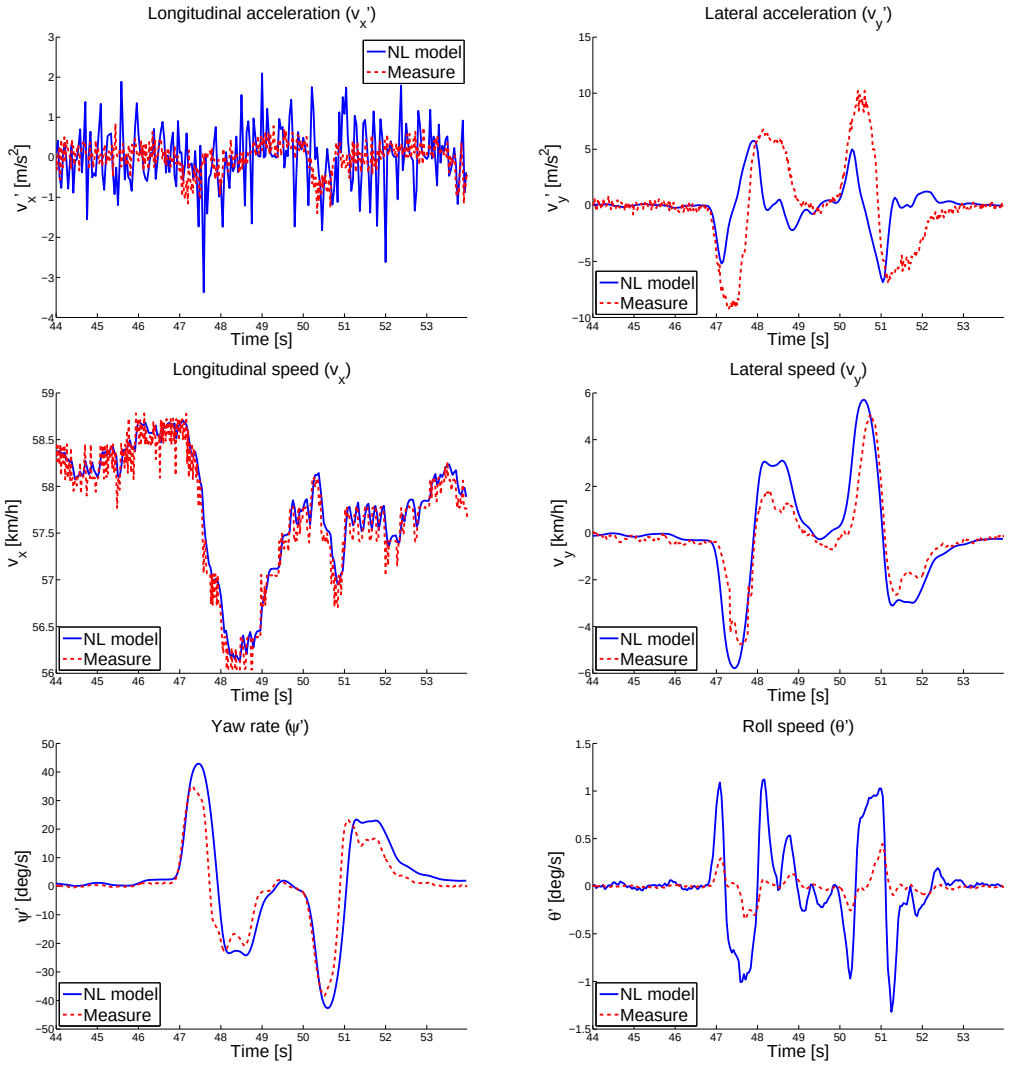

Figure 5.26: Output signals of the "Moose" test ($v = 60km/h$), from top left to bottom right: longitudinal acceleration ($\ddot{x}_s$), lateral acceleration ($\ddot{y}_s$), longitudinal speed ($\dot{x}_s$), lateral speed ($\dot{y}_s$), yaw rate ($\dot{\psi}$) and roll velocity ($\dot{\theta}$) .

5.5.1 Human body comfort, road-holding and handling performances

Human body comfort. The passenger comfort feeling is a combination of many different characterizing factors such as:

- The chassis (e.g. vibrations, noise, etc.) that are somehow controllable; in our case, especially by the suspension control.
- The driver state (e.g. feeling, age, health, general abilities etc.) and environment (e.g. weather) which are not controllable (yet...).

From a general viewpoint, comfort feeling has an impact on the driver reaction time, accuracy, situation evaluation and decision abilities.

Since the driver comfort study is complex and subjective concept, studies are more related to uncomfort analysis. Such studies have been led by modeling the human body as a complex system composed of masses linked by spring and damper elements (that model the muscles) (Girardin *et al.*, 2006). According to this kind of model, some studies have been carried out and pointed some sensitive frequency zones (e.g. for the heart, the head, etc.) according to different disturbances (such as the steering wheel vibrations or the road irregularities).

In this work, human body sensitive functions are neither characterized nor directly treated, but evaluated through the chassis analysis. In our analysis for comfort feeling improvements, we will simply analyze some specific frequency zones on the vertical behavior of the chassis (namely vertical acceleration and displacement), therefore if we reduce amplification of these functions, we will conclude that the passenger comfort is improved.

Road-holding. Compared to the human comfort, road-holding is a vehicle property which characterizes the ability of the vehicle (and more specifically, the wheels) to remain in contact with the road, i.e. to avoid the wheel trepidations introduced by road irregularities, and to guarantee road contact in high load transfer situation (due to stiff cornering situations).

Handling. Together with the road-holding property, handling is a vehicle property that specifies the ability of the vehicle to remain controllable whatever the vehicle and environments situations (e.g. state of the road, irregularities, wind, actuator fault, etc.).

5.5.2 Vertical performance specifications (quarter car)

In order to evaluate the comfort, the vertical motion (z_s) and acceleration ($\ddot{z}_s$) of the chassis are analyzed. The wheel vertical motion (z_{us}) and the suspension deflection (z_{def}) are related to road holding specifications (see Sammier, 2001; Zin, 2005). In the following, four performance objectives are derived from industrial control specifications (Sammier *et al.*, 2003) that are consistent with the ones given in (Gillespie, 1992):

- Comfort at high frequencies:
  The vibration isolation between $[4; 30]$Hz is evaluated by the transfer function $\ddot{z}_s/z_r$. The vertical acceleration of the chassis has to be limited in order to obtain good comfort at high frequencies (> 5Hz), although the human body is not sensitive to vertical accelerations at high frequencies (> 10Hz).

- Comfort at low frequencies:
  The vibration isolation between $[0; 5]$Hz is evaluated by the transfer function z_s/z_r. Ideally, the vertical displacement of the chassis should be the same as that of the road for low frequencies (lower than around 1Hz) and null for high frequencies (higher than around 1Hz). In practice, for low disturbances ($z_r < 3$cm), the maximal gain occurring between 1 and 5Hz of z_s/z_r has to be bounded by 1.8.

- Road holding:
  As indicated before, it is evaluated with the transfer function z_{us}/z_r. For a good road holding, the maximal gain, in the range $[0; 20]$Hz, of the considered transfer function has to be limited to 1.8 (for low disturbance).

- Suspension constraints:
  The transfer z_{def}/z_r is a road holding indicator and also a constraint on the deflection of the actuator evaluated between $[0; 20]$Hz in order to preserve its life cycle.

These four criteria are the one provided in the PhD Thesis of Sammier (2001), according to PSA Peugeot-Citröen requirements. Note that when comfort is studied, the most important transfer is the one defined by z_s/z_r. When road-holding is characterized, the most interesting one is z_{us}/z_r.

As an illustration, Figure 5.27, gives the Bode diagram of the transfers of interest for two different damping values (soft i.e. comfort oriented, $c = 700N/m/s$ and stiff i.e. road-holding oriented, $c = 3000Nm$).

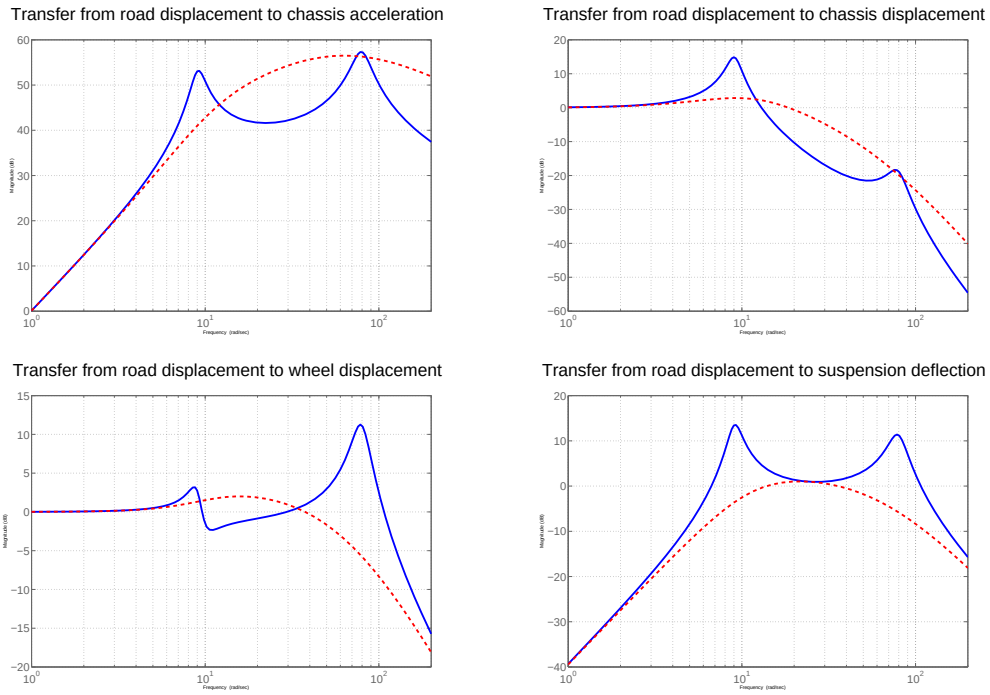

Figure 5.27: Typical Bode diagrams of the different transfer according to road unevenness for soft, (solid blue) and stiff $c = 5000$N/m/s(dashed red) damping suspension.

Upper Bode diagrams of Figure 5.27, associated with comfort specifications are essential to evaluate passenger feeling (acceleration and displacement of the chassis: m_s) and lower Bode diagrams are associated with road-holding characteristic, i.e. behavior of the wheel and the suspension according to road disturbances. By looking at Figure 5.27, one can notice that the stiff suspension (dashed red) has an important acceleration and bounce in the whole frequency space of interest. Conversely, the wheel displacement and deflection are a lot more attenuated, providing thus good road-holding performances.

To evaluate the suspension control approaches with the passive one, the power spectral density (PSD) measure of each of these signals along the frequency and magnitude space of interest is used as the following formula:

$$PSD_{\{f_1,a_1\}\rightarrow\{f_2,a_2\}}(x) = \sqrt{\int_{f_1}^{f_2}\int_{a_1}^{a_2} x^2(f,a)da \cdot df} \tag{5.23}$$

or simply,

$$PSD_{f_1 \to f_2}(x) = \sqrt{\int_{f_1}^{f_2} x^2(f) df} \tag{5.24}$$

where f_1 and f_2 (resp. a_1, a_2) are the lower and higher frequency (resp. magnitude) bounds respectively and x is the signal of interest.

Remark: Industrial criteria The criteria used here, have been derived according to industrial specifications (from PSA Peugeot-Citroën). For further information on these criteria, the reader is invited to read (Sammier *et al.*, 2003).

Example: Application of the PSD on passive suspensions As an illustration, by applying (5.23) to the linear vertical quarter car model with either $c = 700N/M/s$ or $c = 5000N/m/s$, as on Figure 5.27 (for a single disturbance amplitude signal), one obtains the following results summarized in Table 5.3: Results are consistent with the idea of comfort: for a stiff suspension, the PSD is high, hence

Signal	$c = 700N/m/s$	$c = 5000N/m/s$
$\ddot{z}_s/z_r$	5938	14171
z_s/z_r	4.7	5
z_{us}/z_r	28.2	14.2
z_{def}/z_r	30	12.3

Table 5.3: PSD evaluation for $c = 700N/m/s$ and $c = 5000N/m/s$.

the car is uncomfortable, and for a low damping value, the PSD is low, then vehicle is comfortable. Conversely, concerning road-holding, comfortable cars have bad road holding performances compared to uncomfortable ones. Control should find a trade-off to improve comfort & road-holding if possible. ◊

5.5.3 Roll and pitch performances

Regarding the roll and pitch moments, the aim is to minimize the peak amplitude and the steady state gain. Figure 5.28 gives the Bode diagram for two suspension damping value.

As for the suspension, the PSD criteria can be used in order to evaluate the improvement.

5.5.4 Longitudinal, Lateral and Yaw performances

Concerning the handling performances, the frequency criteria are hard to derive, and, as far as the author knows, the literature does not provide extensive results on this subject. The relation between tire parameters and driver evaluation is presented in (Pouly *et al.*, 2007).

Nevertheless, other specifications or diagram can be derived and used according in order to characterize yaw, lateral and longitudinal vehicle performances such as:

- Attenuate the yaw rate peak value in an obstacle avoidance situation.

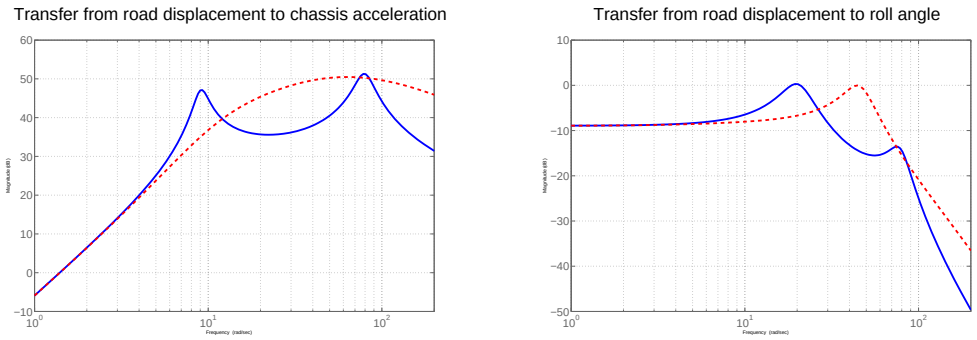

Figure 5.28: Typical Bode diagrams of the transfers according to road unevenness for soft, (solid blue) and stiff $c = 5000$N/m/s(dashed red) damping suspension.

- Attenuate the $\beta(t)$ value, e.g.

$$\max_t |\beta(t)| < 7deg \tag{5.25}$$

- Attenuate the lateral acceleration $\ddot{y}_s(t)$ e.g.

$$\max_t |\ddot{y}_s(t)| < 1g \tag{5.26}$$

  where g is the gravitational constant.

This analysis is brief since criteria to analyze the handling performances are more based on specific tests such as:

- The Moose test.
- Cornering at constant speed.
- Braking in an uneven road surface.
- etc.

Thus, reader can find many different evaluation methods for handling evaluations.

5.6 Concluding remarks

In this chapter, some vehicle models have been introduced, that are widely used in the literature and in this thesis for control synthesis. Some properties and frequency responses have been given in order to provide the reader the necessary background on vehicle models and on the challenging points related to these models.

Moreover a full vehicle model has been "validated" through experimental tests and performance criteria have been introduced together with comfort, road-holding and vehicle handling notions.

In the next chapters, control strategies are presented involving the tools developed in Chapter 3 and the actuators and models described in Chapters 4 and 5.

Chapter 6

Suspension control

6.1 Introduction

This chapter illustrates some of the contributions of this thesis in the domain of suspension control through two cases where the LPV theory is applied to reach specific objectives. Results presented in this chapter both have been obtained thanks to a strong collaboration with P. Gáspár, Z. Szabó and J. Bokor, from the MTA SZTAKI - Hungarian Academy of Sciences (Budapest, Hungary). We present these two results since they represent two interesting (and different) study cases:

1. The first one, based on a half vehicle model, is concerned with the control of two active suspension systems. The proposed LPV controller, designed through a mixed $\mathcal{H}_\infty/\mathcal{H}_2$ method, is scheduled to handle model nonlinearities. We show that the LPV design improves the closed-loop performances and robustness, but also introduces conservatism in the resulting solution. Moreover, the mixed design interest is shown through physical analysis. This contribution has been:

   - Presented at the *10th Mini-conference on Vehicle System Dynamics, Identification and Anomalies (VSDIA)* held in Budapest, Hungary (see Poussot-Vassal *et al.*, 2006*a*).

2. The second one, based on a vertical quarter car model, is concerned with the introduction of a new methodology for semi-active suspension control. The LPV strategy is designed with the $\mathcal{H}_\infty$ performance criteria, and the varying parameter aims at modifying the closed-loop performance objectives in order to satisfy the dissipative constraint characteristic of the semi-active suspension actuators. The proposed solution is compared to existing semi-active strategies showing interesting properties. This contribution has been:

   - Presented at the *3rd IFAC Symposium on System Structure and Control (SSSC)* held in Iguaçu, Brazil (see Poussot-Vassal *et al.*, 2007).
   - Published in *Control Engineering Practice* (see Poussot-Vassal *et al.*, 2008*d*).

The chapter is structured as follows: Section 6.2 describes the first case study; it gives some simulation and computation results and issues. The second study case is illustrated in Section 6.3 where a comparison is made with other semi-active suspension strategies available in the literature (namely, ADD and Mixed SH-ADD, introduced in Chapter 2).

6.2 Mixed qLPV/$\mathcal{H}_\infty/\mathcal{H}_2$ active suspension control

6.2.1 General idea

The mixed qLPV $\mathcal{H}_\infty/\mathcal{H}_2$ method is proposed here for the design of an active suspension system, in which different optimization criteria are applied to guarantee the performance specifications despite the nonlinearities of the suspension system, mainly caused by the changes in the spring coefficients (5.5). It is assumed that the nonlinear dynamics of the vehicle are approximated by LPV (more precisely qLPV) models, in which nonlinear terms are hidden with newly defined scheduling variables available from measured signals. The active suspension controller, based on the LPV model, takes the nonlinear dynamics of the system into consideration. This work extends the strategy presented in Zin *et al.* (2008*a*) to a half vehicle model and in a multi objective framework. Moreover, we analyze the performance trade-off due to the mixed $\mathcal{H}_\infty$ and $\mathcal{H}_2$ design with the Pareto limit as well as the conservatism introduced by an LPV controller.

6.2.2 Problem description

Let consider the half vehicle model roll oriented, as defined in (5.13). The measured signals are the left and right suspension deflections and the selected varying parameters are the stiffness of the left and right suspension springs (i.e. k_l and k_r), function of the deflection. Thus, the system can be described as a qLPV system such as:

$$\Sigma : \left\{ \begin{array}{rcl} \dot{x}(t) & = & A(k_l, k_r)x(t) + Bu(t) \\ y(t) & = & Cx(t) + Du(t) \end{array} \right. \tag{6.1}$$

where $u = [u_l; u_r]$ is the control input, $y = [z_{def_l}; z_{def_r}]$ is the measured signal (suspension deflections) and $\{k_l, k_r\}$ are varying parameters function of $\{z_{def_l}, z_{def_r}\}$, which are state variables of the considered model (and also the system output). The LPV system is thus a qLPV one. Let consider the following polytope, formed by $N = 4$ corners:

$$\mathcal{P}_\rho := \left[\begin{array}{cc} \underline{k}_l & \underline{k}_r \\ \underline{k}_l & \overline{k}_r \\ \overline{k}_l & \underline{k}_r \\ \overline{k}_l & \overline{k}_r \end{array} \right], \quad \begin{array}{l} k_l \in [\underline{k}_l, \overline{k}_l] \\ k_r \in [\underline{k}_r, \overline{k}_r] \end{array} \tag{6.2}$$

The qLPV polytopic system has thus the following form:

$$\begin{array}{rcl} \left[\begin{array}{c|c} A(k_l,k_r) & B(k_l,k_r) \\ \hline C(k_l,k_r) & D(k_l,k_r) \end{array} \right] & = & \alpha_1(k_l,k_r) \left[\begin{array}{c|c} A(\underline{k}_l,\underline{k}_r) & B \\ \hline C & D \end{array} \right] + \alpha_2(k_l,k_r) \left[\begin{array}{c|c} A(\underline{k}_l,\overline{k}_r) & B \\ \hline C & D \end{array} \right] \\ & + & \alpha_3(k_l,k_r) \left[\begin{array}{c|c} A(\overline{k}_l,\underline{k}_r) & B \\ \hline C & D \end{array} \right] + \alpha_4(k_l,k_r) \left[\begin{array}{c|c} A(\overline{k}_l,\overline{k}_r) & B \\ \hline C & D \end{array} \right] \end{array} \tag{6.3}$$

The objective of the controller is to improve the vertical comfort in a given frequency range and to minimize the roll moment. For that purpose, the $\mathcal{H}_\infty$ and $\mathcal{H}_2$ performance criteria are used.

- The $\mathcal{H}_\infty$ performance is used to enforce robustness to model uncertainties and to express frequency-domain performance specifications.
- The $\mathcal{H}_2$ performance can be used to minimize the energy of some signals.

On a half vehicle, the expected performances are multiple. As exposed in Section 5.5, some sensitivity functions can be imposed to modify the sprung and the unsprung masses behavior; for this, the $\mathcal{H}_\infty$ performance suits well. Moreover, from a practical point of view, weights on the control signal have to be specified to prevent actuator saturation; therefore, an $\mathcal{H}_2$ criterion is appropriate. According to these remarks, let consider the following generalized plant given on Figure 6.1 where weights chosen in order to shape the sensitivity functions according to the criteria given in Section 5.5.

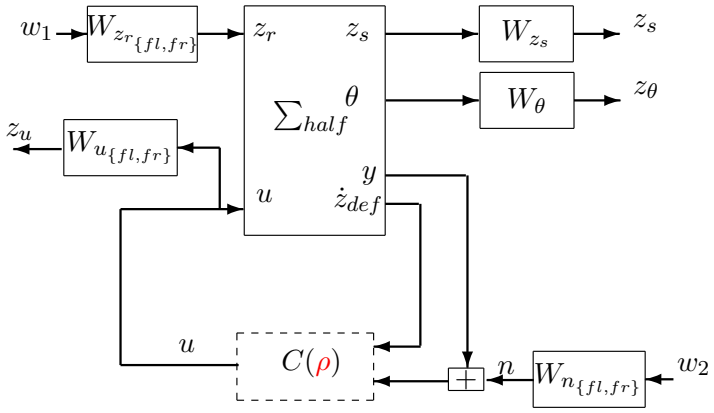

Figure 6.1: Generalized plant

$$\begin{cases} W_{z_s} &= \dfrac{1}{\frac{s}{2\pi 5}+1} \\ W_\theta &= \dfrac{1}{\frac{s}{2\pi}+1} \\ W_{u_{\{l,r\}}} &= 2.10^{-3} \\ W_{zr_{\{l,r\}}} &= 7.10^{-2} \\ W_{n_{\{l,r\}}} &= 10^{-3} \end{cases} \tag{6.4}$$

From now, we will consider the generalized plant as given on Figure 6.1 and synthesize different controllers (with different characteristics):

- Controller 1: an LTI/$\mathcal{H}_\infty$ controller is synthesized where the controlled outputs are $z_\infty = [z_s, z_\theta, z_{u_l}, z_{u_r}]$.
- Controller 2: an LTI/$\mathcal{H}_\infty$/$\mathcal{H}_2$ is synthesized controller where the controlled outputs are $z_\infty = [z_s, z_\theta, z_{u_l}, z_{u_r}]$ for $\mathcal{H}_\infty$ performance and $z_2 = [z_s, z_\theta, z_{u_l}, z_{u_r}]$ for $\mathcal{H}_2$ performance.
- Controller 3: a qLPV/$\mathcal{H}_\infty$/$\mathcal{H}_2$ controller is synthesized where the controlled outputs are $z_\infty = [z_s, z_\theta, z_{u_l}, z_{u_r}]$ for $\mathcal{H}_\infty$ performance and $z_2 = [z_s, z_\theta, z_{u_l}, z_{u_r}]$ for $\mathcal{H}_2$ performance and where the varying parameters are k_l and k_r.

These controllers are synthesized according to LMI results given in Chapter 3. In the following, we compare performances of each of these controllers. First, simulations are done to show the benefit of the mixed synthesis compared to single $\mathcal{H}_\infty$. Secondly, we study the influence of the trade-off of the $\{\gamma_\infty, \gamma_2\}$ couple on Controller 2 (i.e. the repartition between the two performance criteria) on the reached performances. Thirdly, we compare the LTI mixed approach with the qLPV one and show

the interest in the gain-scheduling according of the stiffness parameter. Finally, the Pareto limit is given in order to illustrate the compromise between $\mathcal{H}_\infty$ and $\mathcal{H}_2$ criteria when a mixed controller is designed (for both LTI and qLPv cases).

6.2.3 Simulation - Controller 1 (LTI/$\mathcal{H}_\infty$) vs. Controller 2 (LTI/$\mathcal{H}_\infty$/$\mathcal{H}_2$)

First we show the advantages of the mixed $\mathcal{H}_\infty$/ $\mathcal{H}_2$ (Controller 2) compared to the $\mathcal{H}_\infty$ synthesis (Controller 1). In both designs, γ_∞ is similar. In this simulation, a step road disturbance (of $5cm$, from $t = 1s$ to $t = 2s$) is applied on the left wheel (z_{r_l}), then a roll moment disturbance M_{dx} (of $5000Nm$ between $t = 3s$ to $t = 6s$) caused by a steering manoeuver; controllers performances are compared w.r.t. to the passive suspension.

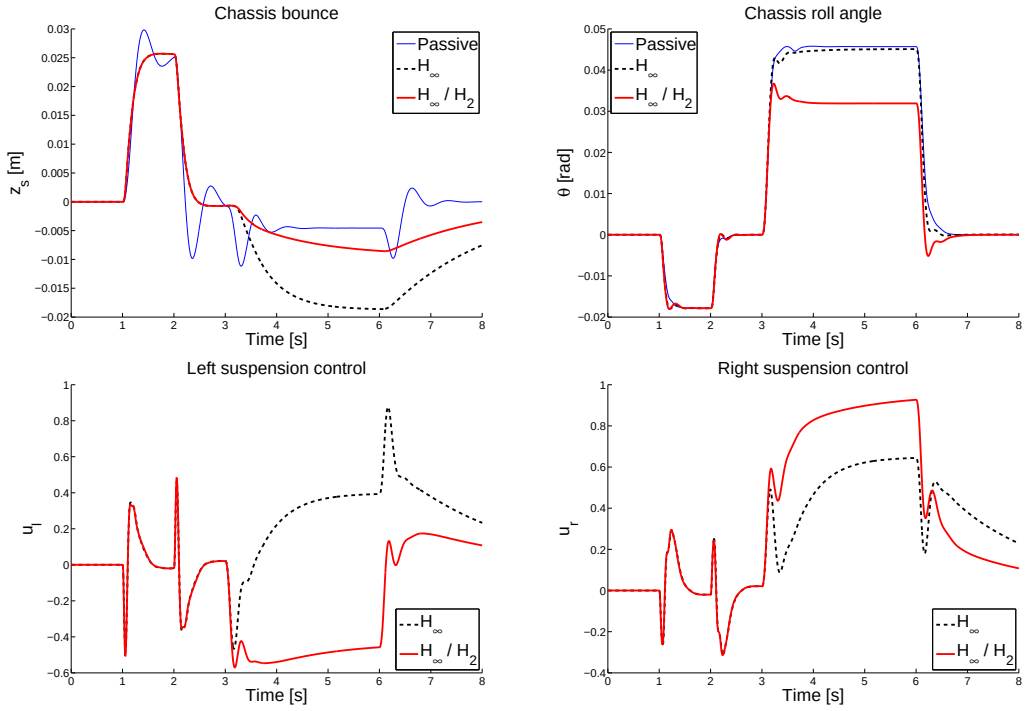

Figure 6.2: Comparison between Controller 1 (dashed) and Controller 2 (solid) design with Passive (solid slim). From top left to bottom right: chassis bounce (z_s), roll angle (θ), left (u_l) and right (u_r) control signals.

By using the mixed synthesis instead of single $\mathcal{H}_\infty$, the roll angle can be significantly reduced (see Figure 6.2).

6.2.4 Simulation - parametrization of Controller 2 (LTI/$\mathcal{H}_\infty$/$\mathcal{H}_2$)

As the mixed case seems to improve the single $\mathcal{H}_\infty$ criterion, one aims at comparing the performances of the LTI mixed synthesis (Controller 2) for different couples $\{\gamma_\infty, \gamma_2\}$ (Figure 6.3). This test aims at illustrating the role of the $\mathcal{H}_2$ criteria. Note that the same experiment as in the previous subsection is performed. In this case, when:

- $\gamma_2 = 4.5$, $\gamma_\infty = 0.25281$ is achieved.

- $\gamma_2 = 1.5$, $\gamma_\infty = 0.26883$ is achieved, and smoother responses and control signals (see Figure 6.3).

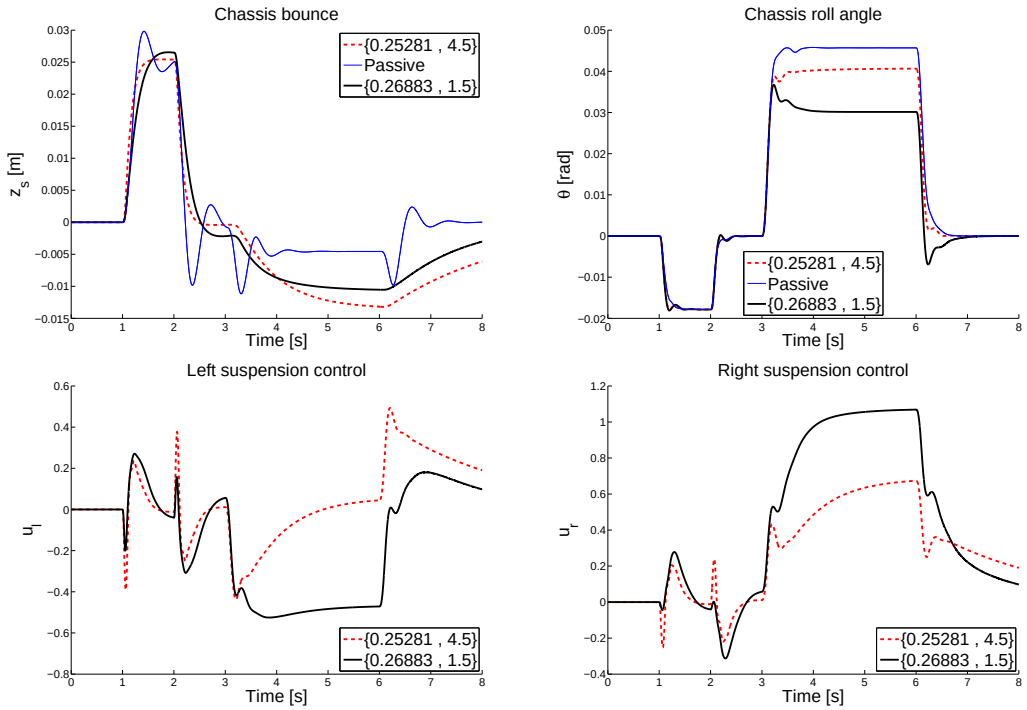

Figure 6.3: Controller 2 performances according to different $\{\gamma_\infty, \gamma_2\}$ couples. From top left to bottom right: chassis bounce (z_s), roll angle (θ), left (u_l) and right (u_r) control signals.

The aim of the $\mathcal{H}_2$ criterion is to minimize the energy and variations of a signal. If one decreases the γ_2 attenuation value, then the value of the γ_∞ increases (see also Pareto limit Figure 6.6). Hence, we observe that the z_s variations are smoother and the roll angle is attenuated by using a smaller attenuation gain on the $\mathcal{H}_2$ criterion (less oscillations, i.e. improvement of the vertical comfort). This emphasize the interest of the $\mathcal{H}_2$ criterion.

6.2.5 Simulation - Controller 2 (LTI/$\mathcal{H}_\infty$/$\mathcal{H}_2$) vs. Controller 3 (qLPV/$\mathcal{H}_\infty$/$\mathcal{H}_2$)

In this simulation set, the mixed LTI (Controller 2) and the mixed qLPV (Controller 3) controllers are compared on simulations. This simulation configuration is the same as previously, but here the added disturbance moment (M_{dx}) on the roll axis is of $8000Nm$ instead of $5000Nm$, which led the system to enter in the springs stiffness nonlinearities. Figures 6.4 and 6.5 show the results obtained.

Here, Controller 3 has been built for parameters $k_{\{l,r\}} \in k_{nom} \times [1, 1.95]$ (i.e. $[\underline{k}_{l,r}, \overline{k}_{l,r}]$), where k_{nom} is the lower value of $k(.)$ (see Figure 5.5) and for a fixed $\gamma_\infty = 0.25$.

As long as the system remains in the linear stiffness zone, the qLPV controller (Controller 3) provides almost the same performances as the controlled LTI one (Controller 2). As an illustration, between $t = 0s$ to $t = 3s$, when a small road disturbance is applied, both behaviors are similar and the scheduling parameters (α_i) do not vary. But, when the system enters in the nonlinearities (e.g. at time $t = 4s$), the qLPV controller schedules its gains to handle the stiffness nonlinearities and

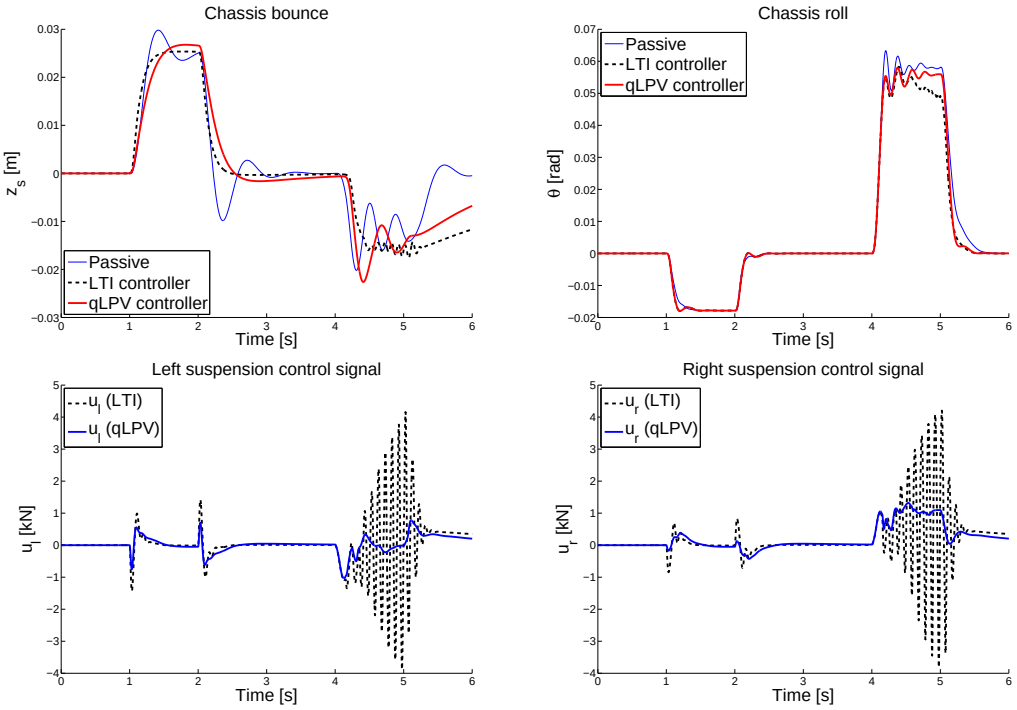

Figure 6.4: Comparison of Controller 2 (dashed) and Controller 3 (solid). From top left to bottom right: chassis bounce (z_s), roll angle (θ), left (u_l) and right (u_r) control signals.

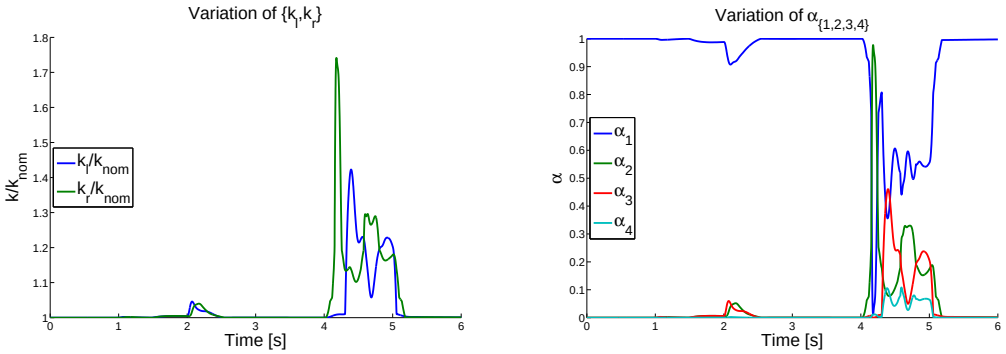

Figure 6.5: Stiffness parameter variations (left) and α parameters.

improves the performances achieved by the LTI one. As such a control tackles the nonlinearities, it enforces robustness and control signals are more adapted to the system, thus the adaptive controller is much more accurate than the invariant one (see Zin, 2005). The α variations (see Figure 6.5) show the obtained scheduling values (α_i) according to the parameters variations (k_l, k_r).

By looking at the control signals (u_l and u_r), one clearly see that the qLPV control provides a control signal less noisy than the LTI controller does. Thus the qLPV solution is much more tractable from an implementation point of view.

Remark: Controller implementation. The qLPV approach is more complex than the LTI one since N controllers have to be implemented ($N = 4$ in our case). Moreover, it requires a real-time scheduling. Nevertheless, as in both syntheses (LTI and qLPV), the same number of measures is used, in terms of sensor, Controller 3 is not more expensive than Controller 2 (the scheduling rule only requires the deflection measure).

6.2.6 Pareto limit

The Pareto limit (introduced in Chapter 3) is illustrated for the mixed $\mathcal{H}_\infty/\mathcal{H}_2$ case. Let recall that it is impossible to minimize both γ_∞ and γ_2. In the literature, the mixed problem is generally solved by minimizing a convex combination of $\mathcal{H}_\infty$ and $\mathcal{H}_2$ that represents a compromise between the two performances. Such a minimization may take the following form,

$$\min_{\{\alpha\in[0,1]\}} \{\alpha\gamma_\infty + (1-\alpha)\gamma_2\} \tag{6.5}$$

Hence a natural problem rises: how to choose α in a smart way. The concept of non-inferiority (also called Pareto optimality) is used here to characterize the objectives. Recall that a non-inferior solution is the one for which an improvement in one objective requires the degradation of an other. In our case, the objectives are given in terms of $\mathcal{H}_\infty$ and $\mathcal{H}_2$ performances. To plot the Pareto optimum, applied to our problem, we iteratively and successively fix γ_∞ and optimize the γ_2. The corresponding results are given in Figure 6.6. This process is done to both LTI (full line) and qLPV cases (dashed lines). Note that for the qLPV case, the Parero limit is computed for different sizes of the varying parameter set, where the left and right stiffness bounds are fixed at different values (note that by increasing the bounds, one increases the polytope size, but also handles more parameter variations).

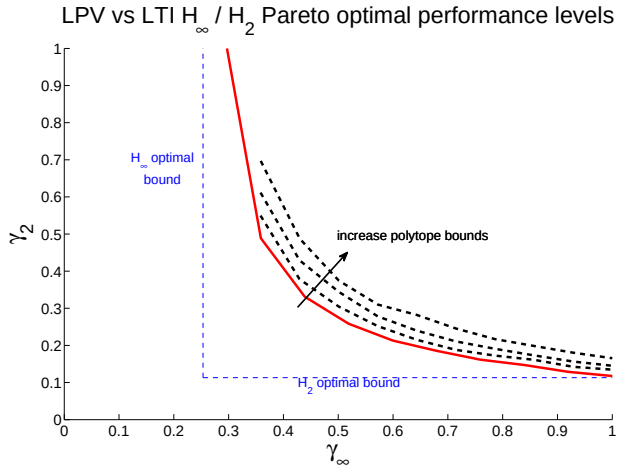

Figure 6.6: Pareto limits of the LTI (solid) and qLPV for $k_{\{l,r\}} \in k_{nom} \times [1, 1.2], [1, 1.5], [1, 2]$ (dashed).

The achievable combinations $\{\gamma_\infty, \gamma_2\}$ are the set of couples located over the Pareto limit. For the LTI case, it illustrates the trade-off. For the qLPV case, the Pareto limit illustrates the conservatism introduced by increasing the polytope size. Thus, it is also useful to measure the conservatism of a method; as an example, by choosing a parameter dependent Lyapunov function, the conservatism may

be reduced. Such a figure can also motivate researches on polytope reduction. Indeed, the more the size of the polytope is increased (bounds of the parameters), the more the curve goes far away from the LTI Pareto optimum (Figure 6.6), and thus, performances are decreased.

6.2.7 Concluding remarks on the active suspension design

This example illustrates an active suspension control synthesis using advanced control tools. Here we have investigated a multi-objective ($\mathcal{H}_\infty/\mathcal{H}_2$) qLPV control applied to a half vehicle model. Attention is made on the advantages of the mixed criteria and on the compromises that have to be done in multi-objective applications. Moreover, a qLPV controller has been designed and shown to improve the system performances, especially when it enters in the nonlinear behavior. Thanks to the scheduling rule, the controller adapts its gains to the system working point. By using the Pareto limit (non-inferior solution), we illustrate the compromise to be done and the conservatism introduced by the polytopic solution.

This example allows to illustrate an active suspension design; it illustrates the control synthesis of an "adaptive" LPV multi-objective controller on a MIMO system. In this case, the LPV design improves the robustness and accuracy of the closed loop system.

In the following, the LPV approach is used to make the closed-loop system performance varying to achieve, in an original way, the semi-active constraint of controlled dampers.

6.3 Semi-active suspension control

This section is concerned with the presentation of one of the main contributions provided in this thesis, which concerns the design and the analysis of a new semi-active suspension controller.

Recently, different kinds of semi-active control strategies, like two-state Skyhook, ADD, Mixed SH-ADD (Skyhook-ADD), model-predictive or simply clipped control, have been developed in the literature (see Section 2.4). Here, we introduce a new semi-active suspension control strategy, that a priori satisfies the principal limitations of a semi-active suspension actuator (i.e. dissipative constraint and force bounds). The proposed approach is based on the LPV theory. It exhibits some interesting advantages compared to already existing methods, such as simple structure for implementation, performance flexibility, robustness, etc. To show the efficiency of the method and to validate the theoretical approach, the proposed methodology is evaluated using the vertical performance criterion and the metric introduced in Section 5.5, through simulations on the nonlinear vertical quarter vehicle model (introduced in Section 5.2). Moreover, some comparisons with other approaches are performed to stress the potentiality of the design.

6.3.1 General idea & Control structure

The control synthesis is based on the vertical quarter car model described by equation (5.2) where $F_k(z_{def}) = k.z_{def}$ and $F_c(\dot{z}_{def}) = c.\dot{z}_{def}$ are linear functions ($c = 1500N/m/s$ and $k = 29500N/m$). The applied control law has the following structure:

$$u = c.\dot{z}_{def} + u^{\mathcal{H}_\infty} \tag{6.6}$$

where c is the nominal linearized damping coefficient of the considered semi-active damper. As an illustration, for an MR damper, c nominal is the one given to provide nominal performances (e.g. when no current is applied to the system). Then $u^{\mathcal{H}_\infty}$ is the additional force provided by the controller. To

account for actuator limitations (see e.g. Chapter 4), a new method is developed based on the LPV polytopic theory using the $\mathcal{H}_\infty$ controller synthesis approach.

From now on, the considered semi-active damper will simply be modeled as a static map of the deflection speed/Force of the Delphi MR damper illustrated in Section 4.2, i.e. a lower and upper bound of the achievable forces, as shown on Figure 6.7.

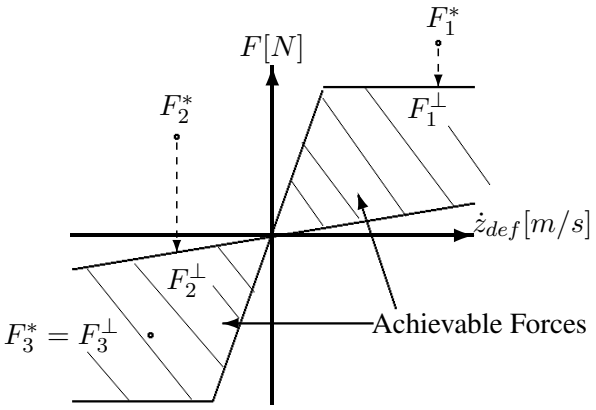

Figure 6.7: Semi-active damper model: achievable zone $D(\dot{z}_{def})$.

This static model is thus a saturation function of the deflection speed. In the following, it will be denoted as $D(\dot{z}_{def})$.

6.3.2 Semi-active proposed approach & Scheduling strategy

In order to meet the semi-activeness and performance requirements, the generalized control scheme is chosen as in Figure 6.8.

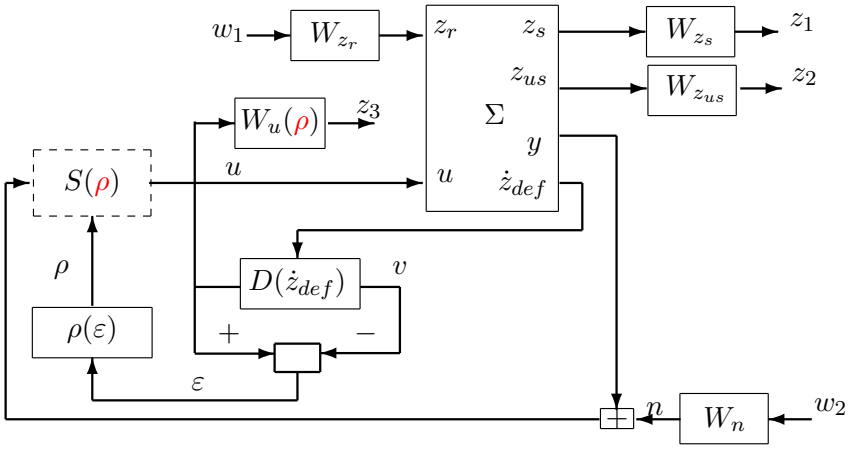

Figure 6.8: Generalized scheme & Scheduling strategy.

The generalized block scheme incorporates the weighting functions ($W_{z_r}, W_n, W_{z_s}, W_{z_{us}}, W_u(\rho)$ described later), and the semi-active actuator model, $D(\dot{z}_{def})$ (as the one presented below, which simply consists in the upper and lower saturations of the considered semi-active actuator).

$\rho(\varepsilon)$ is the scheduling parameter, function of $\varepsilon = u - v$, the difference between the computed force and the achievable one (a force is achievable if it is between the upper and lower bounds of the semi-active considered actuator, as illustrated by the static model $D(\dot{z}_{def})$ on Figure 4.3 and 6.7). $\rho(\varepsilon)$ will be used to satisfy the dissipative damper constraints (see next subsection). The idea is to increase the control gain when the required force is in the allowed quadrants, and otherwise to rely on the passive law designed by the car manufacturer when the forces are outside the allowable space. For that purpose, the following scheduling strategy $\rho(\varepsilon)$ is introduced (and illustrated on Figure 6.9):

$$\rho(\varepsilon) = 10\frac{\mu\varepsilon^4}{\mu\varepsilon^4 + 1/\mu} \tag{6.7}$$

where μ is a design parameter that modifies the slope of the $\rho(\varepsilon)$ function. In the proposed case, μ is chosen sufficiently high (e.g. $\mu = 10^8$) to ensure the semi-active control (see next subsection). On Figure 6.9, the $\rho(\varepsilon)$ function is given for different values of μ.

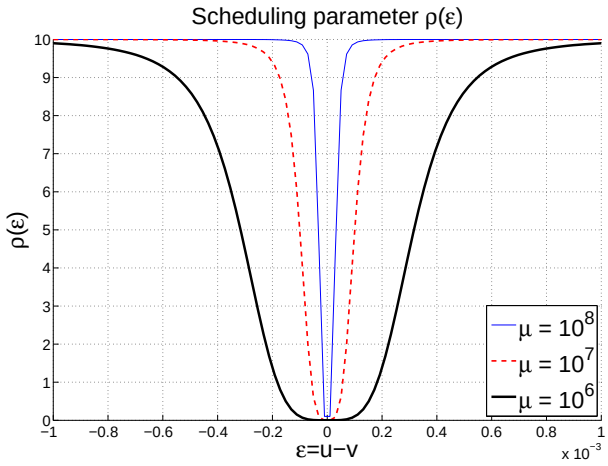

Figure 6.9: $\rho(\varepsilon)$ function, for $\mu = 10^6$ (solid thick), $\mu = 10^7$ (dashed), $\mu = 10^8$ (solid thin).

Remark: About the scheduling parameters $\rho(\epsilon)$.

- The defined $\rho(\varepsilon)$ function is continuous and satisfies $\{\rho(\varepsilon) \in [0, 10]\}, \forall\varepsilon \in \mathbb{R}$. In other terms, ρ belongs to a closed set $[\underline{\rho}, \overline{\rho}]$. This point is essential in the LPV framework, as described in Chapter 3. For numerical implementation purposes, one will consider $\rho \in [0.1, 10]$ instead of $[0, 10]$.
- $\varepsilon \neq 0 (\Leftrightarrow u \neq v)$ means that the required force is outside the allowed range. Conversely, $\varepsilon = 0 (\Leftrightarrow u = v)$ means that the force required by the controller is reachable for the considered semi-active actuator.

The idea is then to synthesize a controller $C(\rho)$ that is tuned according to this parameter in order to satisfy some performance objectives while ensuring the semi-activeness. In other words, to add a force ($u^{\mathcal{H}_\infty}$) when possible, and to rely on the passive solution when no force can be added. For that purpose, the LPV synthesis framework is used and performances are described through the $\mathcal{H}_\infty$ criteria.

6.3.3 LPV Control synthesis

As emphasized previously, the aim is to keep the control signal in the semi-active quadrants (Figure 4.3 and 6.7). In other words, the control law aims at increasing/decreasing the damping coefficient. Here, in the LPV design presented in Figure 6.8, $W_u(\rho)$, which is the performance criterion on the control signal, is ρ dependent. Let remember that in the $\mathcal{H}_\infty$ framework, this weight indicates how large the gain on the control signal can be. Choosing a high $W_u(\rho) = \rho$ forces the control signal to be low, and conversely. Hence, when ρ is large, the control signal is so penalized that it is practically zero, and the closed-loop behavior is the same as the passive quarter vehicle model one. Conversely, when ρ is small, the control signal is no more penalized; hence the controller can achieve performances in the allowed Force/Deflection speed space. This is consistent with the shape of $\rho(\varepsilon)$ in Figure 6.9.

Note that, as the varying parameter enters on the input signal, requirement R2, given in Section 3.6 is not fulfilled for the solvability of the $\mathcal{H}_\infty$ control problem for LPV systems. Therefore, a strictly proper filter $\mathcal{F}$ s.t.

$$\mathcal{F} = \frac{1}{\frac{s}{100} + 1} \tag{6.8}$$

is added to the generalized plant. Thus the new generalized plant description is given as,

$$\begin{bmatrix} \dot{x} \\ z_\infty \\ y \end{bmatrix} = \begin{bmatrix} A(\rho) & B_\infty(\rho) & B \\ C_\infty(\rho) & D_{\infty w}(\rho) & D_{\infty u} \\ C & 0 & 0 \end{bmatrix} \begin{bmatrix} x \\ w_\infty \\ u \end{bmatrix} \tag{6.9}$$

where,

$$\begin{cases} x &= \begin{bmatrix} x_{quarter} & x_{weights} & x_{filter} \end{bmatrix}^T \\ z_\infty &= \begin{bmatrix} W_{z_s} z_s, & W_{z_{us}} z_{us}, & W_u(\rho) u \end{bmatrix}^T \\ w_\infty &= \begin{bmatrix} W_{z_r}^{-1} z_r, & W_n^{-1} n \end{bmatrix}^T \\ y &= z_{def} \\ \rho &\in \begin{bmatrix} \underline{\rho} & \overline{\rho} \end{bmatrix} \end{cases} \tag{6.10}$$

where x is the concatenation of the linearized quarter vehicle model and the weighting function state variables, z_∞ the performance output, w_∞ the weighted input, y the measured signal, and ρ the varying parameter.

According to the performance objectives described in Section 5.5, W_{z_s} (resp. $W_{z_{us}}$) is shaped in order to reduce the amplification of the sprung mass z_s (resp. z_{us}) between $0-5$ Hz (resp. $0-20$ Hz), W_{z_r} and W_n model ground disturbances (z_r) and measurement noise (n) respectively, and $W_u(\rho)$ is used to limit the control signal and achieve the semi-active constraint (see next subsection). The weighting functions are given by:

$$\begin{cases} W_{z_s} &= \frac{\frac{s}{\omega_{11}} + 1}{\frac{s}{\omega_{12}} + 1} \\ W_{z_{def}} &= \frac{1}{\frac{s}{\omega_{21}} + 1} \\ W_{z_r} &= 7.10^{-2} \\ W_n &= 10^{-4} \\ W_u(\rho) &= \rho \frac{1}{\frac{s}{1000} + 1} \\ \rho &\in \begin{bmatrix} 0.01 & 10 \end{bmatrix} \end{cases} \tag{6.11}$$

where $\omega_{11} = 1rd/s$, $\omega_{12} = \sqrt{\frac{k_t}{m_{us}}}rd/s$ and $\omega_{21} = \sqrt{\frac{k_t}{m_s+m_{us}}}rd/s$. These filters are designed to enhance the frequency zone, as described in Section 5.5. Attention is made to avoid constraint in the invariant behavior (see Section 5.2). Figure 6.10 (left) shows $1/W_{z_s}$ and $1/W_{z_{def}}$ weighting functions and Figure 6.10 (right) shows $1/W_u(\rho)$ for $\rho \in [\underline{\rho}, \overline{\rho}]$.

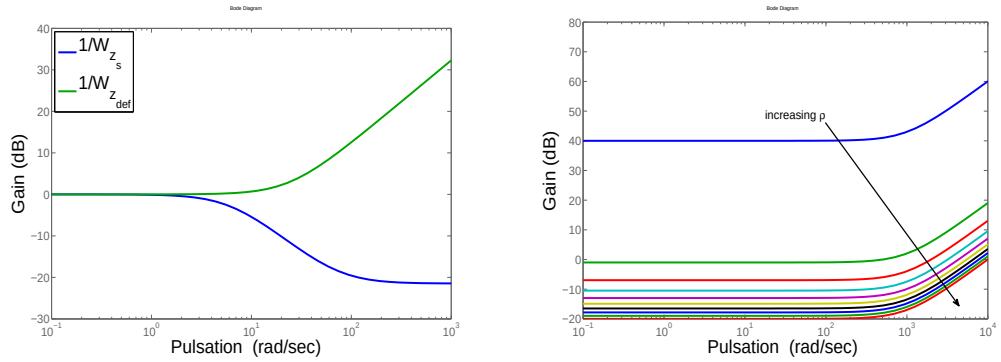

Figure 6.10: Weighting functions used for the LPV $\mathcal{H}_\infty$ synthesis.

Applying the LMI based polytopic LPV/$\mathcal{H}_\infty$ control synthesis (described in Section 3.6) to the generalized plant (6.9) leads to two controllers $C(\underline{\rho})$ and $C(\overline{\rho})$, hence to two closed-loops ($CL(\underline{\rho})$ and $CL(\overline{\rho})$). The applied control law is the convex combination of these two controllers, function of ρ, as described in equation (6.12),

$$\begin{aligned} u &= c_0.\dot{z}_{def} + u^{\mathcal{H}_\infty} \\ u^{\mathcal{H}_\infty} &= \Big[\frac{|\rho-\overline{\rho}|}{\overline{\rho}-\underline{\rho}}S(\underline{\rho}) + \frac{|\rho-\underline{\rho}|}{\overline{\rho}-\underline{\rho}}S(\overline{\rho})\Big]y \end{aligned} \tag{6.12}$$

Hence, the controller $C(\rho)$ and the closed-loop $CL(\rho)$ lie in the following convex hulls:

$$\begin{aligned} C(\rho) &\in \mathbf{Co}\{C(\underline{\rho}), C(\overline{\rho})\} \\ CL(\rho) &\in \mathbf{Co}\{CL(\underline{\rho}), CL(\overline{\rho})\} \end{aligned} \tag{6.13}$$

The system closed-loop frequency responses obtained with the LPV controllers, and for different frozen values of $\rho \in \left[\ \underline{\rho}\ \ \overline{\rho}\ \right]$, are given on Figures 6.11.

Using the criteria introduced in Section 5.5 one can see that when ρ is low, suspension behavior is modified as described by the defined criteria. Thus it is improved in the frequency range of interest.

Note that these closed-loop transfers provide a good frequency behavior (good performances) when ρ is small, improving comfort in the range $0-5$Hz and road holding in the range $0-20$Hz, while, when ρ is high, it perfectly matches with the passive suspension which for the considered Renault Mégane Coupé car is road holding oriented.

Note also that a major interest in using the LPV design is that the internal stability of the closed-loop system is ensured for all $\rho \in \left[\ \underline{\rho}\ \ \overline{\rho}\ \right]$, hence the system is kept under control.

Remark: Frequency diagrams. The Bode diagrams given on Figure 6.11 show the system frequency performance according to different values of the parameter ρ. Remember that the parameter ρ is not chosen by the driver, but imposed by the semi-active model of the damper, and will vary on line.

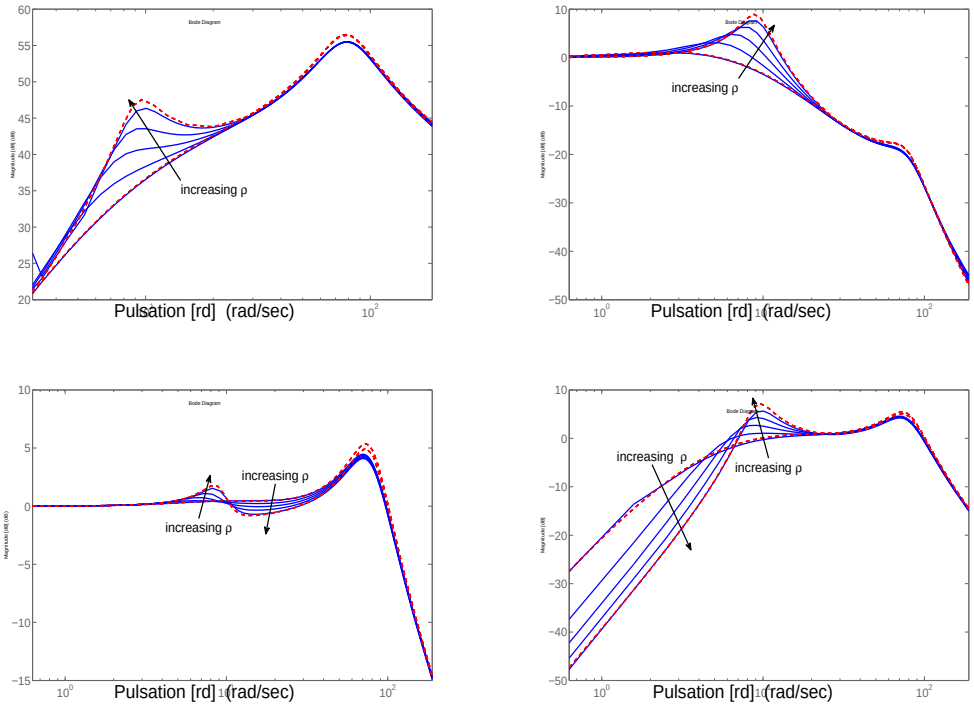

Figure 6.11: Frequency diagrams of the closed-loop for different values of $\rho \in [0.1; 10]$. From top left to bottom right: $\ddot{z}_s/z_r$, z_s/z_r, z_{us}/z_r, z_{def}/z_r.

6.3.4 Implementation issues

Before providing the simulation results, a sketch of implementation in order to apply the proposed strategy is given. Figure 6.12 shows the implementation synopsis, for any kind of semi-active actuators.

In Figure 6.12,

- 'SA mdl' is the model of the semi-active damper considered in the application (here $D(\dot{z}_{def})$, a static model of the upper and lower damping factors of the MR damper).
- $\rho(\varepsilon)$ is the scheduling law given in (6.7).
- 'SA act' is the real considered actuator and its inner loop (e.g. inverse model) of the semi-active damper that modifies the damping coefficient.
- u, v, ε and ρ are the control and scheduling signals as described before.
- Ω is used here to specify the set of input parameters of the real controllable damper 'SA act'. As an illustration, for a MR damper, the real control input is I_{MRD}, the current that modifies the magneto-rheological fluid viscosity.

Hence, in the case of the MR damper actuator, the force u has to be converted into a current (by the means of tables or electrical laws for instance), hence $\Omega = I_{MRD}$. For other kinds of semi-active

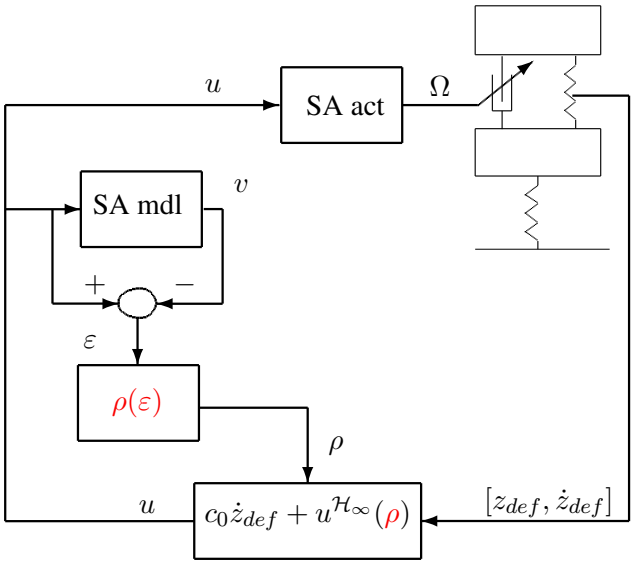

Figure 6.12: Implementation scheme.

actuators, control input can be some mechanical, pneumatic elements or other damper input variables depending on the chosen technology (see e.g. Lord, 2008; Delphi, 2008; Sachs, 2008).

Remark: About the implementation.

- This scheme is the same for any suspension control approaches. The advantage here is that the required force u always remains in the allowed force range of the considered controlled semi-active actuator (thanks to the proposed LPV approach).
- If a dynamical model of the considered actuator (gain, bandwidth limit...) is available, it may be included in the synthesis by the mean of the $W_u(\rho)$ weighting function.

6.3.5 Simulation results, performance evaluation and comparison with other controllers

The proposed control design is evaluated through time and frequency space responses. Evaluations are performed thanks to the introduced metric (see Section 5.5) and compared with other strategies.

6.3.5.1 Other semi-active methods illustrated for comparison

In order to compare the proposed "LPV $\mathcal{H}_\infty$" design, comparison with other strategies are performed. The following controller are used:

- A full "Active $\mathcal{H}_\infty$ " controller (synthesized for $\rho = \underline{\rho}$), with the same weighting function as the one introduced previously.
- A "Clipped $\mathcal{H}_\infty$ " controller, which is the same controller as the "Active $\mathcal{H}_\infty$ " one (see below), but with clipped (saturated) output by function $D(\dot{z}_{def})$.

- The mixed "SH-ADD" semi-active controller defined as:

$$u = c_{in}.\dot{z}_{def} \tag{6.14}$$

where c_{in} is computed as:

$$c_{in} = \begin{cases} c_{min} & \text{if } \left[(\ddot{z}_s^2 - \alpha^2 \dot{z}_s^2) \leq 0 \ \& \ \dot{z}_s \dot{z}_{def} > 0\right] \text{ OR } \left[(\ddot{z}_s^2 - \alpha^2 \dot{z}_s^2) > 0 \ \& \ \dot{z}_s \dot{z}_{def} > 0\right] \\ c_{max} & \text{if } \left[(\ddot{z}_s^2 - \alpha^2 \dot{z}_s^2) \leq 0 \ \& \ \dot{z}_s \dot{z}_{def} \leq 0\right] \text{ OR } \left[(\ddot{z}_s^2 - \alpha^2 \dot{z}_s^2) > 0 \ \& \ \dot{z}_s \dot{z}_{def} \leq 0\right] \end{cases} \tag{6.15}$$

where $\alpha = 2\pi\sqrt{\frac{kt}{mus}}$, is the cut-off frequency at the invariant point, as advised in (Spelta, 2008).

- The "ADD" semi-active method defined as:

$$u = c_{in}.\dot{z}_{def} \tag{6.16}$$

where c_{in} is defined as:

$$c_{in} = \begin{cases} c_{min} & \text{if } \ddot{z}_s \dot{z}_{def} \leq 0 \\ c_{max} & \text{if } \ddot{z}_s \dot{z}_{def} > 0 \end{cases} \tag{6.17}$$

All these strategies will also be compared to the passive suspension with the parameter of the Renault Mégane Coupé. This "Passive" suspension will be our reference model.

6.3.5.2 Time domain simulations

A step road disturbance of magnitude $-1cm$ is generated at $t = 1s$ and of $+1cm$ at $t = 5s$. The suspension control force (SER) and the scheduling parameter variations are shown on Figures 6.13.

Figure 6.13 clearly shows that the forces provided by the "LPV $\mathcal{H}_\infty$" controller remain in the semi-active allowed space and in the achievable range of the considered Delphi MR damper. Moreover, it illustrates the fact that all the semi-active methods remain in the allowed quadrants (note that the "Active $\mathcal{H}_\infty$" controller goes in the active quadrants). Figure 6.13 shows how the ρ parameter varies according to the step. Notice that during the step disturbance, the ρ parameter varies to handle the semi-active constraint.

Figure 6.14 shows on time responses, that the proposed "LPV $\mathcal{H}_\infty$" controller attenuates undesired oscillations for both the chassis acceleration and bounce, the wheel bounce and the suspension deflection. These results stand for illustrating the fact that the proposed design ensures the semi-active constraint. One can see that the "LPV $\mathcal{H}_\infty$" notably reduces the acceleration peak and preserves the suspension deflection. The wheel behavior is very similar for all the proposed designs.

As these results are not complete enough to characterize the quality of the proposed control design, thereafter, the frequency behavior is analyzed and quantified with the PSD metric introduced in 5.5.

6.3.5.3 Frequency domain simulations

The performance metric (5.23) is used to evaluate both passive and controlled nonlinear quarter car models, using the presented MR damper as the semi-active actuator (for all the control strategies). Let recall that the parameters used in the simulations for the passive reference model correspond to the "Renault Mégane Coupé" one, a car satisfying good road holding and handling performances. This means that the proposed semi-active control will not improve the road holding characteristics significantly.

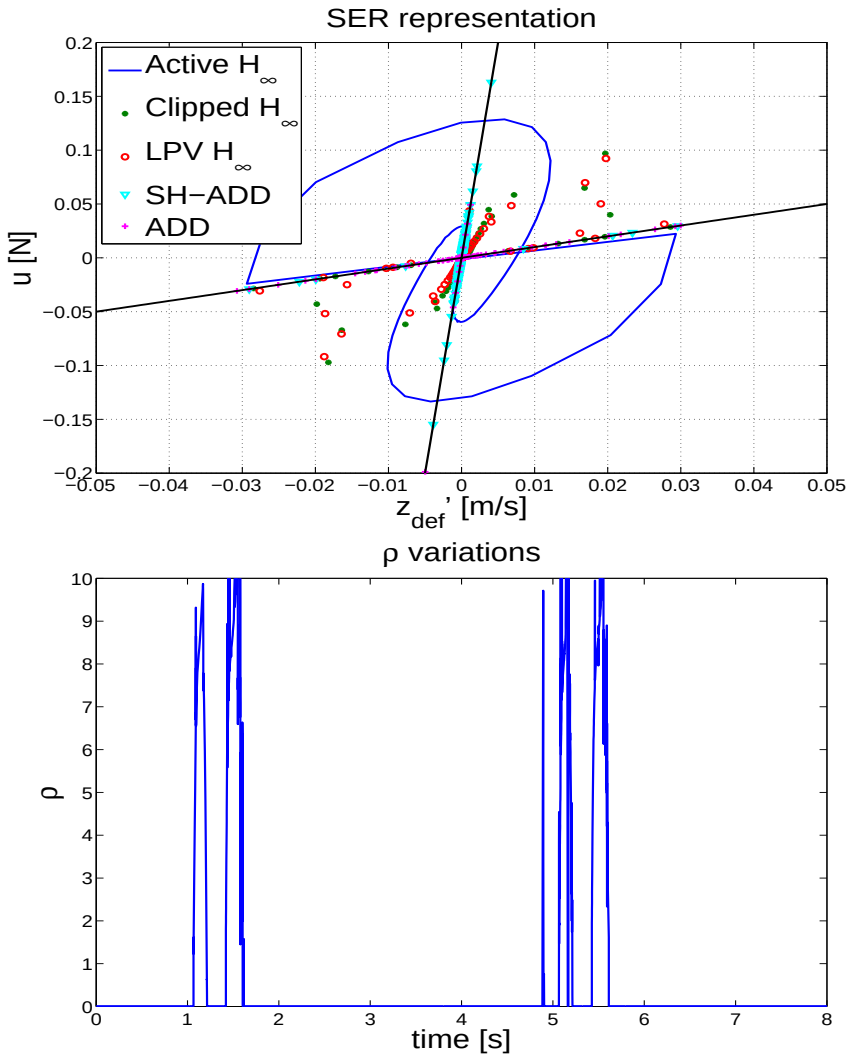

Figure 6.13: Force/Deflection speed diagram (SER) in response to a step road disturbance (top). ρ variation (bottom).

Figure 6.15 shows the nonlinear frequency response (pseudo-Bode) of $\ddot{z}_s/z_r$, z_s/z_r, z_{us}/z_r and z_{def}/z_r (for a given input amplitude of $2cm$).

Figure 6.16 shows the same nonlinear frequency response of $\ddot{z}_s/z_r$, z_s/z_r, z_{us}/z_r and z_{def}/z_r as on Figure 6.15; but here, the gain is evaluated as in absolute value (i.e. not in dB), a linear space frequency is considered (instead of a semi logarithmic pulsation space) and zoom is done on the frequencies of interest (i.e. $[4; 30]$ for $\ddot{z}_s/z_r$, $[0; 5]$ for z_s/z_r, $[0; 20]$ for z_{us}/z_r and $[0; 20]$ for $\ddot{z}_{def}/z_r$)

In Table 6.1, the improvement of each strategy is evaluated as:

$$\frac{\text{Passive PSD} - \text{Controlled PSD}}{\text{Passive PSD}} \tag{6.18}$$

where the PSD denotes the power spectral density as described in Section 5.5. Note that, for these tuning parameters, the:

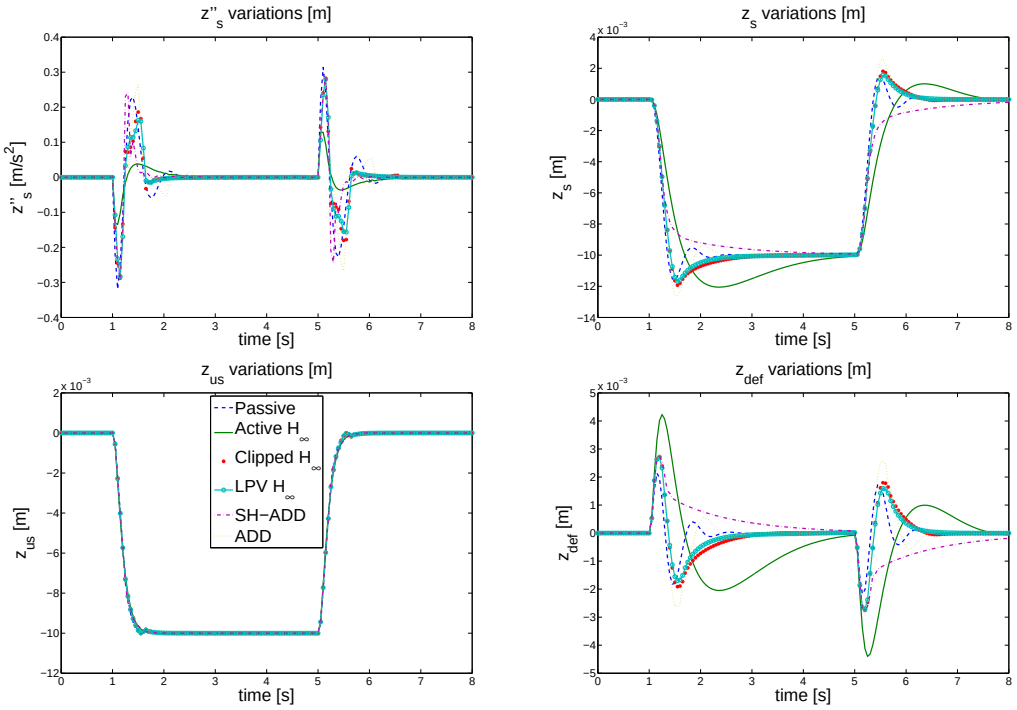

Figure 6.14: Time response of $\ddot{z}_s$, z_s, z_{us} and z_{def} to a step road disturbance (from top left to bottom right).

Signal	Active $\mathcal{H}_\infty$	Clipped $\mathcal{H}_\infty$	LPV/$\mathcal{H}_\infty$	ADD	SH-ADD
$\ddot{z}_s/z_r$ $[4;30]$Hz	4.8%	3.8%	-4.4%	10%	10.8%
z_s/z_r $[0;5]$Hz	52.8%	23.5%	18.9%	16.9%	36.2%
z_{us}/z_r $[0;20]$Hz	3.2%	4.2%	9.9%	-4.9%	-5.8%
z_{def}/z_r $[0;20]$Hz	5.3%	5.7%	10.4%	-7.8%	-4.5%

Table 6.1: Improvement of the semi-active control methods (comparison between "Active $\mathcal{H}_\infty$", "Clipped $\mathcal{H}_\infty$", "LPV $\mathcal{H}_\infty$", "ADD" and "Mixed SH-ADD" control).

- The "Active $\mathcal{H}_\infty$ " controller improves all the transfers (which is not surprising, since the actuator is not limited), but requires an active actuator (see Figure 6.13).
- The Mixed "SH-ADD" (as well as the simple "ADD") provides good comfort results but diminishes road-holding performances (this remark was also predictable since these control laws are comfort oriented).
- The "Clipped $\mathcal{H}_\infty$ " shows good PSD improvements in this test results, as shown in (Sammier, 2001). But it still remains a solution where neither stability nor $\mathcal{H}_\infty$ performances can be guarantee since the control is simply clipped, thus saturated.
- The "LPV $\mathcal{H}_\infty$" strategy leads to good improvements concerning comfort objectives (chassis bounce) and road holding (wheel bounce), which is very satisfactory for the "Renault Mégane

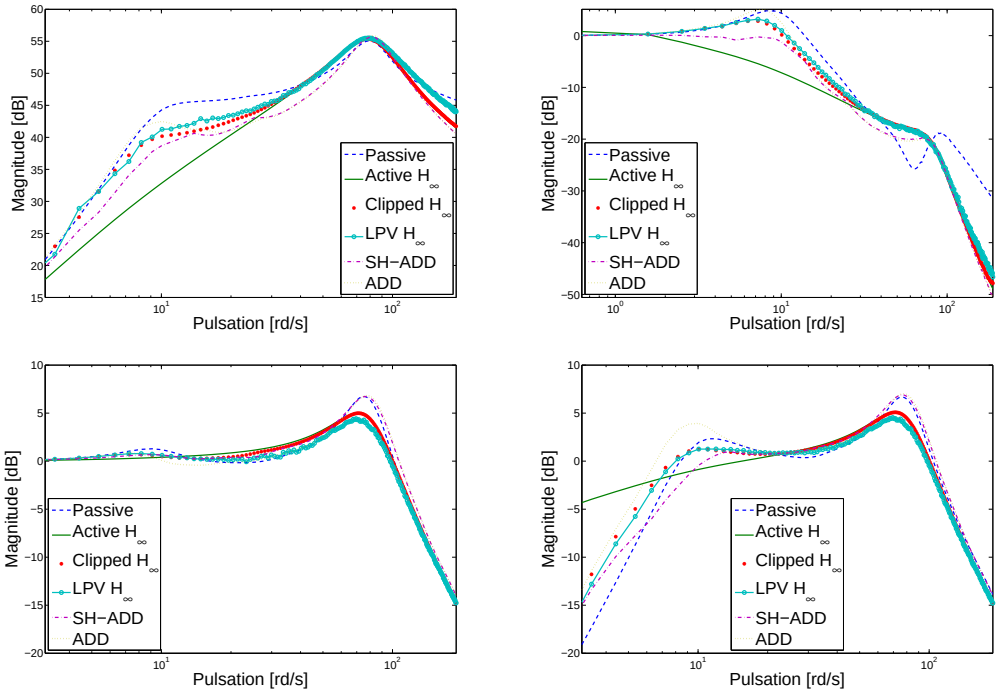

Figure 6.15: Frequency response of the different semi-active control laws of $\ddot{z}_s/z_r$, z_s/z_r, z_{us}/z_r and z_{def}/z_r.

Coupé" (already road-holding oriented). The slight loss of performance in the acceleration is not so significant (see Figure 6.15) and principally concerns hight frequencies ($> 10Hz$).

Note that, by ranking the strategies which improve the passive damper according to each transfer one obtains:

- Chassis acceleration between $[4; 30]Hz$ ($\ddot{z}_s/z_r$) which represents trepidations in the car, one obtains: SH-ADD, ADD, Clipped $\mathcal{H}_\infty$.
- Chassis displacement between $[0; 5]Hz$ (z_s/z_r) which represents passenger comfort in the car, one obtains: SH-ADD, Clipped $\mathcal{H}_\infty$, LPV $\mathcal{H}_\infty$, ADD.
- Wheel displacement between $[0; 20]Hz$ (z_{us}/z_r) which represents vehicle road-holding, one obtains: LPV $\mathcal{H}_\infty$, Clipped $\mathcal{H}_\infty$.
- Suspension deflection between $[0; 20]Hz$ (z_{def}/z_r) which is important for suspension life cycle, one obtains: LPV $\mathcal{H}_\infty$, Clipped $\mathcal{H}_\infty$.

6.3.6 Some remarks and perspectives on semi-active suspension control

In this section, a new strategy to ensure the dissipative constraint for a semi-active suspension is introduced, while keeping the advantages and flexibility of the $\mathcal{H}_\infty$ control design. The main interests of such an approach compared to existing ones are:

1. Flexible design: possibility to apply $\mathcal{H}_\infty$, $\mathcal{H}_2$, Pole placement, Mixed criteria, etc (Note that here only one single tuning design is presented but other weighting functions and/or criteria can be applied).
2. Measurement: only the suspension deflection (and its first derivative) is required.
3. Computation: synthesis leads to two LTI controllers and a simple scheduling strategy based on a static actuator model (no on-line optimization process involved).
4. Internal stability is preserved and the controlled (which is not the case when Clipped design is performed).
5. Implementation: solution tractable for any kind of semi-active actuators.

The proposed control design shows good performances, through both frequency based industrial criteria and time simulation experiments performed on a nonlinear model (compared to existing strategies). Hence this new semi-active strategy exhibits significant improvements on the achieved performances and provides a non negligible design flexibility.

Moreover, compared to LQ and MPC techniques, the implementation of such a controller results in a low cost solution in terms of controller order (time consumption) and sensor requirements which is one of the key points in all embedded solutions. Compared to ADD and SH-ADD, it presents more flexibility but results in a more complex solution. The proposed approach can also be applied to any semi-active actuators (as long as a model is available).

6.4 Concluding remarks

This chapter has emphasized two contributions of this thesis in the suspension domain. In the first one, the suspension system is controlled to enhance heave and roll behaviors, while taking into account the nonlinearities of the spring through the use of a mixed performance qLPV design. In Zin *et al.* (2008*a*), the robustness enhancement bring by the qLPV design is shown for the quarter vehicle case using a single $\mathcal{H}_\infty$ performance criteria. Here the model nonlinearity (of both suspension stiffness) is handled in the control design. Thus, time-domain results show that the robustness of the closed-loop is enhanced but further analysis may be done to prove it (e.g. using μ-analysis or nonlinear frequency analysis). Moreover, an illustration of the Pareto trade-off is given, which also shows the conservatism introduced by the LPV polytopic design.

In the second design, the semi-active constraint is handled through the LPV design. In this approach, the varying parameter is used to modify the control performance (while in the first example, it was used to improve the robustness). The proposed controller shows good performance results compared to well established existing semi-active controllers.

These examples illustrate some of the potentialities of the LPV design. Moreover, in the continuity of these results, some interesting points to be investigated in future works may be:

- To analyze the influence of the polytope size and the improvement led by a parameter dependent Lyapunov function.
- To find a constraint tractable for SDP solvers, to handle the semi-active constraint, to avoid the LPV design and reduce solution conservatism.
- To find a constraint tractable for SDP solvers, to handle the semi-active requirement without using the LPV scheme, to reduce conservatism and avoid scheduling.

In the next chapter, control strategies will be designed for Global Chassis Control (GCC) purpose. Thus, the aim is now to control the whole vehicle dynamics by the use of multiple (kinds of) actuators.

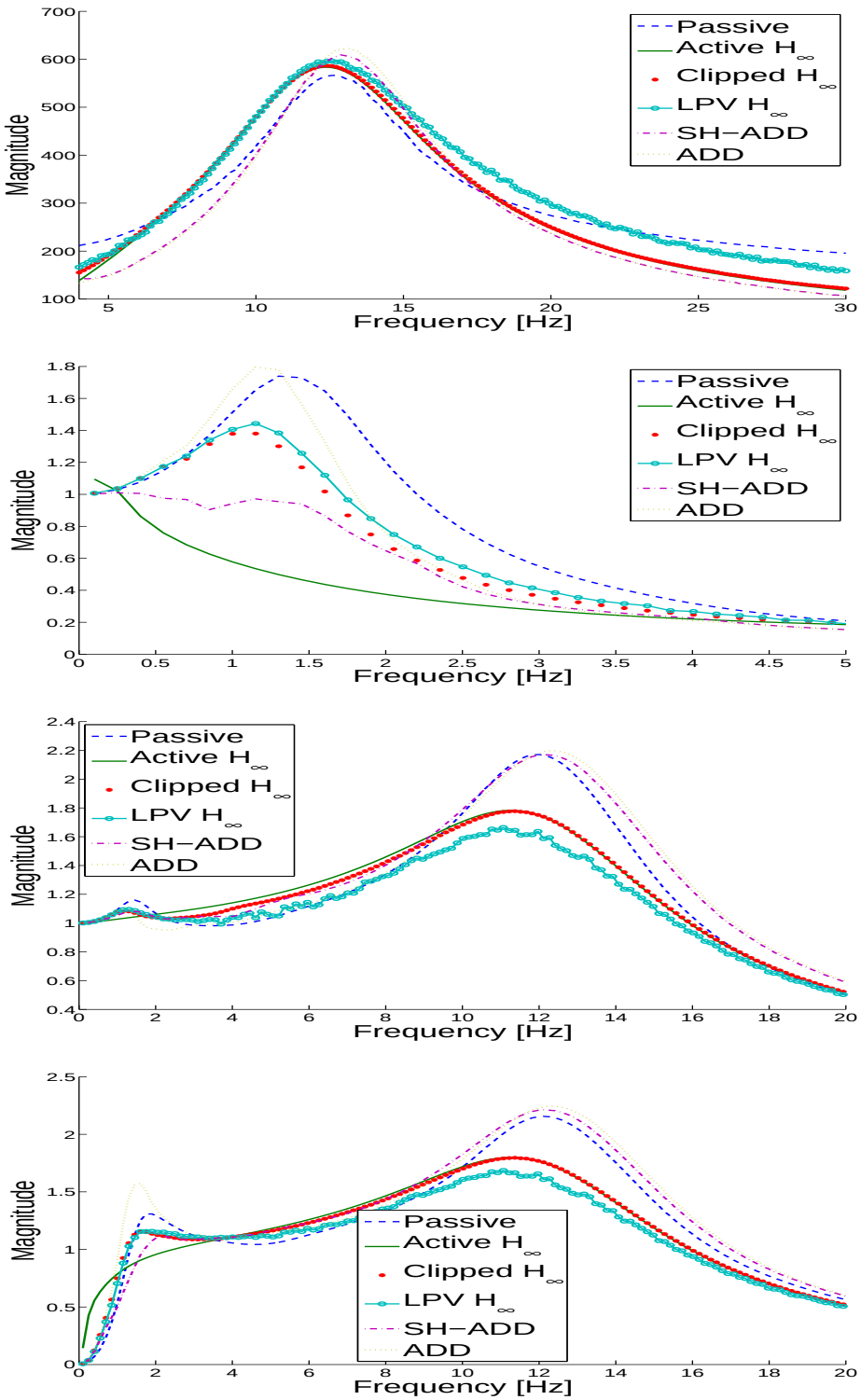

Figure 6.16: Frequency response of the different semi-active control laws of $\ddot{z}_s/z_r$, z_s/z_r, z_{us}/z_r and z_{def}/z_r (linear frequency space and zoom on the frequency space of interest).

Chapter 7

Global chassis control

7.1 Introduction

Chapter 6 was only devoted to suspension systems, were the involved control strategies where "locally" set and validated (e.g. on vertical quarter or half models). It presents some of this work contributions in the suspension field (in both the active and semi-active domain).

This chapter is concerned with the Global Chassis Control (GCC) design. As said in Chapter 2, this problem is crucial in automotive industry and covers many complex theoretical problems (see e.g. Shibahata, 2004; Andreasson and Bunte, 2006; Falcone *et al.*, 2007*c*; Chou and d'Andréa Novel, 2005; Gáspár *et al.*, 2008*b*). According to the author and to papers found in the literature (see e.g. Gáspár *et al.*, 2008*b*), there exist two main different ways to deal with the GCC problem:

- The first one consists in considering the vehicle as a global MIMO system and in designing a controller that solves all the dynamical problems by directly controlling the different actuators with the available measurements. Thus, no local controller (or inner loop) is considered and the proposed controller should solve all the problems by itself (note that this problem is illustrated in the second example, given in Section 7.3). See also (Lu and DePoyster, 2002; Chou and d'Andréa Novel, 2005; Gáspár *et al.*, 2008*b*; Falcone *et al.*, 2007*c*).

- The second solution consists in designing a controller which aims at providing somehow, the reference signals to local controllers, which have been previously designed to solve a local subsystem problem (e.g. ABS). Thus, this controller, more than a controller, monitors the local controllers. Therefore, such a controller solves the global vehicle dynamical problems, playing the role of "super controller". Note that this problem is illustrated in the third example, given in Section 7.4. See also (Falcone *et al.*, 2007*a*).

Consequently, in this chapter, three different GCC structures are introduced, representing the main contributions of this work in the GCC field. Each of these approaches have a specific structure and role, as described thereafter:

1. The first GCC design is based on the latest results obtained by Zin *et al.* (2008*a*). It consists in designing a local suspension controller (in our case, a simple Skyhook control law) and an "anticipation strategy" that modifies the anti-roll repartition. This control structure provides a two stage global controller that, through the four suspensions control, can improve the vehicle attitude and modify the handling performances with a single tuning parameter. This contribution has been:

- Presented at the *4th IFAC Symposium on Mechatronics systems* held in Heidelberg, Germany (see Poussot-Vassal *et al.*, 2006*b*) (concerning the Skyhook parametrization and analysis).
- Accepted for publication in the *International Journal of Vehicle Autonomous Systems: Special Issue on Modeling and Simulation of Complex Mechatronics Systems* (see Poussot-Vassal *et al.*, 2009).

2. The second GCC design involves the four suspensions and the rear braking subsystems. The control strategy is designed in the LPV framework using the $\mathcal{H}_\infty$ control performance. In this formulation, the originality stands for the scheduling parameter that is used to achieve the ABS functionality (i.e. to avoid slipping) and to make vary the performances of the suspension system (as done previously done to handle rollover in (Gáspár *et al.*, 2007)). Moreover, the suspensions and the braking control units are designed in a unified way and work together to improve either comfort (in normal cruise situation) or safety (in emergency braking situations), according to a single monitoring parameter. This contribution has been:
   - Presented at the *17th IFAC World Congress (WC)* held in Seoul, South Korea (see Poussot-Vassal *et al.*, 2008*c*), selected for publication to the special issue of Control Engineering Practice (CEP): "World Congress Application Paper Prize Papers".
   - Submitted to *IEEE Transaction on Control System Technology* (see Poussot-Vassal *et al.*, 2008*e*).
3. The third GCC controller involves the braking and the steering subsystems. This controller focuses on vehicle stability improvement in dangerous situations. Thus, it can be viewed as a new kind of ESC. In this approach, the LPV/$\mathcal{H}_\infty$ controller is a "super controller" that generates a stabilizing reference moment to be achieved by the rear braking system and, if necessary, by the steering system intervention (e.g. in case of actuator failure, high moment requirement, etc.). The interest of this control structure is that it can be integrated to vehicles where local controllers are already implemented. In this strategy, the designed controller provides reference signals to a local braking sliding-mode based controller, recently developed by Tanelli *et al.* (2007*a*) and discussed in (Poussot-Vassal, 2007), and to the steering system. This contribution has been:
   - Accepted to *IEEE Conference on Decision and Control (CDC)*, held in Cancun, Mexico (see Poussot-Vassal *et al.*, 2008*b*).

The chapter is structured as follows: in Section 7.2 the suspension based GCC is described. Section 7.3 describes the design and results of the GCC based on suspension and braking actuators. Finally, the GCC control using braking and steering actuators is described in Section 7.4. All these strategies are validated on the full vehicle model presented in Section 5.4.

7.2 Suspension based GCC

7.2.1 General idea & Objective

The main objective is to control the four semi-active suspensions in order to improve vehicle comfort and handling. The main contribution is to propose a simple methodology to design a global vehicle attitude controller via a two stage strategy:

- A local suspension design (Skyhook controller), tuned following a frequency based industrial criterion.
- A global attitude strategy which provides an anti-roll distribution, improving both vehicle attitude and handling requirements.

The interest of this approach is that it consists in a very simple control structure where a single parameter can modify the vehicle handling in an efficient way. The simplicity of the proposed strategy represents a tractable solution for implementation issues on a real-time embedded system.

7.2.2 Global control overview

Here, the two stage attitude control strategy is introduced. This strategy consists of a local controller (for each of the four controlled damper) derived in order to improve comfort, and in a global strategy, derived to limit vehicle roll and pitch movements to modify handling. The global control design structure is given in Figure 7.1.

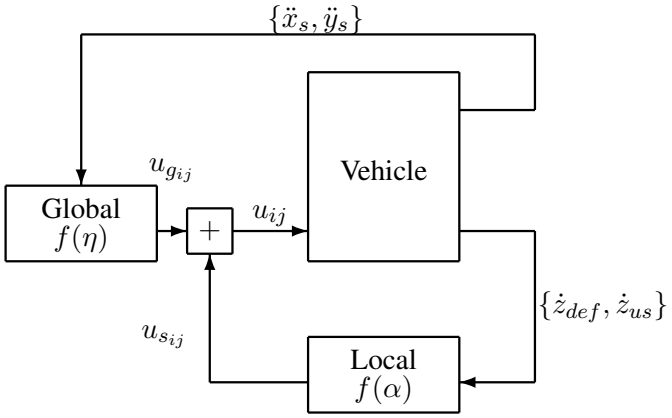

Figure 7.1: Global control structure.

It shows the two stage strategy which controls the four suspensions. Each blocks are detailed thereafter:

- **Vehicle**: is the full nonlinear vehicle model as described in Section 5.4.
- **Local control** ($f(\alpha)$): is a Skyhook control of synthesized for each suspension to improve the vertical behavior. It uses $\dot{z}_{def}$ and $\dot{z}_{us}$ as input signals, and provides u_s.
- **Global control** ($f(\eta)$): as the Anti-roll distribution, set to improve attitude and handling of the vehicle. It uses $\ddot{x}_s$ and $\ddot{y}_s$ as input signals, and provides u_g.

The general control law, that feeds the controlled suspensions, is simply given by $u_{ij} = u_{s_{ij}} + u_{g_{ij}}$. Each block is described in the following subsections. Where $i = \{f, r\}$ and $j = \{l, r\}$.

7.2.3 Local control: Skyhook suspension control ($f(\alpha)$)

The Skyhook control principle (Karnopp *et al.*, 1974; Sammier *et al.*, 2003) is recalled in Figure 7.2. The aim is to isolate the sprung mass from road irregularities by virtually linking this mass to the

sky. The idea of such a two degree of freedom control is to use c_{sky} to adjust the damping coefficient, and α to give a distribution of the damping between the "sky" and the wheel. For $\alpha = 0$, the damper force u_s is independent from the vertical velocity of the axle. It implies oscillations of z_{us}. Using c_{sky}, the damping of the vertical motion of the chassis can be controlled and the choice of α allows to fix the damping of the vertical motion of the axle. As the ideal Skyhook behavior is not reachable for a real controllable damper, it is approximated by equation (7.1),

$$u_s = c_{sky}\dot{z}_{def} + c_{sky}(1-\alpha)\dot{z}_{us} \tag{7.1}$$

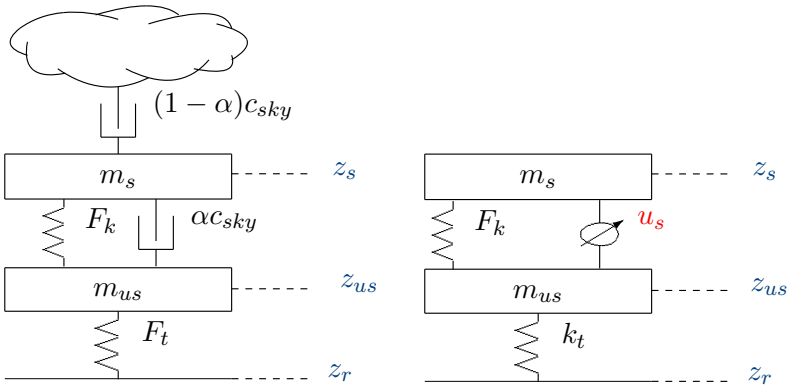

Figure 7.2: Ideal Skyhook principle (left) and Controlled damper (right).

Remark: Skyhook approximation. The control strategy (7.1) is built in order to approach the Skyhook principle from the sprung mass point of view (Sammier, 2001).

Due to the simple two degree of freedom structure, the Skyhook control is simple to implement, which makes it widely used in the industry. Nevertheless, the best way to tune parameters α and c_{sky} is not straightforward (even if it may be done intuitively). In Poussot-Vassal *et al.* (2006*b*), a criterion is proposed to complete this step. It consists in introducing the criterion $J_k(\Upsilon)$, which is a linear weighted combination of criteria given in Section 5.5, defined as:

$$\begin{aligned} J_k(\Upsilon) &= k_c \frac{PSD_{4\to 30}(\ddot{z}_s)}{\max PSD_{4\to 30}(\ddot{z}_s)} + k_c \frac{PSD_{0\to 5}(z_s)}{\max PSD_{0\to 5}(z_s)} \\ &+ k_d \frac{PSD_{0\to 20}(z_{us})}{\max PSD_{0\to 20}(z_{us})} + k_d \frac{PSD_{0\to 20}(z_{def})}{\max PSD_{0\to 20}(z_{def})} \end{aligned}$$

where $\Upsilon \in \mathcal{S}$ is the bounded set of degree of freedom (or parameters) of the considered control law. $k = \{k_c, k_d\}$ with k_c (resp. k_d) the weight related to comfort (resp. road-holding) objectives. Thus, the problem is to find:

$$\Upsilon^* \in \mathcal{S} | \forall \Upsilon \in \mathcal{S}, J_k(\Upsilon^*) \leq J_k(\Upsilon) \tag{7.2}$$

To derive the optimal strategy, one aims at minimizing $J_k(\Upsilon)$ for a given $k = \{k_c, k_d\}$ couple, where the parameter set $\Upsilon \in \mathcal{S} := \{c_{sky} \in [0, 5000], \alpha \in [0, 1]\}$.

Remark: About $\mathcal{S}$. Note that we have chosen $\mathcal{S} := \{c_{sky} \in [0, 5000], \alpha \in [0, 1]\}$ since the considered suspension degree of freedom of the Skyhook control law parameters are defined as $0 \leq \alpha \leq 1$ and $0 \leq c_{sky} \leq 5000$ (c_{sky} is bounded by the considered damper). However, this methodology could be applied with another control law where other tuning parameters may be be optimized (see e.g. Poussot-Vassal *et al.*, 2008*a*) where an $\mathcal{H}_\infty$ controller is tuned using this criteria and where the degrees of freedom are the gains on sensitivity functions.

Figure 7.3 gives the criteria evaluation for $k = \{1, 10\}$ (which focuses on road-holding) and $k = \{10, 1\}$ (which focuses on comfort), evaluated on the vertical quarter car model for the whole parameter set. Moreover, on Figure 7.27, the corresponding Bode diagrams are given and confirm the criteria based optimal values.

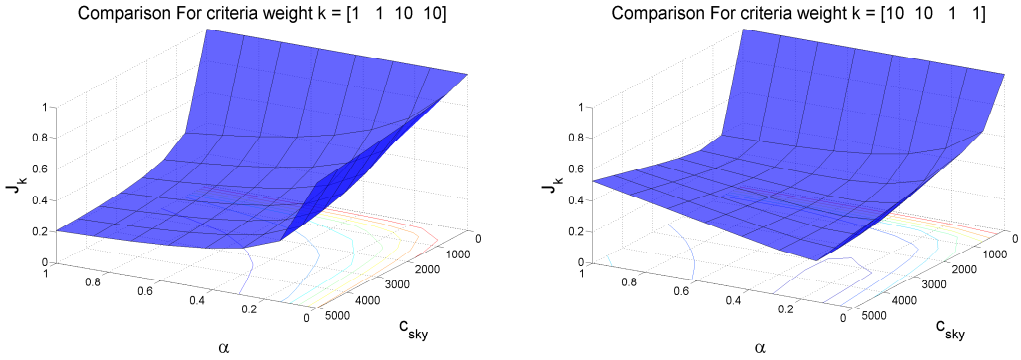

Figure 7.3: $J_{k=\{1,10\}}$ (road-holding, left) and $J_{k=\{10,1\}}$ (comfort, right) criterion as a function of α and c_{sky}.

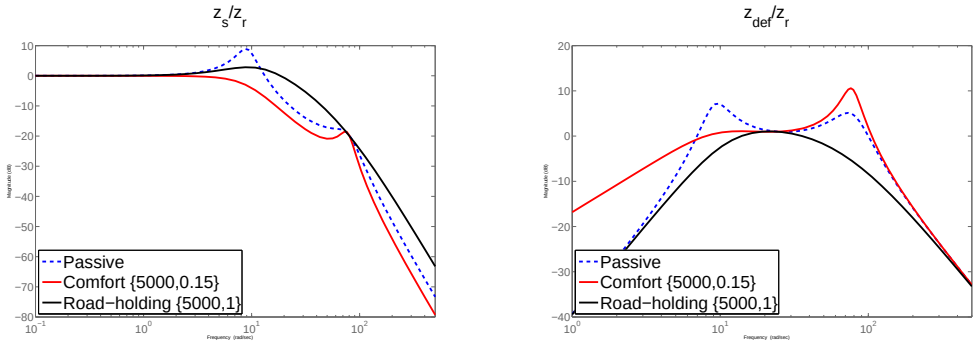

Figure 7.4: Bode diagrams for $\Upsilon^*_{rh} = \{5000, 1\}$ (road-holding) and $\Upsilon^*_c = \{5000, 0.15\}$ (comfort). Left: chassis displacement; right: suspension deflection

The minimum for the road-holding (rh) and comfort (c) configurations are reached for:

$$\begin{array}{rcl} \Upsilon^*_{rh} & = & \{c_{opt}, \alpha_{opt}\} = \{5000, 1\} \\ \Upsilon^*_{c} & = & \{c_{opt}, \alpha_{opt}\} = \{5000, 0.15\} \end{array} \tag{7.3}$$

Note that these results are consistent with the Skyhook control design. Indeed, the α parameter gives the damping distribution, and when equals 1, the sprung mass is no more linked to the sky,

hence the controlled suspension is fully passive. This remark confirms the fact that Skyhook is only interesting for comfort improvements.

As expected, according to the chosen weights $k = \{k_c, k_d\}$, the criterion provides different couples of $\Upsilon^* = \{c^*_{sky}, \alpha^*\}$. The question that raises from this fact is: what is the $k = \{k_c, k_d\}$ couple that globally minimizes the $J_k(\Upsilon)$ criteria? To answer this question, one can:

1. Evaluate the optimal $\Upsilon^* = \{c^*_{sky}, \alpha^*\}$ for varying k couples.
2. Plot $J_k(\Upsilon^*)$ for the different k couples.

Figure 7.5 shows the results for $k_c \in [0, 10]$ and $k_d \in [0, 10]$.

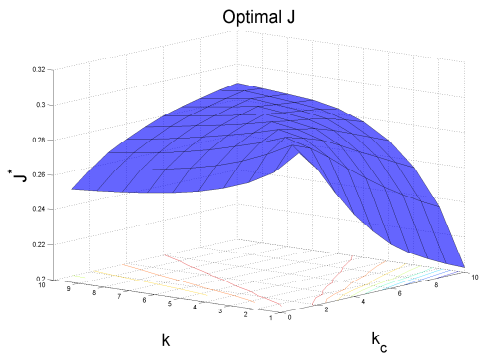

Figure 7.5: Optimal $J_k(\Upsilon^*)$ as a function of the weighting functions $\{k_c, k_d\}$.

Because of the structure of the Skyhook control law (comfort oriented), the best solution (i.e. $J_k(\Upsilon^*)^*$) is obtained for a $k = \{k_c, k_d\}$ tuned to improve comfort, (i.e. $k = \{0, 10\}$). Moreover, the optimal configuration is always achieved with the maximum c_{sky}, therefore, the performance only varies according to the α parameter. As this α parameter influences the behavior of the controlled suspension, it may be used to influence the achieved performances to either enhance handling or vehicle comfort.

7.2.4 Global control: Anti-roll distribution ($f(\eta)$)

In the previous subsection, a strategy and a methodology to choose the parameter values to control individual suspensions based on the quarter car model are developed. Such a kind of strategy is well designed to improve comfort and road-holding w.r.t. ground irregularities but lacks of efficiency when the vehicle is subject to load transfers. Therefore, the objective is to develop a global strategy that reduces the effects of load transfers due to accelerations/decelerations and vehicle steering manoeuvres, by modifying the suspension forces.

To do so, from full vehicle equations (5.21), one aims at imposing $\ddot{z}_s = \ddot{\phi} = \ddot{\theta} = 0$ to reduce attitude oscillations. By replacing the vertical forces $F_{sz_{ij}}$ by $u_{g_{ij}}$, one obtains the global control signals:

$$\begin{array}{rcl} u_{g_{fl}} + u_{g_{fr}} + u_{g_{rl}} + u_{g_{rr}} & = & 0 \\ (u_{g_{fl}} - u_{g_{fr}})t_f + (u_{g_{rl}} - u_{g_{rr}})t_r & = & -mh\ddot{x}_s \\ (u_{g_{rl}} + u_{g_{rr}})l_r - (u_{g_{fl}} + u_{g_{fr}})l_f & = & mh\ddot{y}_s \end{array} \tag{7.4}$$

The resulting equation has four unknown variables and only three equations. To obtain a unique solution, another equation related to the anti-roll bar distribution is introduced. Indeed, this repartition

(denoted as η) exists in all vehicles due to the anti-roll bars and of suspensions. It corresponds to the quantity of anti-roll moment that the front axle has to provide compared to the rear axle. It results in the following equation (Zin, 2005).

$$(1-\eta)(u_{g_{fl}} - u_{g_{fr}})t_f - \eta(u_{g_{rl}} - u_{g_{rr}})t_r \quad = \quad 0 \tag{7.5}$$

where η is the anti-roll distribution parameter. When $\eta \rightarrow 0$ (resp. $\eta \rightarrow 1$), the anti-roll is only done by the rear (resp. front) axle. In (Zin *et al.*, 2008*a*), the author explains how to choose this parameter in order to make the vehicle over/under steering. The higher (resp. lower) η is, the more the vehicle oversteers (resp. understeers).

Therefore, the global control strategy consists in adding the following control input vector to the local suspension control provided by the controller described bellow, corresponding to the solution of the set of equations (7.4)-(7.5):

$$\begin{bmatrix} u_{g_{fl}} \\ u_{g_{fr}} \\ u_{g_{rl}} \\ u_{g_{rr}} \end{bmatrix} = \begin{bmatrix} 1 & 1 & 1 & 1 \\ t_f & -t_f & t_r & -t_r \\ -l_f & -l_f & l_r & l_r \\ (1-\eta)t_f & -(1-\eta)t_f & -\eta t_r & \eta t_r \end{bmatrix}^{-1} \begin{bmatrix} 0 \\ mh\ddot{y}_s \\ -mh\ddot{x}_s \\ 0 \end{bmatrix} \tag{7.6}$$

7.2.5 Simulation results

The validation of the proposed controller structure is done on the full nonlinear vehicle model described in Section 5.4, assuming semi-active suspensions as actuators (see Section 4.2). Typical driving situations are simulated on both passive and controlled vehicle to emphasize the efficiency of the proposed approach.

7.2.5.1 Attitude analysis

First, one aims at analyzing comfort (attitude of the vehicle) and road-holding improvements. The following driving scenario is considered:

1. Vehicle runs at $120km/h$ on a straight line.

2. From $t = 0.2s$ to $t = 0.7s$, a $2cm$ bump occurs on the front wheels ($z_{r_{fj}}$).

3. From $t = 1s$ to $t = 1.5s$, a $2cm$ bump occurs on the right wheels ($z_{r_{ir}}$).

Simulations are performed with a fixed $\eta = 0.5$, that represents a neutral behavior for the anti-roll distribution (as illustrated in Zin (2005) and next subsection). Figure 7.6 compares the chassis attitude ($\ddot{z}_s$, z_s, θ, ϕ) for both comfort ($\{c_{sky} = 5000, \alpha = 0.15\}$) and road-holding ($\{c_{sky} = 5000, \alpha = 1\}$) Skyhook controllers w.r.t. the nonlinear passive reference vehicle representing the Renault Megane Coupé car.

The comfort oriented Skyhook design considerably improves both displacement and acceleration of the chassis while reducing, in a significant way, the roll and pitch angles. The road-holding Skyhook controller does not degrade too much these signals and maintains a correct road-holding. Hence, the α parameter shows to influence the comfort/road-holding compromise.

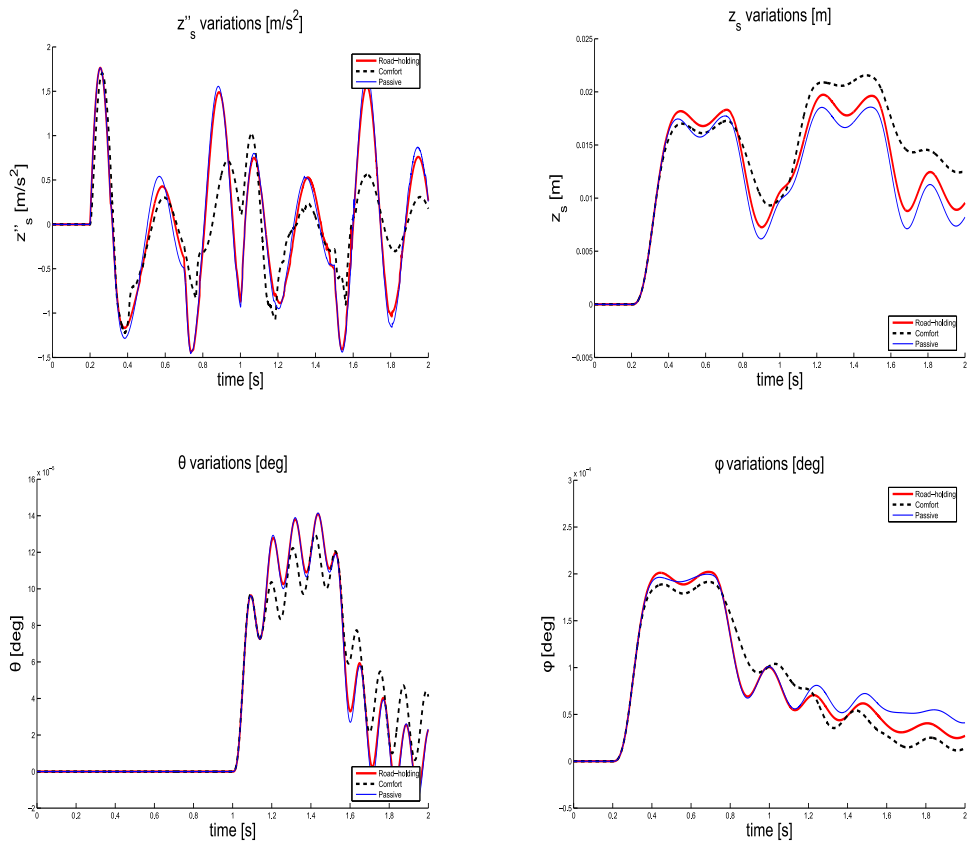

Figure 7.6: Vehicle attitude $\ddot{z}_s$, z_s, θ, ϕ (from top left to bottom right) with $\eta = 0.5$. Passive (solid thin), Comfort (thick dotted), Road-holding (thick solid)

7.2.5.2 Handling analysis

The local suspension strategy is shown to modify the vehicle attitude, emphasizing the benefit of using the anti-roll distribution strategy to improve handling. As explained before, the anti-roll strategy gives an additional degree of freedom that shows to influence vehicle handling. To analyze such a performance variation, the following two driving scenarios are proposed:
Scenario 1:

1. Vehicle runs at $120km/h$.
2. A steering manoeuver to avoid an obstacle on the road starts at $t = 0.1s$ and ends at $t = 1s$ (acting on δ).

Scenario 2:

1. Vehicle runs at $120km/h$.
2. A direction change manoeuver that starts at $t = 0.1s$ and ends at $t = 0.5s$ is performed (acting on δ).

As handling performances are to be analyzed, simulations are performed using the road-holding Skyhook controller (which is shown to improve road-holding). Figures 7.7 and 7.8 show the vehicle path and behavior (to avoid the obstacle) for the different η (Scenario 1).

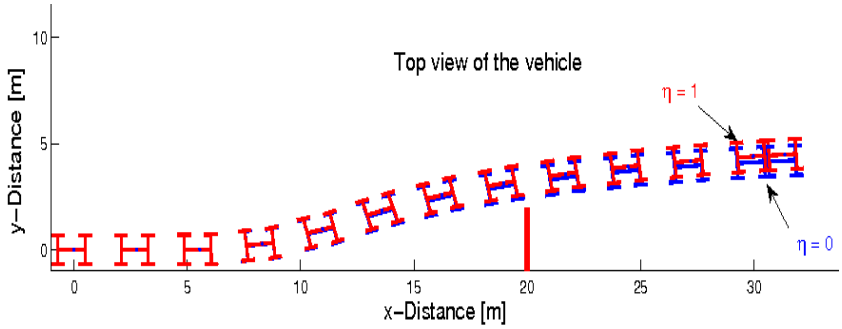

Figure 7.7: Scenario 1: Vehicle path for $\eta = 0$ (understeer) and $\eta = 1$ (oversteer), with $v = 120km/h$.

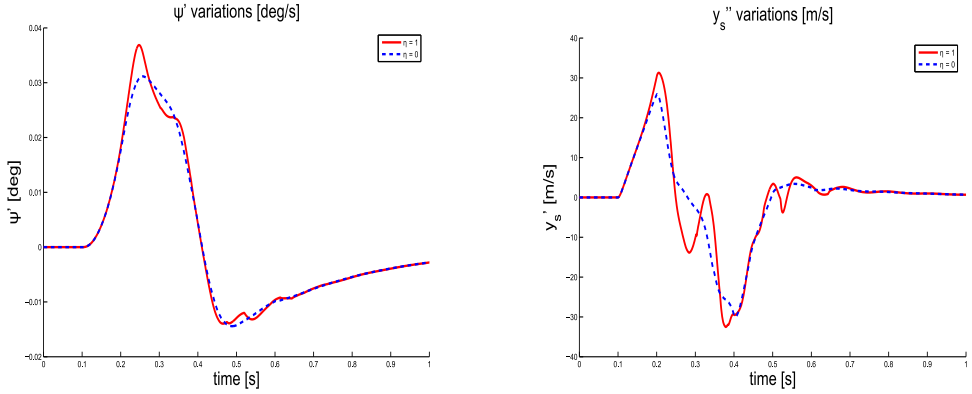

Figure 7.8: Scenario 1: vehicle yaw $\dot{\psi}$ (left) and lateral acceleration $\ddot{y}_s$ (right) for $\eta = 0$ (dotted) and $\eta = 1$ (solid), with $v = 120km/h$.

Figures 7.9 and 7.10 show the vehicle path and behavior for the different η (Scenario 2).

By comparing Figure 7.7 and 7.9, one sees that when $\eta = 1$ (resp. $\eta = 0$), the vehicle oversteers (resp. understeers). When $\eta = 1$ the yaw rate and the lateral acceleration present a higher peak, which is typical of an oversteering vehicle i.e. a vehicle more sensitive to driver manoeuvres (see Figures 7.8 and 7.10).

7.2.6 Concluding remarks

In this example, the full vehicle attitude & handling control are considered. A two-stage control strategy (local & global) is proposed to improve both comfort and handling of the vehicle using semi-active suspensions and anti-roll bar distribution. One of the main interests in this study is that

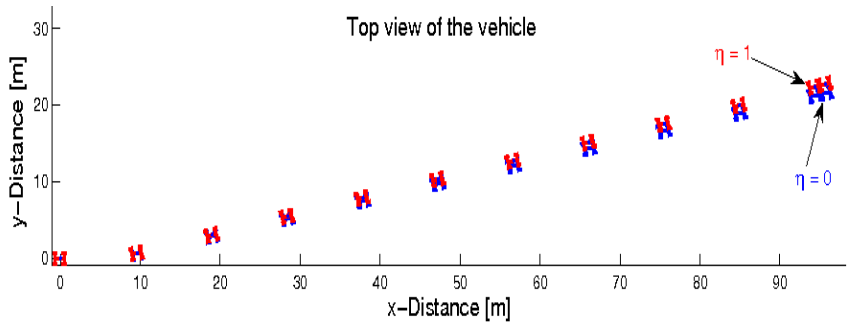

Figure 7.9: Scenario 2: Vehicle path for $\eta = 0$ (understeer) and $\eta = 1$ (oversteer), with $v = 120km/h$.

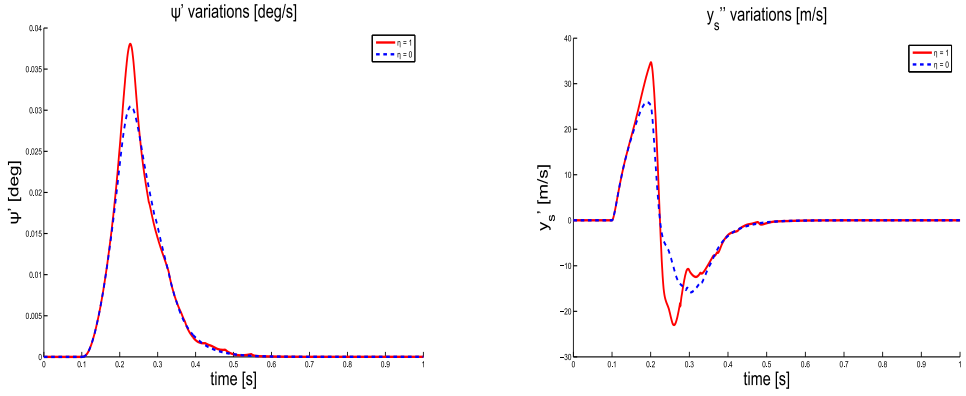

Figure 7.10: Scenario 2: vehicle yaw $\dot{\psi}$ (left) and lateral acceleration $\ddot{y}_s$ (right) for $\eta = 0$ (dotted) and $\eta = 1$ (solid), with $v = 120km/h$.

handling, together with comfort improvements can be modified thanks to a simple suspension strategy. The developed approach uses the simple Skyhook strategy tuned according to an industrial criterion and an anti-roll distribution controller that influences the vehicle comfort and handling performances. The presented strategy gives two main degrees of freedom: α and η. Both are related to comfort and handling objectives:

- $\alpha \mapsto 1$ provides a road-holding oriented control.
- $\alpha \mapsto 0$ provides a comfort oriented control.
- $\eta \mapsto 1$ makes the vehicle oversteering.
- $\eta \mapsto 0$ makes the vehicle understeering.

Based on these remarks, a monitor based on a driving conditions, as exposed in (Ding *et al.*, 2005; Gáspár *et al.*, 2007), could be developed to schedule these parameters in order to adapt the control performances according to the driving situation.

Extensions of this work may concern the analysis and the development of strategies to adapt online the η and α parameters to achieve varying performances according to the driving situations. This analysis illustrates the interest in making the actuators collaborate to solve different vehicle dynamical problems.

7.3 GCC involving Suspension and Braking subsystems

7.3.1 General idea

In this section, the proposed controller is based on the LPV/$\mathcal{H}_\infty$ control design. It involves active suspensions and rear brakes to guarantee comfort in normal cruise situations and to improve vehicle stability when emergency situations are detected through a monitor (e.g. undesirable yaw rate). This contribution extends the one achieved by Gáspár *et al.* (2007), which focuses on rollover prevention. The developed strategy aims at simplifying engineer design, reducing development time in making actuators cooperate, ensuring robustness properties with respect to model uncertainties, and internal stability. The controller is built to handle the strong nonlinearities of the tire braking forces, reproducing in an original way the ABS principle.

7.3.2 General LPV control structure

The main idea is to synthesize two coupled controllers:

- The first is an active suspension one (based on the full vehicle vertical model), that focuses on the vehicle attitude behavior in normal driving situations and improves road holding and handling in emergency or critical ones.
- The second is a rear braking system controller (based on the lateral-longitudinal model) that is activated in emergency situations to prevent critical yaw rate and large lateral acceleration situations (in case of loss of manoeuvrability).
- These controllers collaborate thanks to the use of a monitor that identifies the driving situation (normal, dangerous, critical)..

As both controllers performance objectives might vary, according to the driving situations (normal, emergency, critical) detected by a monitor, these controllers are designed using LPV methods. On Figure 7.11, the whole structure of the control strategy is sketched,

where v denotes the vehicle speed, R_b (resp. R_s) is the scheduling parameter associated to C_{brake}, the braking (resp. C_{susp}, the suspension) controller. $T_{b_{rj}}$ is the rear braking torque, u_{ij} the four active suspension force input. The yaw rate is denoted as $\dot{\psi}$, the rear slip ratio is given by λ_{rj} and $z_{def_{ij}}$ is the suspension deflections. Each block is described thereafter.

7.3.3 Monitor

The aim of the monitor is to give an image of the driving situation and to tune the brake and suspension control objectives to overcome conflicting effects and to avoid wheel slipping. On real vehicles, such a block may be much more complex, but since here, we focus on attitude improvement and yaw stability, we will only consider the following strategy, based on the measurement of the longitudinal slip ratio of the rear wheels (i.e. λ_{rj}). As introduced on Figure 7.11, two monitor variables are computed:

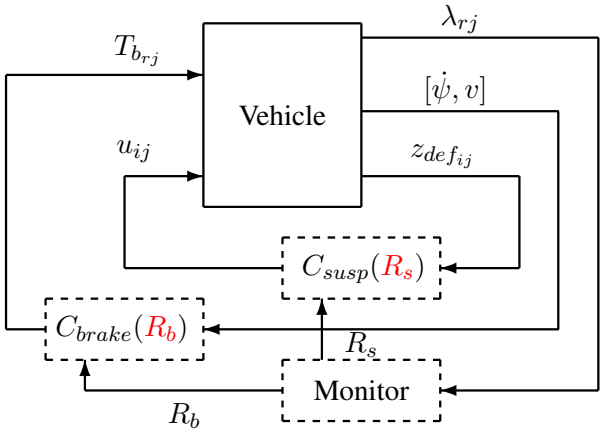

Figure 7.11: General vehicle control structure.

1. **Braking monitor** R_b, defined as:

$$R_b = \min_{j=\{l,r\}} (r_{b_j}) \tag{7.7}$$

which is a function of the absolute value of the slip ratio ($|\lambda_{rj}|$). r_{b_j} is defined as a relay (hysteresis like) function: $\rightarrow 0$ when 'on', $\rightarrow 1$ when 'off'. Switch 'on' (resp. 'off') threshold equal to λ^+ (resp λ^-) (see Figure 7.12).

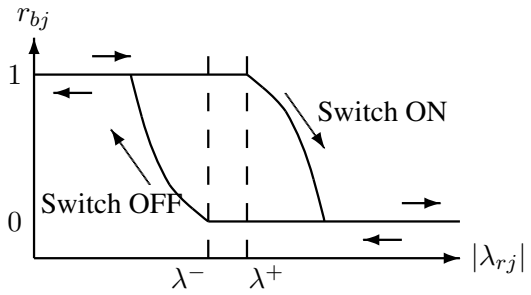

Figure 7.12: r_{bj} as a function of the rear slip $|\lambda_{rj}|$.

When slipping is low, the vehicle is in normal situation, hence $R_b \rightarrow 1$. When the slip ratio increases and became greater than λ^+, a critical situation is detected, thus $R_b \rightarrow 0$. As R_b is function of the slip ratio, the choice of λ^+ (resp. λ^-) is done according to the longitudinal tire friction curve recalled on Figure 7.13. Here, we have chosen $\lambda^+ = 9\%$ and $\lambda^- = 8\%$, in order to select a lower bound of the linear and peak tire friction force with the unstable part of the tire. The braking controller is then tuned according to the R_b parameter. This controller is presented in Section 7.3.4.1.

Note that we chose R_b as the minimum between r_{b_l} and r_{b_r} since we consider that if one wheel is slipping, the situation is dangerous (or critical).

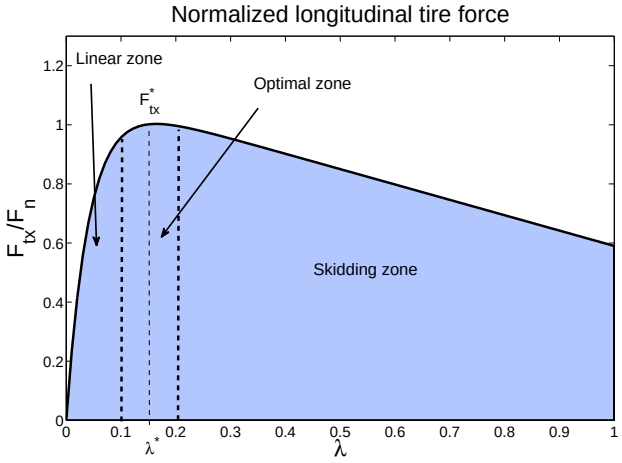

Figure 7.13: Recall of the different braking zones.

2. **Suspension monitor** R_s, defined as follows (see also Figure 7.14):

$$R_s \begin{cases} \rightarrow 1 & \text{when } 1 > R_b > R^2_{crit} \\ = \dfrac{R_b - R^1_{crit}}{R^2_{crit} - R^1_{crit}} & \text{when } R^1_{crit} < R_b < R^2_{crit} \\ \rightarrow 0 & \text{when } 0 < R_b < R^1_{crit} \end{cases} \tag{7.8}$$

When $R_b > R^2_{crit}(= 0.9)$, i.e. when low slip is detected ($< \lambda^-$), the vehicle is not in an emergency situation. When $R_b < R^1_{crit}(= 0.7)$, i.e. when high slip occurs ($> \lambda^+$), a critical situation is reached. Intermediate values of R_b will give intermediate diving situations. Hence, as explained in Section 7.3.4.2, suspension performances will be adjusted according to this parameter (comfort or road-holding).

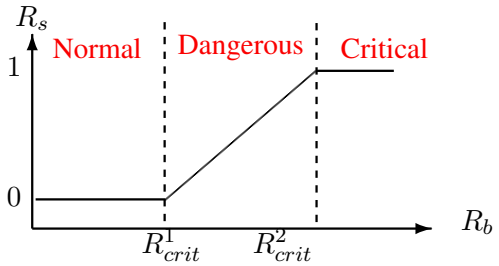

Figure 7.14: R_s as a function of R_b.

In the following, both controllers are derived thanks to the LPV/$\mathcal{H}_\infty$ methodology. These controllers are scheduled by the monitor presented below. Such a synthesis makes possible to smoothly change control performances thanks to parameters (here R_b and R_s), guaranteeing internal stability (avoiding switching) and minimizing the $\mathcal{H}_\infty$ norm (Bruzelius, 2004).

7.3.4 LPV Control design

7.3.4.1 Braking controller: $C_{brake}(R_b)$

The braking system aims at improving handling, avoiding emergency situations such as yaw rate error and large lateral accelerations. But one of the main problems in braking control is to provide an optimal force with respect to the nonlinear tire characteristics. For this purpose, many works concerning tire and brake control have been done in the last decade. Here, this problem is tackled in an original way using the LPV/$\mathcal{H}_\infty$ design methodology where the varying parameter is the brake monitor, which is a new contribution. R_b aims at ensuring that the required braking force remains in the linear stable zone of the tire characteristic and close to the maximal braking force. However, as we aim at attenuating the yaw rate error, caused by lateral forces and yaw moment disturbances that may lead the vehicle to instability, one introduces the following weighting functions and generalized plant, based on the longitudinal lateral model (Figure 7.15):

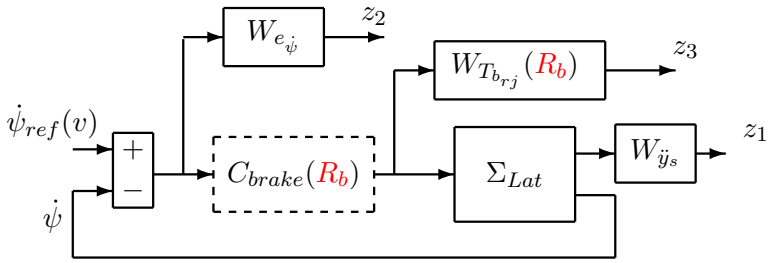

Figure 7.15: Braking system generalized plant.

- $W_{e_{\dot\psi}} = 10^{-2}\frac{s+1000}{s+1}$, defines the sensitivity function with respect to the yaw rate error (reference $\dot\psi_{ref}(v)$ being provided by a nonlinear undisturbed bicycle model, equation (5.15)).
- $W_{\ddot y_s} = 10^{-2}\frac{\frac{s}{2000}+1}{\frac{s}{20}+1}$, is devoted to lateral acceleration attenuation.
- $W_{T_{b_{rj}}}(R_b) = 3R_b10^{-4}$, is a parameter dependent weight acting on the controller output gain.

When $R_b \to 1$, which corresponds to a low slip ratio, the control signal gain would be high. Conversely, when the slip ratio is higher and enters the unstable tire zone, $R_b \to 0$, then the control signal will be attenuated. This mechanism will lead to bring back the slip ratio to lower values. As the R_b parameter is varying in an hysteresis way, the slip ratio will be "trapped" between λ^- and λ^+ when high torque is required, which guarantees a good braking torque and avoids slipping, reproducing the ABS working principle in an original way, as illustrated in the simulations results.

Remark: Double importance of the R_b parameter. More than a monitor on the slip ratio, which is an image of the vehicle state, it should be noted that, as long as the controller design is done on a linear model, in case of high braking control, the force required may exceed the achievable one, given by the tire characteristic, and may lock the wheel, which is dangerous for the passengers and the tire system. Hence, the R_b monitoring step is essential to obtain good braking performances.

7.3.4.2 Suspension controller: $C_{susp}(R_s)$

Attitude control is mainly ensured through the suspension system. The applied suspension control law is given by:

$$u_{ij} = c_0(1 - R_s) + u_{ij}^{\mathcal{H}_\infty}(R_s) \tag{7.9}$$

where c_0 is the nominal damping coefficient and $u_{ij}^{\mathcal{H}_\infty}(R_s)$ is obtained by the $\mathcal{H}_\infty$ design, where some particular frequency based sensitivity functions may be considered (Sammier *et al.*, 2003).

This controller is tuned thanks to the LPV/$\mathcal{H}_\infty$ techniques using a full linear vertical model and the following generalized plant (Figure 7.16) and parameterized weighting functions:

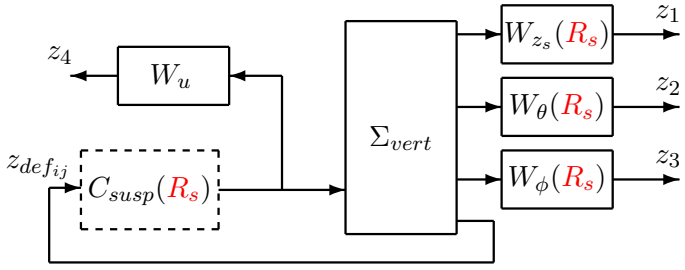

Figure 7.16: Suspension system generalized plant.

- $W_{z_s}(R_s) = \frac{2}{\frac{s}{2\pi f_1}+1}R_s$, is shaped to reduce bounce amplification of the sprung mass (z_s) between $[0, 10]Hz$ ($f_1 = 10Hz$).
- $W_\theta(R_s) = \frac{2}{\frac{s}{2\pi f_2}+1}(1 - R_s)$, attenuates the roll amplification in low frequencies ($f_2 = 8Hz$).
- $W_\phi(R_s) = \frac{2}{\frac{s}{2\pi f_3}+1}(R_s)$, reduces the pitching moment especially in low frequency ($f_3 = 8Hz$).
- $W_u = 10^{-3}$, is used to limit the control input gain.

When $R_b > R_{crit}^2$, the braking operates in the linear zone (tire stable zone), hence, suspensions are tuned to improve comfort (i.e. $R_s \to 1$). Conversely, when $R_b < R_{crit}^1$, the braking becomes critical, hence, suspensions are set to road holding (i.e. $R_s \to 0$).

Figure 7.17 gives the closed-loop Bode diagram for $R_s = \{0, 1\}$ of the roll and pitch angles in response of a moment disturbance, and compare it to the passive reference Renault Mégane Coupé model. Figure 7.18 shows the vertical behavior for $R_s = \{0, 1\}$.

When $R_s \to 1$, the suspension tends to improve comfort, focusing on vertical and pitch dynamics, while deteriorating road-holding and roll.

The roll is attenuated in emergency situations ($R_s \to 0$). The originality relies on the scheduling of the weighting functions that make the controllers function of the suspension monitor (see also Gáspár *et al.*, 2007).

7.3.5 Simulation results

Simulations are performed on the full nonlinear vehicle model given in Section 5.4, including nonlinear suspensions force and values identified on a Renault Mégane Coupé. In the sequel, the

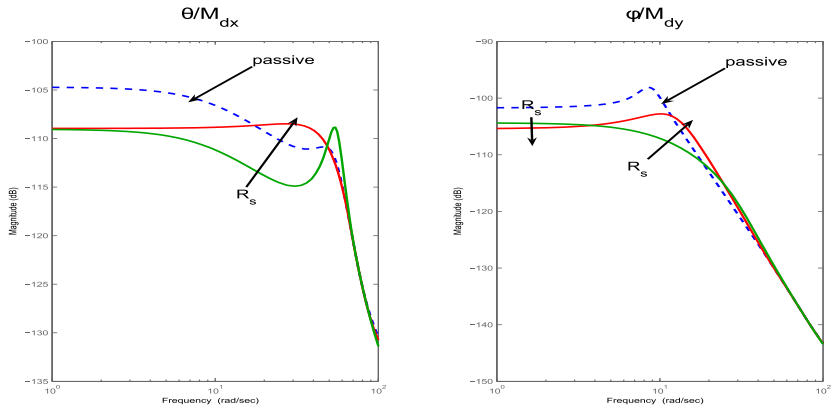

Figure 7.17: Bode diagrams of ϕ/M_{dx} (left) and θ/M_{dy} (right).

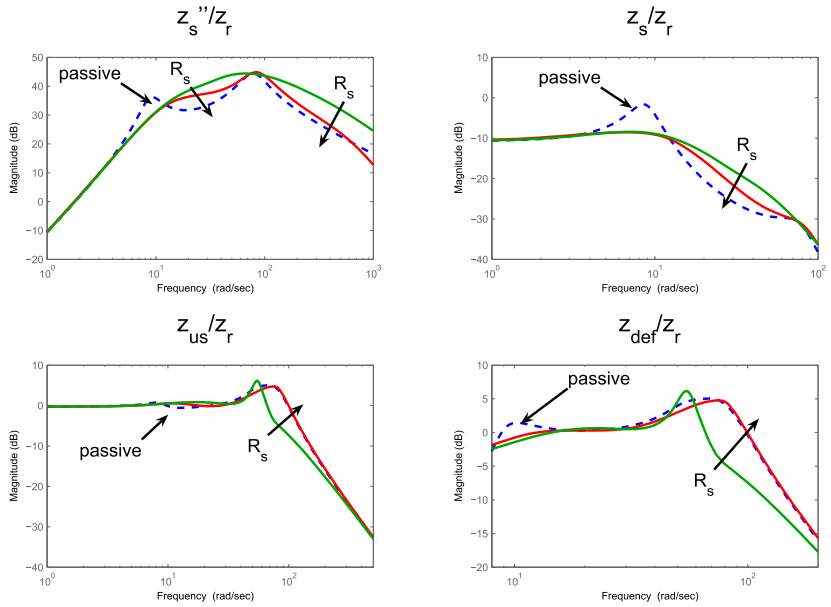

Figure 7.18: From top left to bottom right. Bode diagrams of $\ddot{z}_s/z_r$, z_s/z_r, z_{us}/z_r and z_{def}/z_r.

performances obtained by the proposed gain-scheduled controller, denoted as "LPV", are analyzed and compared to the Renault Mégane Coupé car (without control, denoted as "Reference car") and, for sake of completeness, with a simple LTI/$\mathcal{H}_\infty$ controller (without scheduled gains), denoted as "LTI".

7.3.5.1 Scenario & Monitored signals

The following scenario is used (see also Figure 7.19):

1. The vehicle runs at 130km/h in a straight line.
2. A 5cm bump occurs on the left wheels, $z_{r_{il}}$ (from $t = 0.5$s to $t = 1$s).
3. A double line change manoeuver is performed, acting on δ (from $t = 2$s to $t = 6$s).
4. A lateral wind occurs at vehicle's front, generating an undesirable yaw moment M_{dz} (from $t = 2.5$s to $t = 3$s).
5. A 5cm bump occurs on the left wheels ($z_{r_{il}}$), during the manoeuver (from $t = 3$s to $t = 3.5$s).

The corresponding input signals are given on Figure 7.19. The resulting monitored signals are are

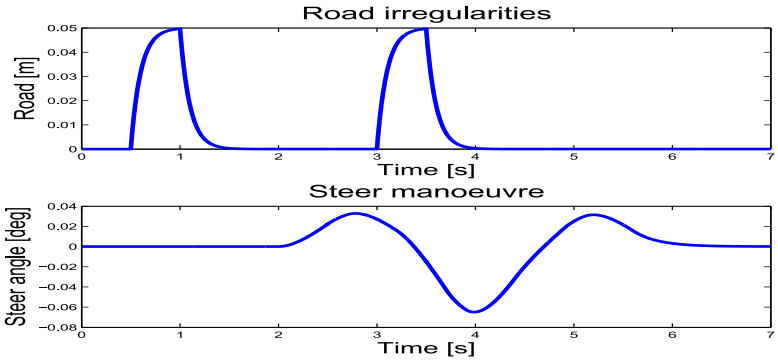

Figure 7.19: Input signals.

shown on Figure 7.20.

At time $t = 2.5$s, a positive yaw moment disturbance is generated, thus, it results in a yaw rate error, hence the rear right wheel brake is activated to overcome the loss of manoeuvrability and the suspensions, usually tuned to improve comfort ($R_s = 1$) are set to road holding mode ($R_s = 0$). As the braking force required is higher than the limit of the actuator ($1200Nm$) and will tend to lock the rear right wheel, the R_b monitor (thanks to the slip ratio measure) attenuates the control gain of the braking controller in order to reduce the torque control and brings back the slip ratio close to the linear and maximum braking forces. It results an anti-locking wheel system. As illustrated on Figure 7.21, the LPV controller avoids wheel locking and provides a braking force around the peak value while the LTI leads to locked wheel, which is very unlikely.

Thanks to the braking monitored value (R_b), that reproduces the ABS principle, the vehicle using the gain-scheduled controller provides a braking force that remains in the optimal zone and avoids slipping.

Moreover, at the end of the manoeuver, the LPV controlled system speed is 118km/h and the LTI one 120km/h; see Figure 7.22. Therefore, the braking achieved by the LPV controller shows to be more efficient than the LTI one.

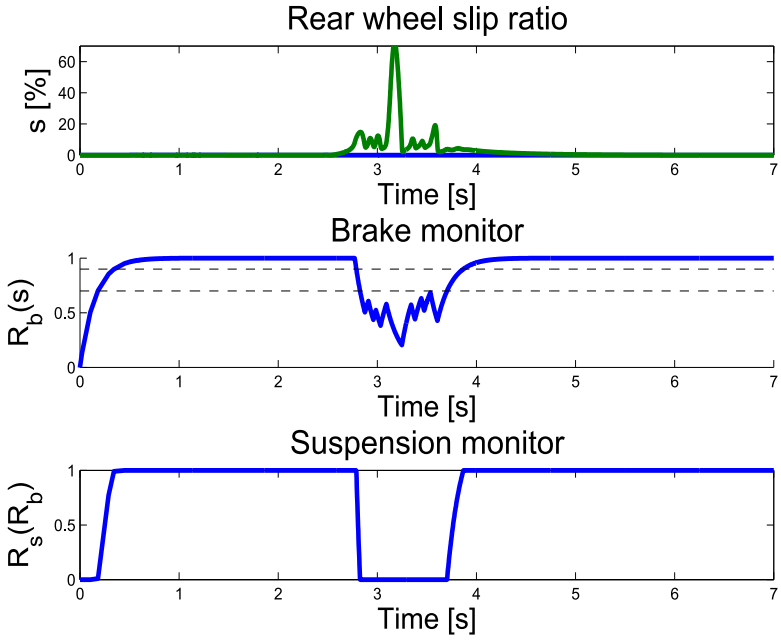

Figure 7.20: Monitored signals.

7.3.5.2 Vehicle attitude & Handling analysis

First, the vertical behavior and the vehicle attitude are illustrated on Figure 7.23.

The results obtained are consistent with the Bode diagrams plots. It is interesting to note here that at the first bump, vertical bounce and acceleration are much more improved than during the second one. Note also that while the LTI controller gives the same performances for the two bumps, the LPV one slightly degrades its comfort performances during the manoeuvre (after 2s), in order to focus on road-holding. On Figure 7.24, the handling performances are analyzed. As observed, the controlled system significantly improves the vehicle handling by attenuating the yaw moment disturbance, allowing the vehicle to limit lateral and yaw errors which may lead to a road exit. As long as the gain-scheduled controller brakes in a better way, it gives an even better result.

Thus, the proposed design shows to adapt the performance objectives according to the situation focussing on comfort in normal cruise situations and on safety when critical situations are detected (degrading comfort). Moreover, even if the braking improvements achieved by the LPV design are not so large, it still provides better results and avoid slipping, compared to the LTI approach.

7.3.6 Concluding remarks

In this section, a global chassis strategy is introduced, involving brake and suspension control systems, in order to handle the compromises between driving situations in a unified way. This work extends previous results obtained in (Gáspár *et al.*, 2007) where the rollover prevention was under consideration. Here, both yaw stability and comfort are improved using gain-scheduled robust methodology. The braking strategy, that reproduces the ABS working principle, is also designed in an original way. The author stresses such a method does not need the exact knowledge of the tire force curve

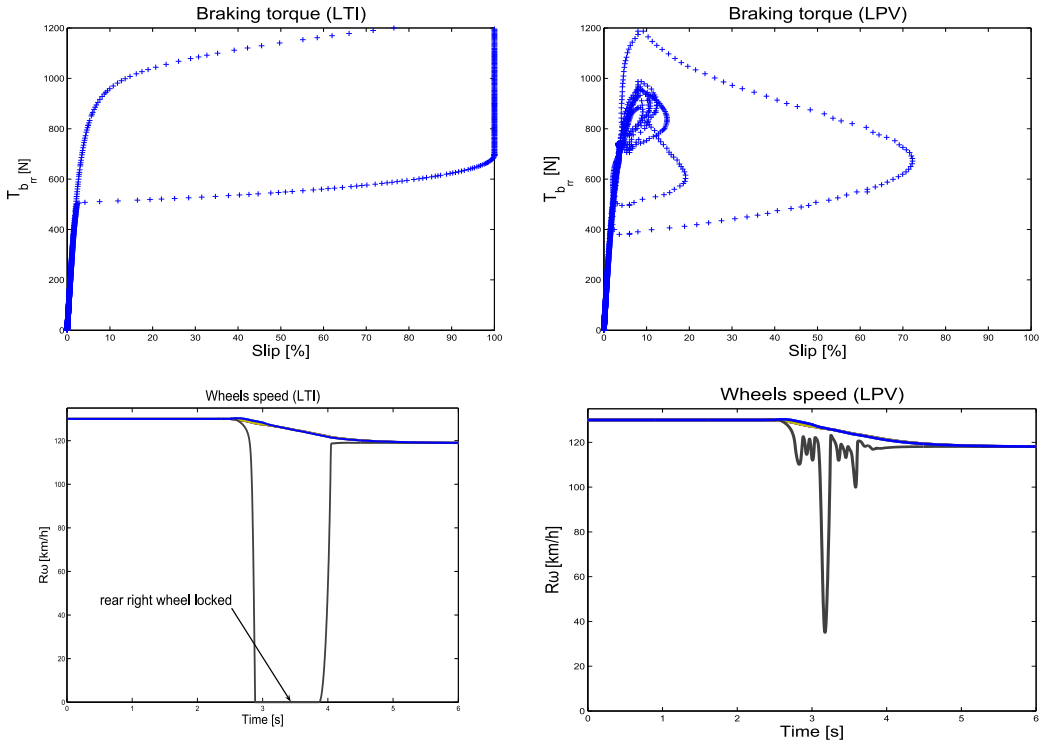

Figure 7.21: Top: Rear right brake control (function of the slip ratio). Bottom: wheels speed. Left: LTI approach, Right: LPV approach.

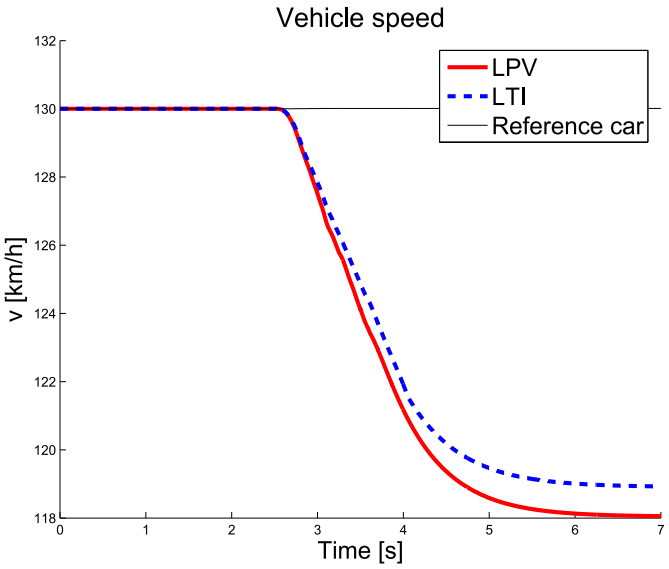

Figure 7.22: Vehicle speed.

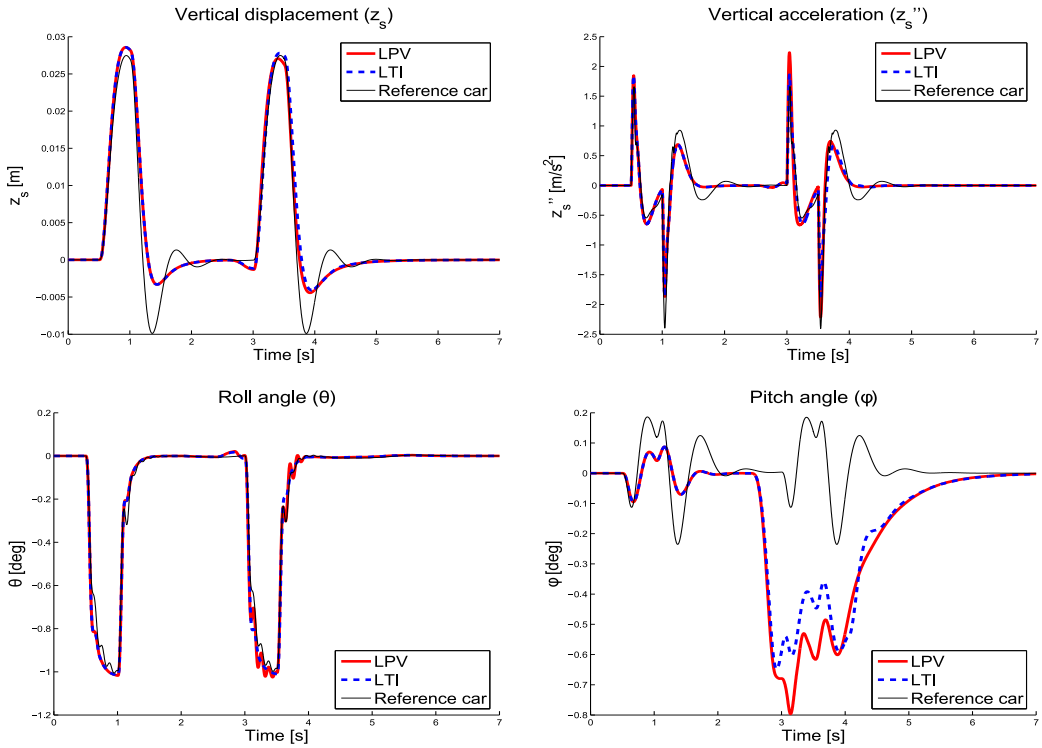

Figure 7.23: Chassis attitude (bounce and orientation).

to guarantee good performances, which is a notable advantage. A rough idea of the linear and peak value zone is enough to obtain good results. By the way, as far as this part is not the main issue, one can use the brake controller (C_{brake}) as a reference torque control for an even much more efficient braking system, as shown in (Falcone *et al.*, 2007*a*) (see also next section).

We show the efficiency of the proposed approach using complex simulations. In practice, the slip ratio is not always available, therefore further investigations should also include its estimation or the sensitivity analysis of the control approach according to this parameter.

The key point of this study is that the GCC, involving different kinds of actuators, is synthesized globally to handle critical dynamical objectives without any local actuator.

7.4 GCC involving Braking and Steering subsystems

7.4.1 General idea

In this section, a Global Chassis Controller (GCC), involving rear Electro-Mechanical Braking (EMB) and front Active Steering (AS) actuators, in order to enhance vehicle handling and safety properties in critical and dangerous driving situations (e.g. large lateral acceleration and yaw rate error) is proposed. To achieve the driving situation dependency, one aims at synthesizing a "super controller" using the Robust ($\mathcal{H}_\infty$) LPV framework where the parameter dependency can be linearly introduced in the control design. To achieve good braking and avoid slipping, the proposed GCC is associated with the Anti-locking Braking System (ABS) control mechanism recently developed by

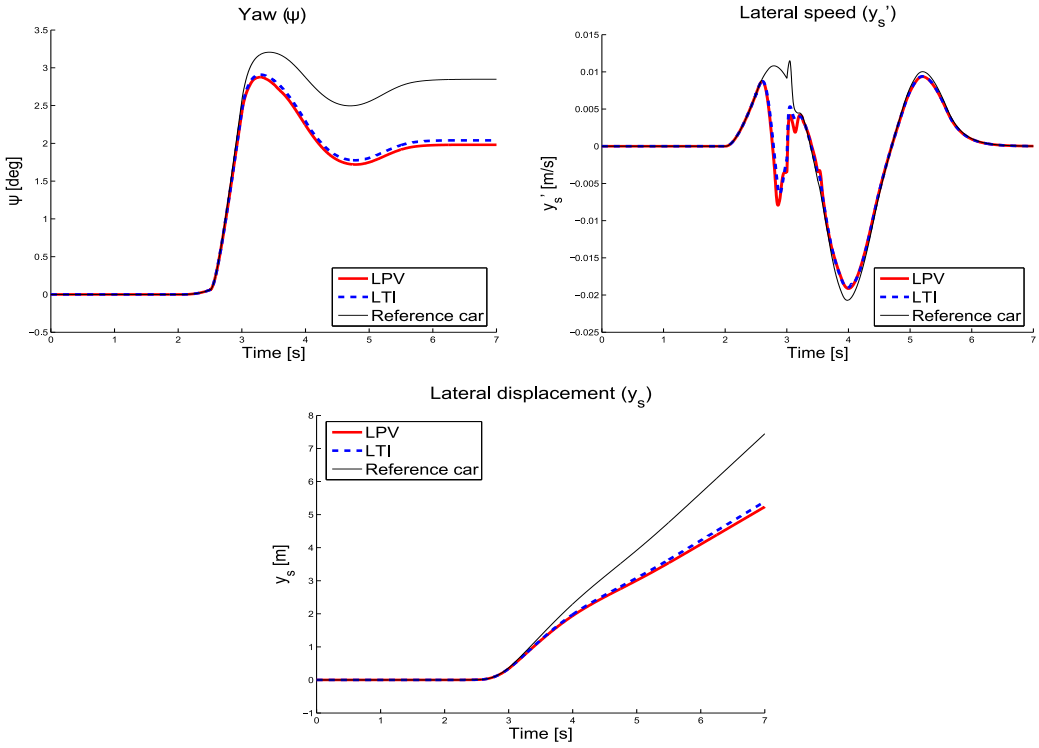

Figure 7.24: Handling performances.

Tanelli *et al.* (2007*a*), which has been shown to be robust w.r.t. the nonlinearities, poor tire measurement problems and road type. Note that in this approach, compared to the one introduced in Section 7.3, the GCC relies on local controllers to achieve local tasks and thus, plays the role of an external controller. It is then compatible with existing strategy for ABS control. Indeed, in Section 7.3, the ABS was handled by the GCC, using the R_b parameter.

The interest of the proposed GCC is that, more than a simple controller, it sets up a hierarchy to the actuators activation and intervention (in two steps):

1. Step 1: when a dangerous situation is detected, the GCC gives a torque reference to the braking system (that avoids slipping, thanks to the ABS local controller).

2. Step 2: if the braking system is not efficient enough and is not able to stabilize the vehicle (e.g. in case of low adherence or braking failure), the steering system is activated to handle the dynamical problem.

Since the solution does not require any on-line optimization, the GCC structure also shows to be easy to implement on commercial vehicles. The originality of the proposed approach, compared to already existing ones, is that the controller can be fully integrated into vehicles where local and efficient controllers already exist (e.g. ABS), and, thanks to the LPV control structure, may adapt the performance objectives according to the driving situation and the actuators efficiency.

7.4.2 Controller design

The structure and the synthesis of a multivariable Global Chassis Controller (GCC) involving steering and rear braking actuators are described thereafter.

7.4.2.1 Global chassis control structure and working principle

The objective is to improve handling and safety by using first the rear braking actuators and to activate then the front active steering system when braking is not efficient enough to achieve the required performance level. Figure 7.25 shows the proposed global control structure including the following blocks:

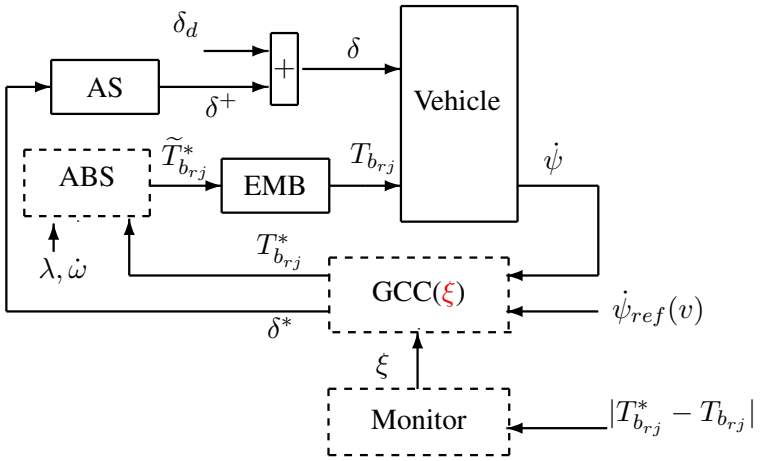

Figure 7.25: Global integrated control structure scheme.

- **Vehicle & Actuators (AS & EMB)**: are the full nonlinear vehicle and actuator models (see Chapter 4 and Section 5.4). Note that $\delta = \delta_d + \delta^+$, where δ_d is the steering angle provided by the driver and δ^+, the steering angle added by the Active Steering (AS) system actuator. $T_{b_{rj}}$ holds for the rear braking torque provided by the Electro-Mechanical Braking (EMB) system.

- **GCC(ξ)**: the proposed global chassis controller provides the desired braking torque ($T^*_{b_{rj}}$) and the additive steering angle (δ^*), scheduled by ξ, the monitoring parameter. The controller inputs are the vehicle yaw rate ($\dot{\psi}$) and the desired yaw rate ($\dot{\psi}_{ref}(v)$), provided by a nonlinear bicycle model given by equations (5.18) (see subsection 7.4.2.2).

- **ABS**: it is the local control implemented on each of the rear wheels that is activated when high slipping occurs, and that provides the braking torque $\widetilde{T}^*_{b_{rj}}$, according to the required one ($T^*_{b_{rj}}$), provided by the GCC(ξ) bloc. This strategy, based on the ABS strategy developped by Tanelli *et al.* (2007*a*), which uses as input signals the slip ratio λ, and the wheel deceleration speed $\dot{\omega}$ (see subsection 7.4.2.3).

- **Monitor**: the scheduling strategy, that supervises the GCC(ξ), is implemented in the monitor. It provides the scheduling parameter ξ, according to a rule, function of $|T^*_{b_{rj}} - T_{b_{rj}}|$, which is considered here as a braking measure efficiency (see subsection 7.4.2.4).

The so called GCC, using parameter dependent performance weighting functions, is synthesized with the polytopic LPV/$\mathcal{H}_\infty$ design, using ξ (function of the brake efficiency measure) as the scheduling variable. Each block is described in the sequel.

Remark: About the direction column. The careful reader could notice that, in this model, the direction column is not considered, thus auto-aligning moments are not modeled. Considering an extension of this results, the vehicle model should contains a direction column subsystem (e.g. as the one presented in Section 4.4) and a local active steering controller could be included to handle the auto-aligning moment disturbance. For sake of simplicity, in this study we assume that the driver provides an angle to the steering wheels, while in a more exact model, the driver provides a torque.

7.4.2.2 LPV generalized plant and LPV/$\mathcal{H}_\infty$ GCC synthesis

The idea is to synthesize a GCC that generates a stabilizing reference moment M_{dz}^*, converted into a braking torque, in order to achieve handling performances and to ensure passenger safety when dangerous situations are detected, and to provide an additive steering angle δ^* when braking is no longer efficient enough to guarantee safety.

Remark: Transformation from moment (M_{dz}^*) to braking force ($T_{b_{rj}}^*$). To convert the stabilizing moment reference (M_{dz}^*) into an effective braking torque, the following transformation is done:

$$\begin{cases} T_{b_{rl}}^* &= \dfrac{RM_{dz}^*}{t_r} \\ T_{b_{rr}}^* &= -\dfrac{RM_{dz}^*}{t_r} \end{cases} \tag{7.10}$$

Remember that the braking torque working space is bounded and given by $T_{b_{rj}} \in \mathcal{T}_b$ where:

$$\mathcal{T}_b := \{T_b \in \mathbb{R} : 0 \leq T_b \leq T_b^{max}\} \tag{7.11}$$

To generate the stabilizing moment (M_{dz}^*) and the steering angle (δ^*), a Dynamical Output Feedback LPV $\mathcal{H}_\infty$ controller is synthesized using an extended bicycle model described as follows, obtained from vehicle dynamical equation (5.21):

$$\begin{aligned} \begin{bmatrix} \dot{v}_y \\ \ddot{\psi} \\ \dot{\beta} \end{bmatrix} &= \begin{bmatrix} 0 & \frac{l_r C_{yr} - l_f C_{yf}}{mv} - v & \frac{C_{yr} - C_{yf}}{m} \\ 0 & -\frac{l_f^2 C_{yf} + l_r^2 C_{yr}}{I_z v} & \frac{l_r C_{yr} - l_f C_{yf}}{I_z} \\ 0 & -1 + \frac{l_r C_{yr} - l_f C_{yf}}{mv^2} & -\frac{C_{yf} + C_{yr}}{mv} \end{bmatrix} \begin{bmatrix} v_y \\ \dot{\psi} \\ \beta \end{bmatrix} + \begin{bmatrix} \frac{C_{yf}}{m} \\ \frac{-l_f C_{yf}}{I_z} \\ \frac{C_{yf}}{mv} \end{bmatrix} \delta^* \\ &+ \begin{bmatrix} 0 \\ \frac{1}{I_z} \\ 0 \end{bmatrix} M_{dz}^* + \begin{bmatrix} \frac{-1}{m} \\ 0 \\ \frac{1}{mv} \end{bmatrix} F_{dy} \end{aligned} \tag{7.12}$$

The generalized scheme is given on Figure 7.26, where the weighting functions are defined below:

- $W_{e_{\dot{\psi}}} = 10\frac{\frac{s}{500}+1}{\frac{s}{50}+1}$, which is used to shape the yaw rate error ($e_{\dot{\psi}} = \dot{\psi}_{ref} - \dot{\psi}$).

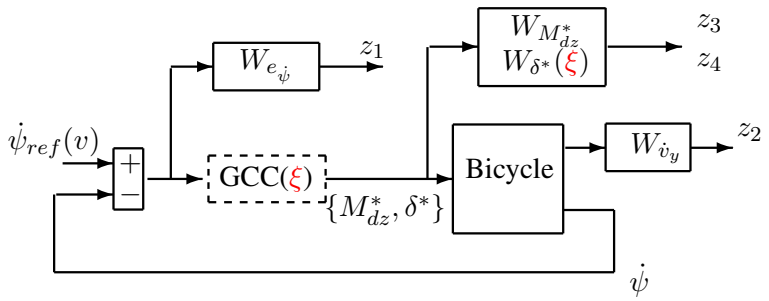

Figure 7.26: Generalized plant for synthesis.

- $W_{\dot v_y} = 10^{-3}$, used to attenuate the lateral acceleration.
- $W_{M^*_{dz}} = 10^{-5}\frac{\frac{s}{10\varpi}+1}{\frac{s}{100\varpi}+1}$, that attenuates the yaw moment control input (where $\varpi = 70$rd/s is the bandwidth of the considered braking actuator).
- $W_{\delta^*}(\xi) = \xi\frac{1}{\frac{s}{1000}+1}$, that attenuates the steering control input according to ξ, and taking into account the AS actuator bandwidth limitations.

Note that the weight on the steering actuator (namely $W_{\delta^*}(\xi)$) is linearly parameterized by the considered varying parameter $\xi(.) \in \mathcal{P}_\xi$, with $\mathcal{P}_\xi$ defined as :

$$\mathcal{P}_\xi := \{\xi \in \mathbb{R} : \underline{\xi} \leq \xi \leq \overline{\xi}\} \tag{7.13}$$

where $\underline{\xi} = 0.1$ and $\overline{\xi} = 10$. Thus, when $\xi = \overline{\xi}$, the steering input is penalized, and, on the contrary, when $\xi = \underline{\xi}$, the steering control signal is no more penalized. As a consequence, the ξ parameter activates or deactivates the steering action.

As this parameter modifies the input matrix, in order to fulfill the LPV polytopic requirements R2, one introduces the filter $\mathcal{F} = \frac{1}{\frac{s}{1000}+1}$. The generalized LPV plant is thus described as,

$$M(\xi) : \left[\begin{array}{c} \dot x \\ \hline z \\ y \end{array}\right] = \left[\begin{array}{c|cc} A(\xi) & B_1(\xi) & B_2 \\ \hline C_1(\xi) & D_{11}(\xi) & D_{12} \\ C_2 & 0 & 0 \end{array}\right] \left[\begin{array}{c} x \\ \hline w \\ u \end{array}\right] \tag{7.14}$$

where x includes the state variables of the system, of the weighing functions and of the filter, $w = F_{dy}$ and $u = [\delta^*, M^*_{dz}]$ are the exogenous and control inputs respectively; $z = [z_1, z_2, z_3, z_4] = [W_{e_{\dot\psi}} e_{\dot\psi}, W_{\dot v_y}\dot v_y, W_{M^*_{dz}} M^*_{dz}, W_{\delta^*}(\xi)\delta^*]$ holds for the controlled output, and $y = \dot\psi_{ref}(v) - \dot\psi$ is the measurement.

The LPV system (7.14) can be described as a polytopic system, i.e. a convex combination of the systems defined at each vertex formed by $\mathcal{P}_\xi$, namely $\Sigma(\underline{\xi})$ and $\Sigma(\overline{\xi})$.

Considering the LPV system (7.14), the solution defined in Chapter 3 by LMIs (3.118) provides a polytopic controller which achieves the $\mathcal{H}_\infty$ varying performances. Using YALMIP interface (Lofberg, 2004) and Sedumi solver (Sturm, 1999), one obtains $\gamma_\infty = 2.32$ and the following controller Bode diagrams (Figure 7.27).

The Bode diagrams given on Figure 7.27 show the steering and braking controller output w.r.t. to ξ. As the steering weight has been described as parameter dependent, we see that when $\xi = \overline{\xi} = 10$, the steering signal is attenuated, and, conversely, when $\xi = \underline{\xi} = 0.1$, the steering gain is larger. As a

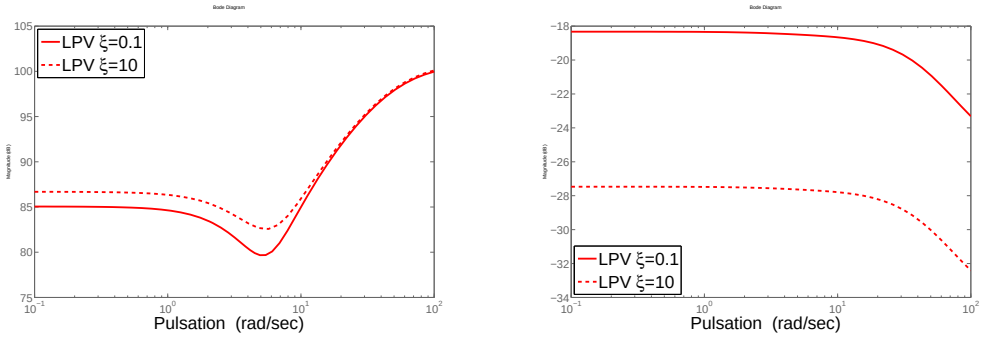

Figure 7.27: Bode diagrams of the Controller outputs M^*_{dz}/y (left) and δ^*/y (right).

consequence, when ξ is low (resp. high), steering is activated (resp. deactivated). Intermediate values will give intermediate behaviors. Finally, remember that, as long as $\xi \in \mathcal{P}_\xi$, the closed loop stability in guaranteed (thanks to the LPV design).

7.4.2.3 Local rear ABS controller

As previously introduced on Figure 7.25, a local ABS controller is used at each rear wheel in order to achieve good braking and avoid slipping (leading to loss of manoeuvrability). Since the GCC synthesis is performed assuming linear lateral tire stiffness (C_f and C_r), a local controller is essential to prevent from too high braking torques that would lead to slipping situations (note that in Section 7.3, an additional parameter, R_b, was introduced to handle the ABS). In this design, we use the ABS sliding-mode based control law given in Tanelli *et al.* (2007*a*) which exhibits good robustness properties w.r.t. actuator bandwidth, road type and measurement noise and which allows to handle the compromise between wheel deceleration low performance and poor slip estimation (see also Poussot-Vassal, 2007).

This strategy, called Mixed Slip and Deceleration (MSD) (Savaresi *et al.*, 2007), consists in regulating ε, a convex combination of the wheel slip ratio λ and of the normalized linear wheel deceleration $\eta = -\frac{\dot{\omega}R}{g}$ measurements around a user defined set point $\overline{\varepsilon}$.

$$\varepsilon = \alpha\lambda - (1-\alpha)\eta \text{ where } (\alpha \in [0,1]) \tag{7.15}$$

Then, for each rear wheel, the ABS control is given by,

$$T_{b_{ABS_{rj}}} = \begin{cases} T_b^{max} & \text{if } \widetilde{e} = \overline{\varepsilon} - \varepsilon > \Delta \\ 0 & \text{if } \widetilde{e} = \overline{\varepsilon} - \varepsilon < -\Delta \\ \dfrac{T_b^{max}}{2} & \text{if } \widetilde{e} = \overline{\varepsilon} - \varepsilon = 0 \\ \dfrac{T_b^{max}}{2}(1 + \widetilde{e}|\widetilde{e}|^{-q}\Delta^{q-1}) & \text{otherwise} \end{cases} \tag{7.16}$$

where $T_b^{max} = 1200Nm$is the maximal braking torque, $q = 0.5$ is a smoothing factor, $\Delta = 0.1$ is a dead-zone defined to avoid chattering and $\overline{\varepsilon} = 0.2$ (for more information on this control law, the reader is invited to refer to (Tanelli *et al.*, 2007*a*; Poussot-Vassal, 2007)). Note that in its original version, this control law results in a switching control. Therefore, q is a parameter which aims at

replacing the switching rule by a hyperbolic tangent like function and Δ to define a dead zone to preserve the control actuator.

To integrate this control law to the proposed GCC structure, this control law is slightly modified as:

$$\widetilde{T}^*_{b_{rj}} = \min\{T_{b_{ABS_{rj}}}, T^*_{b_{rj}}\} \tag{7.17}$$

This modification only stands because when a low torque demand is required by the GCC controller, the ABS mechanism may not be used. Therefore, the ABS is used only when the torque demand leads to skidding situations.

Remark: About the ABS activation and the steering control. Note that when the ABS is activated, it means that the required braking force is higher that the achievable one, thus, the steering system may be activated to generate the stabilizing moment. This activation is handled by the ξ parameter. In the next subsection, this principle is introduced through the notion of braking efficiency measure.

7.4.2.4 Monitor: braking efficiency measure

The aim of the monitor is to schedule the GCC control in order to activate the steering system when braking is no longer efficient enough to guarantee safety. Then, we propose the following scheduling strategy:

$$e = \max(|e_{T_{b_{rj}}}|)\,, j = \{l, r\} \tag{7.18}$$

where $e_{T_{b_{rj}}} = T^*_{b_{rj}} - T_{b_{rj}}$, and define the scheduling parameter $\xi(e)$ as:

$$\xi := \begin{cases} \overline{\xi} & \text{if } e \leq \underline{\chi} \\ \dfrac{\overline{\chi} - e}{\overline{\chi} - \underline{\chi}}\overline{\xi} + \dfrac{e - \underline{\chi}}{\overline{\chi} - \underline{\chi}}\underline{\xi} & \text{if } \underline{\chi} < e < \overline{\chi} \\ \underline{\xi} & \text{if } e \geq \overline{\chi} \end{cases} \tag{7.19}$$

where $\underline{\chi} = \frac{30}{100}T_b^{max}$ and $\overline{\chi} = \frac{70}{100}T_b^{max}$ are user defined brake efficiency measures.

Remark: About $\underline{\chi}$ and $\overline{\chi}$. These parameters are user defined. In this case, they are chosen so that the steering system is deactivated when the difference between the required braking torque and the achievable one is lower than 30% of the maximal braking torque. When this difference becomes greater than 70%, the steering system is fully activated (between 30% and 70%, the steering is linearly activated). Thus in this case, the scheduling is an evaluation of the braking efficiency. Note that other monitor strategies may be employed according to lateral acceleration or to other engineering logics (see e.g. Ding *et al.*, 2005). Thus, the scheduling strategy is an interesting field on research. Note also that, as long as the brake weight is not ξ dependent, the braking actuator remains always active. Thus only the steering actuator may be (de-)activated w.r.t. to ξ.

7.4.3 Simulation results

To validate the proposed GCC strategy, simulations on the full nonlinear model introduced in Section 5.4 have been performed. First, typical driving situations are performed, secondly, performance analyses are done using critical initial stable conditions.

7.4.3.1 Typical driving situations

Simulations are performed on two typical driving situations: for both simulations, a double line change manoeuver is performed on a wet road, with a vehicle initially running at $100km/h$.

1. Situation 1: the simulation is performed assuming a healthy actuator (Figures 7.28 and 7.29).
2. Situation 2: a faulty rear left braking system is considered (Figures 7.30 and 7.31). The rear braking torque is bounded by $50Nm$.

Double line change on wet road, $v_0 = 100km/h$ (healthy actuator). As the road is wet, road/tire adhesion is low and the lateral tire contact forces are strongly diminished. As a consequence, during the manoeuver, the uncontrolled vehicle drifts away from the desired path, as illustrated on Figure 7.28.

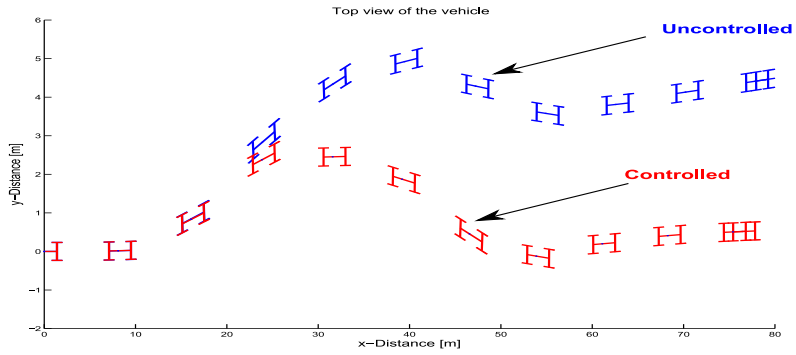

Figure 7.28: Vehicle path after a double line change manoeuver on a WET road with initial speed $v_0 = 100km/h$ without fault on the rear left actuator.

By comparing the yaw rate behaviors given in Figure 7.29-(top), it is clear that the proposed integrated control scheme enhances the vehicle stability and yaw rate tracking, compared to the non controlled one. Figure 7.29-(bottom, left) shows that the scheduling parameter (ξ) slightly varies since the braking system is efficient enough to stabilize the vehicle. Consequently, the control signal mainly involves the braking system; see Figure 7.29-(bottom, right) and the steering control input is almost not activated ($\max |\delta^+| < 0.25$ degree).

Double line change on wet road, $v_0 = 100km/h$ (Fault occurring on the braking system). Here a fault occurs on the rear left braking during the same critical driving situation. Now, the maximal braking torque that can be applied by the rear left braking actuator is bounded by $50Nm$ (the healthy maximal torque is $1200Nm$). Consequently, the vehicle path may be undesirable. To overcome this actuator failure, the steering actuator is activated and the corresponding path is given on 7.30.

As in the previous situation, the handling is clearly improved, even in presence of the faulty actuator. By comparing the yaw rate curves given on Figure 7.31-(top), one can appreciate the improvement brought by the LPV control structure. As the rear left braking system is faulty, when the vehicle would need it, from $t = 1.5s$ to $t = 2.1s$, the GCC controller is scheduled in order to activate the steering system to counteract the undesired behavior, as illustrated on Figure 7.31-(bottom, left). Especially, it

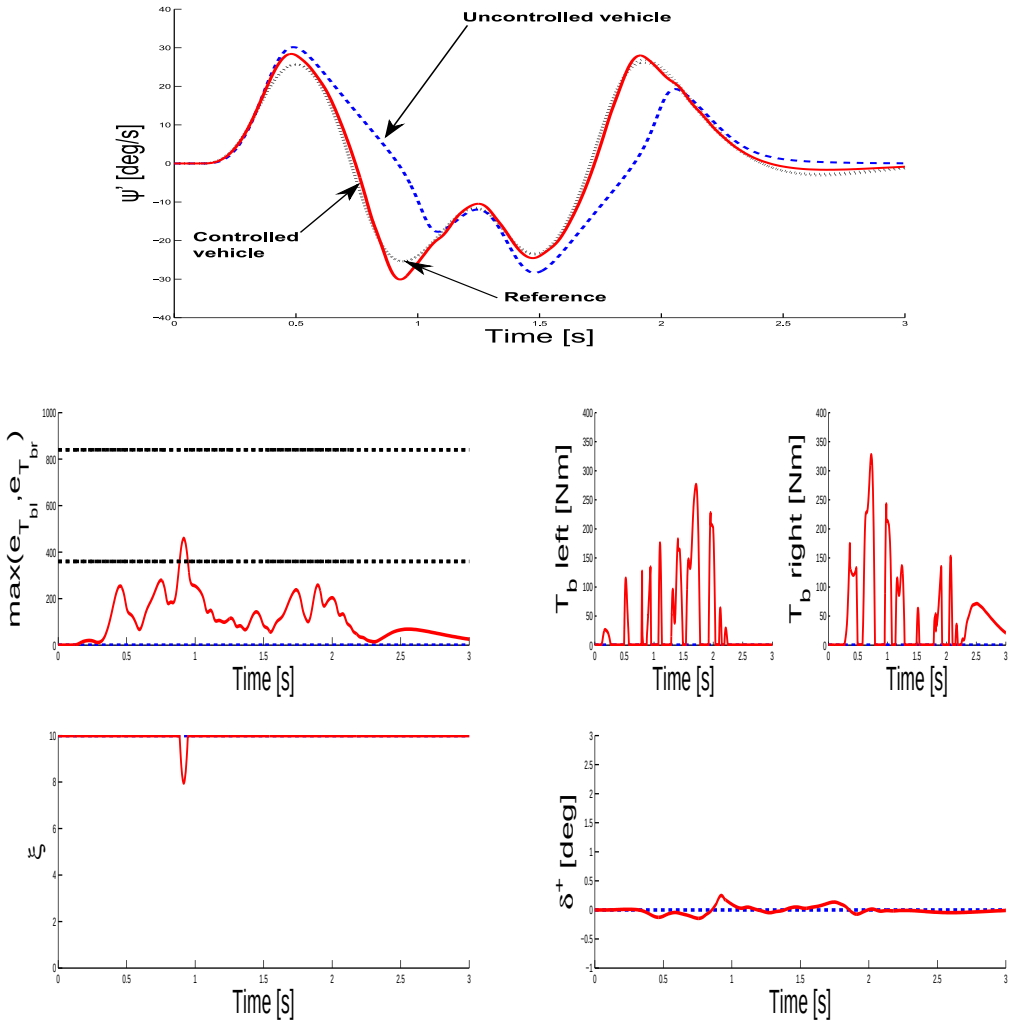

Figure 7.29: Situation 1: simulation of a double line change manoeuver on a WET road with initial speed $v_0 = 100km/h$.

is to note that the ξ parameter decreases during this period (from $\overline{\xi}$ to $\underline{\xi}$), activating in the same time the steering input as shown on Figure 7.31-(bottom, right).

7.4.3.2 Initial state analysis

In this second simulation set, the steering angle provided by the driver is null (i.e. $\delta_d = 0$). One compares the vehicle behavior for different initial conditions of the yaw rates and the side slip angles. Three cases are considered with different road adhesions and vehicle initial speeds. In all these simulations $\dot{\psi}_{ref} = 0$. The performed situations are the following:

- Situation 1: Dry road, $v_0 = 120km/h$ (Figure 7.32)
- Situation 2: Wet road, $v_0 = 120km/h$ (Figure 7.33)

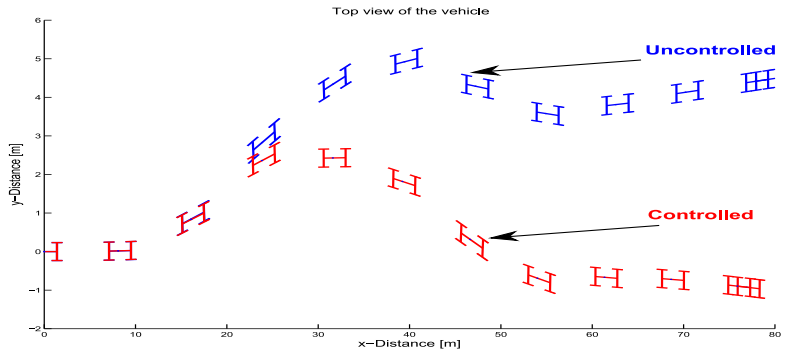

Figure 7.30: Vehicle path after a double line change manoeuver on a WET road with initial speed $v_0 = 100km/h$ with a FAULTY rear left actuator.

- Situation 3: Icy road, $v_0 = 90km/h$ (Figure 7.34)

For all critical initial conditions, the controlled vehicle reaches the safe situation ($\dot{\psi} = 0$ and $\beta_{cog} = 0$) much faster than the uncontrolled system (see top Figures 7.32, 7.33 and 7.34). Moreover, as shown on phase portraits (Figures 7.32, 7.33 and 7.34), the proposed control limits the yaw rate and side slip angle peak values, hence reduces the risk of the vehicle to become unstable. Thanks to the use of an efficient ABS controller on each braking wheel, the braking torque remains low and slipping never occurs. Bottom Figures 7.32, 7.33 and 7.34 show that actuators work simultaneously to overcome the dangerous situation caused by the critical initial conditions.

Remark: About the results. By looking at the phase portraits (top Figures 7.32, 7.33 and 7.34), one sees that at the beginning of the trajectories, controlled and passive results are very similar. This is due to the fact that the yaw rate reference provided in the simulation is not simply 0, but:

$$\ddot{\psi}_{ref} = -10\dot{\psi}_{ref} \tag{7.20}$$

where initial condition $\dot{\psi}^0_{ref}$ is equal to the initial yaw rate condition. This slight modification does not alter the analysis, but is important to avoid a step error when simulation is initialized.

7.5 Some conclusions

The aim of this "super controller" is to enhance the vehicle safety in critical driving situations. For that purpose, a reconfigurable Global Chassis Controller (GCC) structure involving braking and steering subsystems has been proposed in the LPV framework. The control structure consists in scheduling the controller (with ξ, a braking efficiency measure) in order to solve the dynamical problem by the use of rear braking, and, if necessary the intervention of the front steering actuator. This parameter dependent structure is synthesized in the LPV/$\mathcal{H}_\infty$ framework, which guarantees the closed-loop stability and performances for all variations of the parameter in the defined convex set (here, $\xi \in \mathcal{P}_\xi$). The proposed GCC solution is integrated in a vehicle dynamic framework, thus, the obtained controller shows to be robust to fault occurring on the braking system and to critical driving situations.

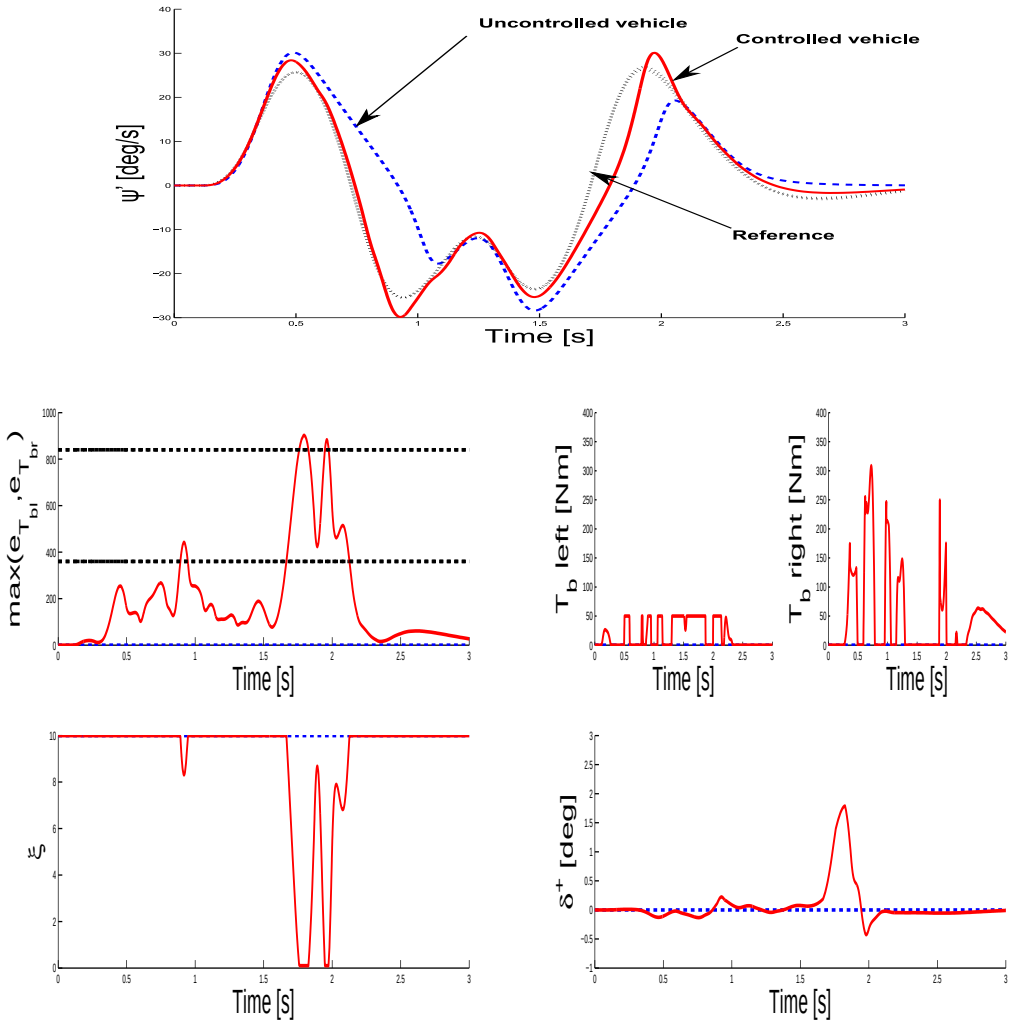

Figure 7.31: Situation 2: Simulation of a double line change manoeuver on a WET road with initial speed $v_0 = 100km/h$, with a FAULTY actuator.

Moreover, as long as the general structure does not involve any on-line optimization process, it is easy to implement the controller on real vehicles, even those where local ABS are already working well. As an illustration, here, the proposed GCC is well integrated with the existing ABS strategy (Tanelli *et al.*, 2007*a*). Simulations of critical driving situations, performed on a complex nonlinear vehicle model, show the effectiveness of the proposed control design.

Further experiments and investigations may be done to handle vehicle speed dependency, and to include a suspension strategy. Moreover, the scheduling strategy should be designed in a more formal way (e.g. using Fault Detection approaches).

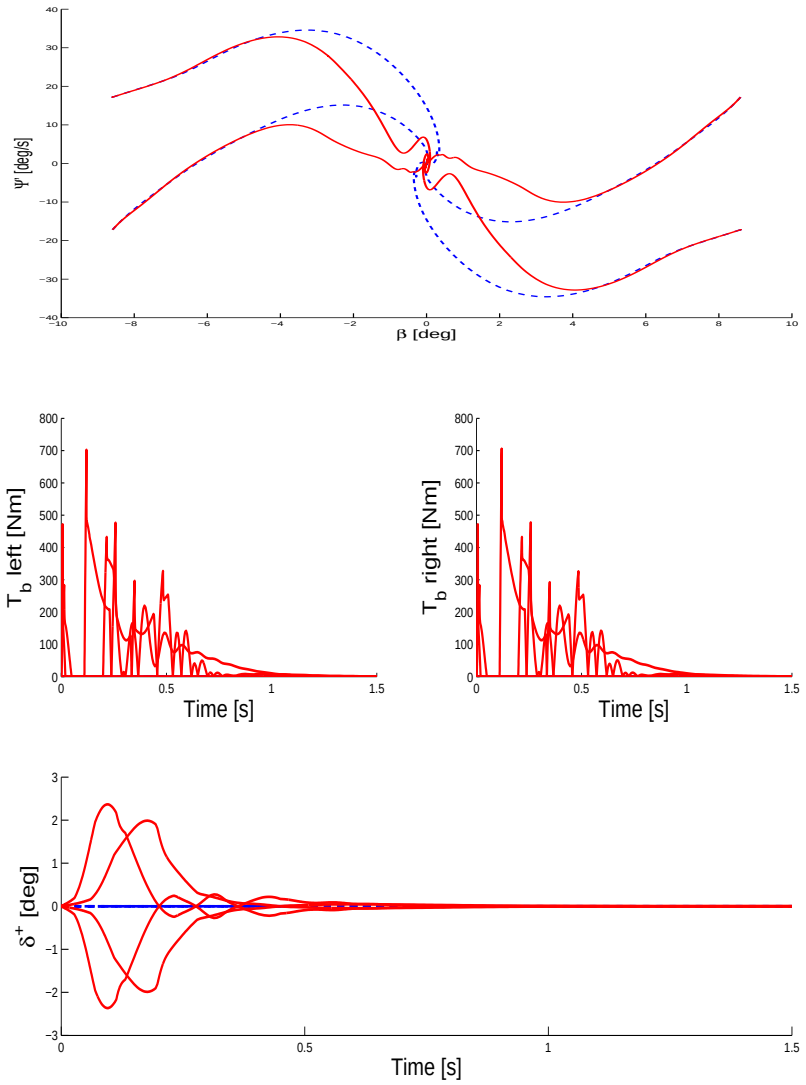

Figure 7.32: Situation 1: simulation on a DRY road with $\delta_d = 0$ and initial speed $v_0 = 120km/h$. Dashed: uncontrolled, Solid: GCC.

7.6 Concluding remarks

In this chapter we have introduced three GCC strategies. These approaches illustrate in an interesting way the different GCC structures and the potentiality of the LPV approach to solve the vehicle dynamical problems. Each of these control designs presents a particular interest:

- The first solution consists in modifying the suspension control law (locally built with a simple Skyhook control law), using an anti-roll distribution strategy. This strategy shows interesting results and provides both comfort and handling improvements by using only the suspension actuators. Such kind of simple control shows the interest of making the actuators collaborate and motivates researches to design controllers that work together to improve the global vehicle

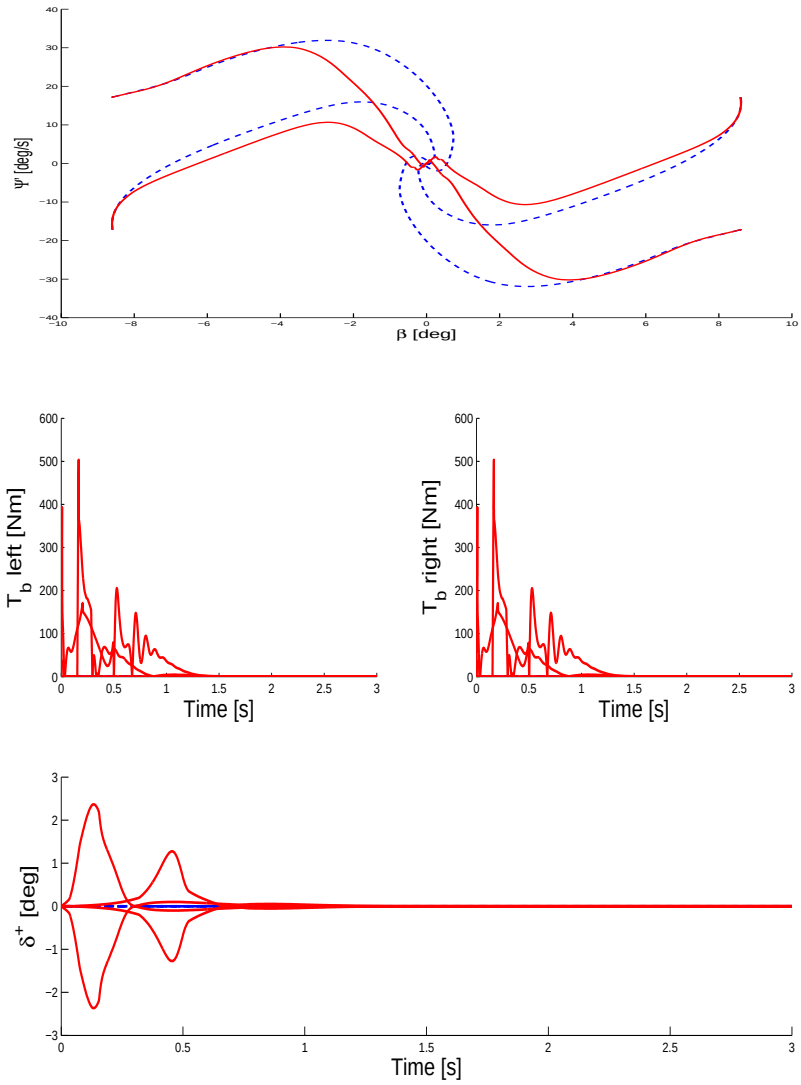

Figure 7.33: Situation 2: simulation on a WET road with $\delta_d = 0$ and initial speed $v_0 = 120km/h$. Dashed: uncontrolled, Solid: GCC.

dynamics.

- The second solution illustrates a GCC strategy that controls different actuators (suspension and braking systems) and provides varying performances according to the vehicle situation. The proposed control is designed, considering an LPV model which provides an interesting framework to introduce parameter dependent performance specifications and to handle system nonlinearities. Therefore, this design has been done considering the vehicle as a MIMO system (without local controllers). We show that the ABS strategy may be handled in another original way (using the parameter variation).

- The third solution proposes a "super controller" that aims at solving the general dynamical

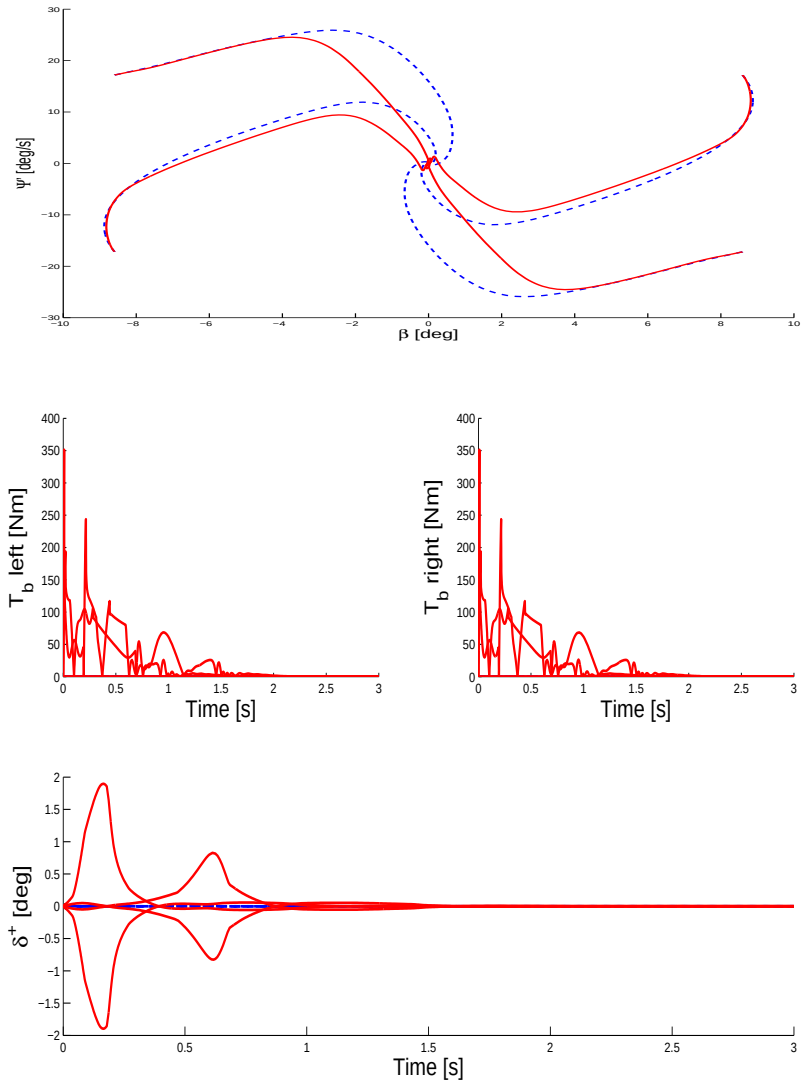

Figure 7.34: Situation 3: simulation on a ICY road with $\delta_d = 0$ and initial speed $v_0 = 90km/h$. Dashed: uncontrolled, Solid: GCC.

control problem supervising the locally designed actuators. The LPV design allows to achieve situation dependent performances. Moreover it exhibits a simple structure which may be easily implemented on commercial cars.

From a general viewpoint, the interest is that the vehicle is viewed as a dynamical object where dynamical performances, under constraints, have to be handled. Some perspectives of this work would be to:

- Compare the proposed strategies with other methods (e.g. Chou and d'Andréa Novel, 2005; Falcone *et al.*, 2007*c*).
- Introduce a metric and/or a methodology to design a scheduling strategies in a more formal way

(as e.g. in Poussot-Vassal *et al.*, 2008*a*).

- Extend the "super controller" scheme by integrating the semi-active suspension strategy developed in Section 6.3 to obtain a GCC involving suspension, braking and steering subsystems.
- Integrate the LPV based ABS strategy to the global scheme presented in Section 7.4.

General conclusions and perspectives

Summary

This thesis is concerned with the study and the analysis of the global chassis control through the use of advanced robust control tools. The underlying objectives are to enhance vehicle comfort and safety characteristics. This work is presented in six chapters.

- In the first chapter, some historical aspects concerning the robust and LMI growing importance in the control community are introduced. A recent state of the art in automotive control is also given, emphasizing the suspension and global chassis applications.
- The second chapter recalls the theoretical tools used in the thesis. Thus, notions such as robustness, convexity, LMIs, LTI and LPV controller synthesis are introduced. This chapter aims at providing the reader the necessary tools to understand the contributions of this work.
- The third chapter presents the main subsystems of the car involved in this work, namely: suspensions, braking and steering actuators. As semi-active suspension systems are of deep interest in this thesis, some representative study cases are also detailed to illustrate some properties of such actuators. These study cases have been made possible, thanks to the collaborations with R. Ramirez-Mendoza, from the Tecnologico de Monterrey, and B. Talon, from the SOBEN company.
- The fourth chapter aims at presenting some of the most widely used vehicle models. These models are based on the subsystems presented in the third chapter. In this chapter, the quarter, half and full (LTI, LPV and nonlinear as well) vehicle models are presented. For sake of completeness, and to validate the models structure and parameters, the full nonlinear model is "validated" with experimental tests held on a real Renault Mégane Coupé vehicle. A part of this work has been done in collaboration with G.L. Gissinger, M. Basset, C. Lamy and G. Pouly, from the MIAM research team, at the "Université de Haute Alsace".
- The fifth chapter presents our contributions in the domain of suspension control. First, an active LPV suspension control strategy is studied including multi-objective performance criteria, illustrating the benefits of the advanced control design methodologies on automotive applications. Secondly, a new semi-active suspension strategy using the LPV approach is proposed and compared with other well known designs. This design shows interesting results and exhibits some powerful properties. A part of this work has been made in strong collaboration with P. Gáspár, Z. Szabó and J. Bokor, from the MTA SZTAKI, Hungarian Academy of Sciences.
- Chapter six develops the main contributions of the thesis in the so called global chassis control field. We introduce different GCC structures, involving suspension, braking and steering actuators. We show the benefits of the advanced control structures designs that use different actuators

to enhance safety, comfort and to handle critical driving situations and actuators failure, which are actual problems. A part of this work has also been made in collaboration with J. Bokor, P. Gáspár and Z. Szabó.

Main contributions

The main contributions of this thesis are essentially methodology oriented. They mainly concern:

- The design of a new semi-active suspension control strategy, using, in an original way, the LPV control approach. This control design presents many interesting properties compared to already existing semi-active strategies. According to the author, this result is interesting since, nowadays, semi-active suspension control is a very challenging problem in the automotive industry and in the research community as well (see Section 6.3).
- The development of different global chassis control (GCC) structures using the LPV framework. In this domain, the main contributions concern:
  - Firstly, the synthesis of a GCC to control suspension and braking systems, the performances of which vary with respect to the vehicle situation and where the complex tire nonlinearities are handled in an original way. In this approach, the controller is globally synthesized to handle the dynamical objectives and to ensure slip stability (i.e. avoid skidding) in an original way, without considering local controllers (see Section 7.3). Thus, even if the approach is different, this work is in the continuity of many others, where GCC are designed to handle all the vehicle problems without using local controllers.
  - Secondly, the synthesis of GCC involving braking and steering actuators, and playing the role of "super controller". This controller is also designed in the LPV framework to achieve situation dependent performances. The main difference with respect to the previously designed GCC is that its structure takes advantage of local controllers (is our case, the ABS controller). Thus, in this design, the GCC handles the dynamical problems by monitoring the locally distributed controllers (see Section 7.4).

  GCC is also a challenging problem where theoretical and experimental researches are still under development.

Perspectives

As a perspective of these results, many interesting points may be explored. Among others, according to the author, the following seem to be of great interest:

- **Modeling & Identification**: Enhance the vehicle modeling step and identify the key variables (i.e. variables that are unknown or varying and that greatly influence the dynamics of the vehicle such as tire stiffness, height of the center of gravity, etc.) to build controllers robust w.r.t. crucial nonlinearities that affect the control performances.
- **LPV design**: Think about a methodology to design scheduling strategies for LPV controller. Indeed, when the scheduling parameter of a LPV controller is used to make the closed-loop performances varying, the way the parameter varies considerably influences the obtained results. Thus a methodology to design in a more mathematical way the scheduling parameter may be

an interesting point of investigation. As far as the author knows, this concept is not covered in the literature yet. A good starting point may be to investigate on Fault Detection Isolation approaches.

- **Suspension design**: Improve the proposed semi-active suspension control strategy in order to be abe to obtain either comfort or road-holding performances while ensuring the dissipative property. Indeed, additional studies may be carried out to ensure the semi-activeness without involving LPV design.
- **GCC design (1)**: Concerning the global chassis control design, an extension of the last structure (given in Section 7.4) may be done by including the new proposed LPV semi-active suspension strategy as a local controller.
- **GCC design (2)**: Based on Section 7.4), a real global chassis controller with suspension, braking and steering local controllers scheduled with a monitor that may adapt the performances according to the vehicle situation (normal, dangerous or critical) and handle actuator failures may be synthesized.
- **Synthesis constraint**: Include in the controller synthesis, the saturation constraints or anti-windup strategies. This step is very important for braking and steering controllers since they are limited in amplitude, but also in variation rate (see e.g. Garcia and Tarbouriech, 2001; Grimm *et al.*, 2003; Hu *et al.*, 2003; Wu and Lu, 2004).
- **Comparisons**: Extensions of the GCC approaches may also include comparisons with other approaches developed in the literature (Chou and d'Andréa Novel, 2005; Falcone *et al.*, 2007*c*).
- **Discretisation & Implementation**: Implement the proposed suspension strategies on a real experimental test bench. This step may introduce some LPV controller discretisation theoretical problems which are of great interest for the expansion of this theory. In Toth *et al.* (2008), authors present some aspects on the discretisation phase. This may be part of the work of S. Aubouet who works with the SOBEN company on a new semi-active dampers technology.
- **Suspension application**: Extend the proposed semi-active suspension structure to real suspension (e.g. the SOBEN one), by including in the design, the structural dynamics of the considered system.

Chapter

Appendix

A.1 LMI-based DOF LTI/$\mathcal{H}_\infty$ solution

The LMI based solution to the Dynamical Output Feedback $\mathcal{H}_\infty$ problem for LTI system is described thereafter. It is based on result given (but not developed) in (Scherer *et al.*, 1997). This proof is interesting since it can be easily extended to $\mathcal{H}_2$, mixed LTI and LPV problems. Let consider the BRL problem given by:

$$\begin{bmatrix} \mathcal{A}^T K + K\mathcal{A} & K\mathcal{B} & \mathcal{C}^T \\ \mathcal{B}^T K & -\gamma_2^2 I & \mathcal{D}^T \\ \mathcal{C} & \mathcal{D} & -I \end{bmatrix} \prec 0 \tag{A.1}$$

where $\mathcal{A}$, $\mathcal{B}$, $\mathcal{C}$ and $\mathcal{D}$ are the closed-loop matrices defined as in (3.86) and where K and γ are the Lyapunov function and $\mathcal{H}_\infty$ bound variables (in the following, for sake of clarity, $D_{22} = 0$ i.e. generalized system is strictly proper).

Proof: $\mathcal{H}_\infty$ LMI solution (for $D_{22} = 0$). Let consider $X = X^T \succ 0$ and $Y = Y^T \succ 0$, then suppose

$$\begin{aligned} K &= \begin{bmatrix} Y & N \\ N^T & Y^T \end{bmatrix} \\ K^{-1} &= \begin{bmatrix} X & M \\ M^T & X^T \end{bmatrix} \\ V_1 &= \begin{bmatrix} X & I_n \\ M^T & 0 \end{bmatrix} \\ KV_1 &= V_2 = \begin{bmatrix} I_n & Y \\ 0 & N^T \end{bmatrix} \end{aligned} \tag{A.2}$$

First note that,

$$\begin{aligned} KK^{-1} = I_n \quad &\Leftrightarrow \quad \begin{bmatrix} YX + NM^T & YM + NX^T \\ N^T X + Y^T M^T & N^T M + Y^T X^T \end{bmatrix} = I_n \\ &\Leftrightarrow \quad \begin{cases} YX + NM^T &= I_n \\ N^T X + Y^T M^T &= 0 \end{cases} \end{aligned} \tag{A.3}$$

Then, define V such that:

$$V = \begin{bmatrix} V_1 & 0 & 0 \\ 0 & I_m & 0 \\ 0 & 0 & I_q \end{bmatrix} \tag{A.4}$$

By left-right multiplying the BRL by V^T and V, one obtains:

$$\begin{bmatrix} V_1^T(\mathcal{A}^T K + K\mathcal{A})V_1 & V_1^T K\mathcal{B} & V_1^T\mathcal{C}^T \\ \mathcal{B}^T K V_1 & -\gamma^2 I_m & \mathcal{D}^T \\ \mathcal{C}V_1 & \mathcal{D} & -I_q \end{bmatrix} \prec 0 \tag{A.5}$$

where,

$$\begin{array}{rcll} V_1^T K\mathcal{A}V_1 & = & V_2^T\mathcal{A}V_1 & \\ & = & \begin{bmatrix} M_{11} & M_{12} \\ M_{21} & M_{22} \end{bmatrix} & \\ & \text{with} & M_{11} = AX + B_2(D_cC_2X + C_cM^T) & \\ & & M_{12} = A + B_2D_cC_2 & \\ & & M_{21} = YAX + YB_2D_cC_2X + NB_cC_2X + YB_2C_cM^T + NA_cM^T & \\ & & M_{22} = YA + (YB_2D_c + NB_c)C_2 & \\ V_1^T K\mathcal{B} & = & V_2^T\mathcal{B} & \\ & = & \begin{bmatrix} B_1 + B_2D_cD_{21} \\ YB_1 + (YB_2D_c + NB_c)D_{21} \end{bmatrix} & \\ \mathcal{C}V_1 & = & \begin{bmatrix} C_1X + D_{12}(D_cC_2X + C_cM^T) & C_1 + D_{12}D_cC_2 \end{bmatrix} & \\ V_1^T K V_1 & = & V_1^T V_2 & \\ & = & \begin{bmatrix} X & I_n \\ I_n & Y \end{bmatrix} & \end{array} \tag{A.6}$$

Then, by introducing the following variable changes:

$$\begin{cases} \widetilde{D} &= D_c \\ \widetilde{C} &= D_cC_2X + C_cM^T \\ \widetilde{B} &= YB_2D_c + NB_c \\ \widetilde{A} &= YAX + YB_2D_cC_2X + NB_cC_2X + YB_2C_cM^T + NA_cM^T \end{cases} \tag{A.7}$$

we finally obtain,

$$\begin{bmatrix} A\mathbf{X} + \mathbf{X}A^T + B_2\widetilde{\mathbf{C}} + \widetilde{\mathbf{C}}^T B_2^T & \widetilde{\mathbf{A}}^T + A + B_2\widetilde{\mathbf{D}}C_2 & B_1 + B_2\widetilde{\mathbf{D}}D_{21} & \mathbf{X}C_1^T + \widetilde{\mathbf{C}}^T D_{12}^T \\ \widetilde{\mathbf{A}} + A^T + C_2^T\widetilde{\mathbf{D}}^T B_2^T & \mathbf{Y}A + A^T\mathbf{Y} + \widetilde{\mathbf{B}}C_2 + C_2^T\widetilde{\mathbf{B}}^T & \mathbf{Y}B_1 + \widetilde{\mathbf{B}}D_{21} & C_1^T + C_2^T\widetilde{\mathbf{D}}^T D_{12}^T \\ B_1^T + D_{21}^T\widetilde{\mathbf{D}}^T B_2^T & B_1^T\mathbf{Y} + D_{21}^T\widetilde{\mathbf{B}}^T & -\gamma_\infty I_{n_u} & D_{11}^T + D_{21}^T\widetilde{\mathbf{D}}^T D_{12}^T \\ C_1\mathbf{X} + D_{12}\widetilde{\mathbf{C}} & C_1 + D_{12}\widetilde{\mathbf{D}}C_2 & D_{11} + D_{12}\widetilde{\mathbf{D}}D_{21} & -\gamma_\infty I_{n_y} \end{bmatrix} \prec 0$$
$$\begin{bmatrix} \mathbf{X} & I_n \\ I_n & \mathbf{Y} \end{bmatrix} \succ 0 \tag{A.8}$$

which is now an LMI in X, Y, $\widetilde{A}$, $\widetilde{B}$, $\widetilde{C}$, $\widetilde{D}$ and γ_∞ that can be solved by a good SDP solver. Therefore, one only have to find M and N such that,

$$MN^T = I_n - XY \tag{A.9}$$

To do so, the singular value decomposition is used together with the Cholesky factorization s.t.:

$$\begin{array}{rcl} I_n - XY & = & U\Sigma V^T \\ & = & UR^T RV^T \end{array} \tag{A.10}$$

where R is the solution of the Cholesky factorization. Then, by identifying, $M = UR^T$ and $N = VR^T$. Then to go back to the solution of the problem, the controller parameters are obtained by the following transformation,

$$\left\{\begin{array}{rcl} D_c &=& \widetilde{D} \\ C_c &=& (\widetilde{C} - D_c C_2 X) M^{-T} \\ B_c &=& N^{-1}(\widetilde{B} - Y B_2 D_c) \\ A_c &=& N^{-1}(\widetilde{A} - YAX - YB_2 D_c C_2 X - NB_c C_2 X - YB_2 C_c M^T) M^{-T} \end{array}\right. \tag{A.11}$$

It is to be noted that one can force the controller to be strictly proper by imposing $\widetilde{D_c} = 0$, which simplify the LMIs previously exposed (this constrain also is widely required for applications purpose). □

B.2 Pseudo-Bode computation

The pseudo-Bode computation allows at plotting frequency responses of a nonlinear model. The computation methods is consists in sending a sinusoidal input signal on input w of the form $w(t) = a\sin(\omega t)$, where a is the signal amplitude, ω is the signal pulsation and t the time duration. Then, after N periods, one measure the gain of the output signal z. Then repeat the sequence for varying ω and/or a. The steps are the following:

1. Excite the system through an input signal at pulsation ω (from ω_{min} to ω_{max}) during N periods.
2. For each pulsation, measure the output signal.
3. Compute the discrete Fourier transform of the signal.
4. Compute the magnitude (and phase).

Remark: About the N periods. It is of importance to send a signal during N (e.g. $N = 10$) periods in order to avoid transient phases, especially in the nonlinear case.

C.3 Some linear algebra

Definition C.3.1 (*Invertible matrix*)

A matrix A is said to be invertible is there exist a unique matrix, denoted A^{-1} such that $AA^{-1} = I$. If so A^{-1} is called the inverse of A. If such a matrix doesn't exists, A is said to be singular.

Property C.3.1 (*Invertible matrix*)

Let A and B two invertible matrices, then,

$$\begin{array}{rcl} (AB)^{-1} &=& B^{-1}A^{-1} \\ (A^T)^{-1} &=& (A^{-1})^T \\ (A^*)^{-1} &=& (A^{-1})^* \end{array} \tag{C.12}$$

Remark: Matrix inversion Consider the following matrix, then it's inverse can be simply derived using this formulae.

$$\begin{bmatrix} A & D \\ C & B \end{bmatrix}^{-1} = \begin{bmatrix} A^{-1} + A^{-1}D(B - CA^{-1}D)^{-1}CA^{-1} & -A^{-1}D(B - CA^{-1}D)^{-1} \\ -(B - CA^{-1}D)^{-1}CA^{-1} & (B - CA^{-1}D)^{-1} \end{bmatrix} \tag{C.13}$$

Definition C.3.2 (*Matrix trace*)

A matrix A trace is defined by,

$$\boldsymbol{Tr}(A) = \sum_{i=1}^{n} a_{ij} \tag{C.14}$$

Property C.3.2 (*Matrix sum and products*)

The following properties hold,

$$\begin{array}{rcl} \boldsymbol{Tr}(AB) & = & \boldsymbol{Tr}(BA) \\ \boldsymbol{Tr}(A+B) & = & \boldsymbol{Tr}(A) + \boldsymbol{Tr}(B) \\ \det(AB) & = & \det(BA) \\ & = & \det(A)\det(B) \end{array} \tag{C.15}$$

Definition C.3.3 (*Eigenvalues, Eigenvector, Spectrum*)

- *Eigenvalues $\lambda_i = \lambda_i(A)$ (where $1 \leq i \leq n$) d'of a A square matrix of order n are the n real or complex zeros of the characteristic polynomial defined as,*

$$\chi_A : \lambda \in \mathbb{C} \text{ s.t. } \chi_A(\lambda) = \det(A - \lambda I) \tag{C.16}$$

- *Then each eigenvalue λ_i is associated a vector p such that,*

$$p \neq 0 \text{ and } Ap = \lambda p \tag{C.17}$$

  called eigenvector of A.

- *Then the A spectrum is given by,*

$$\boldsymbol{spec}(A) = \bigcup_{i=1}^{n} \{\lambda_i(A)\} \tag{C.18}$$

Definition C.3.4 (*Singular values decomposition*)

Let $A \in \mathbb{F}^{m\times n}$. There exist unitary matrices

$$\begin{array}{rcl} U & = & [u_1, u_2, \ldots, u_m] \in \mathbb{F}^{m\times m} \\ V & = & [v_1, v_2, \ldots, v_n] \in \mathbb{F}^{n\times n} \end{array} \tag{C.19}$$

such that,

$$A = U\Sigma V^* \tag{C.20}$$

where,

$$\begin{array}{c} \Sigma = \left[\begin{array}{cc} \Sigma_1 & 0 \\ 0 & 0 \end{array} \right] \\ \Sigma_1 = \textbf{\textit{diag}}(\sigma_1, \ldots, \sigma_p) \\ \sigma_1 \geq \sigma_2 \geq \cdots \geq \sigma_p \geq 0, p = \min(m, n) \end{array} \tag{C.21}$$

$(\sigma_1, \sigma_2 \ldots, \sigma_p)$ are called singular values. Singular value allow to measure the size of a matrix. they are good indicator of the strong and weak input or output directions.

Definition C.3.5 (*Cholesky factorization*)

The Cholesky factorization expresses a symmetric positive definite matrix A as the product of a triangular matrix and its transpose s.t.:

$$A = R^T R \tag{C.22}$$

where R is an upper triangular matrix strictly positive.

D.4 Renault Mégane Coupé parameters

The involved model parameters, identified on a "Renault Mégane Coupé" car, are given on Table D.1.

Symbol	Value	Unit	Signification
m_s	1260	kg	sprung mass
$m_{us_{fj}}$	37.5	kg	front unsprung masses (left, right)
$m_{us_{rj}}$	37.5	kg	rear unsprung masses (left, right)
I_x	250	$kg.m^2$	roll inertia
I_y	1400	$kg.m^2$	pitch inertia
I_z	2000	$kg.m^2$	yaw inertia
t_f	1.4	m	Front axle
t_r	1.4	m	Rear axle
l_f	1.4	m	COG-front distance
l_r	1	m	COG-rear distance
r	0.3	m	nominal wheel radius
h	0.7	m	chassis COG height
k_f	29500	N/m	front suspension linearized stiffness (left, right)
k_{rj}	20000	N/m	rear suspension linearized stiffness (left, right)
c_{fj}	1500	$N/m/s$	front suspension linearized damping (left, right)
c_{rj}	3000	$N/m/s$	rear suspension linearized damping (left, right)
k_{tj}	208000	N/m	tire stiffness (front, rear & left, right)
z_{def}	$[-0.09; 0.05]$	m	suspension bounds (front, rear & left, right)
B_z	0.247		auto-aligning tire parameter (front, rear & left, right)
C_z	2.56		auto-aligning tire parameter (front, rear & left, right)
D_z	-15.53		auto-aligning tire parameter (front, rear & left, right)
E_z	-3.92		auto-aligning tire parameter (front, rear & left, right)
b_y	8.3278		lateral tire parameter (front, rear & left, right)
c_y	1.1009		lateral tire parameter (front, rear & left, right)
d_y	2268		lateral tire parameter (front, rear & left, right)
e_y	-1.1661		lateral tire parameter (front, rear & left, right)

Table D.1: Renault Mégane Coupé parameters (full vehicle)

Bibliography

Abdellahi, E., D. Mehdi and M. M Saad (2000). On the design of active suspension system by $\mathcal{H}_\infty$ and mixed $\mathcal{H}_2/\mathcal{H}_\infty$: An LMI approach. In: *Proceedings of the IEEE American Control Conference (ACC)*. Chicago, Illinois. pp. 4041–4045.

Abedor, J., K. Nagpal and K. Poola (1994). Robust regulation with $\mathcal{H}_2$ performance. *System & Control Letters* **23**, 431–443.

Abedor, J., K. Nagpal, P.P. Khargonekar and K. Poola (1995). Robust regulation in the presence of norm-bounded uncertainty. *IEEE Transaction on Automatic Control* **40**(1), 147–153.

Ackermann, J. and T. Bunte (1996). Yaw disturbance attenuation by robust decoupling of car steering. In: *Proceedings of the 13th IFAC World Congress (WC)*. San Francisco, California. pp. 1–6.

Ahmadian, M. and X. Song (1999). A non parametric model for magneto-rheological dampers. In: *Proceedings of the ASME Design Engineering Technical Conference*. Las Vegas, Nevada, USA.

Alazard, D., C. Cumer, P. Apkarian, M. Gauvrit and G. Ferrerres (1999). *Robustesse et Commande optimale*.

Alvarez, L., R. Horowitz and L. Olmos (2002). Adaptive emergency braking control with observer-based dynamic tire-road friction model and underestimation of friction coefficient. In: *Proceedings of the 5th IFAC World Congress (WC)*. Barcelona, Spain.

Andreasson, J. and T. Bunte (2006). Global chassis control based on inverse vehicle dynamics models. *Vehicle System Dynamics* **44**(supplement), 321–328.

Apkarian, P. and P. Gahinet (1995). A convex characterization of gain scheduled $\mathcal{H}_\infty$ controllers. *IEEE Transaction on Automatic Control* **40**(5), 853–864.

Apkarian, P. and R.J. Adams (1998). Advanced gain-scheduling techniques for uncertain systems. *IEEE Transaction on Control System Technology* **6**(1), 21–32.

Apkarian, P., P. Gahinet and G. Beker (1995). Self-scheduled $\mathcal{H}_\infty$ control of linear parameter-varying systems: A design example. *Automatica* **31**(9), 1251–1262.

Arzelier, D. (2005). *Théorie de Lyapunov, commande robuste et optimisation*.

Arzelier, D. and D. Peaucelle (2004*a*). Multi-objective $\mathcal{H}_2/\mathcal{H}_\infty$/impulse-to-peak synthesis: application to the control of an aerospace launcher. In: *Proceedings of the 16th IFAC Symposium on Automatic Control in Aerospace*. St Petersburg, Russia.

Arzelier, D. and D. Peaucelle (2004*b*). A multiobjective $\mathcal{H}_\infty/\mathcal{H}_2$/p2p synthesis: Application to the control of an aerospace launcher. In: *Proceedings of the 16th IFAC Symposium on Automatic Control in Aerospace*. St. Petersburg, Russia.

Åström, Karl Johan and Björn Wittenmark (1995). *Adaptive Control*. Addison-Wesley. Reading, Massachusetts.

Åström, K.J. and B. Wittenmark (1997). *Computer controlled systems: Theory and design*. Vol. Third edition.

Aubert, D. and S. Mammar (1996). Contrôle latéral automatique d'un véhicule à l'aide d'une caméra: cas du suivi de route. *RTS: Recherche-Transport-Sécurité*.

Aubouet, S. (2007). On modeling and control of a semi-active suspension system (in french). Master's thesis. Grenoble INP - ESISAR. GIPSA-lab (former LAG) & SOBEN.

Aubouet, S., O. Sename, B. Talon, C. Poussot-Vassal and L. Dugard (2008). Performance analysis and simulation of a new industrial semi-active damper. In: *Proceedings of the 17th IFAC World Congress (WC)*. Seoul, South Korea.

Autran, F., F. Bessière, J. Lévine and P. Rouchon (1995). La fonction suspension, du passif à l'actif: l'approche VALEO. In: *Proceedings of the Journées Automatique Automobile*. Bordeaux, France.

Bakker, E., H.B. Pacejka and L. Lidner (1989). A new tire model with an application in vehicle dynamics studies. *SAE Paper*.

Balas, G. J., J. Bokor and Z. Szabo (2003). Invariant subspaces for LPV systems and their application. *IEEE Transaction on Automatic Control* **48**, 2065–2069.

Bambang, R., E. Shimemura and K. Uchida (1993). Mixed $\mathcal{H}_2/\mathcal{H}_\infty$ control with pole placement, state feedback case. In: *Proceedings of the IEEE American Control Conference (ACC)*. San Francisco, California, USA. pp. 2777–2779.

Benson, S.J., Y. Ye and X. Zhang (2000). Solving large-scale sparse semidefinite programs for combinatorial optimization. *SIAM Journal on Optimization* **10**(2), 443–461.

Bergounioux, M. (2001). *Optimisation et contrôle des systèmes linéaires (in French)*. DUNOD.

Bernstein, D.S. and W.M. Haddad (1989). LQG control with an $\mathcal{H}_\infty$ performance bound: A Riccati equation approach. *IEEE Transaction on Automatic Control* **34**(3), 293–305.

Biannic, J.M. (1996). Robust control of parameter varying systems: aerospace applications. PhD thesis (in french). Université Paul Sabatier (ONERA), Toulouse, France.

Bokor, J., Z. Szabo and G. Stikkel (2004). Detection filter design for LPV systems. a geometric approach. *Automatica* **40**, 511–518.

Bonnans, F. (2006). *Optimisation continue (in French)*. DUNOD.

Borrelli, F., M. Baotic, A. Bemporad and M. Morari (2003). An efficient algorithm for computing the state feedback optimal control law for discrete time hybrid systems. In: *Proceedings of the th IEEE American Control Conference (ACC)*. Denver, Colorado, USA.

Botero, J.C., M. Gobbi, G. Mastinu and R. Martorana N.D. Piazza (2007). On the reformulation of the ABS logic by sensing forces and moments at the wheels. In: *Proceedings of the 5th IFAC Symposium on Advances on Automotive Control (AAC)*. Aptos, California.

Boyd, S., L. El-Ghaoui, E. Feron and V. Balakrishnan (1994). *Linear Matrix Inequalities in System and Control Theory*. SIAM Studies in applied mathematics.

Briat, C., O. Sename and J-F. Lafay (2007). A LFT/$\mathcal{H}_\infty$ state-feedback design for linear parameter varying time delay systems. In: *Proceedings of the European Control Conference (ECC)*. Kos, Greece.

Briat, C., O. Sename and J-F. Lafay (2008*a*). Delay-scheduled state-feedback design for time-delay systems with time-varying delays. In: *IFAC World Congress (WC)*. Seoul, South Korea.

Briat, C., O. Sename and J-F. Lafay (2008*b*). Quadratic $\mathcal{H}_\infty$ stabilization of LPV polytopic systems (submitted). In: *47th IEEE Conference on Decision and Control (CDC)*. Cancun, Mexico.

Bruzelius, F. (2004). Linear Parameter-Varying Systems: an approach to gain scheduling. PhD thesis. University of Technology of Göteborg, Sweeden.

Bu, J. and M. Sznaier (2000). A linear matrix inequality approach to synthesizing low-order suboptimal mixed $\mathcal{L}_1/\mathcal{H}_\infty$ controllers. *Automatica* **36**, 957–963.

Burckhardt, M. (1993). *Fahrwerktechnik: Radschlupf-Regelsysteme*. Wrzburg.

Campos-Delgado, D. and K. Zhou (2003). Mixed $\mathcal{L}_1/\mathcal{H}_2/\mathcal{H}_\infty$ control design: Numerical optimization. *International Journal of Robust and Nonlinear Control* **76**(7), 687–697.

Canale, M., L. Fagiano, M. Milanese and P. Borodani (2007). Robust vehicle yaw control using an active differential and IMC techniques. *Control Engineering Practice* **15**(8), 923–941.

Canale, M., M. Milanese and C. Novara (2006). Semi-active suspension control using fast model-predictive techniques. *IEEE Transaction on Control System Technology* **14**(6), 1034–1046.

Canudas, C. and P. Tsiotras (1998). Dynamic tire models for vehicle traction control. In: *Proceedings of the IEEE American Control Conference (ACC)*. Philadelphia, Pennsylvania.

Canudas, C., E. Velenis, P. Tsiotras and G. Gissinger (2003*a*). Dynamic tire friction models for road/tire longitudinal interaction. *Vehicle System Dynamics*.

Canudas, C., M.L. Petersen and A. Shiriaev (2003*b*). A new nonlinear observer for tire/road distributed contact friction. In: *Proceedings of the 42th IEEE Conference on Decision and Control (CDC)*. Hawaii, USA.

Caroux, J., C. Lamy, M. Basset and G. L. Gissinger (2007). Sideslip angle measurement, experimental characterization and evaluation of three different principles. In: *Proceedings of the 6th IFAC Symposium on Intelligent Autonomous Vehicles (IAV)*.

Chen, H. and K-H. Guo (2005). Constrained $\mathcal{H}_\infty$ control of active suspensions: An LMI approach. *IEEE Transaction on Control System Technology* **13**(3), 412–421.

Chilali, M. and P. Gahinet (1996). $\mathcal{H}_\infty$ design with pole placement constraints: an LMI approach. *IEEE Transaction on Automatic Control* **41**(3), 358–367.

Chilali, M., P. Gahinet and P. Apkarian (1999). Robust pole placement in LMI regions. *IEEE Transaction on Automatic Control* **44**(12), 2257–2270.

Chou, H. and B. d'Andréa Novel (2005). Global vehicle control using differential braking torques and active suspension forces. *Vehicle System Dynamics* **43**(4), 261–284.

Ciarlet, P.G. (1998). *Introduction à l'analyse numérique matricielle et à l'optimisation*.

Claeys, X. (2002). Commande latérale des véhicules automobiles avec prise en compte de la dynamique des actionneurs. Application à la conduite en peloton des poids lourds sur autoroute. PhD thesis (in french). INPG, Laboratoire d'Automatique de Grenoble (new GIPSA-lab), Grenoble, France.

Clement, B. and G. Duc (2000). Flexible arm multiobjective control via youla parameterization and LMI optimization. In: *Proceedings of the 3rd IFAC Symposium on Robust Control Design (ROCOND)*. Praha, Czech Republic.

Dahleh, M.A. and J.S. Shamma (1992). Rejection of persistent bounded disturbances: Nonlinear controllers. *System & Control Letters* , 245–252.

de Souza, C.E. and A. Trofino (2005). Gain scheduled $\mathcal{H}_2$ controller synthesis for linear parameter varying systems via parameter-dependent Lyapunov functions. *International Journal of Robust and Nonlinear Control* **16**, 243–257.

Delphi (2005). Delphi magneride. Technical review. Delphi.

Delphi (2008). Delphi website. Technical report. Delphi. http://www.delphi.com.

Denny, M. (2005). The dynamics of antilock brake systems. *European Journal of Physics* **26**, 1007–1016.

Ding, S.X., S. Schneider, E.L. Ding and A. Rehm (2005). Fault tolerant monitoring of vehicle lateral dynamics stabilization systems. In: *Proceedings of the 44th IEEE Conference on Decision and Control (CDC)*. Seville, Spain. pp. 2000–2005.

Doyle, J.C. (1982). Analysis of feddback systems with structured uncertainties. *IEEE Proc., Part D* **129**, 242–250.

Doyle, J.C. and G. Stein (1984). Lecture notes in advances in multivariable control. *ONR/Honeywell Workshop, Minneapolis*.

Doyle, J.C., K. Glover, P. Khargonekar and B. Francis (1989). State space solution to standard $\mathcal{H}_2$ and $\mathcal{H}_\infty$ control problems. *IEEE Transaction on Automatic Control* **34**(8), 831–847.

Doyle, J.C., K. Zhou, K. Glover and B. Bodenheimer (1994). Mixed $\mathcal{H}_2$ and $\mathcal{H}_\infty$ performance objectives: Optimal control. *IEEE Transaction on Automatic Control* **39**(8), 1575–1587.

Drakunov, S., U. Ozguner, P. Dix and B. Ashrafi (1995). ABS control using optimum search via sliding modes. *IEEE Transaction on Control System Technology* **3**(1), 79–85.

El-Ghaoui, L. (1997). *Commande Robuste*. Ecole Nationale des Techniques Avancées / Ecole Polytechnique.

Emura, J., S. Kakizaki, F. Yamaoka and M. Nakamura (1994). Developement on the semi-active suspension system based on the sky-hook damper theory. *Society of Automotive Engineers* pp. 17–26.

Falcone, P., F. Borrelli, H.E. Tseng, J. Asgari and D. Hrovat (2007*a*). Integrated braking and steering model predictive control approach in autonomous vehicles. In: *Proceedings of the 5th IFAC Symposium on Advances on Automotive Control (AAC)*. Aptos, California.

Falcone, P., F. Borrelli, J. Asgari, H.E. Tseng and D. Hrovat (2007*b*). Predictive active steering control for autonomous vehicle systems. *IEEE Transaction on Control System Technology* **15**(3), 566–580.

Falcone, P., M. Tufo, F. Borrelli, J. Asgari and H.E. Tseng (2007*c*). A linear time varying model predictive control approach to the integrated vehicle dynamics control problem in autonomous systems. In: *Proceedings of the 46th IEEE Conference on Decision and Control (CDC)*. New Orleans, Louisiane, USA.

Fialho, I. and G. Balas (2002). Road adaptive active suspension design using linear parameter varying gain scheduling. *IEEE Transaction on Control System Technology* **10**(1), 43–54.

Francis, B. A., J. W. Helton and G. Zames (1984). $\mathcal{H}_\infty$ optimal feedback controllers for linear multivariable systems. *IEEE Transaction on Automatic Control* **29**(1), 888–900.

Francis, B.A. and G. Zames (1984). On $\mathcal{H}_\infty$ optimal sensitivity theory for SISO feedback systems. *IEEE Transaction on Automatic Control* **29**(1), 9–16.

Francis, B.A. and J.C. Doyle (1987). Linear control theory with an $\mathcal{H}_\infty$ criterion. *SIAM Journal of Control and Optimization* **25**, 815–844.

Fu, M. (2004). Pole placement via static output feedback is np-hard. *IEEE Transaction on Automatic Control* **49**(5), 855–857.

Gahinet, P. and P. Apkarian (1994). An linear matrix inequality approach to $\mathcal{H}_\infty$ control. *International Journal of Robust and Nonlinear Control* **4**(4), 421–448.

Gahinet, P., P. Apkarian and M. Chilali (1996). Affine parameter-dependent Lyapunov functions and real parametric uncertainty. *IEEE Transaction on Automatic Control* **41**(3), 436–442.

Garcia, G. and S. Tarbouriech (2001). Letter to the editor on the paper 'Output feedback control with input saturations : LMI design approaches' by g. scorletti, j.p. folcher and l. el-ghaoui. *European Journal of Control* **7**(6), 567–579.

Gáspár, P., I. Szaszi and J. Bokor (1998). Iterative model-based mixed $\mathcal{H}_2/\mathcal{H}_\infty$ control design. In: *Proceedings of the UKACC International Conference on Control*. Swansea, United Kingdom. pp. 652–657.

Gáspár, P., I. Szaszi and J. Bokor (2004). Active suspension design using LPV control. In: *Proceedings of the 1st IFAC Symposium on Advances in Automotive Control (AAC)*. Salerno, Italy. pp. 584–589.

Gáspár, P., Z. Szabó and J. Bokor (2005). The design of an integrated control system in heavy vehicles based on an LPV method. In: *Proceedings of the 44th IEEE Conference on Decision and Control (CDC)*. Seville, Spain. pp. 6722–6727.

Gáspár, P., Z. Szabó and J. Bokor (2008*a*). *Subimitted to International Journal of Vehicle Autonomous Systems*.

Gáspár, P., Z. Szabó and J. Bokor (2008*b*). An integrated vehicle control with actuator reconfiguration. In: *Proceedings of the 17th IFAC World Congress (WC)*. Seoul, South Korea.

Gáspár, P., Z. Szabó, J. Bokor, C. Poussot-Vassal, O. Sename and L. Dugard (2007). Toward global chassis control by integrating the brake and suspension systems. In: *Proceedings of the 5th IFAC Symposium on Advances in Automotive Control (AAC)*. Aptos, California, USA.

Gauthier, C. (2007). Modélisation et commande d'un système common rail. PhD thesis (in french). INPG, Laboratoire d'Automatique de Grenoble (new GIPSA-lab) and Delphi Diesel Systems, Grenoble, France.

Gillespie, T.D. (1992). *Fundamental of vehicle dynamics*. Society of Automotive Engineers, Inc.

Giorgetti, N., A. Bemporad, H.E. Tseng and D. Hrovat (2006). Hybrid model predictive control application toward optimal semi-active suspension. *International Journal of Robust and Nonlinear Control* **79**(5), 521–533.

Girardin, G., T. Peter, G.L. Gissinger and M. Basset (2006). Modélisation non linéaire du comfort dynamique d'un véhicule. In: *Proceedings of the 17th Conférence Internationale Francophone d'Automatique (CIFA)*. Bordeaux, France.

Gissinger, G.L., C. Menare and A. Constans (2003). A mechatronic conception of a new intelligent braking system. *Control Engineering Practice* **11**, 163–170.

Giua, A. and G. Usai (1999). Semiactive suspension design with an optimal gain switching target. *Vehicle System Dynamics* **31**(4), 213–232.

Giua, A., M. Melas, C. Seatzu and G. Usai (2004). Design of a predictive semiactive suspension system. *Vehicle System Dynamics* **41**(4), 277–300.

Glover, K. and J.C. Doyle (1988). State space formulae for all stabilizing controllers that satisfy an $\mathcal{H}_\infty$ norm bound and relations to risk sensitivity. *System & Control Letters* **11**, 167–172.

Grimm, G., J. Hatfield, I. Postlethwaite, A.R. Teel, M.C. Turner and L. Zaccarian (2003). Antiwindup for stable linear systems with input saturation: An LMI-based synthesis. *IEEE Transaction on Automatic Control* **48**(9), 1509–1525.

Gustafsson, F. (1997). Slip-based tire-road friction estimation. *Automatica* **33**(6), 1087–1099.

Henrion, D., D. Arzelier, D. Peaucelle and J.B. Lasserre (2004). On parameter dependent Lyapunov functions for robust stability of linear systems. In: *Proceedings of the 43rd IEEE Conference on Decision and Control*. Atlantis, Paradise Island, Bahamas. pp. 887–892.

Henrion, D., S. Tarbouriech and G. Garcia (1999). Output feedback robust stabilization of uncertain linear systems with saturating controls: An LMI approach. *IEEE Transaction on Automatic Control* **44**(11), 2230–2237.

Hrovat, D. (1997). Survey of advanced suspension developments and related optimal control application. *Automatica* **33**(10), 1781–1817.

Hsu, Y-H. Judy and J.C. Gerdes (2005). Stabilization of a steer-by-wire vehicle at the limits of handling using a feedback linearization. In: *Proceedings of IMECE*. Orlando, Florida. pp. 1–10.

Hu, T., A.R. Teel and L. Zaccarian (2003). Anti-windup synthesis for linear control systems with input saturation: Achieving regional, nonlinear performance. *Automatica* **44**, 512–519.

Iwasaki, T. and R.E. Skelton (1994). All controllers for the general $\mathcal{H}_\infty$ control problem: LMI existence conditions and state space formulas. *Automatica* **30**(8), 1307–1317.

Jacquet, D. (2007). Macroscopic Freeway Modelling and Control. PhD thesis. INPG, Laboratoire d'Automatique de Grenoble (new GIPSA-lab), Grenoble, France.

Johansen, T.A., I. Petersen, J. Kalkkuhl and J. Ludemann (2003). Gain-scheduled wheel slip control in automotive brake systems. *IEEE Transaction on Control System Technology* **11**(6), 799–811.

Jonasson, M. and F. Roos (2008). Design and evaluation of an active electromechanical wheel suspension system. *to appear in Journal of Mechatronics*.

Jungers, M. (2006). Commande Robuste multicritère: une approche par la théorie des jeux. PhD thesis (in french). Ecole Normale Supérieure de Cachan, Laboratoire SATIE, Cachan, France.

Karnopp, D., M.J. Crosby and R.A. Harwood (1974). Vibration control using semi-active force generators. *Journal of Engineering for Industry* **96**, 619–626.

Karnopp, D.C. (1983). Active damping in road vehicle suspension systems. *Vehicle System Dynamics* **12**(6), 296–316.

Kawabe, T., O. Isobe, Y. Watanabe, S. Hanba and Y. Miyasato (1998). New semi-active suspension controller design using quasi-linearization and frequency shaping. *Control Engineering Practice* **6**, 1183–1191.

Kern, S. (2008). On the modeling and control of magneto-rheological dampers. Master's thesis. Grenoble INP - ENSIEG. GIPSA-lab (former LAG) & Tecnologico de Monterrey.

Khargonekar, P.P. and M.A. Rotea (1991). Mixed $\mathcal{H}_2/\mathcal{H}_\infty$ control: A convex optimization approach. *IEEE Transaction on Automatic Control* **36**(7), 824–837.

Kiencke, U. and L. Nielsen (2000). *Automotive Control Systems*.

Kimura, H. (1984). Robust stabilizability for a class of transfer functions. *IEEE Transaction on Automatic Control* **29**(9), 788–793.

Koenig, D. and S. Mammar (2003). Reduced order unknown input kalman filter: Application for vehicle lateral control. In: *Proceedings of the IEEE American Control Conference (ACC)*. Denver, Colorado. pp. 4353–4358.

Koo, J-H., F.D. Goncalves and M. Ahmadian (2004). Investigation of the response time of magnetorheological fluid dampers. *SPIE* **5386**, 63–71.

Krstic, M. and H.H. Wang (2000). Stability of extremum seeking feedback for general nonlinear dynamic systems. *Automatica* **36**, 595–601.

Kwiatkowski, A., S. Trimpe and H. Werner (2007). Less conservative polytopic LPV models for charge control by combining parameter set mapping and set intersection. In: *Proceedings of the 46th IEEE Conference on Decision and Control (CDC)*. New Orleans, Louisiane, USA. pp. 3363–3368.

Lamy, C. and M. Basset (2008). Vision-based determination of wheel camber angle and tire deflection. In: *Proceedings of the 17th IFAC World Congress (WC)*. Seoul, South Korea.

Lofberg, J. (2004). YALMIP : A toolbox for modeling and optimization in matlab. In: *Proceedings of the CACSD Conference*.

Lord (2008). Lord website. Technical report. Lord. http://www.lord.com.

Lu, J. (2004). A frequency-adaptive multi-objective suspension control strategy. *ASME Journal of Dynamic Systems, Measurement and Control* **126**(3), 700–707.

Lu, J. and M. DePoyster (2002). Multiobjective optimal suspension control to achieve integrated ride and handling performance. *IEEE Transaction on Control System Technology* **10**(6), 807–821.

Malik, W., S. Kang and S. Darbha (2006). Synthesis of fixed order stabilizing controllers using frequency response measurements. In: *Proceedings of the 5th IFAC Symposium on Robust Control Design (ROCOND)*. Toulouse, France.

Mammar, S. and D. Koenig (2002). Vehicle handling improvement by active steering. *Vehicle System Dynamics* **38**(3), 211–242.

Margolis (1983). Semi-active control of wheel hop in ground vehicles. *Vehicle System Dynamics* **12**(6), 317–330.

Martinez, J.J. (2005). Inter-distance vehicle control. PhD thesis (in french). INPG, Laboratoire d'Automatique de Grenoble (new GIPSA-lab), Grenoble, France.

Masubuchi, I., A. Ohara and N. Suda (1995). LMI-based controller synthesis: A unified formulation and solution. In: *Proceedings of the IEEE American Control Conference (ACC)*. Seattle, Washington, USA. pp. 3473–3477.

McFarlane, D. and K. Glover (1992). A loop-shaping design procedure using $\mathcal{H}_\infty$ synthesis. *IEEE Transaction on Automatic Control* **37**(6), 759–769.

Milliken, W.F. and D.L. Milliken (1995). *Race car vehicle dynamics*. SAE.

Moreau, X. (1995). La dérivation non entière en isolation vibratoire et son application dans le domaine de l'automobile. La suspension Crone : du concept à la réalisation (in French). PhD thesis. Université de Bordeaux I.

Nesterov, Y. and A. Nemirovskii (1994). *Interior-Point Polynomial Algorithms in Convex Programming*. SIAM Studies in applied mathematics.

Ono, E., K. Asano, M. Sugai, S. Ito nd M. Yamamoto, S. Sawada and Y. Yasui (2003). Estimation of automotive tire force characteristics using wheel velocity. *Control Engineering Practice* **11**, 1361–1370.

Oustaloup, A. and B. Mathieu (1999). *La commande CRONE*. Hermes.

Oustaloup, A., X. Moreau and M. Nouillant (1996). The CRONE suspension. *Control Engineering Practice* **4**(8), 1101–1108.

Peaucelle, D. and D. Arzelier (2002). An iterative method for $\mathcal{H}_\infty/\mathcal{H}_2$ synthesis via static output feedback. In: *Proceedings of the 41st IEEE Conference on Decision and Control (CDC)*. Las Vegas, Nevada, USA.

Pouly, G., J-P. Lauffenburger, M. Basset and T.Wissart (2007). Correlation between objective tire parameters and subjective test driver evaluation. In: *Proceedings of the 5th IFAC symposium on Advances in Automotive Control (AAC)*. Aptos, California, USA.

Poussot-Vassal, C. (2007). Discussion paper on: "Combining Slip and Deceleration Control for Brake-by-Wire Control Systems: a Sliding-Mode Approach". *European Journal of Control* **13**(6), 612–615.

Poussot-Vassal, C., A. Drivet O. Sename, L. Dugard and R. Ramirez-Mendoza (2008*a*). A self tuning suspension controller for multi-body quarter vehicle model. In: *Proceedings of the 17th IFAC World Congress (WC)*. Seoul, South Korea.

Poussot-Vassal, C., O. Sename and L. Dugard (2008*b*). A global chassis controller for handling improvements involving braking and steering systems. In: *Proceedings of the 47th IEEE Conference on Decision and Control (CDC)*. Cancun, Mexico.

Poussot-Vassal, C., O. Sename and L. Dugard (2009). Attitude and handling improvements based on optimal skyhook and feedforward strategy with semi-active suspensions. *International Journal of Vehicle Autonomous Systems: Special Issue on Modelling and Simulation of Complex Mechatronic Systems (to appear)*.

Poussot-Vassal, C., O. Sename, L. Dugard, P. Gáspár, Z. Szabó and J. Bokor (2006*a*). Multi-objective qLPV $\mathcal{H}_\infty/\mathcal{H}_2$ control of a half vehicle. In: *Proceedings of the 10th Mini-conference on Vehicle System Dynamics, Identification and Anomalies (VSDIA)*. Budapest, Hungary.

Poussot-Vassal, C., O. Sename, L. Dugard, P. Gáspár, Z. Szabó and J. Bokor (2007). A LPV based semi-active suspension control strategy. In: *Proceedings of the 3rd IFAC Symposium on System Structure and Control (SSSC)*. Iguaçu, Brazil.

Poussot-Vassal, C., O. Sename, L. Dugard, P. Gáspár, Z. Szabó and J. Bokor (2008*c*). Attitude and handling improvements through gain-scheduled suspensions and brakes control. In: *Proceedings of the 17th IFAC World Congress (WC)*. Seoul, South Korea.

Poussot-Vassal, C., O. Sename, L. Dugard, P. Gáspár, Z. Szabó and J. Bokor (2008*d*). New semi-active suspension control strategy through LPV technique. *Control Engineering Practice* **16**(12), 1519–1534.

Poussot-Vassal, C., O. Sename, L. Dugard, P. Gáspár, Z. Szabó and J. Bokor (2008*e*). Vehicle attitude and handling improvements through gain-scheduled suspensions and brakes control. *Submitted to IEEE Transaction on Control System Technology (under review)*.

Poussot-Vassal, C., O. Sename, L. Dugard, R. Ramirez-Mendoza and L. Flores (2006*b*). Optimal Skyhook control for semi-active suspensions. In: *Proceedings of the 4th IFAC Symposium on Mechatronics Systems*. Heidelberg, Germany. pp. 608–613.

Raharijaona, T. (2004). Commande robuste pour l'assistance latérale de véhicule. PhD thesis (in french). Supelec, Université Paris XI Orsay, Paris, France.

Ramirez-Mendoza, R. (1997). Sur la modélisation et la commande de véhicules automobiles. PhD thesis (in french). INPG, Laboratoire d'Automatique de Grenoble (new GIPSA-lab), Grenoble, France.

Ray, L. (1997). Nonlinear tire force estimation and road friction identification. *Automatica* **33**(10), 1819–1833.

Robert, D. (2007). Contribution à l'interaction commande /ordonnancement. PhD thesis (in french). INPG, Laboratoire d'Automatique de Grenoble (new GIPSA-lab), Grenoble, France.

Robert, D., O. Sename and D. Simon (2006). Synthesis of a sampling period dependent controller using lpv approach. In: *Proceedings of the 5th IFAC Robust Control Design (ROCOND)*. Toulouse, France.

Rossi, C. and G. Lucente (2004). $\mathcal{H}_\infty$ control of automotive semi-active suspensions. In: *Proceedings of the 1st IFAC Symposium on Advances in Automotive Control (AAC)*. Salerno, Italy.

Rotea, M.A. (1993). The generalized $\mathcal{H}_2$ control problem. *Automatica* **29**, 373–385.

Sachs (2008). Sachs website. Technical report. Sachs. http://www.zfsachs.com.

Sammier, D. (2001). On modelling and control of the automotive suspensions. PhD thesis (in french). INPG, Laboratoire d'Automatique de Grenoble (new GIPSA-lab), Grenoble, France.

Sammier, D., O. Sename and L. Dugard (2000). $\mathcal{H}_\infty$ control of active vehicle suspensions. In: *Proceedings of the IEEE International Conference on Control Applications (CCA)*. Anchorage, Alaska. pp. 976–981.

Sammier, D., O. Sename and L. Dugard (2003). Skyhook and $\mathcal{H}_\infty$ control of active vehicle suspensions: some practical aspects. *Vehicle System Dynamics* **39**(4), 279–308.

Sampson, D.J.M. and D. Cebon (2003). Active roll control of single unit heavy road vehicles. *Vehicle System Dynamics* **40**, 229–270.

Savaresi, S.M. and C. Spelta (2007). Mixed sky-hook and ADD: Approaching the filtering limits of a semi-active suspension. *ASME Transactions: Journal of Dynamic Systems, Measurement and Control* **129**(4), 382–392.

Savaresi, S.M. and C. Spelta (2008). A single sensor control strategy for semi-active suspension. *to appear in IEEE Transaction on Control System Technology*.

Savaresi, S.M., E. Siciliani and S. Bittanti (2005*a*). Acceleration driven damper (ADD): an optimal control algorithm for comfort oriented semi-active suspensions. *ASME Transactions: Journal of Dynamic Systems, Measurements and Control* **127**(2), 218–229.

Savaresi, S.M., E. Silani and S. Bittanti (2004). Semi-active suspensions: an optimal control strategy for a quarter-car model. In: *Proceedings of the 1st IFAC Symposium on Advances in Automotive Control (AAC)*. Salerno, Italy. pp. 572–577.

Savaresi, S.M., M. Tanelli and C. Cantoni (2007). Mixed slip-deceleration control in automotive braking systems. *ASME Transactions: Journal of Dynamic Systems, Measurement and Control* **129**(1), 20–31.

Savaresi, S.M., M. Tanelli, P. Langthaler and L. Del Re (2006). Identification of tire-road contact forces by in-tire accelerometers. In: *Proceedings of the 14th IFAC Symposium on System Identification (SYSID)*. Newcastle, Australia.

Savaresi, S.M., S. Bittanti and M. Montiglio (2005*b*). Identification of semi-physical and black-box models: the case of MR-dampers for vehicles control. *Automatica* **41**, 113–117.

Scherer, C. (2004). Robust mixed control and LPV control with full block scaling. Technical report. Delft University of Technology. Mechanical Engineering Systems and Control Group.

Scherer, C. and S. Wieland (2004). *LMI in control (lecture support, DELFT University)*.

Scherer, C., P. Gahinet and M. Chilali (1997). Multiobjective output-feedback control via LMI optimization. *IEEE Transaction on Automatic Control* **42**(7), 896–911.

Scherer, C.W. (1996). Mixed $\mathcal{H}_2/\mathcal{H}_\infty$ control for time-varying and linear parametrically-varying systems. *International Journal of Robust and Nonlinear Control* **6**(9-10), 929–952.

Scherer, C.W. (2000). An effcient solution to multi-objective control problems with LMI objectives. *System & Control Letters* **40**, 43–57.

Schinkel, M. and K. Hunt (2002). Anti-lock braking control using a sliding mode like approach. In: *Proceedings of the IEEE American Control Conference (ACC)*. Anchorage, Alaska.

Scorletti, G. (2004). *An introduction to the LMI optimization in Automatic Control (in French)*.

Scorletti, G., J.P. Folcher and L. El-Ghaoui (2001). Output feedback control with input saturations : LMI design approaches. *European Journal of Control* **7**(6), 567–579.

Seron, M., X.W. Zhuo, J.A. De Dona and J.J. Martinez (2007). An antilock-braking algorithm for an eddy-current-based brake-by-wire. *IEEE Transaction on Control System Technology* **56**(3), 1100–1107.

Seron, M., X.W. Zhuo, J.A. De Dona and J.J. Martinez (2008). Multisensor switching control strategy with fault tolerance guarantees. *Automatica* **44**(1), 88–97.

Shamma, J.S. and M. Athans (1991). Guaranteed properties of linear parameter varying gain scheduled control systems. *Automatica* , 559–564.

Shen, X. and F. Yu (2006). Investigation on integrated vehicle chassis control based on vertical and lateral tyre behaviour correlativity. *Vehicle System Dynamics* **44**(1), 506–519.

Shibahata, Y. (2004). Progress and future direction of chassis control technology. In: *Proceedings of the IFAC*.

Shibahata, Y. (2005). Progress and future direction of chassis control technology. *IFAC Annual Reviews in Control* **29**(1), 151–158.

Shuqui, G., Y. Shaopu and P. Cunzgi (2006). Dynamic modeling of magnetorheological damper behaviors. *Journal of Intelligent Material Systems And Structures* **17**, 3–14.

Spelta, C. (2008). Design and applications of semi-active suspension control systems. PhD thesis. Politecnico di Milano, dipartimento di Elettronica e Informazione, Milano, Italy.

Sturm, Jos F. (1999). Using SeDuMi 1.02, a MATLAB toolbox for optimization over symmetric cones. *Optim. Methods Softw.* **11/12**(1-4), 625–653. Interior point methods.

Sun, W., P.P. Khargonekar and D. Shim (1994). Solution to the positive real control problem. *IEEE Transaction on Automatic Control* **39**(10), 2034–2046.

Svendenius, J. and M. Gafvert (2006). A semi-empirical dynamic tire model for combined-slip forces. *Vehicle System Dynamics* **44**(2), 189–208.

Takahashi, R.H.C., J.F. Camino, D.E. Zampieri and P.L.D. Peres (1998). A multiobjective approach for $\mathcal{H}_2$ and $\mathcal{H}_\infty$ active suspension control. In: *Proceedings of the IEEE American Control Conference (ACC)*. Philadelphia, Pennsylvania. pp. 48–52.

Tanelli, M. (2007). Active Braking Control Systems Design for Road Vehicles. PhD thesis. Politecnico di Milano, dipartimento di Elettronica e Informazione, Milano, Italy.

Tanelli, M. and S.M. Savaresi (2006). Friction curve peak detection by wheel deceleration measurement. In: *Proceedings of the IEEE Conference on Intelligent Transportation Systems (ITSC)*. Toronto, Canada.

Tanelli, M., R. Sartori and S.M. Savaresi (2007*a*). Combining slip and deceleration control for brake-by-wire control systems: a sliding-mode approach. *European Journal of Control* **13**(6), 593–611.

Tanelli, M., R. Sartori and S.M. Savaresi (2007*b*). Sliding mode slip-deceleration control for brake-by-wire control systems. In: *Proceedings of the 5th IFAC Symposium on Advances on Automotive Control (AAC)*. Aptos, California.

Tanelli, M., S.M. Savaresi and C. Cantoni (2006). Longitudinal vehicle speed estimation for traction and brakig systems. In: *Proceedings of the Conference on Control and Applications (CCA)*. Munich, Germany.

Toth, R., F. Felici, P.S.C. Heuberger and P.M.J. Van der Hof (2008). Crutial aspects of zero-order hold lpv state-space system discretization. In: *Proceedings of the 17th IFAC World Congress (WC)*. Seoul, South Korea.

Tseng, H.E. and J.K. Hedrick (1994). Semi-active control laws - optimal and sub-optimal. *Vehicle System Dynamics* **23**(1), 545–569.

Tuan, H. Duong, P. Apkarian and S. Hosoe (2001). Nonlinear $\mathcal{H}_\infty$ control for an integrated suspension system via parametrized linear matrix inequality characterizations. *IEEE Transaction on Control System Technology* **9**(1), 175–185.

Tuan, H.D. and P. Apkarian (1999). Relaxations of parametrized LMI with control applications. *International Journal of Robust and Nonlinear Control* **9**, 59–84.

Velenis, E., P. Tsiotras, C. Canudas and M. Sorine (2005). Dynamic tire friction models for combined longitudinal and lateral vehicle motion. *Vehicle System Dynamics*.

Villagra, J., B. d'Andréa Novel, H. Mounier and M. Pengov (2007). Flatness-based vehicle steering control strategy with SDRE feedback gains tuned via a sensitivity approach. *IEEE Transaction on Control System Technology* **15**(3), 554–565.

Wu, F. and B. Lu (2004). Anti-windup control design for exponentially unstable LTI systems with actuator saturation. *System & Control Letters* **52**, 305–322.

Yi, J., L. Alvarez and R. Horowitz (2003). Emergency braking control with an observer-bsed dynamic tire/road friction model and wheel angular velocity measurement. *Vehicle System Dynamics* **39**(2), 81–97.

Zames, G. (1966). On the input-output stability of time-varying nonlinear feedback systems - parts I and II. *IEEE Transaction on Automatic Control* **11**, 228–238, 465–476.

Zames, G. (1981). Feedback and optimal sensitivity: Model reference transformations, multiplicative seminorms, and approximate inverses. *IEEE Transaction on Automatic Control* **26**(2), 301–320.

Zhou, K., J. Doyle and K. Glover (1996). *Robust and Optimal Control*. New Jersey.

Zin, A. (2005). Robust automotive suspension control toward global chassis control. PhD thesis (in french). INPG, Laboratoire d'Automatique de Grenoble (new GIPSA-lab), Grenoble, France.

Zin, A., O. Sename and L. Dugard (2005). Switched $\mathcal{H}_\infty$ control strategy of automotive active suspensions. In: *Proceedings of the 16th IFAC World Congress (WC)*. Praha, Czech Republic.

Zin, A., O. Sename, M. Basset, L. Dugard and G. Gissinger (2004). A nonlinear vehicle bicycle model for suspension and handling control studies. In: *Proceedings of the IFAC Conference on Advances in Vehicle Control and Safety (AVCS)*. Genova, Italy. pp. 638–643.

Zin, A., O. Sename, P. Gaspar, L. Dugard and J. Bokor (2008*a*). Robust LPV/$\mathcal{H}_\infty$ control for active suspensions with performance adaptation in view of the global chassis control. *Vehicle System Dynamics (to appear, DOI: 10.1080/00423110701684587)*.

Zin, A., O. Sename, P. Gáspár, L. Dugard and J.Bokor (2006). An LPV/$\mathcal{H}_\infty$ active suspension control for global chassis technology: Design and performance analysis. In: *Proceedings of the IEEE American Control Conference (ACC)*. Minneapolis, Minnesota.

Zin, A., O. Sename, P. Gaspar, L. Dugard and J.Bokor (2008*b*). Robust LPV - $\mathcal{H}_\infty$ control for active suspensions with performance adaptation in view of global chassis control. *Vehicle System Dynamics* **46**(10), 889–912.

Zolnierczyk, S. (2008). On the modeling of magneto-rheological dampers. Master's thesis. Grenoble INP. GIPSA-lab (former LAG).

COMMANDE ROBUSTE MULTIVARIABLE LINEAIRE A PARAMETRES VARIANT DE CHASSIS AUTOMOBILE

Résumé : Nous étudions dans cette thèse les problèmes liés à la Commande Globale de Châssis (CGC) automobile. L'objectif est de développer des méthodes pour piloter différents actionneurs du véhicule (suspensions, freinage et direction) afin de les faire collaborer, dans le but d'améliorer le confort et la sécurité, et, de maitriser la dynamique du véhicule. Ce problème est complexe car il implique des dynamiques variées, non linéaires et de fortes contraintes au niveau des actionneurs. Les méthodes et outils utilisés sont issus des récents développements de l'automatique dans le domaine de la commande robuste pour les systèmes linéaires à paramètres variant (LPV). Dans ce contexte, les principaux thèmes développés concernent la modélisation, l'analyse et le contrôle des véhicules automobiles, ainsi que le contrôle robuste des systèmes LPV, utilisant les outils des inégalités linéaires matricielles (LMIs). Les principaux résultats traitent du développement de méthodes LPV pour la synthèse de commande robuste de suspension semi-active et de la synthèse de contrôle global de châssis (CGC) garantissant sécurité et agrément de conduite.

Mots clefs : Dynamique véhicule, Commande Globale de Châssis, Suspensions, Freinage, Direction, LPV, $\mathcal{H}_\infty$, $\mathcal{H}_2$, Multi-objectif, LMIs.

ROBUST MULTIVARIABLE LINEAR PARAMETER VARYING CONTROL OF AUTOMOTIVE CHASSIS

Abstract: In this thesis, the automotive global chassis control problem is treated. The objective is to develop methodologies to control the different vehicle actuators (suspension, braking and steering systems) to enhance comfort and safety, and, to control the ground vehicle dynamics. Since it implies many different and nonlinear phenomena and constrained actuators, this problem turns to be very complex to solve. The tools and methods used are inspired from the recent developments in automatic control, and especially from the one from the robust control community applied to Linear Parameter Varying (LPV) systems. In this framework, we focus on the modeling, the analysis and the control of automotive systems as well as robust control for LPV systems, using the Linear Matrix Inequality (LMI) tools. The main results concern the development of a new semi-active suspension controller and an adaptive global chassis control using the robust LPV approach.

Key words : Vehicle dynamics, Global Chassis Control, Suspensions, Braking, Steering, LPV, $\mathcal{H}_\infty$, $\mathcal{H}_2$, Multi-objective, LMIs.

Discipline : Automatique-Productique
Grenoble Image Parole Signal Automatique - ENSIEG, BP46, 38402 Saint-Martin d'Hères, FRANCE.